SAPIENZA
UNIVERSITÀ DI ROMA

Hydrodynamic characterization of finite-sized particle transport in confined microfluidic systems, Brownian motion and stochastic modeling of particle transport at microscale.

Dottorato in Processi Chimici per l'Industria e per l'Ambiente (XXXV cycle)

Giuseppe Procopio
ID number 1494900

Advisor
Prof. Massimiliano Giona

Academic Year 2021/2022

Thesis defended on 28 April 2023
in front of a Board of Examiners composed by:

Prof. Massimiliano Grosso (Università degli Studi di Cagliari)
Prof. Ernesto Salzano (Università degli Studi di Bologna)
Prof. Francesco Ferella (Università degli Studi dell'Aquila)

Hydrodynamic characterization of finite-sized particle transport in confined microfluidic systems, Brownian motion and stochastic modeling of particle transport at microscale.
PhD thesis. Sapienza University of Rome

This thesis has been typeset by LaTeX and the Sapthesis class.

Author's email: giuseppe.procopio@uniroma1.it

a Silvia, mia madre

Abstract

In this thesis, the peculiar effects of the hydrodynamic confinement on the dynamic of a colloid in the Stokes regime have been addressed theoretically. Practical expressions, useful to investigate the transport of particles in complex geometries, have been provided for force, torque and higher order moments on the particle and for the disturbed velocity field of the fluid.

To begin with, a new formulation of the Stokesian singularity method is developed by introducing a bitensorial distributional formalism. This formalism overcomes the ambiguities of the classical hydrodynamic formulation of the singularity method that limits its application in confined problems. The formalism proposed permits naturally to distinguish between pole and field points of tensorial singular fields and to clearly define each singularity from its associated Stokes problem.

As a consequence of this approach an explicit expression for the singularity operator is provided, giving the disturbance field due to a body once applied to an ambient flow of the fluid. The operator is expressed in terms of the volume moments and its expression is valid regardless of the boundary conditions applied to the surface of the body. The dualism between the singularity operator giving the disturbance flow of a n-th order ambient flow and the n-th order Faxén operator has been investigated. It has been found that this dualism, referred to as the Hinch-Kim dualism, holds only if the boundary conditions satisfy a property that is referred to as the *Boundary-Condition reciprocity* (BC-reciprocity, for short). If this property is fulfilled, the Faxén operators can be expressed in terms of (m, n)-th order geometrical moments of volume forces (defined in Chapter 3). In addition, it is shown that in these cases, the hydromechanics of the fluid-body system is completely determined by the entire system of the Faxén operators. Classical boundary conditions of hydrodynamic practice (involving slippage, fluid-fluid interfaces, porous materials, etc.) are investigated in light of this property. It is found the analytical expression for the 0-th, 1-st and 2-nd Faxén operators for a sphere with Navier-slip boundary conditions.

These results are applied in order to express the hydrodynamics of particles in confined fluids in terms of quantities related to the geometry of the particle and the geometry of the confinement separately using the reflection method. Specifically, closed-form results and practical expressions for the velocity field of the fluid and the functional form of force and torque acting on a particle are derived in terms of: (i) the Faxén operators of the body of the particle (given by its unbounded geometrical moments) and (ii) the multi-poles in the domain of the confinement. The convergence of the reflection method is examined and it is found that the expressions obtained are also valid for distances between particle and walls of the confinement of the same magnitude order, failing only in the limit case of the lubrication range. The reflection solutions obtained with the present theory, approximated to the order $O\left((\ell_b/\ell_d)^5\right)$, are compared with the exact solution of a sphere near a planar wall, and the expressions for forces and torques considering the more general situation of Navier-slip boundary conditions on the body are provided.

A general formulation of the fluctuation-dissipation relations in confined geometries, the paradoxes associated with no-slip boundary conditions close to a solid

boundary, and the modal representation of the inertial kernels for complex fluids complete the present dissertation. Specifically, the general setting of the overdamped approximation in confined geometries is provided, by explicitly expressing the thermal contributions associated with the rigid rototranslational motion of a body. In passing, the extension of fluctuation-dissipation results to non-equilibrium conditions, such as those arising in thermophoretic flows in the presence of a steady temperature profile is developed. The influence of boundary conditions on the fluctuational form of the force acting on a rigid particle near a solid wall is addressed, showing that the classical Stokesian paradox of infinite touching time in the presence of no-slip boundary conditions can be resolved by considering the arbitrarily small slippage effects on both surfaces, leading to an integrable logarithmic singularity. Finally, a preliminary extension of fluid-particle interactions either in a time-dependent Stokes regime or in the presence of complex (viscoelastic) flows is addressed, focusing on the modal representation of the dissipative and fluid inertial memory kernels, and on the fluctional form of the latter. Specifically, it is shown that for a viscoelastic fluid, characterized by a finite and non-vanishing relaxation rate, the generalized Basset kernel is a regular function of time, also close to $t = 0$, which is not the case of a Newtonian fluid for which the Basset kernel scales as $1/\sqrt{t}$.

Contents

Introduction

One of the main characteristics of fluid flows at the microscale is the accurate predictability of their hydrodynamics. Also for this reason, by a detailed design of microfluidic devices, it is possible to realize highly controlled, sensitive and selective processes. This capability, coupled with their main limitation of very small processed volumes, make microfluidic devices mainly employed in middle/high-value applications, concerning fields such as pharmaceutical [213, 246], food [222, 109, 180], environment [239, 247], optics [203, 69, 151], microelectronics [96, 249] and precision mechanics [99, 155].

The predictability of the behavior of a microfluidic system is strictly related to the equations governing fluid motion in the low Reynolds number regime, typical at this length scale. In fact, in most cases, the flow can be considered in the Stokes regime ($Re \to 0$) and, when the inertia becomes significant ($Re \sim 1$), perturbations of the Stokes solution can be enforced [107]. From the mathematical point of view, this means that the configurations assumed by the fluid flows belong to the set of solutions of a well-posed linear problem for which the uniqueness and the convergence in specific functional spaces are ensured [137].

On the other hand, in scaling the size of a fluidic system, other difficulties arise, making the detailed predictability far from being effective by a superficial approach to the design of microfluidic devices. Typical complications occurring in dealing with microfluidic devices can be basically distinguished into two main classes: (i) difficulties extrinsic to the fluid flow, and (ii) difficulties intrinsically related to the peculiarity of the laminar regime of the flow. The complications belonging to the first class can be attributed to typical disturbance phenomena affecting the processes, such as, for example, undesired electrostatic [16] and Casimir forces (becoming significant at microscale [176, 20]) or the noise due to thermal fluctuations affecting especially smaller particles. The second class encompasses difficulties strictly related to transport phenomena in the low Reynolds-number regime such as: the enhanced dispersion of solutes in channels due to the interaction between diffusional processes and the high-velocity gradients of the fluid along the channel sections; the inhibition of mixing processes due to the smallness of convective effects (corresponding to very high Peclet numbers); the long-range interactions between bodies, due mainly to the substantial incompressibility of these flows [84, 83]; the central role of an accurate choice of the appropriate boundary conditions, the simplification of which can lead to considerable errors both quantitatively and qualitatively, or even to evident paradoxes [110, 111, 62, 200]. A more profound knowledge of these phenomena is therefore essential in order to realize a correct design for these devices, overcoming, whenever possible, these difficulties and, eventually, taking advantage from them in the development of innovative processes unachievable at the macroscale.

An important class of microfluidic processes involves transport of colloidal particles. These can be either inactive (such as proteins, nucleic acids, viruses, fibers, and organic and inorganic pollutants) or active colloids (such as biological [145] or artificial microswimmers [170]) transported in devices such as microreactors for protein crystallization [241], T-junctions for cell encapsulation [123], DNA sequencer [160], flow cytometry channels for particle detection [219], separation capillaries by hydrodynamic chromatography [227], etc. In many of these cases, microfluidic devices (having, by definition, micrometric sizes) possess a characteristic length ℓ_d comparable with the characteristic length ℓ_b of the processed particles.

The fact that both particles and flow devices possess characteristic lengthscales of the same order of magnitude implies in turn that particles cannot be considered as pointwise entities such as in the modeling of macroscopic systems, and their size and geometrical properties should be considered. Therefore, in order to correctly investigate the transport properties of these systems, it is necessary to take into account steric hindrance, angular orientations and body deformations with respect to the walls of the device and to the other particles. When considering particles of finite size immersed in the fluid, also particle-fluid hydrodynamic interactions become more complex than in pointwise models, for which hydrodynamic interactions can be simply represented by a Stokes coefficient relating drag forces to the velocity of particles and where the particle velocity can be considered equal to that of the fluid (when external flows are present and in the absence of specific forces acting on the particles, such as the Lorentz force for ferromagnetic particles in an electrically neutral fluid). In fact, the main effects of fluid-body interactions can be summarized as:

- the motion of the fluid is disturbed by the body and therefore the velocity field in the domain of the fluid is different from the ambient fluid flow;
- the particle velocity is different from the velocity of the ambient flow at the particle position, and therefore the particles flow rates can be considerably discordant from those expected from the pointwise model;
- forces and torques on particles are related to translational and angular velocities by a more general linear relation represented by a resistance matrix which takes into account anisotropy, lift forces, coupling between rotations/translations and forces/torques, and which reduces to a simple coefficient (isotropic matrix) only in the case the particle is spherical and located far away from the device walls.

Another implication of size similarity between particles and devices, coupled with the slow spatial decay of Stokesian perturbations $O(1/r)$, where r is the distance from the perturbation point of application, regards the hydrodynamic interactions between particles and boundaries of the flow domain. In fact, whenever an interface in the vicinity of the particle is considered (such as the walls surrounding the fluid, the interface with another fluid or the presence of other particles), the homogeneity symmetry of the unbounded fluid is broken, and thus the resistance to the motion of the particle in the confined system becomes dependent on the particle position.

Specifically, the more the fluid is confined, the higher the resistance becomes [104]. Therefore, the resistance on a particle translating at the center of a channel with a square section is lower than the resistance of a particle translating at the center of the inscribed, and higher than resistance of a particle at the centerline of the circumscribed channel with circular cross-sections, and the resistance of particles within a dilute suspension will be lower than that in a concentrate one.

Finally, the motion of smaller particles in microfluidic systems is affected by thermal fluctuations that cause an erratic particle movement also in quiescent fluids which is responsible for colloidal diffusive transport. Also, these fluctuations forces, strictly related to the hydrodynamic resistance by the fluctuation-dissipation theorem [133, 134] are significantly affected by the heterogeneity and anisotropy of confined environments typical of microfluidic devices.

In order to realize an accurate design of microfluidic systems, keeping a strict control of the transport processes occurring within them, colloidal particle dynamics should be accounted for in detail, and it requires a careful description of the different forces acting on the generic colloidal particle in the diluted case. The total force $\boldsymbol{F}$ and torque $\boldsymbol{T}$ acting on a rigid colloid, considered in an assigned external potential $\Phi(\boldsymbol{x})$, can be resumed by the Newton equation

$$\begin{pmatrix} \boldsymbol{F} \\ \boldsymbol{T} \end{pmatrix} = \begin{pmatrix} \boldsymbol{F}_{res} \\ \boldsymbol{T}_{res} \end{pmatrix} + \begin{pmatrix} \boldsymbol{F}_{flow} \\ \boldsymbol{T}_{flow} \end{pmatrix} + \begin{pmatrix} \boldsymbol{F}_{stocha} \\ \boldsymbol{T}_{stocha} \end{pmatrix} - \begin{pmatrix} \nabla\Phi(\boldsymbol{x}) \\ 0 \end{pmatrix} \tag{0.1}$$

where $\boldsymbol{F}_{res}$ and $\boldsymbol{T}_{res}$ are force and torque contributions associated with the dissipative hydrodynamic resistance of the solvent fluid, $\boldsymbol{F}_{flow}$ and $\boldsymbol{T}_{flow}$ are force and torque exerted on the particle by to the ambient flow (e.g. a pressure-driven flow), while $\boldsymbol{F}_{stocha}$ and $\boldsymbol{T}_{stocha}$ are stochastic force and torque acting on the particle due to the thermal agitation of the fluid molecules. In eq (0.1), $\Phi(\mathbf{x})$ is an external potential possibly acting on the particle.

The effect of the hydrodynamic confinement on a rigid particle in a Stokesian fluid as regards the hydrodynamic resistance, determines a linear functional law relating the force $\boldsymbol{F}_{res}$ and torque $\boldsymbol{T}_{res}$ to the translational $\boldsymbol{U}$ and angular velocity $\boldsymbol{\omega}$ of the particle, that can be expressed in tensorial form as

$$\begin{pmatrix} \boldsymbol{F}_{res} \\ \boldsymbol{T}_{res} \end{pmatrix} = -\boldsymbol{H}(\boldsymbol{x}) \begin{pmatrix} \boldsymbol{U} \\ \boldsymbol{\omega} \end{pmatrix} \tag{0.2}$$

where $\boldsymbol{H}(\boldsymbol{x})$ is the position-dependent 6×6 overall resistance matrix of the hydrodynamic interactions, characterized by a block structure

$$\boldsymbol{H}(\boldsymbol{x}) = \begin{pmatrix} \boldsymbol{\eta}(\boldsymbol{x}) & \boldsymbol{C}^{(1)}(\boldsymbol{x}) \\ \boldsymbol{C}^{(2)}(\boldsymbol{x}) & \boldsymbol{\eta}^{\omega}(\boldsymbol{x}) \end{pmatrix} \tag{0.3}$$

where $\boldsymbol{\eta}$, and $\boldsymbol{\eta}^{\omega}$ are the translational and rotational friction matrices, respectively, and $\boldsymbol{C}^{(1)}$, and $\boldsymbol{C}^{(2)}$ the roto-translational coupling matrices. Either by thermodynamical [138] or mechanical arguments [98] (see Chapter 3 and 4), it is possible to prove that $\boldsymbol{\eta}$ and $\boldsymbol{\eta}^{\omega}$ are symmetric and positive definite matrices, while $\boldsymbol{C}^{(1)}$ and $\boldsymbol{C}^{(2)}$ satisfy the property $\boldsymbol{C}^{(2)} = \left[\boldsymbol{C}^{(1)}\right]^{t}$, where the superscript "t" indicates the transpose. Correspondingly, the overall resistance matrix $\boldsymbol{H}(\boldsymbol{x})$ is symmetric and positive definite.

As regards the hydrodynamic force $\boldsymbol{F}_{flow}$ and torque $\boldsymbol{T}_{flow}$ deriving by the action of the ambient flow on the colloidal particle, their representation is by far more complex than that expressed by eq. (0.2) for the hydrodynamic resistances. This is due to the fact that for a generic ambient flow $\boldsymbol{u}(\boldsymbol{x})$, all its derivatives need to be considered. However, in the case that the fluid is considered unbounded (therefore the nearest interfaces are far enough from the particle), by the generalized Faxén law [194, pp. 51-52] it is possible to express them by linear functionals (operators) $\mathcal{F}\{\,\}$ and $\mathcal{T}\{\,\}$ of $\boldsymbol{u}(\boldsymbol{x})$ for the force and the torque, respectively, i.e.,

$$\begin{pmatrix} \boldsymbol{F}_{flow} \\ \boldsymbol{T}_{flow} \end{pmatrix} = \begin{pmatrix} \mathcal{F} \\ \mathcal{T} \end{pmatrix} \{\boldsymbol{u}(\boldsymbol{x})\} \tag{0.4}$$

where $\mathcal{F}\{\,\}$ and $\mathcal{T}\{\,\}$ depend solely on the geometry of the particle. As it will be addressed in detail in Chapter 4, it is possible to express the force and torque on the particle due to a generic ambient flow as in eq. (0.4) also for confined systems, but, in this case, the linear operators depend also on the position $\boldsymbol{x}$ of the colloid, i.e.,

$$\begin{pmatrix} \boldsymbol{F}_{flow} \\ \boldsymbol{T}_{flow} \end{pmatrix} = \begin{pmatrix} \mathcal{F}_x \\ \mathcal{T}_x \end{pmatrix} \{\boldsymbol{u}(\boldsymbol{x})\} \tag{0.5}$$

Following the original approach due to Einstein and Langevin [134], in the case that the fluid is described by means of an instantaneous response (Stoke's regime), it is natural to represent $\mathbf{F}_{\text{stocha}}$ and $\mathbf{T}_{\text{stocha}}$ in the form of a linear superposition of vector-valued Wiener processes, i.e. as

$$\begin{aligned} \mathbf{F}_{\text{stocha}}(\mathbf{x})dt &= \boldsymbol{\alpha}(\mathbf{x})\, d\mathbf{w}(t) + \boldsymbol{\gamma}(\mathbf{x})\, d\mathbf{w}^{\omega}(t) \\ \mathbf{T}_{\text{stocha}}(\mathbf{x})dt &= \boldsymbol{\varepsilon}(\mathbf{x})\, d\mathbf{w}(t) + \boldsymbol{\beta}(\mathbf{x})\, d\mathbf{w}^{\omega}(t) \end{aligned} \tag{0.6}$$

where $d\mathbf{w}(t) = (dw_1(t),\, d_2(t),\, dw_3(t))$ and $d\mathbf{w}^{\omega}(t) = (dw_1^{\omega}(t),\, dw_2^{\omega}(t),\, dw_3^{\omega}(t))$ are the increments in the time interval $(t, t+dt)$ of two mutually independent vector-valued Wiener processes. This observation is a consequence of the fact that Wiener processes are also memoryless, in the meaning that if one defines $\boldsymbol{\xi}(t) = d\mathbf{w}(t)/dt = (\xi_1(t), \xi_2(t), \xi_3(t))$, interpreted in a distributional meaning, the correlation function of $\boldsymbol{\xi}(t)$ is

$$\langle \xi_i(t_0, +t)\, \xi_j(t_0) \rangle = \delta(t)\, \delta_{i,j} \tag{0.7}$$

i.e. the stochastic forcing is delta-correlated (here $\langle\cdot\rangle$ indicates indifferently either ensemble or temporal averages owing to ergodicity, and $t_0 > 0$ is any time instant, owing to the stationarity of the process) [77].

In order to achieve a deeper understanding of the behavior of colloids transported in microfluidic systems, in this thesis all the terms entering eq. (0.1) have been investigated, providing from theoretical grounds, practical expressions for $\boldsymbol{H}(\boldsymbol{x})$, $(\mathcal{F}, \mathcal{T})$, $(\mathcal{F}_x, \mathcal{T}_x)$ and for the matrices $(\boldsymbol{\alpha}, \boldsymbol{\beta}, \boldsymbol{\gamma}, \boldsymbol{\epsilon})$, addressing their properties and their application limit.

Specifically, Chapter 1 addresses a succinct review of the basics concepts in the theory of the Stokes flows useful for further developments.

Chapters 2, 3 and 4 focus the attention on the purely hydrodynamic terms entering eq. (0.1), i.e.

$$\begin{pmatrix} \boldsymbol{F}_{hydro} \\ \boldsymbol{T}_{hydro} \end{pmatrix} = \begin{pmatrix} \boldsymbol{F}_{res} \\ \boldsymbol{T}_{res} \end{pmatrix} + \begin{pmatrix} \boldsymbol{F}_{flow} \\ \boldsymbol{T}_{flow} \end{pmatrix}$$

providing, by using a Singularity Method [194, 130], their explicit relations to the ambient flow, in a form as general as possible, and applying these relations to specific case studies. Although hydrodynamic problems at the microscale can be approached by means of typical numerical methods for solving the Stokes equation (such as finite elements method [235, 53] and boundary integral method [194]), a deeper mathematical understanding of fluid-particle interactions is beneficial in order to overcome, by means of explicit analytical solutions, the limitations and the shortcomings of the numerical approaches, to improve current numerical methods (such as Stokesian dynamics [22]) and develop new ones, and to explain and predict the non-intuitive flow and transport phenomena that may occur at the microscale.

For this reason, as the first step in tackling the problem, Chapter 2 introduces a new mathematical bitensorial distributional formalism for the singularity method in Stokes flows, able to describe the multi-body hydrodynamic interactions and overcoming the ambiguities and imprecisions that arise in the classical singularity formalism that, although irrelevant in unbounded systems, may become hindering whenever confined problems are considered. In fact, the principal ambiguities and imprecisions in the classical singularity method are:

- the singular solutions are not well defined, especially as regards the bounded singular solutions, by its own associated non-homogeneous Stokes problems;
- the point where tensorial transformations are applied generates confusion between field and pole points.

The bitensorial formalism [211, 230, 56], specifically developed for handling the Green functions in field-theoretical developments within the theory of general relativity makes a clear distinction between pole and field points of singular fields, (i) allowing an unambiguous mathematical manipulation of the singularities, (ii) providing a clear definition of the principal singular solutions introduced in the theory of the Stokes flow, (iii) specifying the associated non-homogeneous equations and boundary conditions, (iv) obtaining the most common unbounded singularities as a particular case of the more general bounded counterparts.

As a direct application of this approach, it is found that the same operator determining the disturbance flow due to a Stokeslet, provides a reflection principle for any no-slip bounded solution in the same confined geometry. Finally, by applying this result to the classical problem of the singularities bounded by a no-slip plane the already-known image system for the sourcelet and couplet and the not-yet-known image system for the source doublet and stresslet are obtained.

In Chapter 3, the problem of a particle in a generic ambient flow in an unbounded fluid is addressed, with the aim of describing the entire hydrodynamics of the problem, i.e. both the disturbance flow due to the presence of the body in the fluid and all the moments (forces, torques, stresses) that the fluid exerts on the particle. As it is known [194, 130], in the case of no-slip boundary condition on the body, the Faxén operators giving the force $\mathcal{F}$ and the torque $\mathcal{T}$ on the particle if applied to the generic ambient flow, furnishes also the flow due to the particle translating and rotating in the fluid, respectively, once applied to the pole of a Stokeslet (i.e. to the unbounded Green function of the Stokes equations). This property is referred to in the thesis as the Hinch-Kim dualism. The corresponding dualism is valid also for higher-order moments/fluid motion. To begin with, the occurrence of the Hinch-Kim dualism for more general boundary conditions of common hydrodynamic application are investigated, and it is proved that the necessary condition upon which dualism holds is that boundary condition should belong to a specific subclass that it is referred to as BC-reciprocal. To the class of BC-reciprocal conditions belong: boundary conditions for rigid bodies, Newtonian drops at the mechanical equilibrium, porous bodies modeled by the Brinkman equation, while deforming linear elastic bodies, deforming Newtonian drops, non-Newtonian drops and porous bodies modeled by the Darcy equation do not have this property. Finally, it is shown that, whenever BC-reciprocity holds, the system of Faxén operators describes completely the entire hydromechanics of a particle in a Stokes flow, and that any Faxén operator can be derived from the system of the n-th order moments on the particle in m-th order ambient fields.

As a direct application of the theory, for the Navier-slip boundary conditions on a rigid body, it is found that the n-th order Faxén operators are determined by the n-th order surface tractions, and the analytical expression for the 0-th, 1-st and 2-nd Faxén operators for a sphere with Navier-slip boundary conditions are provided.

The results obtained in the preceding Chapters are applied in Chapter 4 in order to build the exact solution of the Stokes flow around a body in a confined fluid starting from the simpler problems of the singularities of the bounded flow (i.e., all the derivatives of the Green function) and the Faxén operators of the particle in the unbounded domain. To this aim, the reflection method [98] is used and its convergence, still an open question in the general case, is addressed, finding that the solution provided by the reflection method is valid for distances between the particle and confined walls of the same order of magnitude of the size of the particle, $\ell_d \sim \ell_b$, and it may fail for very small gaps $\ell_d \ll \ell_b$. As a direct application of this analysis, the reflection solution obtained with the present theory (using Faxén operators and bounded multi-pole available in the literature), approximated to the order $O((\ell_b/\ell_d)^5)$, is compared and contrasted with the exact solution of a sphere near a planar wall, obtaining an excellent agreement. This result is not only important in itself, but it indicates that the present approach can be applied to obtain higher-order solutions to generic problems involving particles of arbitrary shapes (ellipsoids, spheroids, etc.), and more general confinements (cylindrical channels, rectangular channels, etc.) from the exact, approximated or numerical expressions for the two basic building blocks of the present theory: the Green function for the confinement, and the moments of the particle in the unbounded case. As a novel result obtained by the theory, the expression for the force and torque on a rigid spherical particle near a planar wall in the more general case of Navier-slip boundary conditions on the particle is obtained.

Chapter 5 addresses the stochastic description of the thermal forces, developing the fluctuation-dissipation relations for confined geometries. Particular attention is oriented towards the formulation of the overdamped approximation, as it involves non-trivial issues in the elimination of the fast velocity variables, considering the Stratonovich integral calculus. This is a consequence of the fact that for small but finite particle inertia, the trajectories of micrometric particles are Lipshitz continuous, and owing to the Wong-Zakai theorem, their limit process, does not coincide with the Ito formulation of the Langevin equations, but with the Stratonovich interpretation. Moreover, the implication of the singularities in the hydrodynamic resistances for a particle approaching a solid wall are discussed, in connection with the paradoxes arising from this property, focusing attention to the fact, that the generalization of the no-slip condition to the Navier's slip may cure some of them.

Chapter 6, addresses the description of more general classes of fluids, possessing both dissipative and inertial memory effects, and extending the fluid-particle interactions to time-dependent Stokes regime, and connects the representation of the associated kernels, in order to obtain a feasible formulation of particle dynamics in this case. Specifically, the modal decomposition of fluid inertial kernels, generalizing the Basset kernel to the case of viscoelastic fluids is developed, and it is shown that in the viscoelastic case, owing to the finite propagation velocity of the shear stresses, the generalized Basset kernel is nonsingular at time $t = 0$.

Chapter 1

Fundamentals of fluid-body interaction in the Stokes regime

1.1 General Properties

In this chapter, the fundamental theorems for Stokes flows are briefly reviewed, as they represent the starting point for the original developments addressed in the subsequent chapters.

The equations governing a fluid flow in the vanishing Reynolds number regime defined in a domain $D_f \in \mathbb{R}^3$ are the well-known Stokes equations

$$\begin{cases} -\nabla \cdot \boldsymbol{\sigma}(\boldsymbol{x}) = \mu \Delta \, \boldsymbol{v}(\boldsymbol{x}) - \nabla s(\boldsymbol{x}) = -\boldsymbol{\psi}(\boldsymbol{x}) \\ \nabla \cdot \boldsymbol{v}(\boldsymbol{x}) = 0; \qquad \boldsymbol{x} \in D_f \end{cases} \tag{1.1}$$

where μ is the viscosity of the fluid, $\boldsymbol{v}(\boldsymbol{x})$ the velocity of the fluid element at the point $\boldsymbol{x} \in D_f$, $s(\boldsymbol{x})$ the pressure field, $\boldsymbol{\psi}(\boldsymbol{x})$ an external volume force field and $\boldsymbol{\sigma}(\boldsymbol{x})$ the stress tensor for a Newtonian fluid, hence

$$\boldsymbol{\sigma}(\boldsymbol{x}) = s(\boldsymbol{x}) I - 2\mu \boldsymbol{e}(\boldsymbol{x}); \qquad \boldsymbol{e}(\boldsymbol{x}) = \frac{\nabla \boldsymbol{v}(\boldsymbol{x}) + \nabla \boldsymbol{v}(\boldsymbol{x})^t}{2} \tag{1.2}$$

where I is the identity matrix, $\boldsymbol{e}(\boldsymbol{x})$ the strain rate tensor and the superscript t denotes the transpose operator of a matrix.

The system of eqs. (1.1) requires boundary conditions at the boundary of the fluid domain ∂D_f depending on the physical nature of the interface. In Chapter 3, several boundary conditions at the fluid-body interface are addressed. Here we consider exclusively the Navier-slip boundary condition, which is the most commonly class of mixed boundary conditions assumed at the fluid-solid interface. As deduced by Navier [179], a slippage occurs at the interface between the fluid and a fixed body, and this slippage generates a linear opposite resistance by the surface of the body. Enforcing the impermeability constraint, the boundary conditions become

$$\begin{cases} \boldsymbol{v}(\boldsymbol{x}) \cdot \boldsymbol{n}(\boldsymbol{x}) = 0 \\ \boldsymbol{n}(\boldsymbol{x}) \cdot \boldsymbol{\sigma}(\boldsymbol{x}) \cdot \boldsymbol{t}(\boldsymbol{x}) = -\dfrac{\mu}{\lambda} \boldsymbol{v}(\boldsymbol{x}) \cdot \boldsymbol{t}(\boldsymbol{x}) \qquad \boldsymbol{x} \in \partial D_f \end{cases} \tag{1.3}$$

where $\boldsymbol{n}(\boldsymbol{x})$ is the unit normal to the surface oriented towards the fluid (i.e. the external unit vector to the body), $\boldsymbol{t}(\boldsymbol{x}) = I - \boldsymbol{n}(\boldsymbol{x}) \otimes \boldsymbol{n}(\boldsymbol{x})$ and λ, is the so-called slip length which depends on the chemical characteristics of the interface. When the slip length λ is much smaller than the characteristic size of the fluid system ℓ, hence for $\lambda \ll \ell$, boundary conditions (1.3) reduce to no-slip boundary condition

$$\boldsymbol{v}(\boldsymbol{x}) = 0, \qquad \boldsymbol{x} \in \partial D_f \tag{1.4}$$

corresponding to complete adherence between the fluid and the body at the interface. Typical intrinsic slip length orders are $\lambda \sim 1 \div 100\,nm$ [146], therefore it is important to consider slip at the interface especially in dealing with smaller colloids. However, artifacts at the interface, such as the presence of gas bubbles or surface roughness, can significantly enhance the slippage at the interface making necessary to consider it also in dealing with larger particles.

From the system of the eqs. (1.1) and (1.3) it is possible to deduce several properties of Stokes flows, the first two of which are straightforward.

i) Stokes equations and boundary conditions are *linear*. Therefore, given two distinct solutions $\boldsymbol{v}'(\boldsymbol{x})$ and $\boldsymbol{v}''(\boldsymbol{x})$ of eqs. (1.1) and (1.3) and given two 3×3 constant matrices $\boldsymbol{A}$ and $\boldsymbol{B}$, their linear superposition

$$\boldsymbol{v}(\boldsymbol{x}) = \boldsymbol{A} \cdot \boldsymbol{v}'(\boldsymbol{x}) + \boldsymbol{B} \cdot \boldsymbol{v}''(\boldsymbol{x}) \tag{1.5}$$

is still a Stokes flow, solution of eqs. (1.1) and (1.3).

ii) Material derivative vanishes in the Stokes regime, therefore if boundary conditions change in time according to a given law (say for example the boundary $\partial D_f(t)$ changes in time, as in moving boundary problems), the time evolution of the flow $\boldsymbol{v}(\boldsymbol{x}, t) = \boldsymbol{v}_t(\boldsymbol{x})$ is a collection of *instantaneous* solutions of the Stokes equations, independently of the history of the flow, in which time appears solely as a parameter.

Other properties are less intuitive; however, their proofs can be found in classical monographs [98, 194, 130].

iii) A very useful property of Stokes flows is the *reciprocity* holding between two solutions of the Stokes equations (1.1) with different external volume force fields and boundary conditions. This theorem, firstly formulated by Lorentz [156, pp.23-26], states that if $(\boldsymbol{v}'(\boldsymbol{x}), \boldsymbol{\sigma}'(\boldsymbol{x}))$ and $(\boldsymbol{v}''(\boldsymbol{x}), \boldsymbol{\sigma}''(\boldsymbol{x}))$ are two solutions of the Stokes eqs. (1.1) in the domain D_f with distinct boundary conditions on ∂D_f and with $\boldsymbol{\psi}'(\boldsymbol{x})$ and $\boldsymbol{\psi}''(\boldsymbol{x})$ as external volume force field respectively, then

$$\int_{\partial D_f} (\boldsymbol{v}'(\boldsymbol{x}) \cdot \boldsymbol{\sigma}''(\boldsymbol{x}) - \boldsymbol{v}''(\boldsymbol{x}) \cdot \boldsymbol{\sigma}'(\boldsymbol{x})) \cdot \boldsymbol{n}(\boldsymbol{x}) dS = \int_{D_f} (\boldsymbol{v}'(\boldsymbol{x}) \cdot \boldsymbol{\psi}''(\boldsymbol{x}) - \boldsymbol{v}''(\boldsymbol{x}) \cdot \boldsymbol{\psi}'(\boldsymbol{x})) dV \tag{1.6}$$

where dS and dV are the surface, and the volume elements, respectively. Eq. (1.6) becomes in differential form

$$\nabla \cdot (\boldsymbol{v}'(\boldsymbol{x}) \cdot \boldsymbol{\sigma}''(\boldsymbol{x}) - \boldsymbol{v}''(\boldsymbol{x}) \cdot \boldsymbol{\sigma}'(\boldsymbol{x})) = \boldsymbol{v}'(\boldsymbol{x}) \cdot \boldsymbol{\psi}''(\boldsymbol{x}) - \boldsymbol{v}''(\boldsymbol{x}) \cdot \boldsymbol{\psi}'(\boldsymbol{x}) \tag{1.7}$$

As it will be shown in the remainder, the relation between two distinct Stokes flows provided by eqs. (1.6) and (1.7) permit us to obtain the analytical expressions for complex flows in terms of simpler ones, and to deduce interesting relations for the hydromechanics of bodies. An exhaustive discussion on the importance of the Lorentz reciprocal theorem in fluid dynamics is addressed in [163]. Proofs of the Lorentz reciprocal theorem, in the form eq. (1.6) and eq. (1.7), are reported in [130, p. 19] and in [194, p. 9]; whereas in [98, pp. 85] it is proved a generalization of the theorem to the case the two solutions refer to two different fluids with viscosity μ' and μ''.

iv) Another fundamental theorem for Stokes flow, firstly established by Helmholtz (see [98, p. 91] or [5, p. 227]), is the *minimum dissipation theorem.* According to this theorem, the velocity field $\boldsymbol{v}(\boldsymbol{x})$ solution of (1.1) produces the minimum dissipation energy in the domain of the fluid [5, 138]

$$\Phi[\boldsymbol{v}(\boldsymbol{x})] = 2\mu \int_{D_f} \boldsymbol{e}(\boldsymbol{x}) : \boldsymbol{e}(\boldsymbol{x}) dV \tag{1.8}$$

among all the incompressible flows $\boldsymbol{v}^{\#}(\boldsymbol{x})$ with equal boundary conditions. Therefore, given a generic incompressible flow

$$\begin{cases} \nabla \cdot \boldsymbol{v}^{\#}(\boldsymbol{x}) = 0, & \boldsymbol{x} \in D_f \\ \boldsymbol{v}^{\#}(\boldsymbol{x}) = \boldsymbol{v}(\boldsymbol{x}), & \boldsymbol{x} \in \partial D_f \end{cases} \tag{1.9}$$

with $\boldsymbol{e}^{\#}(\boldsymbol{x}) = (\nabla \boldsymbol{v}^{\#}(\boldsymbol{x}) + \nabla \boldsymbol{v}^{\#}(\boldsymbol{x})^t)/2$, then

$$\int_{D_f} \boldsymbol{e}^{\#}(\boldsymbol{x}) : \boldsymbol{e}^{\#}(\boldsymbol{x}) dV \geq \int_{D_f} \boldsymbol{e}(\boldsymbol{x}) : \boldsymbol{e}(\boldsymbol{x}) dV \tag{1.10}$$

v) As a corollary of the minimum dissipation energy theorem [93, p. 24], the Stokes flow is *unique*. More precisely, two solutions $\boldsymbol{v}'(\boldsymbol{x})$ and $\boldsymbol{v}''(\boldsymbol{x})$ of the Stokes eqs. (1.1), attaining the same values for all $\boldsymbol{x} \in \partial D_f$, are one and the same flow, i.e., $\boldsymbol{v}'(\boldsymbol{x}) = \boldsymbol{v}''(\boldsymbol{x})$ for all $\boldsymbol{x} \in D_f$. In point of fact, as they solve the Stokes equations, they both minimize the dissipation energy and therefore their associated strain rate tensors are equal $\boldsymbol{e}'(\boldsymbol{x}) = \boldsymbol{e}''(\boldsymbol{x})$. As consequence, the difference flow $\boldsymbol{v}'(\boldsymbol{x}) - \boldsymbol{v}''(\boldsymbol{x})$ is at most constant, hence a rigid motion. Enforcing the boundary condition, this constant should be vanishing and thus $\boldsymbol{v}'(\boldsymbol{x}) = \boldsymbol{v}''(\boldsymbol{x})$ in the entire domain D_f.

vi) As a direct consequence of linearity and uniqueness, any Stokes flow is *reversible.* This means that, if the flow $\boldsymbol{v}'(\boldsymbol{x})$ is a solution of the Stokes equations satisfying a boundary condition, say $\boldsymbol{v}'(\boldsymbol{x}) = \boldsymbol{v}^S(\boldsymbol{x})$, the flow that satisfies the same boundary conditions with reversed sign, i.e., $\boldsymbol{v}''(\boldsymbol{x}) = -\boldsymbol{v}^S(\boldsymbol{x})$, is exactly the initial flow with the reversed sign, i.e., $\boldsymbol{v}''(\boldsymbol{x}) = -\boldsymbol{v}'(\boldsymbol{x})$. Since a change in sign of the solution involves (by linearity) also a change in the sign of the hydrodynamics forces and torques acting on the immersed bodies, reversibility has important implications on the motion of bodies in fluids at micro-scale, such as on the schemes which micro-swimmers need to adopt to move (see for example the Purcell scallop theorem [204, 145, pp. 25-26]), and on the suppression of lift forces on bodies in certain symmetric systems [148, pp. 438-439]).

A fundamental solution of the Stokes flow is the unbounded Green function of the system of equations (1.1), obtained by assuming an external volume force field

$\boldsymbol{\psi}(\boldsymbol{x}) = \boldsymbol{\phi}\,\delta(\boldsymbol{x}-\boldsymbol{\xi})$ centered in a point $\boldsymbol{\xi} \in \mathbb{R}^3$ and requiring for the velocity to vanish at infinity,

$$\begin{cases} -\nabla\cdot\boldsymbol{\sigma}^*(\boldsymbol{x},\boldsymbol{\xi}) = \mu\Delta\,\boldsymbol{v}^*(\boldsymbol{x},\boldsymbol{\xi}) - \nabla s^*(\boldsymbol{x},\boldsymbol{\xi}) = -\boldsymbol{\phi}\,\delta(\boldsymbol{x}-\boldsymbol{\xi}) \\ \nabla\cdot\boldsymbol{v}^*(\boldsymbol{x},\boldsymbol{\xi}) = 0; \qquad \boldsymbol{x},\boldsymbol{\xi}\in\mathbb{R}^3 \\ \boldsymbol{v}^*(\boldsymbol{x},\boldsymbol{\xi}) = 0, \qquad \boldsymbol{x}\to\infty \end{cases} \tag{1.11}$$

The solution of eqs. (1.11), called the Oseen tensor [185, p. 98] or *Stokeslet*, can be obtained by several approaches [137, 194, 84, 154], and it can be expressed as follows

$$\begin{aligned} \boldsymbol{v}^*(\boldsymbol{x},\boldsymbol{\xi}) &= \frac{\boldsymbol{S}(\boldsymbol{x},\boldsymbol{\xi})\cdot\boldsymbol{\phi}}{8\pi\mu} \\ p^*(\boldsymbol{x},\boldsymbol{\xi}) &= \frac{\boldsymbol{P}(\boldsymbol{x},\boldsymbol{\xi})\cdot\boldsymbol{\phi}}{8\pi} \\ \boldsymbol{\sigma}^*(\boldsymbol{x},\boldsymbol{\xi}) &= \frac{\boldsymbol{\Pi}(\boldsymbol{x},\boldsymbol{\xi})\cdot\boldsymbol{\phi}}{8\pi} \end{aligned} \tag{1.12}$$

where $\boldsymbol{S}(\boldsymbol{x},\boldsymbol{\xi})$, $\boldsymbol{P}(\boldsymbol{x},\boldsymbol{\xi})$ and $\boldsymbol{\Pi}(\boldsymbol{x},\boldsymbol{\xi})$ are tensors with entries

$$\begin{aligned} S_{ij}(\boldsymbol{x},\boldsymbol{\xi}) &= \frac{\delta_{ij}}{r} + \frac{(\boldsymbol{x}-\boldsymbol{\xi})_i(\boldsymbol{x}-\boldsymbol{\xi})_j}{r^3} \\ P_j(\boldsymbol{x},\boldsymbol{\xi}) &= \frac{2(\boldsymbol{x}-\boldsymbol{\xi})_j}{r^3} \\ \Pi_{ijk}(\boldsymbol{x},\boldsymbol{\xi}) &= \frac{6(\boldsymbol{x}-\boldsymbol{\xi})_i(\boldsymbol{x}-\boldsymbol{\xi})_j(\boldsymbol{x}-\boldsymbol{\xi})_k}{r^5} \end{aligned} \tag{1.13}$$

$i,j,k = 1,2,3$, where $r = \sqrt{(\boldsymbol{x}-\boldsymbol{\xi})\cdot(\boldsymbol{x}-\boldsymbol{\xi})}$ and "$\cdot$" indicates the Euclidean scalar product.

The Stokeslet solution is the kernel by which it is possible to construct the Ladyzhenskaya volume potential [137, p. 49], providing any solutions of eqs. (1.1) vanishing at infinity

$$\begin{aligned} \boldsymbol{v}(\boldsymbol{x}) &= \int \frac{\boldsymbol{S}(\boldsymbol{x},\boldsymbol{\xi})\cdot\boldsymbol{\psi}(\boldsymbol{\xi})}{8\pi\mu}dV(\boldsymbol{\xi}) \\ p(\boldsymbol{x}) &= \int \frac{\boldsymbol{P}(\boldsymbol{x},\boldsymbol{\xi})\cdot\boldsymbol{\psi}(\boldsymbol{\xi})}{8\pi}dV(\boldsymbol{\xi}) \\ \boldsymbol{\sigma}(\boldsymbol{x}) &= \int \frac{\boldsymbol{\Pi}(\boldsymbol{x},\boldsymbol{\xi})\cdot\boldsymbol{\psi}(\boldsymbol{\xi})}{8\pi}dV(\boldsymbol{\xi}) \end{aligned} \tag{1.14}$$

where $dV(\boldsymbol{\xi})$ is the volume element at $\boldsymbol{\xi}\in\mathbb{R}^3$.

If the fluid domain is bounded, the system of equation (1.11) with homogeneous boundary conditions becomes

$$\begin{cases} -\nabla\cdot\boldsymbol{\sigma}^*(\boldsymbol{x},\boldsymbol{\xi}) = \mu\Delta\,\boldsymbol{v}^*(\boldsymbol{x},\boldsymbol{\xi}) - \nabla s^*(\boldsymbol{x},\boldsymbol{\xi}) = -\boldsymbol{\phi}\,\delta(\boldsymbol{x}-\boldsymbol{\xi}) \\ \nabla\cdot\boldsymbol{v}^*(\boldsymbol{x},\boldsymbol{\xi}) = 0; \qquad \boldsymbol{x},\boldsymbol{\xi}\in D_f \\ \boldsymbol{v}^*(\boldsymbol{x},\boldsymbol{\xi}) = 0, \qquad \boldsymbol{x}\in\partial D_f \end{cases} \tag{1.15}$$

and the solution can be also expressed as

$$\begin{aligned} \boldsymbol{v}^*(\boldsymbol{x},\boldsymbol{\xi}) &= \frac{\boldsymbol{G}(\boldsymbol{x},\boldsymbol{\xi})\cdot\boldsymbol{\phi}}{8\pi\mu} \\ p^*(\boldsymbol{x},\boldsymbol{\xi}) &= \frac{\boldsymbol{\mathcal{P}}(\boldsymbol{x},\boldsymbol{\xi})\cdot\boldsymbol{\phi}}{8\pi} \\ \boldsymbol{\sigma}^*(\boldsymbol{x},\boldsymbol{\xi}) &= \frac{\boldsymbol{\Sigma}(\boldsymbol{x},\boldsymbol{\xi})\cdot\boldsymbol{\phi}}{8\pi} \end{aligned} \tag{1.16}$$

where $\boldsymbol{G}(\boldsymbol{x},\boldsymbol{\xi})$, $\boldsymbol{\mathcal{P}}(\boldsymbol{x},\boldsymbol{\xi})$ and $\boldsymbol{\Sigma}(\boldsymbol{x},\boldsymbol{\xi})$ are kernels, depending on the geometry of the domain D_f, by means of which it is possible to construct the volume potentials analogous to eqs. (1.14) [137, p. 63]. Examples of fluid domains for which the Green function $\boldsymbol{G}(\boldsymbol{x},\boldsymbol{\xi})$ is available in the literature are: the half space [18], the space enclosed between two parallel walls [152], the space enclosed by cylindrical boundary [153], the space enclosed in spherical boundaries [185, 164], the space outside a sphere [185, 165].

A remarkable property of the Stokes Green functions, valid for all the domains, is the reciprocal symmetry of its entries

$$G_{ij}(\boldsymbol{x},\boldsymbol{\xi}) = G_{ji}(\boldsymbol{\xi},\boldsymbol{x}) \tag{1.17}$$

see [194, pp. 76-77] for the proof.

By applying the Lorentz reciprocal theorem eq. (1.6) to the Stokeslet solution $\boldsymbol{v}'(\boldsymbol{x}) = \boldsymbol{v}^*(\boldsymbol{x},\boldsymbol{\xi})$ in eqs. (1.12) and (1.13) with $\boldsymbol{\xi} \in D_f$ and to a generic solution $\boldsymbol{v}''(\boldsymbol{x}) = \boldsymbol{v}(\boldsymbol{x})$, and by using the property eq. (1.17) for the Stokeslet, it is possible to obtain the boundary integral expressions for the Stokes flow [137, p. 52]

$$\begin{aligned} 8\pi\mu\,\boldsymbol{v}(\boldsymbol{x}) &= \int_{D_f} \boldsymbol{S}(\boldsymbol{x},\boldsymbol{\xi})\cdot\boldsymbol{\psi}(\boldsymbol{\xi})dV(\boldsymbol{\xi}) \\ &+ \int_{\partial D_f} (\mu\,\boldsymbol{v}(\boldsymbol{\xi})\cdot\boldsymbol{\Pi}(\boldsymbol{x},\boldsymbol{\xi}) - \boldsymbol{S}(\boldsymbol{x},\boldsymbol{\xi})\cdot\boldsymbol{\sigma}(\boldsymbol{\xi}))\cdot\boldsymbol{n}(\boldsymbol{\xi})dS(\boldsymbol{\xi}) \end{aligned} \tag{1.18}$$

that, in accordance with the uniqueness of the Stokes solutions, expresses that the flow is univocally determined by its values at the boundary of the domain.

1.2 A single body in Stokes flow

Next, let us focus on the case of a body immersed in the unbounded Stokes fluid. The domain of the body is $D_b \subset \mathbb{R}^3$ with boundaries ∂D_b and therefore, the domain of the fluid is $D_f \equiv \mathbb{R}^3/D_b$ with boundaries $\partial D_f \equiv \partial D_b \cup \partial D_\infty$, where ∂D_∞ is an ideal surface at infinity. The *ambient flow* of the fluid (i.e. the flow of the fluid without the body inclusion) is $\boldsymbol{u}(\boldsymbol{x})$ with associated pressure $p(\boldsymbol{x})$ and stress tensor $\boldsymbol{\pi}(\boldsymbol{x})$, solution of the Stokes equations

$$\begin{cases} -\nabla\cdot\boldsymbol{\pi}(\boldsymbol{x}) = \mu\Delta\boldsymbol{u}(\boldsymbol{x}) - \nabla p(\boldsymbol{x}) = 0 \\ \nabla\cdot\boldsymbol{u}(\boldsymbol{x}) = 0 \qquad \boldsymbol{x}\in\mathbb{R}^3 \end{cases} \tag{1.19}$$

The presence of the body in the fluid generates a *disturbance flow* at the boundaries of the body ∂D_b, that we generically call $\boldsymbol{w}^S(\boldsymbol{x})$. Thus, a disturbance flow $\boldsymbol{w}(\boldsymbol{x})$ in the domain of the fluid with associated pressure $q(\boldsymbol{x})$ and stress tensor $\boldsymbol{\tau}(\boldsymbol{x})$ is a solution of the Stokes equations

$$\begin{cases} -\nabla \cdot \boldsymbol{\tau}(\boldsymbol{x}) = \mu \Delta \boldsymbol{w}(\boldsymbol{x}) - \nabla q(\boldsymbol{x}) = 0 \\ \nabla \cdot \boldsymbol{w}(\boldsymbol{x}) = 0 \qquad \boldsymbol{x} \in D_f \\ \boldsymbol{w}(\boldsymbol{x}) = \boldsymbol{w}^S(\boldsymbol{x}),\ \boldsymbol{\tau}(\boldsymbol{x}) = \boldsymbol{\tau}^S(\boldsymbol{x}) \qquad \boldsymbol{x} \in \partial D_b \end{cases} \tag{1.20}$$

where $\boldsymbol{\tau}^S(\boldsymbol{x})$ is the stress tensor of the disturbance flow at the surface of the body.

The total field, or *disturbed flow*, $(\boldsymbol{v}(\boldsymbol{x}), \boldsymbol{\sigma}(\boldsymbol{x})) = (\boldsymbol{u}(\boldsymbol{x}), \boldsymbol{\pi}(\boldsymbol{x})) + (\boldsymbol{w}(\boldsymbol{x}), \boldsymbol{\tau}(\boldsymbol{x}))$ is a solution of the Stokes equations

$$\begin{cases} -\nabla \cdot \boldsymbol{\sigma}(\boldsymbol{x}) = \mu \Delta \boldsymbol{v}(\boldsymbol{x}) - \nabla s(\boldsymbol{x}) = 0 \\ \nabla \cdot \boldsymbol{v}(\boldsymbol{x}) = 0 \qquad \boldsymbol{x} \in D_f \\ \boldsymbol{v}(\boldsymbol{x}) = \boldsymbol{v}^S(\boldsymbol{x}),\ \boldsymbol{\sigma}(\boldsymbol{x}) = \boldsymbol{\sigma}^S(\boldsymbol{x}) \qquad \boldsymbol{x} \in \partial D_b \\ \boldsymbol{v}(\boldsymbol{x}) = \boldsymbol{u}(\boldsymbol{x}) \qquad \boldsymbol{x} \to \infty \end{cases} \tag{1.21}$$

$s(\boldsymbol{x}) = p(\boldsymbol{x}) + q(\boldsymbol{x})$ being the total pressure field , $\boldsymbol{v}^S(\boldsymbol{x}) = \boldsymbol{w}^S(\boldsymbol{x}) + \boldsymbol{u}(\boldsymbol{x})$ and $\boldsymbol{\sigma}^S(\boldsymbol{x}) = \boldsymbol{\tau}^S(\boldsymbol{x}) + \boldsymbol{\pi}(\boldsymbol{x})$ the total velocity field and stress tensor at the surface of the body.

Assumingno-slip boundary conditions, i.e. $\boldsymbol{w}^S(\boldsymbol{x}) = -\boldsymbol{u}(\boldsymbol{x})$ at the the interface with the body, and no external forces on the fluid $\boldsymbol{\psi}(\boldsymbol{x}) = 0$, and considering that as $\boldsymbol{x} \to \infty$ the disturbed field vanishes and $\boldsymbol{v}(\boldsymbol{x}) \to \boldsymbol{u}(\boldsymbol{x})$, boundary integrals (1.18) becomes

$$\begin{aligned} \boldsymbol{v}(\boldsymbol{x}) &= \frac{1}{8\pi\mu} \int_{\partial D_\infty} (\mu \boldsymbol{u}(\boldsymbol{x}) \cdot \boldsymbol{\Pi}(\boldsymbol{x}, \boldsymbol{\zeta}) - \boldsymbol{S}(\boldsymbol{x}, \boldsymbol{\zeta}) \cdot \boldsymbol{\pi}(\boldsymbol{\zeta})) \cdot \boldsymbol{n}(\boldsymbol{\zeta}) dS(\boldsymbol{\zeta}) \\ &- \frac{1}{8\pi\mu} \int_{\partial D_b} \boldsymbol{S}(\boldsymbol{x}, \boldsymbol{\zeta}) \cdot \boldsymbol{\sigma}(\boldsymbol{\zeta}) \cdot \boldsymbol{n}(\boldsymbol{\zeta}) dS(\boldsymbol{\zeta}) \end{aligned} \tag{1.22}$$

Since the first integral on the r.h.s is the boundary integral representation of the ambient flow, regular on the surface of the body, the disturbance field is

$$\boldsymbol{w}(\boldsymbol{x}) = -\frac{1}{8\pi\mu} \int_{\partial D_b} \boldsymbol{S}(\boldsymbol{x}, \boldsymbol{\zeta}) \cdot \boldsymbol{h}(\boldsymbol{\zeta}) dS(\boldsymbol{\zeta}) \tag{1.23}$$

where $\boldsymbol{h}(\boldsymbol{x}) = \boldsymbol{\sigma}(\boldsymbol{x}) \cdot \boldsymbol{n}(\boldsymbol{x})$ is the surface traction of the total disturbed field.

By expanding the Stokeslet field at the point $\boldsymbol{\zeta} \in \partial D_b$ around an interior point of the body $\boldsymbol{\xi} \in D_b$, we obtain the *multi-pole expansion* [130, p. 27], or *singular representation* [194, p. 201], of a disturbance flow

$$8\pi\mu\, \boldsymbol{w}(\boldsymbol{x}) = \boldsymbol{S}(\boldsymbol{x}, \boldsymbol{\xi}) \cdot \boldsymbol{M}^{(0)} + \nabla_\xi \boldsymbol{S}(\boldsymbol{x}, \boldsymbol{\xi}) : \boldsymbol{M}^{(1)}(\boldsymbol{\xi}) + \nabla_\xi \nabla_\xi \boldsymbol{S}(\boldsymbol{x}, \boldsymbol{\xi}) \vdots \frac{\boldsymbol{M}^{(2)}(\boldsymbol{\xi})}{2!} + ... \tag{1.24}$$

where ∇_ξ is the gradient operator at the point $\boldsymbol{\xi}$, $\boldsymbol{M}^{(n)}(\boldsymbol{\xi})$ are n-th order surface moments of the traction $\boldsymbol{h}(\boldsymbol{\zeta})$

$$\boldsymbol{M}^{(n)}(\boldsymbol{\xi}) = \int_{\partial D_b} \overbrace{(\boldsymbol{\zeta} - \boldsymbol{\xi}) \ldots (\boldsymbol{\zeta} - \boldsymbol{\xi})}^{n \text{ times}} \cdot \boldsymbol{h}(\boldsymbol{\zeta}) dS(\boldsymbol{\zeta}), \qquad n = 0, 1, 2, ... \tag{1.25}$$

and

$$\overbrace{\nabla_\xi \dots \nabla_\xi}^{n \text{ times}} \boldsymbol{S}(\boldsymbol{x}, \boldsymbol{\xi})$$

are multi-poles, or higher order singularities, in the unbounded domain, obtained by differentiating the Stokeslet at its pole point $\boldsymbol{\xi}$.

From equation (1.24) we can deduce that the flow around a body with no-slip boundary conditions can be always represented as a linear superposition of unbounded multi-pole solutions. This result provides various advantages in the applications, since it permits us to represent in a simple way some flows around bodies with complex shapes, providing a way to estimate their far fields by computing the leading order terms in the series. In addition, when the body admits specific symmetries, such as in the case of spheres, ellipsoids or slender bodies, the expansion (1.24) reduces to a limited set of multi-poles if singularities are centered on a manifold following the symmetry of the body, and therefore, in this case, it is possible to obtain the exact expressions of the solutions in a simple form. As a simple example, the singular form of the Stokes solution of the disturbance field generated by a sphere with radius R_p in a constant ambient flow $\boldsymbol{u}(\boldsymbol{x}) = -\boldsymbol{U}$ (hence, the field generated by a translating sphere with a velocity $\boldsymbol{U}$) is

$$\boldsymbol{w}(\boldsymbol{x}) = \left(\frac{3R_p}{4} \boldsymbol{S}(\boldsymbol{x}, \boldsymbol{\xi}) + \frac{R_p^3}{8} \Delta_\xi \boldsymbol{S}(\boldsymbol{x}, \boldsymbol{\xi}) \right) \cdot \boldsymbol{U} \tag{1.26}$$

$\boldsymbol{\xi}$ being the center of the sphere.

While for a sphere in a rotating fluid $\boldsymbol{u}(\boldsymbol{x}) = -\boldsymbol{\Omega} \times (\boldsymbol{x} - \boldsymbol{\xi})$

$$\boldsymbol{w}(\boldsymbol{x}) = \frac{R_p^3}{2} \nabla_\xi \times \boldsymbol{S}(\boldsymbol{x}, \boldsymbol{\xi}) \cdot \boldsymbol{\Omega} \tag{1.27}$$

Many other useful singularity solutions are available in the literature, such as the disturbance flow for a sphere in a symmetric linear ambient flow [105], or for translating [41] and rotating [40] spheroids, etc.

However, the procedure for finding the exact solution consists mainly of a trial-and-tentative approach, by guessing the types of singularities constituting the singular representation from physical considerations, and finding the associated intensities that match the boundary conditions [194, pp. 201-212]. In Chapter 3, a systematic procedure to obtain the multi-pole expansions by which the disturbance field due to a sphere in a quadratic ambient flow is obtained in closed form.

The other fundamental issue we are interested in dealing with immersed bodies, is the analytic expression for the hydrodynamics forces

$$\boldsymbol{F} = -\int_{\partial D_f} \boldsymbol{\sigma}(\boldsymbol{x}) \cdot \boldsymbol{n}(\boldsymbol{x}) \, dS \tag{1.28}$$

torques

$$\boldsymbol{T}(\boldsymbol{\xi}) = -\int_{\partial D_f} (\boldsymbol{x} - \boldsymbol{\xi}) \times \boldsymbol{\sigma}(\boldsymbol{x}) \cdot \boldsymbol{n}(\boldsymbol{x}) \, dS \tag{1.29}$$

and other moments that the fluid exerts on bodies. A very powerful theorem provided by Faxén states that the forces and torques acting on a sphere with no-slip boundary conditions and radius R_p due to a generic ambient flow $\boldsymbol{u}(\boldsymbol{x})$ past the sphere are

$$\boldsymbol{F} = 8\pi\mu \left(\frac{3R_p}{4} \boldsymbol{u}(\boldsymbol{\xi}) + \frac{R_p^3}{8} \Delta_\xi \boldsymbol{u}(\boldsymbol{\xi}) \right) \tag{1.30}$$

$\boldsymbol{\xi}$ being the center of the sphere, while for torque on a sphere in a rotating fluid $\boldsymbol{u}(\boldsymbol{x}) = -\boldsymbol{\Omega} \times (\boldsymbol{x} - \boldsymbol{\xi})$, and

$$\boldsymbol{T}(\boldsymbol{\xi}) = 8\pi\mu \frac{R_p^3}{2} \nabla_\xi \times \boldsymbol{u}(\boldsymbol{\xi}) \tag{1.31}$$

For the original proof provided by Faxén see [185, p. 111-113], while for a simplified proof see [148, p. 571]. As hypothesized firstly by Hinch [105] and then proved by Kim [128], the extraordinary similarity between eqs. (1.26) and (1.27) with eqs. (1.30) and (1.31) is not a coincidence, but a consequence of the Lorentz reciprocal theorem of Stokes flows. This dualism can be helpful in several numerical and analytical applications, it is widely employed in Stokesian dynamics [61, 228] and in rheology of suspensions [7, 105]. As we will see in the next chapters, it is valid also for higher order moments. However, as addressed in Chapter 3, its extension to bodies with boundary conditions different from the no-slip ones is not straightforward and the reciprocity of the Stokes flows does not ensure its validity when other boundary conditions are assumed at the interface.

Chapter 2

Bitensorial formulation of the singularity method for Stokes flows

2.1 Introduction

As seen in the Chapter 1, one advantageous strategy to investigate the hydrodynamics of bodies immersed in Stokes flows, is to represent the flow by a set of singular solutions with poles internal to the body, which match the prescribed boundary conditions if placed on opportune manifolds with appropriate intensities. In fact, since the pioneering works of Lorentz [156], Oseen [185] and Burger [181], the use of fundamental solutions has become a common and widely applied approach (referred to as the method of hydrodynamic singularities) for solving incompressible Stokes flows [130, 194, 148]. Important theoretical results in low-Reynolds number hydrodynamics have been obtained in this way, for instance, in quantifying the resistance of an arbitrarily shaped particle in a confined fluid [46], in constructing exact solutions for simple flows [40, 41], in expressing the Generalized Faxén theorem [128] for generic immersed bodies. Furthermore, hydrodynamic singularities represent also one of the principal tools in numerical methods, such as Stokesian dynamics [22], Method of Fundamental Solutions [135] or Multipole Methods [216].

Depending on the presence of a solid boundary at a finite distance from the pole of the singularity, a distinction can be made between unbounded and bounded singularities [194]. In dealing with bounded singularities we consider, throughout this thesis, exclusively no-slip conditions at the boundaries.

In the unbounded case, all the hydrodynamic singularities can be constructed starting from the Stokeslet, by applying to it a differential operator at the pole or at the source point as in eq. (1.24). The relative simplicity in constructing hydrodynamic fields as a linear superposition of a collection of unbounded singularities has made the use of singular solutions extremely popular in the analytical description of velocity fields originated by the motion of solid bodies with different geometries in a Stokes fluid, thus simplifying considerably their representation with respect to those obtained by means of other approaches involving polar coordinates or multipole expansions [130]. Some well-known examples of solutions of hydrodynamic problems expressed in the singular representation refer to the motion of solid spheres [33], ellipsoids [40, 41, 128, 129], tori [119] or slender bodies [97, 2, 3, 6] in unbounded Stokes fluids. Moreover, the singular representation of the solutions of the Stokes flow has been used for characterizing the locomotion of microorganisms [97, 18], and the rheological behavior of suspensions and complex fluids [7, 105].

In the overwhelming majority of these works, the singularity functions are represented in a Cartesian reference system, since either the flow domain is unbounded, or, in the bounded case, the singularities lie on a flat manifold (mainly points and lines). In point of fact, a general theory of the Stokes singularities should take into account any possible system configuration, that can, in principle, be constituted by curved boundaries (such as cylindrical channels, spheroidal capsules, wavy surfaces etc.), and immersed curved objects (helical flagella, biconcave disk-shaped cells etc.), for which it is convenient to associate singularities lying on curved manifolds due to their symmetries. Therefore, it may happen that the appropriate coordinate system for specific hydrodynamic problems is curvilinear. As well known, Navier-Stokes fields are invariant under coordinate transformations and, it is easy to show, that hydrodynamic singularities are invariant also at the pole.

Tensor calculus [210] is the natural geometric framework for addressing invariance with respect to coordinate systems. In dealing with the singularity approach to Stokes flows, the singular fields depend at least on two points (and in principle, are multi-point functions), the source (at the pole of the singularity) and the field point (at the fluid element position). Consequently, a generalization of tensor calculus is required, represented by the bitensorial formalism [211, 230, 56], specifically developed for handling the Green functions in field theoretical developments within the theory of general relativity. The bitensor calculus, developed originally by Ruse [211], and further extended by Synge [230] and De Witt [56] for describing multi-point dependent fields in general relativity, is an extension of the tensor calculus that allows us to distinguish between the components of two-point dependent tensors (such as the Stokes singularities) and to make operations between them by means of the so called parallel propagator. A thorough analysis of bitensor calculus can be found in [190], while Appendix 2.A succinctly reviews the main concepts used in the remainder of this chapter.

One goal of the present chapter is to develop a bitensorial formalism that ensures and preserves in a simple way invariant relations for the hydrodynamic singularity functions both at the source and the field points. In a broader perspective, the aim of this work is not only to transfer the bitensor formalism to the analysis of the hydrodynamic Green functions, which is a useful task in itself, as it makes the Stokesian formalism clear and unambiguous, but also to derive out of this formalism new hydrodynamic properties and operators. A significant example involves the generalization of the Faxén operator associated with an immersed body developed in Chapter 3 and the convenient description of the hydrodynamics of particles in confined fluids developed in Chapter 4.

The chapter is organized as follows. Section 2.2 introduces the tensor algebra within the framework of the Stokes equations. In Section 2.3, it is shown how bitensor calculus eliminates the formal ambiguities (related to the meaning of the tensorial indices, and to the action of linear operators on tensorial singularities) occurring in the current formulation of Stokesian hydrodynamics [130, 194] and it allows us to obtain a clear definition of singular solutions of Stokes flow (bounded and unbounded), specifying the associated homogeneous equations and boundary conditions.

Since the Stokes singularities can be viewed as generalized functions (or distributions), the generalized function theory [79] and its connections with the theory of moments [124] are applied to bitensorial quantities of hydrodynamic interest in Section 2.4. Specifically, it is shown that the linear operator providing the singularity system of a bounded flow is uniquely specified by the system of moments associated with the forces acting on the obstacle. Although the present definition of moments is altogether different from that proposed in [115], where, assuming no-slip boundary conditions, the moments are defined by surface integrals of the stress tensor, the two approaches yield the same final result as regard the expression of the disturbance field, showing that the no-slip boundary condition assumption is unnecessary. This represents the only intersection point between the present theory and the one developed by Ichiki [115] in the particular case of no-slip spheres in a Stokes flow.

In Section 2.5, the operator yielding the disturbance field associated with a Stokeslet is considered showing that it is directly related to the reflection operator [220, 126] of the geometry considered. This result is applied in Section 2.6 to the singularities near a plane wall. The characterization of the singularities bounded by a no-slip planar wall has been analyzed in the literature either as a reflection problem [156, 102, 149] or using a system of image singularities [18, 19]. These two approaches are reviewed in [130]. In Section 2.6, it is shown that the present formalism highlights the equivalence between these two approaches. In fact, the same differential operator furnishes directly either the Lorentz's mirror form of the solution, if applied at the field point, or the Blakes' singularity solution form, if applied at the source point of the Stokeslet. Moreover, since the position of the pole enters as a variable in the reflection operator, this formalism overcomes the original shortcomings in obtaining the higher order bounded singularities by differentiating the Green's function at the pole, due to the fact that, in Blake's solutions, the distance of the pole from the plane enters as a parameter. In this way, we obtain unknown (Source Dipole and Stresslet) and known (Rotlet and Sourcelet) bounded singularities, the latter ones already derived in [19] by means of a more elaborate Fourier-Hankel transform.

2.2 Covariant formulation of Stokes equations

If a Newtonian fluid, possessing viscosity μ, is subjected to a volume force field $\boldsymbol{\psi}(\boldsymbol{x})$, the controvariant components of the stress field $\boldsymbol{\sigma}(\boldsymbol{x})$, the velocity $\boldsymbol{v}(\boldsymbol{x})$ and the scalar pressure field $p(\boldsymbol{x})$ are solution, for vanishing Reynolds number, and under steady conditions, of the Stokes equations [72]

$$\begin{cases} -\nabla_b \sigma^{ab}(\boldsymbol{x}) = \mu \Delta_x v^a(\boldsymbol{x}) - \nabla^a p(\boldsymbol{x}) = -\psi^a(\boldsymbol{x}) \\ \nabla_a v^a(\boldsymbol{x}) = 0 \qquad \boldsymbol{x} \in D_f \end{cases} \tag{2.1}$$

$a = 1, 2, 3$ where D_f is the fluid domain. Throughout this chapter, the Einstein summation convention is adopted. The operators ∇_a and ∇^a in eq. (2.1) represent the covariant and controvariant derivatives, respectively, related by the transformation

$\nabla_a = g_{ab}\nabla^b$, where $g_{ab} = g_{ab}(\boldsymbol{x})$ is the metric tensor [231] and $\Delta_x = g^{ab}\nabla_a\nabla_b$ is the Laplacian operator at the point $\boldsymbol{x}$. For a rank-2 tensor $T^a_{\ b}$ in mixed representation, its covariant derivative reads

$$\nabla_c T^a_{\ b} = T^a_{\ b;c} = \frac{\partial T^a_{\ b}}{\partial x^c} + \Gamma^a_{mc} T^m_{\ b} - \Gamma^n_{bc} T^a_{\ n} \tag{2.2}$$

where $T^a_{\ b;c}$ is an alternative and more compact notation for the covariant derivative of $T^a_{\ b}$, and Γ^a_{mc} are the Christoffel symbols

$$\Gamma^a_{mc} = \frac{1}{2}\, g^{al} \left(\frac{\partial g_{lm}}{\partial x^c} + \frac{\partial g_{lc}}{\partial x^m} - \frac{\partial g_{mc}}{\partial x^l} \right) \tag{2.3}$$

Henceforth, we will use both the notations $\nabla_c T^a_{\ b}$ and $T^a_{\ b;c}$ for the covariant derivatives.

The component of the associated stress tensor for a Newtonian incompressible fluid are therefore expressed by [72]

$$\sigma^{ab} = pg^{ab} - \mu(\nabla^b v^a + \nabla^a v^b) = pg^{ab} - \mu(v^{a;b} + v^{b;a}) \tag{2.4}$$

As well known, the controvariant components of the generic tensorial field $\boldsymbol{\psi}(\boldsymbol{x}) = (\psi^a(\boldsymbol{x}))$ change from the coordinate system $\{x^a\}$ to a new system $\{\tilde{x}^a\}$ via a linear transformation defined by the matrix $\left(\frac{\partial \tilde{x}^b}{\partial x^a}\right)$

$$\tilde{\psi}^b(\boldsymbol{x}) = \psi^a(\boldsymbol{x})\, \frac{\partial \tilde{x}^b}{\partial x^a} \tag{2.5}$$

whereas the inverse matrix at the point $\boldsymbol{x}$ yields the transformation of the covariant components

$$\tilde{\psi}_b(\boldsymbol{x}) = \psi_a(\boldsymbol{x})\, \frac{\partial \tilde{x}^a}{\partial x^b} \tag{2.6}$$

2.3 Bitensorial fundamental solutions of the Stokes flow

In this Section we extend the tensorial notation to the case of the fundamental solutions of the Stokes flow, with the aim of obtaining a clear definition of its singular solutions. From the theory of distributions, we can write the fields entering eq. (2.1) equipped with homogeneous Dirichlet boundary condition at ∂D_f as volume potentials [137], with a kernel $\mathrm{G}^a_{\ \alpha}(\boldsymbol{x},\boldsymbol{\xi})$ for the velocity field

$$v^a(\boldsymbol{x}) = \int \mathrm{G}^a_{\ \alpha}(\boldsymbol{x},\boldsymbol{\xi})\, \frac{\psi^\alpha(\boldsymbol{\xi})}{8\pi\mu} \sqrt{g(\boldsymbol{\xi})}\, d^3\xi \tag{2.7}$$

and a kernel $\mathrm{P}_\alpha(\boldsymbol{x},\boldsymbol{\xi})$ for the pressure field

$$p(\boldsymbol{x}) = \int \mathrm{P}_\alpha(\boldsymbol{x},\boldsymbol{\xi})\, \frac{\psi^\alpha(\boldsymbol{\xi})}{8\pi} \sqrt{g(\boldsymbol{\xi})}\, d^3\xi \tag{2.8}$$

where $\psi^\alpha(\boldsymbol{\xi})$ are the controvariant components of the force field at a source point $\boldsymbol{\xi}$, $g(\boldsymbol{\xi}) = \det(g^{ab}(\boldsymbol{\xi}))$ and $d^3\xi = d\xi^1 d\xi^2 d\xi^3$. Observe that the coordinate representation of the source point $\boldsymbol{\xi}$ could in principle be different from that of the field point $\boldsymbol{x}$. This fact is notationally highlighted throughout the chapter, by using greek letters instead of latin ones for any index $\alpha = 1, 2, 3$ referred to the entries of tensorial entities evaluated at the source point. Therefore, the transformations for the controvariant and covariant components of $\boldsymbol{\psi}(\boldsymbol{\xi})$ at the source point read

$$\psi^{\beta'}(\boldsymbol{\xi}') = \psi^{\alpha}(\boldsymbol{\xi})\,\frac{\partial \xi^{\beta'}}{\partial \xi^{\alpha}}\,, \qquad f_{\beta'}(\boldsymbol{\xi}) = \psi_{\alpha}(\boldsymbol{\xi})\,\frac{\partial \xi^{\alpha}}{\partial \xi^{\beta'}} \tag{2.9}$$

where $\xi^{\beta'}$ are the components of $\boldsymbol{\xi}'$. This notation, with primed indices to indicate the transformed coordinated, will be used throughout the chapter.

The kernels $\mathrm{G}^{a}{}_{\alpha}(\boldsymbol{x},\boldsymbol{\xi})$ and $\mathrm{P}_{\alpha}(\boldsymbol{x},\boldsymbol{\xi})$ are two-point dependent distributions, with tensorial character both at $\boldsymbol{x}$ and $\boldsymbol{\xi}$, thus corresponding to bitensorial quantities [211, 56, 230, 190]. This is a common feature of any fundamental solutions (or Green functions) in mathematical physics. Further details on the theory of bitensors are succintly reviewed in Appendix 2.A. Specifically, the kernel entries $\mathrm{G}^{a}{}_{\alpha}(\boldsymbol{x},\boldsymbol{\xi})$ are the components of a bitensor with vectorial character both at the source and the field point, and consequently their transformation in new coordinate systems both at the source and the field points takes the form

$$\mathrm{G}^{b'}{}_{\beta'}(\boldsymbol{x}',\boldsymbol{\xi}') = \mathrm{G}^{a}{}_{\alpha}(\boldsymbol{x},\boldsymbol{\xi})\,\frac{\partial x^{b'}}{\partial x^{a}}\frac{\partial \xi^{\alpha}}{\partial \xi^{\beta'}} \tag{2.10}$$

whereas the transformation rule for the pressure bitensor, with scalar character at the field point $\boldsymbol{x}$ and vectorial at the source point $\boldsymbol{\xi}$, is given by

$$\mathrm{P}_{\beta'}(\boldsymbol{x},\boldsymbol{\xi}') = \mathrm{P}_{\alpha}(\boldsymbol{x},\boldsymbol{\xi})\,\frac{\partial \xi^{\alpha}}{\partial \xi^{\beta'}} \tag{2.11}$$

Finally, using the invariance properties of the Dirac delta function [190] and the parallel transport of tensorial quantities, it is possible to express the force field entering eq. (2.1) as

$$\psi^{a}(\boldsymbol{x}) = \int g^{a}{}_{\alpha}(\boldsymbol{x},\boldsymbol{\xi})\psi^{\alpha}(\boldsymbol{\xi})\delta(\boldsymbol{x},\boldsymbol{\xi})\sqrt{g(\boldsymbol{\xi})}d^{3}\xi; \qquad \delta(\boldsymbol{x},\boldsymbol{\xi}) = \frac{\delta(\boldsymbol{x}-\boldsymbol{\xi})}{\sqrt{g(\boldsymbol{\xi})}} \tag{2.12}$$

where $g^{a}{}_{\alpha}(\boldsymbol{x},\boldsymbol{\xi})$ is the parallel propagator bitensor, which propagates in a parallel way a vector along the unique geodesics connecting $\boldsymbol{x}$ to $\boldsymbol{\xi}$. In a distributional meaning, it follows that $g^{a}_{\alpha}(\boldsymbol{x},\boldsymbol{\xi})\delta(\boldsymbol{x},\boldsymbol{\xi}) = \delta^{a}{}_{\alpha}\delta(\boldsymbol{x},\boldsymbol{\xi})$ being $\boldsymbol{x}$ and $\boldsymbol{\xi}$ coincident.

By substituting eqs. (2.7), (2.8) and (2.12) in eq. (2.1), we obtain the bitensorial Green function equations of the Stokes flow, yielding the velocity and pressure at the field point $\boldsymbol{x}$ due to an impulsive force acting at the source point $\boldsymbol{\xi}$

$$\begin{cases} -\nabla_{b}\Sigma^{ab}_{\alpha}(\boldsymbol{x},\boldsymbol{\xi}) = \Delta_{x}\mathrm{G}^{a}{}_{\alpha}(\boldsymbol{x},\boldsymbol{\xi}) - \nabla^{a}\mathrm{P}_{\alpha}(\boldsymbol{x},\boldsymbol{\xi}) = -8\pi\delta^{a}_{\alpha}\delta(\boldsymbol{x},\boldsymbol{\xi}) \\ \nabla_{a}\mathrm{G}^{a}{}_{\alpha}(\boldsymbol{x},\boldsymbol{\xi}) = 0 \\ \mathrm{G}^{a}{}_{\alpha}(\boldsymbol{x},\boldsymbol{\xi})|_{\boldsymbol{x}\in\partial D_f} = 0 \end{cases} \tag{2.13}$$

From eq. (2.4), the stress field $\Sigma^{ab}_{\alpha}(\boldsymbol{x},\boldsymbol{\xi})$ associated with the Green function is defined by

$$\Sigma^{ab}_{\alpha}(\boldsymbol{x},\boldsymbol{\xi}) = \mathrm{P}_{\alpha}(\boldsymbol{x},\boldsymbol{\xi})g^{ab}(\boldsymbol{x}) - (\mathrm{G}^{a;b}_{\alpha}(\boldsymbol{x},\boldsymbol{\xi}) + \mathrm{G}^{b;a}_{\alpha}(\boldsymbol{x},\boldsymbol{\xi})) \tag{2.14}$$

In the case the source point is kept fixed, bitensors become simple tensors depending only on the field point. Therefore, by choosing the force field $\boldsymbol{\psi}(\boldsymbol{\xi}) = \boldsymbol{\psi}_0\delta(\boldsymbol{\xi}-\boldsymbol{\xi}_0)$, from eqs. (2.7) and (2.8), we obtain the velocity/pressure fields due to an impulsive force with intensity $\boldsymbol{\psi}_0$ placed at a singular point $\boldsymbol{\xi}_0$

$$v^a(\boldsymbol{x}) = \frac{\psi_0^\alpha}{8\pi\mu}\mathrm{G}^a{}_\alpha(\boldsymbol{x},\boldsymbol{\xi}_0) \tag{2.15}$$

$$p(\boldsymbol{x}) = \frac{\psi_0^\alpha}{8\pi}\mathrm{P}_\alpha(\boldsymbol{x},\boldsymbol{\xi}_0) \tag{2.16}$$

for which the stress tensor $\sigma^{ab}(\boldsymbol{x})$ takes the form

$$\sigma^{ab}(\boldsymbol{x}) = \frac{\psi_0^\alpha}{8\pi}\Sigma^{ab}_\alpha(\boldsymbol{x},\boldsymbol{\xi}_0) \tag{2.17}$$

The reciprocity relation [130, 194] for the Green function in bitensorial notation becomes

$$\mathrm{G}^a{}_\alpha(\boldsymbol{x},\boldsymbol{\xi}) = \mathrm{G}_\alpha{}^a(\boldsymbol{\xi},\boldsymbol{x}) \tag{2.18}$$

By exchanging $\boldsymbol{x} \leftrightarrow \boldsymbol{\xi}$, and thus $a \leftrightarrow \alpha$, and enforcing the reciprocity relation (2.18), it follows that $\mathrm{G}^a{}_\alpha(\boldsymbol{x},\boldsymbol{\xi})$ is also the solution of the system

$$\begin{cases} -\nabla^\beta\Sigma^a_{\alpha\beta}(\boldsymbol{\xi},\boldsymbol{x}) = \Delta_\xi\mathrm{G}^a{}_\alpha(\boldsymbol{x},\boldsymbol{\xi}) - \nabla_\alpha\mathrm{P}^a(\boldsymbol{\xi},\boldsymbol{x}) = -8\pi\delta^a_\alpha\delta(\boldsymbol{x},\boldsymbol{\xi}) \\ \nabla^\alpha\mathrm{G}^a{}_\alpha(\boldsymbol{x},\boldsymbol{\xi}) = 0 \\ \mathrm{G}^a{}_\alpha(\boldsymbol{x},\boldsymbol{\xi})|_{\boldsymbol{\xi}\in\partial D_f} = 0 \end{cases} \tag{2.19}$$

where $\Delta_\xi = g^{\alpha\beta}(\boldsymbol{\xi})\nabla_\alpha\nabla_\beta$ is the Laplacian at point $\boldsymbol{\xi}$. In this case, the associated stress field becomes

$$\Sigma^a_{\alpha\beta}(\boldsymbol{\xi},\boldsymbol{x}) = \mathrm{P}^a(\boldsymbol{\xi},\boldsymbol{x})g_{\alpha\beta}(\boldsymbol{\xi}) - (\mathrm{G}^a{}_{\alpha;\beta}(\boldsymbol{x},\boldsymbol{\xi}) + \mathrm{G}^a{}_{\beta;\alpha}(\boldsymbol{x},\boldsymbol{\xi})) \tag{2.20}$$

Since the Green function vanishes at $\boldsymbol{\xi} \in \partial D_f$ for any $\boldsymbol{x}$, $\mathrm{P}_\alpha(\boldsymbol{x},\boldsymbol{\xi})$ must be constant for $\boldsymbol{\xi} \in \partial D_f$ due to eq. (2.13), and therefore can be set equal to zero. Furthermore, the pressure scalar-vector $\mathrm{P}_\alpha(\boldsymbol{x},\boldsymbol{\xi})$ is a potential scalar field at $\boldsymbol{x}$ possessing the following properties

$$\begin{aligned} &\Delta_x\mathrm{P}_\alpha(\boldsymbol{x},\boldsymbol{\xi}) = 8\pi\nabla_\alpha\delta(\boldsymbol{x},\boldsymbol{\xi}) \\ &\nabla^\alpha\mathrm{P}_\alpha(\boldsymbol{x},\boldsymbol{\xi}) = 8\pi\delta(\boldsymbol{x},\boldsymbol{\xi}) \\ &\mathrm{P}_\alpha(\boldsymbol{x},\boldsymbol{\xi})|_{\boldsymbol{\xi}\in\partial D_f} = 0 \end{aligned} \tag{2.21}$$

The first relation stems from eq. (2.13), by taking the divergence with respect to $\boldsymbol{x}$, while the second relation follows by taking the divergence with respect to $\boldsymbol{\xi}$, enforcing the second relation in eq. (2.19). In a similar way, $\mathrm{P}^a(\boldsymbol{\xi},\boldsymbol{x})$ fulfills the relations

$$\begin{aligned} &\Delta_\xi\mathrm{P}^a(\boldsymbol{\xi},\boldsymbol{x}) = 8\pi\nabla^a\delta(\boldsymbol{x},\boldsymbol{\xi}) \\ &\nabla_a\mathrm{P}^a(\boldsymbol{\xi},\boldsymbol{x}) = 8\pi\delta(\boldsymbol{x},\boldsymbol{\xi}) \\ &\mathrm{P}^a(\boldsymbol{\xi},\boldsymbol{x})|_{\boldsymbol{x}\in\partial D_f} = 0 \end{aligned} \tag{2.22}$$

Observe that eq. (2.21) for $\mathrm{P}_\alpha(\boldsymbol{x},\boldsymbol{\xi})$, and likewise eq. (2.22) for $\mathrm{P}^a(\boldsymbol{\xi},\boldsymbol{x})$ do not constitute a boundary value problem for the pressure variable, as the boundary condition is assigned for a variable ($\boldsymbol{\xi}$ in eq. (2.21)) different from that involved in the differential equation ($\boldsymbol{x}$ in eq. (2.21)), thus representing a collection of properties fulfilled by the pressure field.

To obtain the higher order singularities, the Green function should be differentiated at the pole $\boldsymbol{\xi}$ maintaining homogeneous Dirichlet conditions at the field point. The first derivative at the pole yields the Stokesian dipole, the second derivative the Stokesian quadrupole and so on.

The Stokesian dipole ${\rm G}^a{}_{\alpha;\beta}(\boldsymbol{x},\boldsymbol{\xi})$ can also be expressed as superposition of two other singular solutions of the Stokes equations: a symmetric and an antisymmetric tensor field at the source points

$$ {\rm G}^a{}_{\alpha;\beta}(\boldsymbol{x},\boldsymbol{\xi}) = {\rm E}^a{}_{\alpha\beta}(\boldsymbol{x},\boldsymbol{\xi}) + \varepsilon_{\gamma\alpha\beta}\Omega^{a\gamma}(\boldsymbol{x},\boldsymbol{\xi}) \tag{2.23} $$

where

$$ {\rm E}^a{}_{\alpha\beta}(\boldsymbol{x},\boldsymbol{\xi}) = \frac{1}{2}({\rm G}^a{}_{\alpha;\beta}(\boldsymbol{x},\boldsymbol{\xi}) + {\rm G}^a{}_{\beta;\alpha}(\boldsymbol{x},\boldsymbol{\xi})) \tag{2.24} $$

is the field due to a singular strain of the fluid at the source point, and

$$ \Omega^{a\gamma}(\boldsymbol{x},\boldsymbol{\xi}) = \frac{\varepsilon^{\gamma\epsilon\eta}}{2}{\rm G}^a{}_{\epsilon;\eta}(\boldsymbol{x},\boldsymbol{\xi}) \tag{2.25} $$

where $\varepsilon_{\alpha\beta\gamma}$ is the Levi-Civita symbol (in the italian mathematical literature also called the Ricci tensor [72]), is the field due to a singular rotation of the fluid at the source point.

The symmetric strain component is the solution of the Stokes system of equations

$$ \begin{cases} \Delta_x {\rm E}^a{}_{\alpha\beta}(\boldsymbol{x},\boldsymbol{\xi}) - \frac{1}{2}\,\nabla^a\left({\rm P}_{\alpha;\beta}(\boldsymbol{x},\boldsymbol{\xi}) + {\rm P}_{\beta;\alpha}(\boldsymbol{x},\boldsymbol{\xi})\right) = -4\pi(\delta^a_\alpha\nabla_\beta + \delta^a_\beta\nabla_\alpha)\delta(\boldsymbol{x},\boldsymbol{\xi}) \\ \nabla_a {\rm E}^a{}_{\alpha\beta}(\boldsymbol{x},\boldsymbol{\xi}) = 0 \\ {\rm E}^a{}_{\alpha\beta}(\boldsymbol{x},\boldsymbol{\xi})|_{\boldsymbol{x}\in\partial D_f} = 0 \end{cases} \tag{2.26} $$

which can be also computed directly from eqs. (2.19),(2.20) by exchanging source and field points in the pressure and stress fields related to the solution of the Green function

$$ {\rm E}^a{}_{\alpha;\beta}(\boldsymbol{x},\boldsymbol{\xi}) = \frac{g_{\alpha\beta}(\boldsymbol{\xi})}{2}{\rm P}^a(\boldsymbol{\xi},\boldsymbol{x}) - \frac{1}{2}\Sigma^a_{\alpha\beta}(\boldsymbol{\xi},\boldsymbol{x}) \tag{2.27} $$

The antisymmetric part of the Stokes dipole corresponds to the solution of the Stokes system

$$ \begin{cases} \Delta_x \Omega^{a\gamma}(\boldsymbol{x},\boldsymbol{\xi}) - \frac{1}{2}\varepsilon^{\gamma\epsilon\eta}\nabla^a{\rm P}_{\epsilon;\eta}(\boldsymbol{x},\boldsymbol{\xi}) = -4\pi\delta^a_\epsilon\varepsilon^{\gamma\epsilon\eta}\nabla_\eta\delta(\boldsymbol{x},\boldsymbol{\xi}) \\ \nabla_a\Omega^{a\gamma}(\boldsymbol{x},\boldsymbol{\xi}) = 0 \\ \Omega^{a\gamma}(\boldsymbol{x},\boldsymbol{\xi})\big|_{\boldsymbol{x}\in\partial D_f} = 0 \end{cases} \tag{2.28} $$

A further differentiation at the pole defines the Stokes quadrupole. Specifically, by applying the Laplacian operator $\Delta_\xi/2$ to the Green function, we obtain the so called Source Dipole

$$ \begin{cases} \Delta_x {\rm D}^a{}_\alpha(\boldsymbol{x},\boldsymbol{\xi}) - \frac{1}{2}\nabla^a\Delta_\xi{\rm P}_\alpha(\boldsymbol{x},\boldsymbol{\xi}) = -4\pi\delta^a_\alpha\Delta_\xi\delta(\boldsymbol{x},\boldsymbol{\xi}) \\ \nabla_a{\rm D}^a{}_\alpha(\boldsymbol{x},\boldsymbol{\xi}) = 0 \\ {\rm D}^a{}_\alpha(\boldsymbol{x},\boldsymbol{\xi})\big|_{\boldsymbol{x}\in\partial D_f} = 0 \end{cases} \tag{2.29} $$

Also the solution of this system can be obtained by exchanging source and field points in the gradient of the pressure field associated with the Green function. In point of fact, from the first relation in eq. (2.19), we have

$$\mathrm{D}^a{}_\alpha(\boldsymbol{x},\boldsymbol{\xi}) = -\frac{\Delta_\xi \mathrm{G}^a{}_\alpha(\boldsymbol{x},\boldsymbol{\xi})}{2} = -\frac{\nabla_\alpha \mathsf{P}^a(\boldsymbol{\xi},\boldsymbol{x})}{2} + 4\pi\delta^a_\alpha\delta(\boldsymbol{x},\boldsymbol{\xi}) \tag{2.30}$$

2.3.1 Unbounded singularities

In this paragraph, unbounded singularities are briefly analyzed. Due to translational invariance, the singularities in $\mathbb{R}^3$, depend solely on the vector $\boldsymbol{x}-\boldsymbol{\xi}$. Henceforth, the unbounded singular functions will be indicated by sans-serif capital letters. The Green function $\mathsf{S}^a{}_\alpha(\boldsymbol{x}-\boldsymbol{\xi})$, usually referred to as the Stokeslet, is the solution of the Stokes problem

$$\begin{cases} -\nabla_b\Sigma^{ab}_\alpha(\boldsymbol{x}-\boldsymbol{\xi}) = \Delta_x\mathsf{S}^a{}_\alpha(\boldsymbol{x}-\boldsymbol{\xi}) - \nabla^a\mathsf{P}_\alpha(\boldsymbol{x}-\boldsymbol{\xi}) = -8\pi\delta^a_\alpha\delta(\boldsymbol{x},\boldsymbol{\xi}) \\ \nabla_a\mathsf{S}^a{}_\alpha(\boldsymbol{x}-\boldsymbol{\xi}) = 0 \\ \mathsf{S}^a{}_\alpha(\boldsymbol{x}-\boldsymbol{\xi})\big|_{|\boldsymbol{x}-\boldsymbol{\xi}|\to\infty} = 0 \end{cases} \tag{2.31}$$

Since the Laplacian is invariant under translation (and, more generally, under Euclidean transformations [217]), we have for a generic function $f(\boldsymbol{x}-\boldsymbol{\xi})$, $\Delta_{x-\xi}f(\boldsymbol{x}-\boldsymbol{\xi}) = \Delta_x f(\boldsymbol{x}-\boldsymbol{\xi}) = \Delta_\xi f(\boldsymbol{x}-\boldsymbol{\xi})$. Therefore, it is possible to express the pressure in eq. (2.21) as the solution of the harmonic problem

$$\begin{cases} \Delta_\xi\mathsf{P}_\alpha(\boldsymbol{x}-\boldsymbol{\xi}) = 8\pi\nabla_\alpha\delta(\boldsymbol{x},\boldsymbol{\xi}) \\ \mathsf{P}_\alpha(\boldsymbol{x}-\boldsymbol{\xi})\big|_{|\boldsymbol{x}-\boldsymbol{\xi}|\to\infty} = 0 \end{cases} \tag{2.32}$$

thus

$$\mathsf{P}_\alpha(\boldsymbol{x}-\boldsymbol{\xi}) = 2\nabla_\alpha\frac{1}{|\boldsymbol{x}-\boldsymbol{\xi}|} = \frac{2(\boldsymbol{x}-\boldsymbol{\xi})_\alpha}{r^3} \tag{2.33}$$

while the associated velocity and stress-tensor fields are given by [194, 84]

$$\mathsf{S}^a{}_\alpha(\boldsymbol{x}-\boldsymbol{\xi}) = (\delta^a_\alpha\Delta_\xi - \nabla_\alpha\nabla^a)|\boldsymbol{x}-\boldsymbol{\xi}| = \frac{\delta^a_\alpha}{|\boldsymbol{x}-\boldsymbol{\xi}|} + \frac{(\boldsymbol{x}-\boldsymbol{\xi})^a(\boldsymbol{x}-\boldsymbol{\xi})_\alpha}{|\boldsymbol{x}-\boldsymbol{\xi}|^3} \tag{2.34}$$

$$\Sigma^{ab}_\alpha(\boldsymbol{x}-\boldsymbol{\xi}) = \frac{6(\boldsymbol{x}-\boldsymbol{\xi})^a(\boldsymbol{x}-\boldsymbol{\xi})^b(\boldsymbol{x}-\boldsymbol{\xi})_\alpha}{r^5} \tag{2.35}$$

As $\mathsf{P}_{\alpha;\beta}(\boldsymbol{x}-\boldsymbol{\xi}) = \mathsf{P}_{\beta;\alpha}(\boldsymbol{x}-\boldsymbol{\xi})$, the symmetric part of the Stokes dipole corresponds to the solution of the problem

$$\begin{cases} \Delta_x\mathsf{E}^a{}_{\alpha\beta}(\boldsymbol{x}-\boldsymbol{\xi}) - \nabla^a\mathsf{P}_{\alpha;\beta}(\boldsymbol{x}-\boldsymbol{\xi}) = -4\pi(\delta^a_\alpha\nabla_\beta + \delta^a_\beta\nabla_\alpha)\delta(\boldsymbol{x},\boldsymbol{\xi}) \\ \nabla_a\mathsf{E}^a{}_{\alpha\beta}(\boldsymbol{x}-\boldsymbol{\xi}) = 0 \\ \mathsf{E}^a{}_{\alpha\beta}(\boldsymbol{x}-\boldsymbol{\xi})\big|_{|\boldsymbol{x}-\boldsymbol{\xi}|\to\infty} = 0 \end{cases} \tag{2.36}$$

and due to eq. (2.27) it takes the expression

$$\mathsf{E}^a{}_{\alpha\beta}(\boldsymbol{x}-\boldsymbol{\xi}) = \frac{g_{\alpha\beta}(\boldsymbol{\xi})}{2}\mathsf{P}^a(\boldsymbol{\xi}-\boldsymbol{x}) - \frac{1}{2}\Sigma^a_{\alpha\beta}(\boldsymbol{\xi}-\boldsymbol{x}) \tag{2.37}$$

This field can be viewed as the superposition of two terms: the contribution $\mathsf{M}^a(\boldsymbol{x}-\boldsymbol{\xi}) = -\mathsf{P}^a(\boldsymbol{\xi}-\boldsymbol{x})/2$, which is the solution of a Stokes problem everywhere but at the pole

$$\begin{cases} \Delta_x \mathsf{M}^a(\boldsymbol{x}-\boldsymbol{\xi}) = -4\pi\nabla^a\delta(\boldsymbol{x},\boldsymbol{\xi}) \\ \nabla_a \mathsf{M}^a(\boldsymbol{x}-\boldsymbol{\xi}) = -4\pi\delta(\boldsymbol{x},\boldsymbol{\xi}) \\ \mathsf{M}^a(\boldsymbol{x}-\boldsymbol{\xi})\big|_{|\boldsymbol{x}-\boldsymbol{\xi}|\to\infty} = 0 \end{cases} \tag{2.38}$$

Strictly speaking, the field $\mathsf{M}^a(\boldsymbol{x}-\boldsymbol{\xi})$, usually called the Sourcelet [19, 194], is not a Stokesian singular solution, since its divergence does not vanish at the pole and, thus, it does not satisfy the overall mass balance over the fluid. It can be physically interpreted as the velocity field stemming from a pointwise fluid source (or sink, if the sign is reversed) at the pole. Its bounded counterpart can be defined solely for external problems, so that it could match the regularity condition and the overall mass balance at infinity. However, it cannot be generally neither obtained from the Green function (as the Green function is divergence-free), nor it is related to the Green function pressure field, as in the unbounded case.

Similarly, also the second term is not a singular Stokesian solution. In fact, the field $\mathsf{T}^a_{\alpha\beta}(\boldsymbol{x}-\boldsymbol{\xi}) = \Sigma^a_{\alpha\beta}(\boldsymbol{\xi}-\boldsymbol{x})/2$, called the Stresslet, is the solution of the problem

$$\begin{cases} \Delta_x \mathsf{T}^a_{\alpha\beta}(\boldsymbol{x}-\boldsymbol{\xi}) - \nabla^a \mathsf{P}_{\alpha;\beta}(\boldsymbol{x}-\boldsymbol{\xi}) = -4\pi(g_{\alpha\beta}(\boldsymbol{\xi})\nabla^a + \delta^a_\alpha\nabla_\beta + \delta^a_\beta\nabla_\alpha)\delta(\boldsymbol{x},\boldsymbol{\xi}) \\ \nabla_a \mathsf{T}^a_{\alpha\beta}(\boldsymbol{x}-\boldsymbol{\xi}) = -4\pi g_{\alpha\beta}(\boldsymbol{\xi})\delta(\boldsymbol{x},\boldsymbol{\xi}) \\ \mathsf{T}^a_{\alpha\beta}(\boldsymbol{x}-\boldsymbol{\xi})\big|_{|\boldsymbol{x}-\boldsymbol{\xi}|\to\infty} = 0 \end{cases} \tag{2.39}$$

possessing non vanishing divergence. Therefore, the symmetric Strainlet eq. (2.37) can be expressed as

$$\mathsf{E}^a{}_{\alpha\beta}(\boldsymbol{x}-\boldsymbol{\xi}) = -g_{\alpha\beta}(\boldsymbol{\xi})\mathsf{M}^a(\boldsymbol{x}-\boldsymbol{\xi}) + \mathsf{T}^a_{\alpha\beta}(\boldsymbol{x}-\boldsymbol{\xi}) \tag{2.40}$$

Next consider the antisymmetric term defined by eq. (2.25). In unbounded flows $\Omega^{a\gamma}(\boldsymbol{x}-\boldsymbol{\xi})$ is referred to as the Rotlet. Since $\varepsilon^{\gamma\epsilon\eta}\mathsf{P}_{\epsilon;\eta}(\boldsymbol{x}-\boldsymbol{\xi}) = 0$, the Rotlet is a constant pressure solution of the Stokes system

$$\begin{cases} \Delta_x \Omega^{a\gamma}(\boldsymbol{x}-\boldsymbol{\xi}) = -4\pi\delta^a_\epsilon\varepsilon^{\gamma\epsilon\eta}\nabla_\eta\delta(\boldsymbol{x},\boldsymbol{\xi}) \\ \nabla_a \Omega^{a\gamma}(\boldsymbol{x}-\boldsymbol{\xi}) = 0 \\ \Omega^{a\gamma}(\boldsymbol{x}-\boldsymbol{\xi})\big|_{|\boldsymbol{x}-\boldsymbol{\xi}|\to\infty} = 0 \end{cases} \tag{2.41}$$

the analytic expression of which is

$$\Omega^{a\gamma}(\boldsymbol{x}-\boldsymbol{\xi}) = -\delta^a_\epsilon\varepsilon^{\gamma\epsilon\eta}\nabla_\eta\frac{1}{|\boldsymbol{x}-\boldsymbol{\xi}|} \tag{2.42}$$

Another low order irrotational singularity of the Stokes problem is the solution of eq. (2.29) in unbounded domain, namely

$$\begin{cases} \Delta_x \mathsf{D}^a{}_\alpha(\boldsymbol{x}-\boldsymbol{\xi}) = -4\pi(\delta^a_\alpha\Delta_\xi - \nabla^a\nabla_\alpha)\delta(\boldsymbol{x},\boldsymbol{\xi}) \\ \nabla_a \mathsf{D}^a{}_\alpha(\boldsymbol{x}-\boldsymbol{\xi}) = 0 \\ \mathsf{D}^a{}_\alpha(\boldsymbol{x}-\boldsymbol{\xi})\big|_{|\boldsymbol{x}-\boldsymbol{\xi}|\to\infty} = 0 \end{cases} \tag{2.43}$$

This solution, referred to as the Source Doublet, can be obtained from eq. (2.31) and from the definition of $\mathsf{M}^a(\boldsymbol{x}-\boldsymbol{\xi})$

$$\mathsf{D}^a{}_\alpha(\boldsymbol{x}-\boldsymbol{\xi}) = -\frac{\Delta_\xi \mathsf{S}^a{}_\alpha(\boldsymbol{x}-\boldsymbol{\xi})}{2} = \nabla_\alpha \mathsf{M}^a(\boldsymbol{x}-\boldsymbol{\xi}) + 4\pi\delta^a_\alpha \delta(\boldsymbol{x},\boldsymbol{\xi}) \tag{2.44}$$

2.4 Singular representation of bounded flows

In the previous Section we have discussed how all the singularities of bounded flows can be obtained by differentiating the Stokeslet at its pole. In this Section, we develop a method to obtain the singular representation of a Stokes flow in a given domain D_f containing solid boundaries by means of a linear operator applied to the Stokeslet in the external domain $D_{ext} \equiv \mathbb{R}^3/D_f$, and yielding the disturbance field in D_f. More precisely, consider a given solution $\boldsymbol{u}(\boldsymbol{x})$ of the Stokes equation in D_f, attaining arbitrary values at the boundaries ∂D_f (at which, the Stokes problem dictates no-slip boundary conditions). The velocity field $\boldsymbol{u}(\boldsymbol{x})$ is referred to as the *ambient flow*. In order to match the no-slip boundary condition, a *disturbance flow* $\boldsymbol{w}(\boldsymbol{x})$ should be added so that $\boldsymbol{v}(\boldsymbol{x}) = \boldsymbol{w}(\boldsymbol{x}) + \boldsymbol{u}(\boldsymbol{x})$ is the Stokes solution within D_f satisfying the no-slip conditions on ∂D_f. Thus, the disturbance flow is a solution of the equations

$$\begin{cases} \mu\,\Delta_x w^a(\boldsymbol{x}) - \nabla^a q(\boldsymbol{x}) = 0 & \boldsymbol{x} \in D_f \\ \nabla_a w^a(\boldsymbol{x}) = 0 & \\ w^a(\boldsymbol{x}) = -u^a(\boldsymbol{x}) & \boldsymbol{x} \in \partial D_f \end{cases} \tag{2.45}$$

where $q(\boldsymbol{x})$ is the associated pressure field. It is convenient to extend this problem over the whole physical space $\mathbb{R}^3$ in order to obtain its singular representation. To this purpose, we can formulate the problem defined by eqs. (2.45) in the form of the non-homogeneous unbounded Stokes equations in $\mathbb{R}^3$ as

$$\begin{cases} \mu\,\Delta_x w^a(\boldsymbol{x}) - \nabla^a q(\boldsymbol{x}) = -\psi^a(\boldsymbol{x}) & \boldsymbol{x} \in \mathbb{R}^3 \\ \nabla_a w^a(\boldsymbol{x}) = 0 & \end{cases} \tag{2.46}$$

with the condition that $\psi^a(\boldsymbol{x})$ are distributions defined on a compact support in D_{ext}, and satisfying the integral equation

$$\int_{D_{ext}} \mathsf{S}^a{}_\alpha(\boldsymbol{x},\boldsymbol{\xi}) \frac{\psi^\alpha(\boldsymbol{\xi})}{8\pi\mu} \sqrt{g(\boldsymbol{\xi})} d^3\xi = -u^a(\boldsymbol{x}) \qquad \boldsymbol{x} \in \partial D_f \tag{2.47}$$

Let us introduce the n-th order tensorial moments of the function $\boldsymbol{\psi}(\boldsymbol{x})$, extending the scalar moment theory [124], as

$$M^\alpha_{\boldsymbol{\alpha}_n}(\boldsymbol{\xi}) = \int_{D_{ext}} g^\alpha{}_a(\boldsymbol{\xi},\boldsymbol{x}) g_{\alpha_1}^{a_1}(\boldsymbol{\xi},\boldsymbol{x}) ... g_{\alpha_n}^{a_n}(\boldsymbol{\xi},\boldsymbol{x}) \psi^a(\boldsymbol{x}) (\boldsymbol{x}-\boldsymbol{\xi})_{a_1} ... (\boldsymbol{x}-\boldsymbol{\xi})_{\boldsymbol{a}_n} \sqrt{g(\boldsymbol{x})} d^3x\,, \qquad \boldsymbol{\xi} \in D_{ext} \tag{2.48}$$

or, using the scalar-product notation on the external domain

$$M^\alpha_{\boldsymbol{\alpha}_n}(\boldsymbol{\xi}) = \langle g^\alpha{}_a(\boldsymbol{\xi},\boldsymbol{x})\psi^a(\boldsymbol{x}), g_{\boldsymbol{\alpha}_n}^{\boldsymbol{a}_n}(\boldsymbol{\xi},\boldsymbol{x})(\boldsymbol{x}-\boldsymbol{\xi})_{\boldsymbol{a}_n} \rangle \tag{2.49}$$

where $\langle \cdot, \cdot \rangle$ indicates the scalar product in $D_{ext} \equiv \mathbb{R}^3/D_f$, $\boldsymbol{a}_n = (a_1, \dots, a_n)$ is a multi-index, $g_{\boldsymbol{\alpha}_n}^{\boldsymbol{a}_n}(\boldsymbol{\xi},\boldsymbol{x}) = g_{\alpha_1}^{a_1}(\boldsymbol{\xi},\boldsymbol{x}) ... g_{\alpha_n}^{a_n}(\boldsymbol{\xi},\boldsymbol{x})$ and $(\boldsymbol{x}-\boldsymbol{\xi})_{\boldsymbol{a}_n} = (\boldsymbol{x}-\boldsymbol{\xi})_{a_1} ... (\boldsymbol{x}-\boldsymbol{\xi})_{a_n}$.

It is shown in Chapter 3 that the moments $M^{a}{}_{\boldsymbol{a}_n}(\boldsymbol{\xi})$ can be reduced to the surface integrals. In the case no-slip boundary conditions are assumed, becomes

$$M^{\alpha}{}_{\boldsymbol{\alpha}_n}(\boldsymbol{\xi}) = \int_{\partial D_f} g^{\alpha}{}_{a}(\boldsymbol{\xi},\boldsymbol{x}) g_{\boldsymbol{\alpha}_n}^{\boldsymbol{a}_n}(\boldsymbol{\xi},\boldsymbol{x})(\boldsymbol{x}-\boldsymbol{\xi})_{\boldsymbol{a}_n} \sigma^{ab}(\boldsymbol{x})\, n_b(\boldsymbol{x})\, dS(\boldsymbol{x}) \qquad (2.50)$$

where $\boldsymbol{\sigma}(\boldsymbol{x})$ is the stress tensor related to the total velocity field $\boldsymbol{v}(\boldsymbol{x})$, and $n_b(\boldsymbol{x})$ the covariant components of the inwardly oriented normal unit vector at points $\boldsymbol{x}$ of ∂D_f. Therefore, given a reference point $\boldsymbol{\xi}$, all the moments on the volume D_{ext} are uniquely determined by the stress field at the surface, since eq. (2.50) does not depend on the chosen function $\boldsymbol{\psi}(\boldsymbol{x})$.

Consider the tensorial Taylor expansion [212] of the components of the vectorial test function $\boldsymbol{\phi}(\boldsymbol{x})$ around a given point $\boldsymbol{\xi} \in D_{ext}$

$$\phi^{a}(\boldsymbol{x}) = \sum_{n=0}^{\infty} (-1)^n \frac{g^{a}{}_{\alpha}(\boldsymbol{x},\boldsymbol{\xi}) \nabla_{\boldsymbol{\alpha}_n} \phi^{\alpha}(\boldsymbol{\xi})}{n!} (\boldsymbol{\xi}-\boldsymbol{x})^{\boldsymbol{\alpha}_n} \qquad (2.51)$$

where $\nabla_{\boldsymbol{\alpha}_n} = \nabla_{\alpha_1} \cdots \nabla_{\alpha_n}$. Owing to the bitensorial notation, there is no ambiguity in the definition of $\nabla_{\boldsymbol{\alpha}_n}$ as greek indices refer to the source point.

Applying the test function to the momentum balance equation entering eq. (2.46) we have

$$\begin{aligned} \langle \psi^a, \phi_a \rangle &= \sum_{n=0}^{\infty} \left\langle \psi^a, (-1)^n \frac{g_a{}^{\alpha}(\boldsymbol{x},\boldsymbol{\xi}) \nabla^{\boldsymbol{\alpha}_n} \phi_{\alpha}(\boldsymbol{\xi})}{n!} (\boldsymbol{\xi}-\boldsymbol{x})_{\boldsymbol{\alpha}_n} \right\rangle \\ &= \sum_{n=0}^{\infty} \frac{\nabla^{\boldsymbol{\alpha}_n} \phi_{\alpha}(\boldsymbol{\xi})}{n!} M^{\alpha}{}_{\boldsymbol{\alpha}_n}(\boldsymbol{\xi}) \end{aligned} \qquad (2.52)$$

where we have made use of the relations $g_a{}^{\alpha}(\boldsymbol{x},\boldsymbol{\xi}) = g^{\alpha}{}_{a}(\boldsymbol{\xi},\boldsymbol{x})$ and $(\boldsymbol{x}-\boldsymbol{\xi})^{\boldsymbol{\alpha}_n} = (-1)^n(\boldsymbol{\xi}-\boldsymbol{x})^{\boldsymbol{\alpha}_n} = (\boldsymbol{x}-\boldsymbol{\xi})^{\boldsymbol{a}_n} g_{\boldsymbol{a}_n}^{\boldsymbol{\alpha}_n}(\boldsymbol{\xi},\mathrm{x})$ see Appendix A.

Since the derivatives of the test functions can be formulated in scalar-product notation as

$$\nabla^{\boldsymbol{\alpha}_n} \phi_{\alpha}(\boldsymbol{\xi}) = (-1)^n \left\langle \nabla^{\boldsymbol{\alpha}_n} g^{a}{}_{\alpha}(\boldsymbol{x},\boldsymbol{\xi}) \delta(\boldsymbol{x},\boldsymbol{\xi}), \phi_a(\boldsymbol{x}) \right\rangle \qquad (2.53)$$

substituting eq. (2.53) into eq. (2.52), the function $\boldsymbol{\psi}(\boldsymbol{x})$ can be finally expressed as

$$\psi^{a}(\boldsymbol{x}) = \sum_{n=0}^{\infty} (-1)^n \frac{M^{\alpha}{}_{\boldsymbol{\alpha}_n}(\boldsymbol{\xi})}{n!} \nabla^{\boldsymbol{\alpha}_n} g^{a}{}_{\alpha}(\boldsymbol{x},\boldsymbol{\xi}) \delta(\boldsymbol{x},\boldsymbol{\xi}) \qquad (2.54)$$

Although the moments depend on the reference points $\boldsymbol{\xi}$, the summation in equation (2.54) does not depend on $\boldsymbol{\xi}$. Therefore, eq. (2.54) can be generalized by considering $\boldsymbol{\xi}$ as a point of an arbitrary k-dimensional ($k \leq 3$) set of points Ω, averaging eq. (2.54) over Ω,

$$\psi^{a}(\boldsymbol{x}) = \frac{1}{\mathrm{meas}(\Omega)} \int_{\Omega} d\Omega(\boldsymbol{\xi}) \sum_{n=0}^{\infty} (-1)^n \frac{M^{\alpha}{}_{\boldsymbol{\alpha}_n}(\boldsymbol{\xi})}{n!} \nabla^{\boldsymbol{\alpha}_n} g^{a}{}_{\alpha}(\boldsymbol{x},\boldsymbol{\xi}) \delta(\boldsymbol{x},\boldsymbol{\xi}) \qquad (2.55)$$

where $d\Omega(\boldsymbol{\xi})$ is the measure element and

$$\mathrm{meas}(\Omega) = \int_{\Omega} d\Omega(\boldsymbol{\xi})$$

is the Lebesgue measure of Ω. Depending on the symmetries of the flow geometry, the set Ω can be chosen in some particular cases as to reduce the infinite summation entering eq. (2.55) to a finite number of terms.

From the structure of eq. (2.54) we can introduce a differential operator

$$\mathcal{D}^{*\alpha} = \sum_{n=0}^{\infty} (-1)^n \frac{M^{\alpha}_{\ \boldsymbol{\alpha}_n}(\boldsymbol{\xi})}{n!} \nabla^{\boldsymbol{\alpha}_n} \tag{2.56}$$

that in eq. (2.54) acts on the Dirac delta function. In a similar way, if eq. (2.54) is generalized by eq. (2.55), the operator $\mathcal{D}^{*\alpha}$ attains an integro-differential representation

$$\mathcal{D}^{*\alpha} = \frac{1}{\mathrm{meas}(\Omega)} \int_{\Omega} d\Omega(\boldsymbol{\xi}) \sum_{n=0}^{\infty} (-1)^n \frac{M^{\alpha}_{\ \boldsymbol{\alpha}_n}(\boldsymbol{\xi})}{n!} \nabla^{\boldsymbol{\alpha}_n} \tag{2.57}$$

so that $\psi^a = \mathcal{D}^{*\alpha} g^a_{\ \alpha}(\boldsymbol{x},\boldsymbol{\xi})\delta(\boldsymbol{x},\boldsymbol{\xi})$. Its adjoint $\mathcal{D}$, $\langle \mathcal{D}^{*a} f, g\rangle = \langle f, \mathcal{D} g\rangle$, is expressed by

$$\mathcal{D}^{\alpha} = \frac{1}{\mathrm{meas}(\Omega)} \int_{\Omega} d\Omega(\boldsymbol{\xi}) \sum_{n=0}^{\infty} \frac{M^{\alpha}_{\ \boldsymbol{\alpha}_n}(\boldsymbol{\xi})}{n!} \nabla^{\boldsymbol{\alpha}_n} \tag{2.58}$$

Therefore, the problem defined by eq. (2.46) can be reformulated as

$$\begin{cases} \mu\, \Delta_x w^a(\boldsymbol{x}) - \nabla^a q(\boldsymbol{x}) = -\mathcal{D}^{*\alpha} g^a_{\ \alpha}(\boldsymbol{x},\boldsymbol{\xi})\delta(\boldsymbol{x},\boldsymbol{\xi}) & \boldsymbol{x} \in \mathbb{R}^3,\ \boldsymbol{\xi} \in D_{ext} \\ \nabla_a w^a(\boldsymbol{x}) = 0 \end{cases} \tag{2.59}$$

and the singular representation of the velocity field $\boldsymbol{w}(\boldsymbol{x})$ follows from equations (2.7)-(2.8), namely

$$w^a(\boldsymbol{x}) = \left\langle \mathcal{D}^{*\alpha}\delta(\boldsymbol{\xi}',\boldsymbol{\xi}), \frac{\mathsf{S}^a_{\ \alpha}(\boldsymbol{x}-\boldsymbol{\xi}')}{8\pi\mu} \right\rangle = \frac{\mathcal{D}^{\alpha}\mathsf{S}^a_{\ \alpha}(\boldsymbol{x}-\boldsymbol{\xi})}{8\pi\mu} \tag{2.60}$$

and

$$p(\boldsymbol{x}) = \left\langle \mathcal{D}^{*\alpha}\delta(\boldsymbol{\xi}',\boldsymbol{\xi}), \frac{\mathsf{P}_{\ \alpha}(\boldsymbol{x}-\boldsymbol{\xi}')}{8\pi} \right\rangle = \frac{\mathcal{D}^{\alpha}\mathsf{P}_{\ \alpha}(\boldsymbol{x}-\boldsymbol{\xi})}{8\pi} \tag{2.61}$$

where the scalar products in eqs. (2.60), (2.61) correspond to an integration over $\boldsymbol{\xi}'$. Thus the operator $\boldsymbol{\mathcal{D}}$ defined by the (2.58) provides the singular expansion, of the flow at the source point $\boldsymbol{\xi}$.

The procedure outlined above, based on the generalized function theory, provides an explicit expression for the operator $\boldsymbol{\mathcal{D}}$ in the form of a series expansion the coefficients of which are the moments. The main advantages of this explicit representation are: (i) for a specific flow problem the terms in the series expansion of the operator can be obtained numerically with arbitrary precision, (ii) it is possible to manipulate its formal structure in order to obtain new relations as will be shown in the next Sections.

2.5 Reflection operator

In hydrodynamics problems involving bounded flows and confined geometries, the Green function ${\rm G}^a{}_{\alpha'}(\boldsymbol{x},\boldsymbol{\zeta})$, solution of the equations

$$\begin{cases} -\nabla_b \Sigma^{ab}_{\alpha'}(\boldsymbol{x},\boldsymbol{\zeta}) = \Delta_x {\rm G}^a{}_{\alpha'}(\boldsymbol{x},\boldsymbol{\zeta}) - \nabla^a {\rm P}_{\alpha'}(\boldsymbol{x},\boldsymbol{\zeta}) = -8\pi g^a{}_{\alpha'}(\boldsymbol{x},\boldsymbol{\zeta})\delta(\boldsymbol{x},\boldsymbol{\zeta}) \\ \nabla_a {\rm G}^a{}_{\alpha'}(\boldsymbol{x},\boldsymbol{\zeta}) = 0; \qquad \boldsymbol{x},\boldsymbol{\zeta} \in D_f \\ {\rm G}^a{}_{\alpha'}(\boldsymbol{x},\boldsymbol{\zeta}) = 0; \qquad \boldsymbol{x} \in \partial D_f \end{cases} \tag{2.62}$$

(referred for short to as the bounded Green function) plays a central role as it provides the volume potential in the fluid domain D_f, starting from which any flow with no-slip boundary conditions at ∂D_f, can be constructed.

Bounded Green function are available in the literature for a handful of simple geometries, as reviewed in [194]. In special cases, such as for the Green function of a fluid bounded by a plane [18] or outside a sphere [185, 164] (see also [130]), a representation of the bounded Green function in terms of unbounded singularities placed outside the fluid domain is available. This representation is referred to as the image system [130], which is particularly handy for analytical and numerical calculations whenever the set of singularities is either finite or localized on simple manifolds. The latter property characterizes flows with suitable and simple symmetries while, for generic bounded flows, an image system of singularities is not available.

Based on the theory developed in Section 2.4, this Section addresses the properties of the operator providing the image system for a generic bounded Green function. To this aim, let us to consider as the ambient field the unbounded flow due to a Stokeslet centered at the point $\boldsymbol{\zeta} \in D_f$ and let us use the primed indices, say $\alpha', \beta', ...,$ for referring to this point

$$u^a(\boldsymbol{x}) = \frac{\psi_0^{\alpha'}}{8\pi\mu} {\rm S}^a{}_{\alpha'}(\boldsymbol{x}-\boldsymbol{\zeta}) \tag{2.63}$$

As a consequence, the boundary condition for the disturbance field is given by

$$w^a(\boldsymbol{x}) = -u^a(\boldsymbol{x}) = -\frac{\psi_0^{\alpha'}}{8\pi\mu} {\rm S}^a{}_{\alpha'}(\boldsymbol{x}-\boldsymbol{\zeta}), \qquad \boldsymbol{x} \in \partial D_f \tag{2.64}$$

Owing to linearity, let us define the field ${\rm W}^a{}_{\alpha'}(\boldsymbol{x},\boldsymbol{\zeta})$, depending on $\boldsymbol{\zeta}$, but regular at this point, such that

$$w^a(\boldsymbol{x}) = \frac{\psi_0^{\alpha'}}{8\pi\mu} {\rm W}^a{}_{\alpha'}(\boldsymbol{x},\boldsymbol{\zeta}) \tag{2.65}$$

The theory developed in Section 2.4 can be applied, and enforcing eq. (2.60) the field ${\rm W}^a{}_{\alpha'}$ is given by

$${\rm W}^a{}_{\alpha'}(\boldsymbol{x},\boldsymbol{\zeta}) = \mathcal{D}^\alpha{}_{\alpha'} {\rm S}^a{}_\alpha(\boldsymbol{x}-\boldsymbol{\xi}) \tag{2.66}$$

where

$$\mathcal{D}^\alpha{}_{\alpha'} = \frac{1}{\text{meas}(\Omega)} \int_\Omega d\Omega(\boldsymbol{\xi}) \sum_{n=0}^\infty \frac{M^\alpha_{\alpha'\boldsymbol{\alpha}_n}(\boldsymbol{\xi},\boldsymbol{\zeta})}{n!} \nabla^{\boldsymbol{\alpha}_n}$$

$$M^\alpha_{\alpha'\boldsymbol{\alpha}_n}(\boldsymbol{\xi},\boldsymbol{\zeta}) = -\int_{\partial D_f} (\boldsymbol{x}-\boldsymbol{\xi})_{\boldsymbol{\alpha}_n} g^\alpha{}_a(\boldsymbol{\xi},\boldsymbol{x}) \frac{\Sigma^{ab}_{\alpha'}(\boldsymbol{x},\boldsymbol{\zeta})}{8\pi} n_b(\boldsymbol{x}) dS(\boldsymbol{x}) \tag{2.67}$$

Therefore, the Green function solution of eq. (2.62) can be expressed as the sum of two contributions: a singular part, due to the Stokeslet centered in the point $\boldsymbol{\zeta}$, and a regular part due to the integro-differential operator $\mathcal{D}^{\alpha}{}_{\alpha'}$ acting on the poles of the Stokeslet outside the domain of the fluid

$$\mathrm{G}^{a}{}_{\alpha'}(\boldsymbol{x},\boldsymbol{\zeta}) = \mathsf{S}^{a}{}_{\alpha'}(\boldsymbol{x}-\boldsymbol{\zeta}) + \mathcal{D}^{\alpha}{}_{\alpha'}\mathsf{S}^{a}{}_{\alpha}(\boldsymbol{x}-\boldsymbol{\xi}) \tag{2.68}$$

Owing to the properties of the Green functions, the same result can be obtained by applying the operator $\mathcal{D}^{\alpha}{}_{\alpha'}$ at the field point. In point of fact, making use of the reciprocal identities for the Green functions, $\mathrm{G}^{a}{}_{\alpha'}(\boldsymbol{x},\boldsymbol{\zeta}) = \mathrm{G}_{\alpha'}{}^{a}(\boldsymbol{\zeta},\boldsymbol{x})$ and $\mathsf{S}^{a}{}_{\alpha'}(\boldsymbol{x},\boldsymbol{\zeta}) = \mathsf{S}_{\alpha'}{}^{a}(\boldsymbol{\zeta},\boldsymbol{x})$, it follows that

$$\mathrm{G}^{a}{}_{\alpha'}(\boldsymbol{x},\boldsymbol{\zeta}) = \mathrm{G}_{\alpha'}{}^{a}(\boldsymbol{\zeta},\boldsymbol{x}) = \mathsf{S}_{\alpha'}{}^{a}(\boldsymbol{\zeta}-\boldsymbol{x}) + \mathcal{D}_{\alpha}{}^{a}\mathsf{S}_{\alpha'}{}^{\alpha}(\boldsymbol{\zeta}-\boldsymbol{\xi}) = \mathsf{S}^{a}{}_{\alpha'}(\boldsymbol{x}-\boldsymbol{\zeta}) + \mathcal{D}_{\alpha}{}^{a}\mathsf{S}^{\alpha}{}_{\alpha'}(\boldsymbol{\xi}-\boldsymbol{\zeta}) \tag{2.69}$$

where, due to the reciprocity, the point $\boldsymbol{\xi}$ (corresponding in eq. (2.66) to a source point) has been transformed into a field point outside the domain. By changing the dummy variable $(\boldsymbol{\xi}\to\boldsymbol{y})\in D_b$ and the index $\alpha,\beta,...\to a',b',...$ in order to keep the convention that field points are associated with latin lettering, the Green function can be expressed as

$$\mathrm{G}^{a}{}_{\alpha'}(\boldsymbol{x},\boldsymbol{\zeta}) = \mathsf{S}^{a}{}_{\alpha'}(\boldsymbol{x}-\boldsymbol{\zeta}) + \mathcal{D}_{a'}{}^{a}\mathsf{S}^{a'}{}_{\alpha'}(\boldsymbol{y}-\boldsymbol{\zeta}) \tag{2.70}$$

where now

$$\mathcal{D}_{a'}{}^{a} = \frac{1}{\mathrm{meas}(\Omega)}\int_{\Omega} d\Omega(\boldsymbol{y})\sum_{n=0}^{\infty}\frac{M_{a'}^{a\boldsymbol{a}'_n}(\boldsymbol{y},\boldsymbol{x})}{n!}\nabla_{\boldsymbol{a}'_n}$$

$$M_{a'}^{a\boldsymbol{a}'_n}(\boldsymbol{y},\boldsymbol{x}) = -\int_{\partial D_f} g_{a'}{}^{a''}(\boldsymbol{y},\boldsymbol{z})(\boldsymbol{z}-\boldsymbol{y})^{\boldsymbol{a}'_n}\frac{\Sigma_{a''}^{ab''}(\boldsymbol{z},\boldsymbol{x})}{8\pi}n_{b''}(\boldsymbol{z})dS(\boldsymbol{z}) \tag{2.71}$$

Although equations (2.68) and (2.71) are equivalent, their physical meaning in slightly different. In eq. (2.68), the Green function is expressed as a combination of singular solutions of the unbounded Stokes equation, with poles in Ω, weighted by the moments that, in turn, depend on the pole $\boldsymbol{\zeta}$ entering the original problem eq. (2.62). Conversely, in equation (2.71) the field variable enters in the expression of the operator $\mathcal{D}_{a'}{}^{a}$ through the moments, and the regular part, solution of the Stokes equations as a whole, is a combination of terms each of which individually is not a solution of the Stokes equation.

The operators $\mathcal{D}^{\alpha}{}_{\alpha'}$ defined by eq. (2.67), depend on the pole $\boldsymbol{\zeta}$ via the moments, and consequently, for each $\boldsymbol{\zeta}$, a new system of moments is defined, determining a different operator $\mathcal{D}^{\alpha}{}_{\alpha'}$. For this reason, it is convenient to introduce a new operator, independent of the position of the pole, and such that, its action on the Stokeslet outside the domain of the fluid furnishes the Green function. To this purpose, let us assume that the geometry of the problem is such that there exists a bijective correspondence between points inside $\boldsymbol{\zeta}$ and outside $\boldsymbol{\xi}$ the domain of the fluid, defined by a smooth and invertible function r,

$$\boldsymbol{\xi} = r^{-1}(\boldsymbol{\zeta}), \qquad \boldsymbol{\zeta} = r(\boldsymbol{\xi}) \tag{2.72}$$

As addressed in Appendix 2.A, and following the Ruse approach to bitensor calculus [211], eq. (2.72) enables us to view $\boldsymbol{\xi}$ and $\boldsymbol{\zeta}$ as conjugate points in two different metric spaces, such that tensorial quantities defined at a point in one of the two spaces can be transported to the conjugate point of the other space via the parallel propagator

$$g_{\alpha\beta}(\boldsymbol{\xi}) = g_{\alpha}^{\ \alpha'}(\boldsymbol{\xi},\boldsymbol{\zeta}) g_{\beta}^{\ \beta'}(\boldsymbol{\xi},\boldsymbol{\zeta}) g_{\alpha'\beta'}(\boldsymbol{\zeta}) \tag{2.73}$$

where the parallel propagator is given by

$$g^{\alpha}_{\ \alpha'}(\boldsymbol{\xi},\boldsymbol{\zeta}) = \frac{\partial \xi^{\alpha}}{\partial \zeta^{\alpha'}} \tag{2.74}$$

It follows from eq. (2.73) and from the above bitensorial interpretation of the bijective correspondence eq. (2.72) between point in the flow domain and image points outside it, that the stress tensor $\Sigma^{ab}_{\alpha'}(\boldsymbol{x},\boldsymbol{\zeta})$ can be parallel transported from the point $\boldsymbol{\zeta}$ to the point $\boldsymbol{\xi}$

$$\Sigma^{ab}_{\alpha}(\boldsymbol{x}, r(\boldsymbol{\xi})) = g_{\alpha}^{\ \alpha'}(\boldsymbol{\zeta},\boldsymbol{\xi}) \Sigma^{ab}_{\alpha'}(\boldsymbol{x},\boldsymbol{\zeta}) \tag{2.75}$$

Substituting eq. (2.75) into eq. (2.67) one obtains

$$M^{\alpha}_{\alpha'\boldsymbol{\alpha}_n}(\boldsymbol{\xi},\boldsymbol{\zeta}) = g^{\ \beta}_{\alpha'}(\boldsymbol{\xi},\boldsymbol{\zeta}) M^{\alpha}_{\beta\boldsymbol{\alpha}_n}(\boldsymbol{\xi}, r(\boldsymbol{\xi})) \tag{2.76}$$

where

$$M^{\alpha}_{\beta\boldsymbol{\alpha}_n}(\boldsymbol{\xi}, r(\boldsymbol{\xi})) = -\int_{\partial D_f} (\boldsymbol{x}-\boldsymbol{\xi})_{\boldsymbol{\alpha}_n} g^{\alpha}_{\ a}(\boldsymbol{\xi},\boldsymbol{x}) \frac{\Sigma^{ab}_{\beta}(\boldsymbol{x}, r(\boldsymbol{\xi}))}{8\pi} n_b(\boldsymbol{x}) dS(\boldsymbol{x}) \tag{2.77}$$

Enforcing eq. (2.76), it is possible to express the operator $\mathcal{D}^{\alpha}_{\ \alpha'}$ in terms of a reflection operator independent of the pole $\boldsymbol{\zeta}$, and such that the functional dependence on $\boldsymbol{\zeta}$ is encompassed in the parallel propagator. For highlighting this delicate issue, let us consider the simplest case where Ω reduces to a point $r(\boldsymbol{\zeta})$. In this case, it follows from eq. (2.76) that the operator $\mathcal{D}^{\alpha}_{\ \alpha'}$ attains the form

$$\mathcal{D}^{\alpha}_{\ \alpha'} = g^{\ \beta}_{\alpha'}(\boldsymbol{\zeta},\boldsymbol{\xi}) \mathcal{R}^{\alpha}_{\beta}, \qquad \mathcal{R}^{\alpha}_{\beta} = \sum_{n=0}^{\infty} \frac{M^{\alpha}_{\beta\boldsymbol{\alpha}_n}(\boldsymbol{\xi}, r(\boldsymbol{\xi}))}{n!} \nabla^{\boldsymbol{\alpha}_n} \tag{2.78}$$

The operator $\mathcal{R}^{\alpha}_{\beta}$ furnishes the regular part of the Green function starting from the Stokeslet, independently on the source point $\boldsymbol{\zeta}$ and, for the reasons discussed below, it can be referred to as the reflection operator of the bounded flow problem.

By eqs. (2.68) and (2.70), the operator $\mathcal{R}^{\alpha}_{\beta}$ can be applied on equal footing either at the source or at the field point. In the first case, the Green function reads

$$\mathrm{G}^{a}_{\ \alpha'}(\boldsymbol{x},\boldsymbol{\zeta}) = \mathsf{S}^{a}_{\ \alpha'}(\boldsymbol{x}-\boldsymbol{\zeta}) + g^{\ \beta}_{\alpha'}(\boldsymbol{\zeta},\boldsymbol{\xi}) \mathcal{R}^{\alpha}_{\beta} \mathsf{S}^{a}_{\ \alpha}(\boldsymbol{x}-\boldsymbol{\xi}) \tag{2.79}$$

In the second case, i.e., by applying the operator at the field point, an alternative representation of the Green function follows

$$\mathrm{G}^{a}_{\ \alpha'}(\boldsymbol{x},\boldsymbol{\zeta}) = \mathsf{S}^{a}_{\ \alpha'}(\boldsymbol{x}-\boldsymbol{\zeta}) + g^{a}_{\ b'}(\boldsymbol{x},\boldsymbol{y}) \mathcal{R}^{b'}_{a'} \mathsf{S}^{a'}_{\ \alpha'}(\boldsymbol{y}-\boldsymbol{\zeta}) \tag{2.80}$$

where $\boldsymbol{y} = r^{-1}(\boldsymbol{x})$ and $\boldsymbol{x} = r(\boldsymbol{y})$. The latter expression permits to interpret the regular part of the Green function as a "reflected field" of the ambient flow, that in the present case is given by a Stokeslet centered at the point $\boldsymbol{\zeta}$. In fact, the operator $\mathcal{R}_{a'}^{\ b}$ furnishes a continuation of the Stokes solution with homogeneous Dirichlet boundary conditions in the external domain, usually referred as a reflection principle [220, 126]. To show this, consider the integral form of a generic solution vanishing at the boundary ∂D_f [137]

$$v^a(\boldsymbol{x}) = -\int_{\partial D_f} \frac{\sigma^{\alpha'\beta'}(\boldsymbol{\zeta})n_{\beta'}(\boldsymbol{\zeta})}{8\pi\mu} \mathsf{S}^a_{\ \alpha'}(\boldsymbol{x}-\boldsymbol{\zeta})dS(\boldsymbol{\zeta}) \qquad \boldsymbol{x} \in D_f \tag{2.81}$$

and its continuation in $\mathbb{R}^3/D_f$,

$$v^{a'}(\boldsymbol{y}) = \int_{\partial D_f} \frac{\sigma^{\alpha\beta}(\boldsymbol{\xi})n_{\beta}(\boldsymbol{\xi})}{8\pi\mu} \mathsf{S}^{a'}_{\ \alpha}(\boldsymbol{y}-\boldsymbol{\xi})dS(\boldsymbol{\xi}) \qquad \boldsymbol{y} \in \mathbb{R}^3/D_f \tag{2.82}$$

Since, by the definition of the disturbed field

$$g_{\alpha'}^{\ \beta}(\boldsymbol{\zeta},\boldsymbol{\xi})\mathcal{R}^{\alpha}_{\beta}\mathsf{S}^a_{\ \alpha}(\boldsymbol{x}-\boldsymbol{\xi}) = -\mathsf{S}^a_{\ \alpha'}(\boldsymbol{x}-\boldsymbol{\zeta}), \qquad \boldsymbol{x} \in \partial D_f \tag{2.83}$$

by using the reciprocal identity $\mathsf{S}^a_{\ \alpha'}(\boldsymbol{x}-\boldsymbol{\zeta}) = \mathsf{S}_{\alpha'}^{\ a}(\boldsymbol{\zeta}-\boldsymbol{x})$ and exchanging latin and greek letters, it easy to verify that

$$g^a_{\ b'}(\boldsymbol{x},\boldsymbol{y})\mathcal{R}^{b'}_{a'}\mathsf{S}^{a'}_{\ \alpha'}(\boldsymbol{y}-\boldsymbol{\zeta}) = -\mathsf{S}^a_{\ \alpha'}(\boldsymbol{x}-\boldsymbol{\zeta}), \qquad \boldsymbol{\zeta} \in \partial D_f \tag{2.84}$$

Therefore, by applying the operator $\mathcal{R}^{b'}_{a'}$ at the field in (2.82) we obtain at the r.h.s of eq. (2.82) the field defined by eq. (2.81) and the reflection formula can be derived

$$v^a(\boldsymbol{x}) = g^a_{\ b'}(\boldsymbol{x},\boldsymbol{y})\mathcal{R}^{b'}_{a'}v^{a'}(r(\boldsymbol{x})) \tag{2.85}$$

The reflection formula in eq. (2.85) requires in principle the estimate of infinite terms as the operator $\mathcal{R}^{b'}_{a'}$ admits in general a series expansion in terms of the countable system of moments. It is known from harmonic function theory, that if the reflection operator (e.g. associated with an electrostatic problem) possesses a finite number of non-vanishing terms, then the boundary is either a plane or a sphere [66] and the relation equivalent to eq. (2.85) is referred as a point-to-point reflection principle. In the case of the solutions of the Stokes problem, that involves biharmonic functions, it is known that a point-to-point reflection principle does not hold even for spherical boundaries, and a weaker point-to-set principle [76, 66, 102] should be considered, where a bijective relation occurs between a point $\boldsymbol{x}$ in the fluid domain and a set parameterized by its conjugate point $\boldsymbol{y} = r(\mathbf{x})$ in the complementary domain.

Eq. (2.78) and the analysis developed in the previous Section indicate the close relation (duality) between the image system of singularities of a bounded flow problem and the formulation of a reflection principle, as the two problems are governed by essentially the same operators $\mathcal{D}^{\alpha}_{\ \alpha'}$ and $\mathcal{R}^{\alpha}_{\beta}$, parallel transported between a source point and its conjugate image. The duality between image system and reflection principle has been practically neglected in Stokesian hydrodynamics. Several works have investigated the image system of singularities near a plane [18, 19] or near spherical boundaries [164], and, almost independently, parallel works on reflected fields near a planar [150] and spherical boundaries [102] has been published. The main difficulty in recognizing a common formal structure underlying image systems and reflection principle in Stokesian hydrodynamics stems from the tensorial nature of the operators involved, and by the need of a parallel transport between conjugate points. The introduction of the bitensorial formalism for hydrodynamic Green functions has made possible to highlight this issue.

The duality between the image system of singularities and the existence of a reflection principle make it possible to transfer and apply methods and techniques developed for solving one of these two problems to the other one. The next Section provides an application of this principle in connection with the problem of singularities bounded by planar boundaries.

2.6 Singular fields bounded by a single plane

Below, the results found in Section 2.5 are applied to the problem of the singularities of a flow bounded by a rigid plane. In this case, the function r transforming points $\boldsymbol{x} \in D_f$ into conjugate points $\boldsymbol{y} \in \mathbb{R}^3/D_f$ is given by the mirror operator $\boldsymbol{J} = \boldsymbol{I} - 2\,\boldsymbol{n} \otimes \boldsymbol{n}$, $\boldsymbol{I}$ being the identity matrix, and $\boldsymbol{n}$ the unit normal to the plane, so that $\boldsymbol{y} = \boldsymbol{J} \cdot \boldsymbol{x}$ and $\boldsymbol{x} = \boldsymbol{J} \cdot \boldsymbol{y}$, since $\boldsymbol{J}^2 = \boldsymbol{I}$.

Consider a Cartesian coordinate system (X_1, X_2, X_3) with the origin on the plane and such that the flow domain corresponds to $X_3 > 0$. Let $\boldsymbol{x} \in D_f$ with coordinates (x_1,x_2,x_3), and its mirror point $\boldsymbol{y} \in \mathbb{R}^3/D_f$ with coordinates $y_{a'} = J_{a'a} x_a$.

The parallel propagator (see Appendix 2.A) between these conjugate points is given by

$$g_{aa'}(\boldsymbol{x}, \boldsymbol{y}) = \frac{\partial y^{a'}}{\partial x^a} = J_{aa'} \tag{2.86}$$

The reflection operator acting at the point $\boldsymbol{y}$, corresponding to eq. (2.85) is the so called Lorentz mirror operator [156, 102]

$$\mathcal{R}_{a'b'} = -J_{a'b'} - 2(\boldsymbol{y} \cdot \boldsymbol{n}) \nabla_{a'} \delta_{3b'} + (\boldsymbol{y} \cdot \boldsymbol{n})^2 \Delta_x \delta_{a'b'} \tag{2.87}$$

The Green function of the Stokes flow centered at the source point $\boldsymbol{\zeta} \in D_f$ can be obtained either by applying the reflection operator at the field point, according to eq. (2.80), or at the source point, according to eq. (2.79). In the first case we have

$$\begin{aligned} \mathrm{G}_{a\alpha'}(\boldsymbol{x}, \boldsymbol{\zeta}) &= \mathsf{S}_{a\alpha'}(\boldsymbol{x} - \boldsymbol{\zeta}) + J_{ab'}[-J_{b'a'} - 2y_3 \nabla_{b'} \delta_{3a'} + y_3^2 \Delta_x \delta_{b'a'}] \mathsf{S}_{a'\alpha'}(\boldsymbol{y} - \boldsymbol{\zeta}) = \\ \mathsf{S}_{a\alpha'}(\boldsymbol{x} - \boldsymbol{\zeta}) &- \mathsf{S}_{a\alpha'}(\boldsymbol{J} \cdot \boldsymbol{x} - \boldsymbol{\zeta}) + 2x_3 J_{ab'}[\nabla_{b'} \mathsf{S}_{3\alpha'}(\boldsymbol{J} \cdot \boldsymbol{x} - \boldsymbol{\zeta}) + \frac{x_3}{2} \Delta_x \mathsf{S}_{b'\alpha'}(\boldsymbol{J} \cdot \boldsymbol{x} - \boldsymbol{\zeta})] \end{aligned} \tag{2.88}$$

while the application at the source point provides

$$\begin{aligned} \mathrm{G}_{a\alpha'}(\boldsymbol{x}, \boldsymbol{\zeta}) &= \mathsf{S}_{a\alpha'}(\boldsymbol{x} - \boldsymbol{\zeta}) + J_{\alpha'\beta}[-J_{\beta\alpha} - 2(\boldsymbol{\xi} \cdot \boldsymbol{n}) \nabla_\beta \delta_{3\alpha} + (\boldsymbol{\xi} \cdot \boldsymbol{n})^2 \Delta_\xi \delta_{\beta\alpha}] \mathsf{S}_{a\alpha}(\boldsymbol{x} - \boldsymbol{\xi}) = \\ \mathsf{S}_{a\alpha'}(\boldsymbol{x} - \boldsymbol{\zeta}) &- \mathsf{S}_{a\alpha'}(\boldsymbol{x} - \boldsymbol{\xi}) - 2(\boldsymbol{\xi} \cdot \boldsymbol{n}) J_{\alpha'\beta}[\nabla_\beta \mathsf{S}_{a3}(\boldsymbol{x} - \boldsymbol{\xi}) - \frac{(\boldsymbol{\xi} \cdot \boldsymbol{n})}{2} \Delta_\xi \mathsf{S}_{a\beta}(\boldsymbol{x} - \boldsymbol{\xi})] \end{aligned} \tag{2.89}$$

with the expression for the pressure

$$\mathrm{P}_{\alpha'}(\boldsymbol{x}, \boldsymbol{\zeta}) = \mathsf{P}_{\alpha'}(\boldsymbol{x} - \boldsymbol{\zeta}) - \mathsf{P}_{\alpha'}(\boldsymbol{x} - \boldsymbol{\xi}) - 2(\boldsymbol{\xi} \cdot \boldsymbol{n}) J_{\alpha'\beta} \nabla_\beta \mathsf{P}_3(\boldsymbol{x} - \boldsymbol{\xi}) \tag{2.90}$$

and for the stress tensor

$$\Sigma_{ab\alpha'}(\boldsymbol{x},\boldsymbol{\zeta}) =$$
$$\Sigma_{ab\alpha'}(\boldsymbol{x}-\boldsymbol{\zeta}) - \Sigma_{ab\alpha'}(\boldsymbol{x}-\boldsymbol{\xi}) - 2(\boldsymbol{\xi}\cdot\boldsymbol{n})J_{\alpha'\alpha}[\nabla_\alpha \Sigma_{ab3}(\boldsymbol{x}-\boldsymbol{\xi}) - \frac{(\boldsymbol{\xi}\cdot\boldsymbol{n})}{2}\Delta_\xi \Sigma_{ab\alpha}(\boldsymbol{x}-\boldsymbol{\xi})]$$

Since the pole is fixed at $\boldsymbol{\xi} = \boldsymbol{J}\cdot\boldsymbol{\zeta} = (0,0,-h)$, we obtain the singular form

$$\mathrm{G}_{a\alpha'}(\boldsymbol{x},\boldsymbol{\zeta}) = \mathsf{S}_{a\alpha'}(\boldsymbol{x}-\boldsymbol{\zeta}) - \mathsf{S}_{a\alpha'}(\boldsymbol{x}-\boldsymbol{\xi}) + 2hJ_{\alpha'\beta}[\mathsf{S}_{a3;\beta}(\boldsymbol{x}-\boldsymbol{\xi}) - h\mathsf{D}_{a\beta}(\boldsymbol{x}-\boldsymbol{\xi})] \quad (2.91)$$

and

$$\mathrm{P}_{\alpha'}(\boldsymbol{x},\boldsymbol{\zeta}) = \mathsf{P}_{\alpha'}(\boldsymbol{x}-\boldsymbol{\zeta}) - \mathsf{P}_{\alpha'}(\boldsymbol{x}-\boldsymbol{\xi}) + 2hJ_{\alpha'\beta}\nabla_\beta \mathsf{P}_3(\boldsymbol{x}-\boldsymbol{\xi}) \quad (2.92)$$

$$\Sigma_{ab\alpha'}(\boldsymbol{x},\boldsymbol{\zeta}) = \Sigma_{ab\alpha'}(\boldsymbol{x}-\boldsymbol{\zeta}) - \Sigma_{ab\alpha'}(\boldsymbol{x}-\boldsymbol{\xi}) + 2hJ_{\alpha'\alpha}\left[\nabla_\alpha \Sigma_{ab3}(\boldsymbol{x}-\boldsymbol{\xi}) + \frac{h}{2}\Delta_\xi \Sigma_{ab\alpha}(\boldsymbol{x}-\boldsymbol{\xi})\right] \quad (2.93)$$

The singular representation of the Green function eq. (2.91), here obtained simply by applying the Lorentz reflection operator at the source point, coincides with the result obtained by Blake using a much more elaborate approach involving the Fourier-Hankel transforms [18, 19].

Blake and Chwang in [18, 19] have obtained the singular reflection systems related to bounded Stokeslet, Sourcelet and Rotlet by applying the Fourier-Hankel transforms to separate and distict problems specified by the boundary conditions adopted. In point of fact, the operator formalism developed in Section 2.5 permits to obtain any higher-order singularity in a unitary way, by simply differentiating the Green's function at the pole, eqs. (2.89)-(2.91).

To begin with, consider the bounded Source Dipole $\mathrm{D}_{a\alpha'}(\boldsymbol{x},\boldsymbol{\zeta})$ defined by (2.30), applying the Laplacian operator $-\Delta_\zeta/2$ to the expression (2.89). Being the Laplacian operator invariant with respect to any Euclidean transformation, and thus under the reflection transformation $\boldsymbol{\zeta} = \boldsymbol{J}\cdot\boldsymbol{\xi}$, we have $\Delta_\xi = \Delta_\zeta$, and therefore

$$\begin{aligned}\mathrm{D}_{a\alpha'}(\boldsymbol{x},\boldsymbol{\zeta}) &= \mathsf{D}_{a\alpha'}(\boldsymbol{x}-\boldsymbol{\zeta}) - \mathsf{D}_{a\alpha'}(\boldsymbol{x}-\boldsymbol{\xi})\\ &+J_{\alpha'\beta}\Delta_\xi[(\boldsymbol{\xi}\cdot\boldsymbol{n})\nabla_\beta \mathsf{S}_{a3}(\boldsymbol{x}-\boldsymbol{\xi})] + J_{\alpha'\beta}\Delta_\xi[(\boldsymbol{\xi}\cdot\boldsymbol{n})^2\mathsf{D}_{a\beta}(\boldsymbol{x}-\boldsymbol{\xi})]\end{aligned} \quad (2.94)$$

where, enforcing the identity,

$$\Delta_\xi \mathsf{S}_{a3;\beta}(\boldsymbol{x}-\boldsymbol{\xi}) = \nabla_\beta\Delta_\xi \mathsf{S}_{a3}(\boldsymbol{x}-\boldsymbol{\xi}) = -2\mathsf{D}_{a3;\beta}(\boldsymbol{x}-\boldsymbol{\xi}) \quad (2.95)$$

the third term at the r.h.s of eq. (2.94) reads

$$\begin{aligned}&J_{\alpha'\beta}\Delta_\xi[(\boldsymbol{\xi}\cdot\boldsymbol{n})\nabla_\beta \mathsf{S}_{a3}(\boldsymbol{x}-\boldsymbol{\xi})] =\\ &J_{\alpha'\beta}\nabla_\gamma(\delta_{\gamma 3}\mathsf{S}_{a3;\beta}(\boldsymbol{x}-\boldsymbol{\xi}) + \xi_3 \mathsf{S}_{a3;\beta\gamma}(\boldsymbol{x}-\boldsymbol{\xi})) =\\ &J_{\alpha'\beta}(2\mathsf{S}_{a3;\beta 3}(\boldsymbol{x}-\boldsymbol{\xi}) - 2\xi_3\mathsf{D}_{a3;\beta}(\boldsymbol{x}-\boldsymbol{\xi}))\end{aligned} \quad (2.96)$$

The fourth term in eq. (2.94) can be simplified as

$$\begin{aligned}&J_{\alpha'\beta}\Delta_\xi[(\boldsymbol{\xi}\cdot\boldsymbol{n})^2\mathsf{D}_{a\beta}(\boldsymbol{x}-\boldsymbol{\xi})] =\\ &J_{\alpha'\beta}\nabla_\gamma(2\delta_{3\gamma}\xi_3\mathsf{D}_{a\beta}(\boldsymbol{x}-\boldsymbol{\xi}) + \xi_3^2\mathsf{D}_{a\beta;\gamma}(\boldsymbol{x}-\boldsymbol{\xi})) =\\ &J_{\alpha'\beta}(2\mathsf{D}_{a\beta}(\boldsymbol{x}-\boldsymbol{\xi}) + 4\xi_3\mathsf{D}_{a\beta;3}(\boldsymbol{x}-\boldsymbol{\xi}))\end{aligned} \quad (2.97)$$

so that the singular representation of the Source Dipole reads

$$\mathrm{D}_{a\alpha'}(\boldsymbol{x},\boldsymbol{\zeta}) = \mathsf{D}_{a\alpha'}(\boldsymbol{x}-\boldsymbol{\zeta}) - \mathsf{D}_{a\alpha'}(\boldsymbol{x}-\boldsymbol{\xi}) + 2J_{\alpha'\beta}\Big(\mathsf{D}_{a\beta}(\boldsymbol{x}-\boldsymbol{\xi}) + \mathsf{S}_{a3;\beta3}(\boldsymbol{x}-\boldsymbol{\xi}) + \xi_3\mathsf{D}_{a3;\beta}(\boldsymbol{x}-\boldsymbol{\xi})\Big) \tag{2.98}$$

and since $\xi_3 = -h$, eq. (2.98) becomes

$$\mathrm{D}_{a\alpha'}(\boldsymbol{x},\boldsymbol{\zeta}) = \mathsf{D}_{a\alpha'}(\boldsymbol{x}-\boldsymbol{\zeta}) - \mathsf{D}_{a\alpha'}(\boldsymbol{x}-\boldsymbol{\xi}) + 2J_{\alpha'\beta}\Big(\mathsf{D}_{a\beta}(\boldsymbol{x}-\boldsymbol{\xi}) + \mathsf{S}_{a3;\beta3}(\boldsymbol{x}-\boldsymbol{\xi}) - h\mathsf{D}_{a3;\beta}(\boldsymbol{x}-\boldsymbol{\xi})\Big) \tag{2.99}$$

The associated pressure field can obtained by applying the same operator $-\Delta_\zeta/2 = -\Delta_\xi/2$ to the pressure Green function eq. (2.90). Since the unbounded pressure field is a potential vector field with respect to the source point coordinates, the only non vanishing contribution is given by the third term at the r.h.s of eq. (2.90), and therefore

$$-\frac{\Delta_\zeta \mathrm{P}_{\alpha'}(\boldsymbol{x},\boldsymbol{\zeta})}{2} = 4\pi(\nabla_{\alpha'}\delta(\boldsymbol{x}-\boldsymbol{\zeta}) - \delta_{\alpha'\alpha}\nabla_\alpha\delta(\boldsymbol{x}-\boldsymbol{\xi})) - J_{\alpha'\beta}\Delta_\xi\left(\xi_3\nabla_\beta\mathsf{P}_3(\boldsymbol{x}-\boldsymbol{\xi})\right) =$$
$$4\pi(\nabla_{\alpha'}\delta(\boldsymbol{x}-\boldsymbol{\zeta}) - \delta_{\alpha'\alpha}\nabla_\alpha\delta(\boldsymbol{x}-\boldsymbol{\xi})) - 2J_{\alpha'\beta}\delta_{3\gamma}\nabla_\beta\nabla_\gamma\mathsf{P}_3(\boldsymbol{x}-\boldsymbol{\xi}) \tag{2.100}$$

Fig. 2.1 provides the schematic representation of the unbounded singularities at the image pole necessary to cancel the velocity field at the plane due to the unbounded Source Doubled at the pole in the fluid domain. Panel (a) refers to $\mathrm{D}_{a1} = D_{a2}$, panel (b) to D_{a3}. The vector plot of the bounded Source Dipole defined by eq. (2.99) is depicted in Fig. 2.2.

In the far field, $|\boldsymbol{x}| >> h$, we have

$$\mathrm{D}_{a\alpha'}(\boldsymbol{x},\boldsymbol{\zeta}) = 2J_{\alpha'\alpha}\Big(\mathsf{D}_{a\alpha}(\boldsymbol{x}) + \mathsf{S}_{3\alpha;3a}(\boldsymbol{x})\Big) + o(1/|\boldsymbol{x}|^3), \qquad |\boldsymbol{x}| \gg |\boldsymbol{\zeta}| \tag{2.101}$$

To obtain the Stokes Doublet eq. (2.22), we can apply the covariant derivative at the pole of the Green function. The bounded solution of the Rotlet (2.28) giving the antisymmetric part of the Stokes doublet can be found, according to eq. (2.25), by applying the curl at the pole of the Green function to obtain

$$\Omega_{a\gamma'}(\boldsymbol{x},\boldsymbol{\zeta}) = \Omega_{a\gamma'}(\boldsymbol{x}-\boldsymbol{\zeta}) - \Omega_{a\gamma'}(\boldsymbol{x}-\boldsymbol{\xi}) + 2\epsilon_{\beta'\gamma'3}\Big(\mathsf{E}_{a3\beta'}(\boldsymbol{x}-\boldsymbol{\xi}) + \xi_3\mathsf{D}_{a\beta'}(\boldsymbol{x}-\boldsymbol{\xi})\Big) \tag{2.102}$$

and the associated pressure reads

$$\frac{\varepsilon_{\gamma'\epsilon'\eta'}\nabla_{\eta'}\mathrm{P}_{\epsilon'}(\boldsymbol{x},\boldsymbol{\zeta})}{2} = \varepsilon_{\gamma'\epsilon'\eta'}\nabla_{\eta'}\xi_3 J_{\epsilon'\beta}\nabla_\beta\mathsf{P}_3(\boldsymbol{x}-\boldsymbol{\xi}) = \varepsilon_{\gamma'\epsilon'3}\delta_{\epsilon'\beta}\nabla_3\nabla_\beta\mathsf{P}_3(\boldsymbol{x}-\boldsymbol{\xi}) \tag{2.103}$$

In the far field we have the asymptotic scaling

$$\Omega_{a\alpha'}(\boldsymbol{x},\boldsymbol{\zeta}) = 2\epsilon_{\beta'\alpha'3}\mathsf{T}_{a3\beta'}(\boldsymbol{x})(1-\delta_{\alpha3}) + o(1/|\boldsymbol{x}|^2), \qquad |\boldsymbol{x}| \gg |\boldsymbol{\zeta}| \tag{2.104}$$

The vector plot of the Rotlet is depicted in Fig. 2.3.

To obtain the bounded Strainlet eq. (2.26), i.e. the symmetric part of the Stokes Doublet, we could evaluate $(\nabla_{\beta'}\mathrm{G}_{a\alpha'} + \nabla_{\alpha'}\mathrm{G}_{a\beta'})/2$. Alternatively, it is more

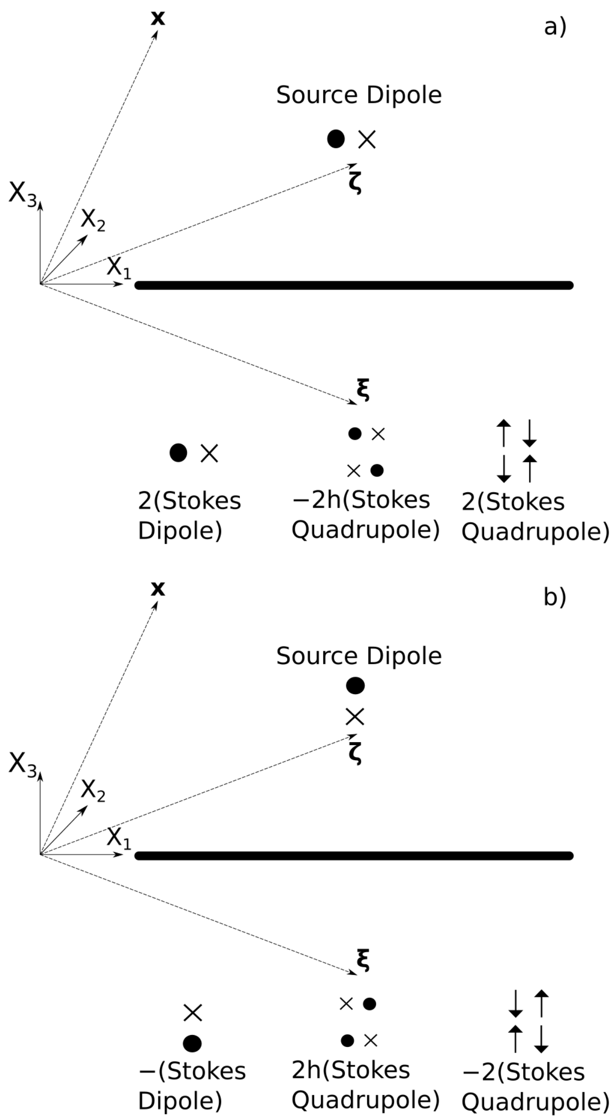

Figure 2.1. Schematic representation of the system of singularities associated with the Source Dipole $\mathrm{D}_{a\alpha'}(\boldsymbol{x},\boldsymbol{\xi})$ confined by a planar wall, represented by the thick horizontal lines. Singularities are centered in two points, the pole above the plane $\boldsymbol{\zeta}$ and its imagine below the plane $\boldsymbol{\xi} = \boldsymbol{J}\cdot\boldsymbol{\zeta}$. Panel (a) refers to the image system of a Source Dipole parallel to the plane (thus, with $\alpha' = 1, 2$), whereas panel (b) to a Source Dipole perpendicular to the plane (thus, $\alpha' = 3$). The symbols have the following meaning: • represents an unbounded Sourcelet, × an unbounded sink (a Sourcelet with reversed sign), the arrow → a concentrated force. The arrow's direction corresponds to the direction of the force.

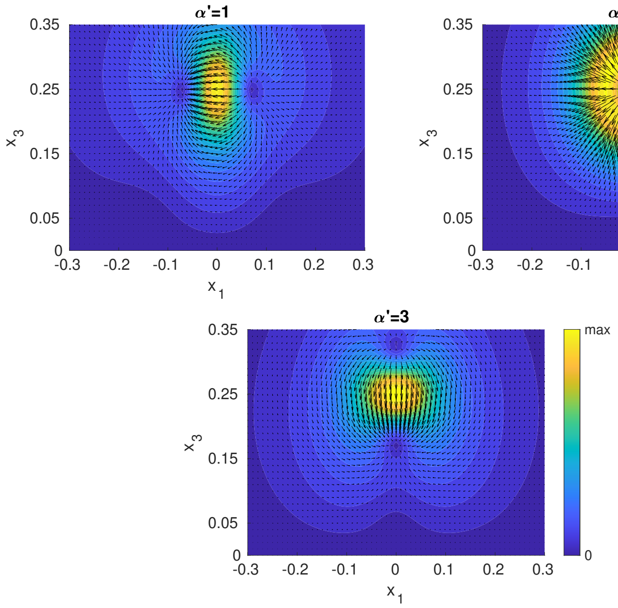

Figure 2.2. Vector plot of the components $(\mathrm{D}_{1\alpha'}(\boldsymbol{x},\boldsymbol{\zeta}),\mathrm{D}_{3\alpha'}(\boldsymbol{x},\boldsymbol{\zeta}))$ of the Source Dipole with pole in $\boldsymbol{\zeta}=(0,0,0.25)$, evaluated on the plane $x_2=0.1$. The color map refers to the intensity $|(\mathrm{D}_{1\alpha'}(\boldsymbol{x},\boldsymbol{\zeta}),\mathrm{D}_{3\alpha'}(\boldsymbol{x},\boldsymbol{\zeta}))|$.

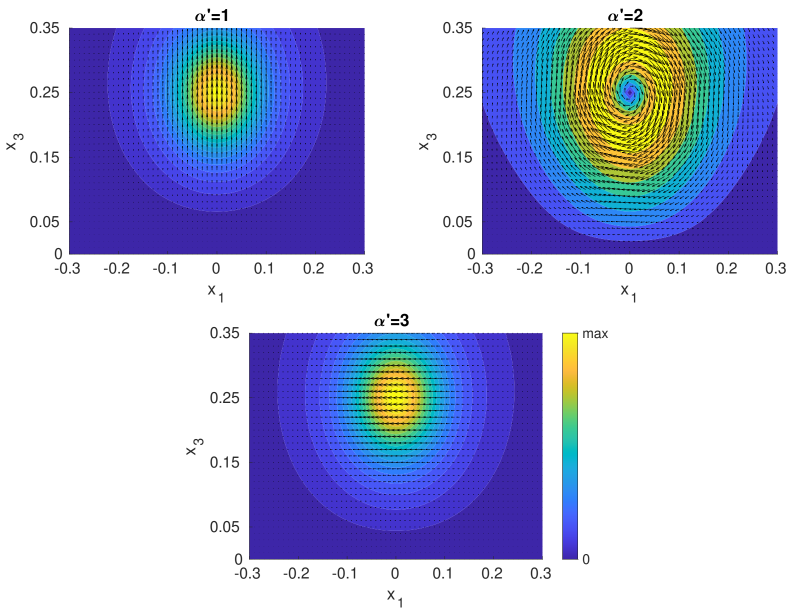

Figure 2.3. Vector plot of the components $(\Omega_{1\alpha'}(\boldsymbol{x},\boldsymbol{\zeta}),\Omega_{3\alpha'}(\boldsymbol{x},\boldsymbol{\zeta}))$ of the Rotlet with pole in $\boldsymbol{\zeta}=(0,0,0.25)$ evaluated on the plane $x_2=0.1$. The color map refers to the intensity $|(\Omega_{1\alpha'}(\boldsymbol{x},\boldsymbol{\zeta}),\Omega_{3\alpha'}(\boldsymbol{x},\boldsymbol{\zeta}))|$.

convenient to use eq. (2.27), substituting in it eq. (2.90) for the pressure, and eq. (2.91) for the stress tensor of the bounded Green function

$$\mathrm{E}_{a\alpha'\beta'}(\boldsymbol{x},\boldsymbol{\zeta}) = \frac{\delta_{\alpha'\beta'}}{2}\mathrm{P}_a(\boldsymbol{\zeta},\boldsymbol{x}) - \frac{1}{2}\Sigma_{\alpha'\beta' a}(\boldsymbol{\zeta},\boldsymbol{x}) \tag{2.105}$$

where

$$\mathrm{P}_a(\boldsymbol{\zeta},\boldsymbol{x}) = \mathsf{P}_a(\boldsymbol{\zeta}-\boldsymbol{x}) - \mathsf{P}_a(\boldsymbol{\zeta}-\boldsymbol{y}) - 2(\boldsymbol{y}\cdot\boldsymbol{n})J_{aa'}\nabla_{a'}\mathsf{P}_3(\boldsymbol{\zeta}-\boldsymbol{y}) \tag{2.106}$$

and

$$\begin{aligned}\Sigma_{\alpha'\beta' a}(\boldsymbol{\zeta},\boldsymbol{x}) &= \mathsf{\Sigma}_{\alpha'\beta' a}(\boldsymbol{\zeta}-\boldsymbol{x}) - \mathsf{\Sigma}_{\alpha'\beta' a}(\boldsymbol{\zeta}-\boldsymbol{y})\\ &-2(\boldsymbol{y}\cdot\boldsymbol{n})J_{aa'}[\nabla_{a'}\mathsf{\Sigma}_{\alpha'\beta' 3}(\boldsymbol{\zeta}-\boldsymbol{y}) - \frac{(\boldsymbol{y}\cdot\boldsymbol{n})}{2}\Delta_y\mathsf{\Sigma}_{\alpha'\beta' a'}(\boldsymbol{\zeta}-\boldsymbol{y})]\end{aligned} \tag{2.107}$$

Since $\Delta_\xi = \Delta_\zeta = \Delta_x = \Delta_y$, in this particular case, where the boundary of the fluid is a plane, it is possible to define the bounded Source $\mathrm{M}_a(\boldsymbol{x},\boldsymbol{\zeta}) = -\mathrm{P}_a(\boldsymbol{\zeta},\boldsymbol{x})/2$ and the bounded Stresslet $\mathrm{T}_{a\alpha'\beta'}(\boldsymbol{x},\boldsymbol{\zeta}) = -\Sigma_{\alpha'\beta' a}(\boldsymbol{\zeta},\boldsymbol{x})/2$, that are the bounded counterparts of the Sourcelet defined in eq. (2.38) and the Stresslet in eq. (2.39). Therefore, the Strainlet can be expressed as

$$\mathrm{E}_{a\alpha'\beta'}(\boldsymbol{x},\boldsymbol{\zeta}) = -\delta_{\alpha'\beta'}\mathrm{M}_a(\boldsymbol{x},\boldsymbol{\zeta}) + \mathrm{T}_{a\alpha'\beta'}(\boldsymbol{x},\boldsymbol{\zeta}) \tag{2.108}$$

By making the following transformation

$$\boldsymbol{y}\cdot\boldsymbol{n} = y_3 = (\boldsymbol{y}-\boldsymbol{\xi})_3 + \xi_3 \tag{2.109}$$

we obtain for $\mathrm{M}_a(\boldsymbol{x},\boldsymbol{\zeta})$ and $\mathrm{T}_{a\alpha'\beta'}(\boldsymbol{x},\boldsymbol{\zeta})$ the following expressions

$$\mathrm{M}_a(\boldsymbol{x},\boldsymbol{\zeta}) = \mathsf{M}_a(\boldsymbol{x}-\boldsymbol{\zeta}) - \mathsf{M}_a(\boldsymbol{x}-\boldsymbol{\xi}) + 2\Big(\mathsf{T}_{a33}(\boldsymbol{x}-\boldsymbol{\xi}) + \xi_3\mathsf{D}_{a3}(\boldsymbol{x}-\boldsymbol{\xi})\Big) \tag{2.110}$$

$$\begin{aligned}\mathrm{T}_{a\alpha'\beta'}(\boldsymbol{x},\boldsymbol{\zeta}) &= \mathsf{T}_{a\alpha'\beta'}(\boldsymbol{x}-\boldsymbol{\zeta}) + 2\delta_{\alpha'\beta'}\mathsf{T}_{a33}(\boldsymbol{x}-\boldsymbol{\xi}) - J_{\alpha'\alpha}J_{\beta'\beta}\mathsf{T}_{a\alpha\beta}(\boldsymbol{x}-\boldsymbol{\xi})+\\ +2J_{\alpha'\alpha}J_{\beta'\beta}\xi_3&\Big(-\xi_3\mathsf{D}_{a\alpha;\beta}(\boldsymbol{x}-\boldsymbol{\xi})-\mathsf{S}_{a3;\alpha\beta}(\boldsymbol{x}-\boldsymbol{\xi})-\delta_{3\beta}\mathsf{D}_{a\alpha}(\boldsymbol{x}-\boldsymbol{\xi})-\delta_{3\alpha}\mathsf{D}_{a\beta}(\boldsymbol{x}-\boldsymbol{\xi})+\delta_{\alpha\beta}\mathsf{D}_{3a}(\boldsymbol{x}-\boldsymbol{\xi})\Big)\end{aligned} \tag{2.111}$$

which possess the following far-field asymptotics

$$\mathrm{M}_a(\boldsymbol{x},\boldsymbol{\zeta}) = 2\mathsf{T}_{a33}(\boldsymbol{x}) + o(1/|\boldsymbol{x}|^2), \qquad |\boldsymbol{x}| \gg |\boldsymbol{\zeta}| \tag{2.112}$$

$$\mathrm{T}_{a\alpha'\beta'}(\boldsymbol{x},\boldsymbol{\zeta}) = 2\mathsf{T}_{a\alpha\beta}(\boldsymbol{x})(1-\delta_{\alpha\beta}-\delta_{\alpha1}\delta_{\beta2}-\delta_{\alpha2}\delta_{\beta1})+2\mathsf{T}_{a33}(\boldsymbol{x})\delta_{\alpha\beta}+o(1/|\boldsymbol{x}|^2), \qquad |\boldsymbol{x}| \gg |\boldsymbol{\zeta}| \tag{2.113}$$

Gathering eqs. (2.110) and (2.111) and substituting them into eq. (2.108), the analytic expression for the bounded Strainlet follows

$$\begin{aligned}\mathrm{E}_{a\alpha'\beta'}(\boldsymbol{x},\boldsymbol{\zeta}) &= \mathsf{E}_{a\alpha'\beta'}(\boldsymbol{x}-\boldsymbol{\zeta}) - J_{\alpha'\alpha}J_{\beta'\beta}\mathsf{E}_{a\alpha\beta}(\boldsymbol{x}-\boldsymbol{\xi})+\\ +2J_{\alpha'\alpha}J_{\beta'\beta}\xi_3&\Big(-\xi_3\mathsf{D}_{a\alpha;\beta}(\boldsymbol{x}-\boldsymbol{\xi})-\mathsf{S}_{a3;\alpha\beta}(\boldsymbol{x}-\boldsymbol{\xi})-\delta_{3\beta}\mathsf{D}_{a\alpha}(\boldsymbol{x}-\boldsymbol{\xi})-\delta_{3\alpha}\mathsf{D}_{a\beta}(\boldsymbol{x}-\boldsymbol{\xi})\Big)\end{aligned} \tag{2.114}$$

and putting $\xi_3 = -h$, one obtains

$$\mathrm{E}_{a\alpha'\beta'}(\boldsymbol{x},\boldsymbol{\zeta}) = \mathsf{E}_{a\alpha'\beta'}(\boldsymbol{x}-\boldsymbol{\zeta}) - J_{\alpha'\alpha}J_{\beta'\beta}\mathsf{E}_{a\alpha\beta}(\boldsymbol{x}-\boldsymbol{\xi})+ \\ -2hJ_{\alpha'\alpha}J_{\beta'\beta}\Big(h\mathsf{D}_{a\alpha;\beta}(\boldsymbol{x}-\boldsymbol{\xi}) - \mathsf{S}_{a3;\alpha\beta}(\boldsymbol{x}-\boldsymbol{\xi}) - \delta_{3\beta}\mathsf{D}_{a\alpha}(\boldsymbol{x}-\boldsymbol{\xi}) - \delta_{3\alpha}\mathsf{D}_{a\beta}(\boldsymbol{x}-\boldsymbol{\xi})\Big) \tag{2.115}$$

The vector plot of the bounded Strainlet is depicted in Fig. 2.4.

Appendix

2.A Biensor calculus

The development of bitensor calculus has followed two parallel pathways: an algebraic [211] and purely geometric approach [230, 56]. As the algebraic approach is particularly relevant in the present hydrodynamic theory of bounded Green functions, and moreover it is scarsely mentioned in the literature, this brief review on bitensor calculus is mainly focused on this formulation, addressing its connection with the geometric theory at the end of this Appendix.

In [211], Ruse defines bitensors as follows: Let $\boldsymbol{x} = (x^1, ..., x^n)$ and $\boldsymbol{\xi} = (\xi^1, ..., \xi^m)$ be two set of independent variables and let $\psi^{a'}(\boldsymbol{x})$, $a' = 1, \dots, n$ be n functions dependent on $\boldsymbol{x}$ and $\phi^{\alpha'}(\boldsymbol{\xi})$, $\alpha' = 1, \dots, m$, m functions dependent on $\boldsymbol{\xi}$, such that we can define the new variables

$$x^{b'} = \psi^{b'}(\boldsymbol{x}), \;\; b' = 1, \dots, n, \qquad \xi^{\beta'} = \phi^{\beta'}(\boldsymbol{\xi}), \;\; \beta' = 1, \dots, m$$

Let $T^{a\alpha}(\boldsymbol{x},\boldsymbol{\xi})$ denote the array of $n \times m$ functions depending on both x^a and ξ^α

$$\begin{pmatrix} T^{11}(\boldsymbol{x},\boldsymbol{\xi}) & ... & T^{1m}(\boldsymbol{x},\boldsymbol{\xi}) \\ ... & ... & ... \\ T^{n1}(\boldsymbol{x},\boldsymbol{\xi}) & ... & T^{nm}(\boldsymbol{x},\boldsymbol{\xi}) \end{pmatrix} \tag{2.116}$$

Moreover, let $T^{a'\alpha}(\mathrm{x}',\boldsymbol{\xi})$ be a set of functions depending on the variables $\boldsymbol{x}'$ and $\boldsymbol{\xi}$, $T^{a\alpha'}(\boldsymbol{x},\boldsymbol{\xi}')$ a set of functions depending on the variables $\boldsymbol{x}$ and $\boldsymbol{\xi}'$, $T^{a'\alpha'}(\boldsymbol{x}',\boldsymbol{\xi}')$ a set of functions depending on the variables $\boldsymbol{x}'$ and $\boldsymbol{\xi}'$. If these functions are related by the equations

$$T^{a\alpha}(\boldsymbol{x}',\boldsymbol{\xi}) = T^{b\alpha}(\boldsymbol{x},\boldsymbol{\xi})\,\frac{\partial x^{a'}}{\partial x^b} \tag{2.117}$$

$$T^{a\alpha'}(\boldsymbol{x},\boldsymbol{\xi}') = T^{a\beta}(\boldsymbol{x},\boldsymbol{\xi})\,\frac{\partial \xi^{\alpha'}}{\partial \xi^\beta} \tag{2.118}$$

$$T^{a'\alpha'}(\boldsymbol{x}',\boldsymbol{\xi}') = T^{b\beta}(\boldsymbol{x},\boldsymbol{\xi})\,\frac{\partial x^{a'}}{\partial x^b}\frac{\partial \xi^{\alpha'}}{\partial \xi^\beta} \tag{2.119}$$

then they are the components of the bivector $\boldsymbol{T}$ expressed in the systems of coordinates $(\boldsymbol{x},\boldsymbol{\xi})$, $(\boldsymbol{x}',\boldsymbol{\xi})$, $(\boldsymbol{x},\boldsymbol{\xi}')$, $(\boldsymbol{x}',\boldsymbol{\xi}')$, respectively. More generally a set of $n^{r+s} \times m^{p+q}$ functions are the components of a bitensor $\boldsymbol{T}$, if they are related by the equations

$$T^{a'_1 \dots a'_r \alpha_1 \dots \alpha_q}_{b'_1 \dots b'_s \beta_1 \dots \beta_p}(\boldsymbol{x}',\boldsymbol{\xi}) = T^{c_1 \dots c_r \alpha_1 \dots \alpha_q}_{d_1 \dots d_s \beta_1 \dots \beta_p}(\boldsymbol{x},\boldsymbol{\xi})\,\frac{\partial x^{a'_1}}{\partial x^{c_1}} \cdots \frac{\partial x^{a'_r}}{\partial x^{c_r}}\frac{\partial x^{d_1}}{\partial x^{b'_1}} \cdots \frac{\partial x^{d_s}}{\partial x^{b'_s}} \tag{2.120}$$

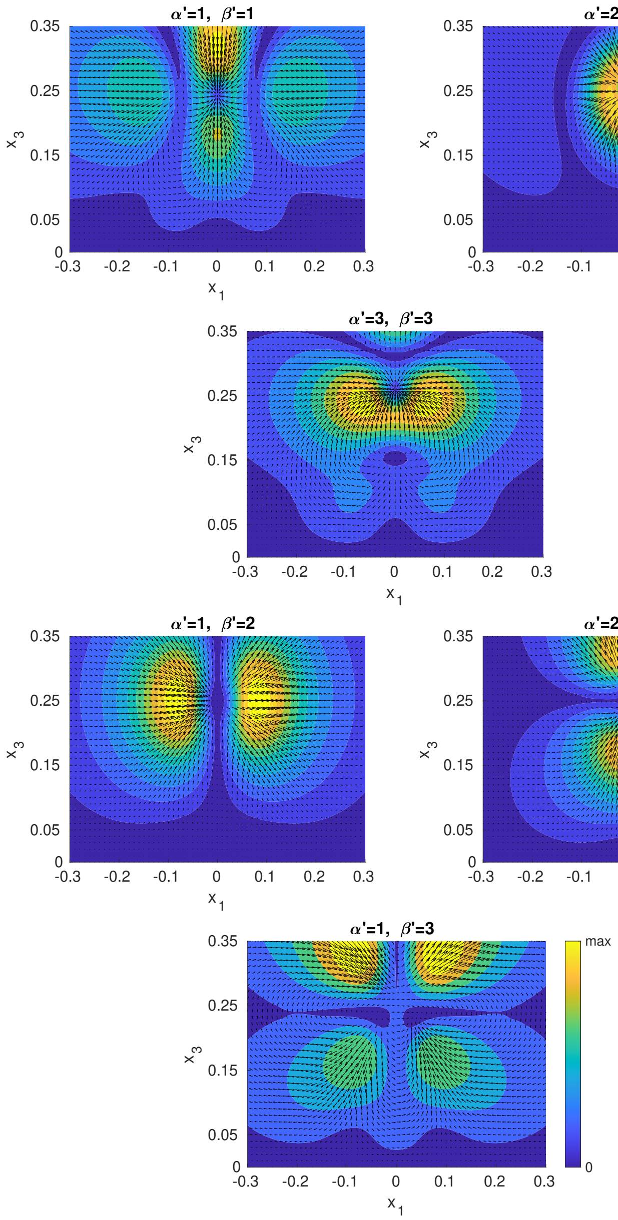

Figure 2.4. Vector plot of the components $(\mathrm{E}_{1\alpha'\beta'}(\boldsymbol{x},\boldsymbol{\zeta}), \mathrm{E}_{3\alpha'\beta'}(\boldsymbol{x},\boldsymbol{\zeta}))$ of the Strainlet with pole in $\boldsymbol{\zeta} = (0, 0, 0.25)$ evaluated on the plane $x_2 = 0.1$. The color map refers to the intensity $|(\mathrm{E}_{1\alpha'\beta'}(\boldsymbol{x},\boldsymbol{\zeta}), \mathrm{E}_{3\alpha'\beta'}(\boldsymbol{x},\boldsymbol{\zeta}))|$.

$$T^{a_1\ldots a_r\alpha'_1\ldots\alpha'_q}_{b_1\ldots b_s\beta'_1\ldots\beta'_p}(\boldsymbol{x},\boldsymbol{\xi}') = T^{a_1\ldots a_r\gamma_1\ldots\gamma_q}_{b_1\ldots b_s\delta_1\ldots\delta_p}(\boldsymbol{x},\boldsymbol{\xi})\frac{\partial\xi^{\alpha'_1}}{\partial\xi^{\gamma_1}}\cdots\frac{\partial\xi^{\alpha'_q}}{\partial\xi^{\gamma'_q}}\frac{\partial\xi^{\delta_1}}{\partial\xi^{\beta'_1}}\cdots\frac{\partial\xi^{\delta_p}}{\partial\xi^{\beta'_p}} \tag{2.121}$$

$$T^{a'_1\ldots a'_r\alpha'_1\ldots\alpha'_q}_{b'_1\ldots b'_s\beta'_1\ldots\beta'_p}(\boldsymbol{x}',\boldsymbol{\xi}') = T^{c_1\ldots c_r\gamma_1\ldots\gamma_q}_{d_1\ldots d_s\delta_1\ldots\delta_p}(\boldsymbol{x},\boldsymbol{\xi})\frac{\partial x^{a'_1}}{\partial x^{c_1}}\cdots\frac{\partial x^{a'_r}}{\partial x^{c_r}}\frac{\partial x^{d_1}}{\partial x^{b'_1}}\cdots\frac{\partial x^{d_s}}{\partial x^{b'_s}}\frac{\partial\xi^{\alpha'_1}}{\partial\xi^{\gamma_1}}\cdots\frac{\partial\xi^{\alpha'_q}}{\partial\xi^{\gamma_q}}\frac{\partial\xi^{\delta_1}}{\partial\xi^{\beta'_1}}\cdots\frac{\partial\xi^{\delta_p}}{\partial\xi^{\beta'_p}} \tag{2.122}$$

If $\boldsymbol{\xi}$ is kept fixed, then $T^{a1}...T^{am}$ are the components $(a = 1, \ldots, n)$ of m ordinary vectors at $\boldsymbol{x}$, whereas if $\boldsymbol{x}$ is kept fixed $T^{1\alpha}...T^{n\alpha}$ are the components $(\alpha = 1, \ldots, m)$ of n vectors at $\boldsymbol{\xi}$. The bitensor $T^{a\alpha}$ is, then, named vector-vector bitensor and, more generally, the bitensor $T^{a_1\ldots a_r\alpha_1\ldots\alpha_q}_{b_1\ldots b_s\beta_1\ldots\beta_p}$ is named $(r+s)$tensor-$(p+q)$tensor.

Next consider two symmetric scalar-(2)tensor $g_{ab}(\boldsymbol{x},\boldsymbol{\xi})$ and $\gamma_{\alpha\beta}(\boldsymbol{x},\boldsymbol{\xi})$, and suppose that $\boldsymbol{x}$ and $\boldsymbol{\xi}$ are two systems of coordinates of two distinct Riemannian spaces defined respectively by the two metric forms

$$ds^2 = g_{ab}(\boldsymbol{x},\boldsymbol{\xi})\, dx^a dx^b \tag{2.123}$$

$$d\sigma^2 = \gamma_{\alpha\beta}(\boldsymbol{x},\boldsymbol{\xi})\, d\xi^\alpha d\xi^\beta \tag{2.124}$$

Eqs. (2.123)-(2.124) define a multiple-infinite set of Riemannian spaces. In fact, fixed the set of variables $\boldsymbol{\xi}$, eq. (2.123) determines a Riemannian space, while fixing $\boldsymbol{x}$, a Riemannian space is determined by eq. (2.124). In the case that $n = m$, it is possible to define a vector-vector bitensor $k^a{}_\alpha(\boldsymbol{x},\boldsymbol{\xi})$, belonging to both spaces, so that

$$g_{ab}(\boldsymbol{x},\boldsymbol{\xi}) = k_a{}^\alpha(\boldsymbol{x},\boldsymbol{\xi})\, k_b{}^\beta(\boldsymbol{x},\boldsymbol{\xi})\, \gamma_{\alpha\beta}(\boldsymbol{x},\boldsymbol{\xi}) \tag{2.125}$$

which represents a system of $n(n+1)/2$ equations for the n^2 unknown components of $k^a{}_\alpha$ (due to the symmetry of g_{ab} and $\gamma_{\alpha\beta}$).

Note that, keeping either $\boldsymbol{x}$ or $\boldsymbol{\xi}$ fixed, the n ordinary vectors $k^1{}_\alpha...k^n{}_\alpha$ and $k^a{}_1...k^a{}_n$ are orthogonal to each other

$$k^c{}_\beta k_b{}^\beta = \delta^c_b \tag{2.126}$$

and similarly

$$k^b{}_\gamma k_b{}^\beta = \delta^\beta_\gamma \tag{2.127}$$

A particular case occurs when $g_{ab}(\boldsymbol{x},\boldsymbol{\xi}) = g_{ab}(\boldsymbol{x})$ does not depend on $\boldsymbol{\xi}$ and moreover $\gamma_{\alpha,\beta}(\boldsymbol{x},\boldsymbol{\xi}) = g_{\alpha\beta}(\boldsymbol{\xi})$. In this case, the two metric spaces defined by eqs. (2.123)-(2.124) represent the same metric space at two different points, and eq. (2.125) becomes

$$g_{ab}(\boldsymbol{x}) = k_a{}^\alpha(\boldsymbol{x},\boldsymbol{\xi})\, k_b{}^\beta(\boldsymbol{x},\boldsymbol{\xi})\, g_{\alpha\beta}(\boldsymbol{\xi}) \tag{2.128}$$

In Euclidean spaces, it is always possible to express the component of the metric tensors $g_{ab}(\boldsymbol{x})$, $g_{\alpha\beta}(\boldsymbol{\xi})$ in the same Cartesian coordinate system $X_{(i)} =$

$(X_{(1)}, X_{(2)}, X_{(3)})$, $(i) = 1, 2, 3$ being the indices for the Cartesian components. Thus, from eq. (2.128) one has

$$I_{(ij)} \frac{\partial X^{(i)}}{\partial x^a} \frac{\partial X^{(j)}}{\partial x^b} = k_a{}^{\alpha}(\boldsymbol{x}, \boldsymbol{\xi}) k_b{}^{\beta}(\boldsymbol{x}, \boldsymbol{\xi}) \frac{\partial X^{(i)}}{\partial \xi^\alpha} \frac{\partial X^{(j)}}{\partial \xi^\beta} I_{(ij)} \tag{2.129}$$

where $I_{(ij)} = \text{diag}(1, 1, 1)$ from which it follows that

$$k_a{}^{\alpha}(\boldsymbol{x}, \boldsymbol{\xi}) = \frac{\partial X^{(i)}}{\partial x^a} \frac{\partial \xi^\alpha}{\partial X^{(i)}} \tag{2.130}$$

that reduces to $k_a{}^{\alpha}(\boldsymbol{x}, \boldsymbol{\xi}) = \delta^a_\alpha$ if we choose the same coordinate system at both points.

If the coordinates of the two points are related by a bijective transformation

$$\xi^\alpha = \psi^\alpha(\boldsymbol{x}); \qquad x^a = g^\alpha(\boldsymbol{\xi}) \tag{2.131}$$

we can consider ξ^α and x^a as two set of coordinates of the same point and, by classical tensor calculus, we have

$$g_{ab}(\boldsymbol{x}) = \frac{\partial \xi^\alpha}{\partial x^a} \frac{\partial \xi^\beta}{\partial x^b} \, g_{\alpha\beta}(\boldsymbol{\xi}) \tag{2.132}$$

Comparing eq. (2.132) with eq. (2.128), we find

$$k^a{}_\alpha(x^a, \xi^\alpha) = \frac{\partial \xi^\alpha}{\partial x^a} \tag{2.133}$$

therefore, an ordinary transformation in the classical tensor calculus, can be viewed as a transformation between two metric spaces

$$ds^2 = g_{ab}(g^a(\boldsymbol{\xi})) \, dx^a \, dx^b \tag{2.134}$$

$$d\sigma^2 = g_{\alpha\beta}(\psi^\alpha(\boldsymbol{x})) \, d\xi^\alpha \, d\xi^\beta \tag{2.135}$$

If the two points belong to a generic Riemannian space, it is not always possible to express the components in the same Cartesian coordinate system. However, we can define, at one point, say $\boldsymbol{x}$, a triad of vector $e^a_{(i)}(\boldsymbol{x})$, forming locally an orthonormal basis, so that [72, 231]

$$g_{ab}(\boldsymbol{x}) e^a_{(i)}(\boldsymbol{x}) e^b_{(j)}(\boldsymbol{x}) = I_{(ij)}; \qquad e^a_{(i)}(\boldsymbol{x}) e^{(i)}_b(\boldsymbol{x}) = \delta^a_b \tag{2.136}$$

Parallel transporting the vectors $e^a_{(i)}(\boldsymbol{x})$ from the point $\boldsymbol{x}$ to the point $\boldsymbol{\xi}$, i.e., integrating the differential equation

$$\frac{De^a_{(i)}(\boldsymbol{z})}{Du} = \frac{\partial e^a_{(i)}(\boldsymbol{z})}{\partial z^k} \frac{dz^k}{du} + \Gamma^a_{bk} e^a_{(i)}(\boldsymbol{z}) \frac{dz^k}{du} = 0 \tag{2.137}$$

along the geodetics connecting the point $\boldsymbol{x}$ to $\boldsymbol{\xi}$, $\boldsymbol{z}(u)$ being a generic point on the geodetics identified by the parameter u and such that $\boldsymbol{z}(0) = \boldsymbol{x}$, we obtain the triad of vectors at the point $\boldsymbol{\xi}$, that is still orthonormal. Thus,

$$g_{\alpha\beta}(\boldsymbol{\xi}) \, e^\alpha_{(i)}(\boldsymbol{\xi}) \, e^\beta_{(j)}(\boldsymbol{\xi}) = I_{(ij)} \, , \qquad e^\alpha_{(i)}(\boldsymbol{\xi}) \, e^{(i)}_\beta(\boldsymbol{\xi}) = \delta^\alpha_\beta \tag{2.138}$$

Using eq. (2.136) and eq. (2.138), it is possible to express both the metric tensors $g_{ab}(\boldsymbol{x})$ and $g_{\alpha\beta}(\boldsymbol{\xi})$ in a common orthonormal basis. Eq. (2.129) thus, becomes

$$I_{(ij)}\, e_a^{(i)}(\boldsymbol{x})\, e_b^{(j)}(\boldsymbol{x}) = k_a{}^\alpha(\boldsymbol{x},\boldsymbol{\xi})\, k_b{}^\beta(\boldsymbol{x},\boldsymbol{\xi}) e_\alpha^{(i)}(\boldsymbol{\xi})\, e_\beta^{(j)}(\boldsymbol{\xi})\, I_{(ij)} \tag{2.139}$$

obtaining the more general expression for the parallel propagator

$$k_a{}^\alpha(\boldsymbol{x},\boldsymbol{\xi}) = e_a^{(i)}(\boldsymbol{x}) e_{(i)}^\alpha(\boldsymbol{\xi}) = k^\alpha{}_a(\boldsymbol{\xi},\boldsymbol{x}) \tag{2.140}$$

In the case the two points $\boldsymbol{x}$ and $\boldsymbol{\xi}$ become coincident, we have

$$\lim_{\boldsymbol{\xi}\to\boldsymbol{x}} \boldsymbol{k}(\boldsymbol{x},\boldsymbol{\xi}) = \lim_{\boldsymbol{\xi}\to\boldsymbol{x}} [k_a{}^\alpha(\boldsymbol{x},\boldsymbol{\xi})] = \lim_{\boldsymbol{\xi}\to\boldsymbol{x}} [e_a^{(i)}(\boldsymbol{x})\, e_{(i)}^\alpha(\boldsymbol{\xi})] = [\delta_a^\alpha] = \boldsymbol{I} \tag{2.141}$$

where $[\cdot]$ indicate the whole tensorial entity. Consequently,

$$\lim_{\boldsymbol{\xi}\to\boldsymbol{x}} k_{a\alpha}(x^a,\xi^\alpha) = \lim_{\boldsymbol{\xi}\to\boldsymbol{x}}\; g_{ab}(\boldsymbol{x})\, k^b{}_\alpha(\boldsymbol{x},\boldsymbol{\xi}) = g_{ab}(\boldsymbol{x})\,, \qquad \lim_{\boldsymbol{x}\to\boldsymbol{\xi}} k_{a\alpha}(\boldsymbol{x},\boldsymbol{\xi}) = g_{\alpha\beta}(\boldsymbol{\xi}) \tag{2.142}$$

Therefore, it is customary to use the same symbol for indicating either the parallel propagator or the metric tensor

$$g_a{}^\alpha(\boldsymbol{x},\boldsymbol{\xi}) = k_a{}^\alpha(\boldsymbol{x},\boldsymbol{\xi})$$

To make an example, consider a unit vector $p^a(\boldsymbol{x})$ at $\boldsymbol{x}$,

$$g_{ab}(\boldsymbol{x}) p^a(\boldsymbol{x}) p^b(\boldsymbol{x}) = 1 \tag{2.143}$$

Using the definition of the parallel propagator eq . (2.128)

$$g_{\alpha\beta}(\boldsymbol{\xi})\, k_a{}^\alpha(\boldsymbol{x},\boldsymbol{\xi})\, p^a(\boldsymbol{x})\, k_b{}^\beta(\boldsymbol{x},\boldsymbol{\xi})\, p^b(\boldsymbol{x}) = g_{\alpha\beta}(\boldsymbol{\xi})\, p^\alpha(\boldsymbol{\xi})\, p^\beta(\boldsymbol{\xi}) = 1 \tag{2.144}$$

we have

$$p^\alpha(\boldsymbol{\xi}) = p^a(\boldsymbol{x})\, k_a{}^\alpha(\boldsymbol{x},\boldsymbol{\xi}) \tag{2.145}$$

that represents the unit vector parallel-transported from the point $\boldsymbol{x}$ to the point $\boldsymbol{\xi}$. In fact, since

$$p^\alpha(\boldsymbol{\xi}) = p^a(\boldsymbol{x}) e_{(i)}^\alpha(\boldsymbol{\xi}) e_a^{(i)}(\boldsymbol{x}) \tag{2.146}$$

we have in the triad basis

$$p^{(i)}(\boldsymbol{\xi}) = p^\alpha(\xi^\alpha)\, e_\alpha^{(i)}(\boldsymbol{\xi}) = p^a(\boldsymbol{x})\, e_a^{(i)}(\boldsymbol{x}) = p^{(i)}(\boldsymbol{x}) \tag{2.147}$$

and thus the components of the vector $p^\alpha(\boldsymbol{\xi})$ in the common triad basis coincide with those of $p^a(\boldsymbol{x})$. From this result, and from the property

$$v^a(\boldsymbol{x})\, p_a(\boldsymbol{x}) = v^a(\boldsymbol{x})\, g_a{}^\alpha(\boldsymbol{x},\boldsymbol{\xi})\, p_\alpha(\boldsymbol{\xi}) = v^\alpha(\boldsymbol{\xi})\, p_\alpha(\boldsymbol{\xi}) \tag{2.148}$$

it follows that any vector $v^a(\boldsymbol{x})$ can be the parallel transported from $\boldsymbol{x}$ to $\boldsymbol{\xi}$‘ via the relation

$$v^\alpha(\boldsymbol{\xi}) = v^a(\boldsymbol{x})\, g_a{}^\alpha(\boldsymbol{x},\boldsymbol{\xi}) \tag{2.149}$$

To conclude, an important bitensor is the so called Synge's world function [230], that is a measure of the geodetic distance between the points $\boldsymbol{x}$ and $\boldsymbol{\xi}$, defined as

$$W(\boldsymbol{x},\boldsymbol{\xi}) = \frac{1}{2}\int_{\boldsymbol{\xi}}^{\boldsymbol{x}} ds^2 \tag{2.150}$$

In Euclidean spaces, it can be explicited as as

$$W(\boldsymbol{x},\boldsymbol{\xi}) = \frac{1}{2} I_{(ij)}(x^{(i)} - \xi^{(i)})(x^{(j)} - \xi^{(j)}) \tag{2.151}$$

$x^{(i)}$ and $\xi^{(i)}$ being the Cartesian coordinates of the two points. Its derivative at $\boldsymbol{x}$ is

$$W_a(\boldsymbol{x},\boldsymbol{\xi}) = (x^{(i)} - \xi^{(i)})\, I_{(ij)} \frac{\partial X^{(j)}}{\partial x^a} = (\boldsymbol{x} - \boldsymbol{\xi})_a \tag{2.152}$$

while the corresponding derivative at $\boldsymbol{\xi}$ reads

$$W_\alpha(\boldsymbol{x},\boldsymbol{\xi}) = (\xi^{(i)} - x^{(i)})\, I_{(ij)} \frac{\partial X^{(j)}}{\partial \xi^\alpha} = (\boldsymbol{\xi} - \boldsymbol{x})_\alpha = -\delta^a_\alpha (\boldsymbol{x} - \boldsymbol{\xi})_a \tag{2.153}$$

Let $(\boldsymbol{x} - \boldsymbol{\xi})_\alpha = g_\alpha{}^a(\boldsymbol{\xi},\boldsymbol{x})(\boldsymbol{x} - \boldsymbol{\xi})_a$ and $(\boldsymbol{\xi} - \boldsymbol{x})_a = g_a{}^\alpha(\boldsymbol{x},\boldsymbol{\xi})(\boldsymbol{\xi} - \boldsymbol{x})_\alpha$. From eq. (2.153) we have

$$\begin{aligned}(\boldsymbol{x} - \boldsymbol{\xi})_{\alpha_1}...(\boldsymbol{x} - \boldsymbol{\xi})_{\alpha_n} &= (-1)^n(\boldsymbol{\xi} - \boldsymbol{x})_{\alpha_1}...(\boldsymbol{\xi} - \boldsymbol{x})_{\alpha_n}\\ (\boldsymbol{\xi} - \boldsymbol{x})_{a_1}...(\boldsymbol{\xi} - \boldsymbol{x})_{a_n} &= (-1)^n(\boldsymbol{x} - \boldsymbol{\xi})_{a_1}...(\boldsymbol{x} - \boldsymbol{\xi})_{a_n}\end{aligned} \tag{2.154}$$

that is a useful relation in moment analysis.

Chapter 3

Singularity and Faxén operators and the Hinch-Kim's dualism

3.1 Introduction

One of the most powerful mathematical tools to investigate particle-fluid interactions is, when available, the so called Faxén operator, which is the operator that once applied to a generic ambient flow (defined as the flow of the fluid without the disturbance due to the particle inclusion), furnishes forces, torques, stresses and higher-order moments on the particle, without the need of solving the specific hydrodynamic problem. The introduction of this operator is originally due to Hilding Faxén (hence the name, see [185] or [98]), who found that the force acting on a sphere with no-slip boundary conditions immersed in a generic ambient flow can be expressed in a simple way in terms of the value of the ambient field and of its Laplacian at the center of the sphere. Moreover, the torque is proportional to the vorticity of the ambient field at the center of the sphere. The Faxén laws for the no-slip sphere are, essentially, an application to the solutions of the Stokes equations [194] of the mean value theorem for biharmonic (the velocity solution of the Stokes equations) and harmonic (the vorticity) functions, yielding, respectively, the 0-th and the asymmetric 1-st order moments of surface traction on the surface of the sphere.

Thereafter, many authors have obtained Faxén operators for several combinations of surface moments, shapes of immersed bodies, boundary conditions, fluid regimes. In the case of the stationary Stokes regime, literature results include the analytic expressions for the Faxén operators of lower orders, specifically: the symmetric 1-st order operator for a sphere with no-slip boundary conditions [9], 0-th and 1-st order for spheroids [101, 128] and, more generally for ellipsoids [25, 129] with no-slip boundary conditions, 0-th and 1-st order for a spherical Newtonian drop [103, 207], 0-th and asymmetric 1-st order operators for a sphere with Navier-slip boundary conditions [197], 0-th and asymmetric 1-st order operators for porous spheres using the Darcy model [188], and 0-th and 1-st order using the Brinkman model [71, 187]. Faxén operators for spheres has been obtained in other flow regimes: 0-th and asymmetric 1-st order operators for a sphere with no-slip boundary conditions in unsteady Stokes flow [169, 167, 245] and for the linearized compressible Navier-

Stokes flow [12], 0-th order operator for a spherical Newtonian drop [122], 0-th and asymmetric 1-st operators for a sphere with Navier-slip boundary conditions in unsteady Stokes flows [70, 196], 0-th and 1-st order operators for porous spheres using the Brinkman model [121], 0-th order Faxén counterpart for a sphere in a potential flow [233].

By definition, a Faxén operator is independent of the ambient flow and the viscosity of the fluids, and depends solely on the geometrical structure of the body and on the parameters specifying the boundary conditions. An explicit expression of the Faxén operator for forces and torques has been given by Brenner [25] for bodies with no-slip conditions and arbitrary shape in terms of an infinite series of differential operators with polidiadic coefficients. The Brenner coefficients depend only on the geometry of the body and correspond to: i) the moments of the surface traction associated with the solution of the Stokes problem for the translating body in the unbounded fluid (in the case of the Faxén operator for the force), and, ii) the moments of the surface traction related the solution of the Stokes problem for the rotating body in the unbounded fluid (in the case of the Faxén operator for the torque).

Hinch [105] observed that the operator applied to the pole of the unbounded Green function of the Stokes flow (usually referred to as the Stokeslet [130]) and returning the disturbance field generated by a no-slip sphere in a symmetric linear flow is exactly the 1-order symmetric Faxén operator found by Batchelor and Green [9], thus intuitively concluding that this is not a simple coincidence but the consequence of the Lorentz reciprocal theorem for the Stokes flows. The dualism between the singularity representation of the flow generated by an arbitrary body immersed in a fluid and the Faxén operators of the body have been proved in a conclusive way by Kim [128] by means of the Lorentz reciprocal theorem. More precisely, in the case no-slip boundary conditions at the body surface are assumed, the Faxén operator for the force of a body with an arbitrary shape coincides (up to a multiplicative constant $8\pi\mu$, where μ is the viscosity of the fluid) with the operator that, applied to the pole of the Stokeslet, yields the velocity field of the fluid due to the translations of the body. The extension of the dualism between higher-order Faxén operators (torques, stresslet, etc.) and higher order singularity operators (giving the field for rotations, strains, etc.) is a straightforward consequence of the Kim's proof. In this thesis, this correspondence is referred as the *Hinch-Kim dualism*.

Hinch-Kim dualism implies several important consequences of theoretical and practical interest: i) by solving a single hydrodynamic problem (either analytically or numerically) it is possible to obtain a Faxén operator even for particles with complex shapes (at least for the leading order terms), ii) the flow generated by an immersed particle can be represented in a compact way by its Faxén operator, the leading-order terms of which can be evaluated using the Brenner polidiadic expansion even for particles with complex shapes, iii) long range particle-particle and particle-channel interactions can be investigated taking advantage of this symmetry in order to obtain hydrodynamic properties of complex systems of particles [9, 8, 105, 21, 166], of active microswimmers near walls [226, 136, 57], of microfluidic flow and separation devices [28, 229], either applying theoretical approaches or by means of numerical methods, such as the Stokesian dynamics [22].

The last two decades have seen a growing interest in generalizing the nature of the boundary conditions, going beyond the no-slip case, and in investigating the interactions with ambient flows more complex then purely constant and linear fields. This is mainly due to: i) the rise of microfluidics [241], where surfaces are chemically treated and the properties of the resulting solid-liquid interfaces exploited, hinging for a more detailed hydrodynamic description [146], ii) the development of the hydromechanics of biological particles [145], where the assumption of rigid translating and rotating particles equipped with no-slip boundary conditions is evidently too simplified and limiting, and where it has been verified that the inclusion of only lower order moments, such as forces, torques and stresslets, is not sufficient to explain many interesting hydrodynamics behaviors of biological particles [178].

The scope of this contribution is to generalize and extend the results obtained for the singularity and Faxén operators and their mutual relationships enforcing no-slip at the solid boundaries to generic boundary conditions and to ambient flows of any order. This extension yields several novel results related to: i) the analytic expression for the singularity operator in terms of volume moments, ii) the definition of an analytic criterion upon which the Hinch-Kim duality holds, iii) the application of this criterion to a broad class of boundary conditions of hydrodynamic interest. The main technical tool in the present theory is the bitensorial distributional analysis developed in Chapter 2, in which the moments with respect to the volume forces acting on the body - instead of the moments associated with the surface tractions considered in the literature - are introduced and applied in order to express the singularity expansion of a disturbance flow. Incidentally, these two hierarchies of moments coincide in the no-slip case. The advantage of this approach is that it makes it possible to obtain a general expression for the singularity operator of a disturbance flow in terms of an infinite series of differential operators with the moments of the volume forces as coefficients, independently of the boundary conditions assumed at the fluid-body interface.

The chapter is organized as follows. Section 3.2 the problem briefly is formulated in a suitable manner for the topic of the chapter. In Section 3.3 it is provided the definition of the (n, m)-th order geometrical moments as the m-th order moments on the body immersed in an n-th order ambient field, and it is shown that the n-th order singularity operator of an arbitrary body can be expressed in series of differential operators with the (n, m)-th order geometrical moments as coefficients. In Section 3.4, it is investigated the Hinch-Kim dualism between n-th order singularity operators and n-th order Faxén operator for an arbitrary body. It is shown that the dualism is not a general property deriving from the Lorentz reciprocity theorem, as it applies solely to a subclass of boundary conditions assumed at the surface of the body, and defined by a parity condition that we call *boundary condition reciprocity*. It is shown that, whenever this dualism holds (hence reciprocal boundary conditions are considered), the Brenner expression for the Faxén operators can be generalized by considering the moments of the volume forces. In addition, it is possible to generalize also the property found in [201], namely that the hydromechanics of a body in Stokes flows is completely described by the entire set of its Faxén operators (or geometrical moments). A similar investigation of the Hinch-Kim dualism has been carried out by Dolata and Zia [59] following a method, completely different from the present approach, based on energetic considerations and expressing the reciprocity between operators instead of fields. Although their main result (the conditions under which the dualism hold) can be mapped into the present theory, these authors have reached some misleading conclusions, such as the validity of the dualism for porous particles modeled by the Darcy law. In the present chapter, it is shown that this is not the case. In fact, in the second part of this work (from Section 3.5 to Section 3.7) it is analyzed a broad class of typical hydrodynamic boundary conditions, determining, case by case, whether the dualism holds or not. In Section 3.5, the boundary conditions at the solid-fluid interface are investigated, finding that the dualism holds for rigid bodies with Navier-slip boundary conditions (even with a non uniform slip length along the surface), but not for linear elastic bodies in deformation. In Section 3.6, the dualism for fluid-fluid boundary conditions is analyzed, finding that it is verified solely for Newtonian drops at the mechanical equilibrium. In Section 3.7, it is considered the case of porous bodies, finding that the dualism applies in the Brinkman model for porous media, but not for the Darcy model. Finally, it is used the analytical approach developed in the previous Sections to obtain a closed-form expression for the 0-th (already available in literature [197]), 1-st and 2-nd (to the best of our knowledge, not yet present in the literature) order Faxén operators for a sphere with Navier-slip boundary conditions.

3.2 Formulation of the problem

Consider a body immersed in a unbounded Stokes fluid. The domain of the body is $D_b \subset \mathbb{R}^3$ with boundaries ∂D_b and the domain of the fluid is $D_f \equiv \mathbb{R}^3/D_b$ with boundaries $\partial D_f \equiv \partial D_b \cup \partial D_\infty$, where ∂D_∞ is an ideal surface at infinity. The *ambient flow* of the fluid (i.e. the flow of the fluid without the body inclusion) is $\boldsymbol{u}(\boldsymbol{x})$ with associated pressure $p(\boldsymbol{x})$ and stress tensor $\boldsymbol{\pi}(\boldsymbol{x})$, solution of the Stokes equations

$$\begin{cases} -\nabla \cdot \boldsymbol{\pi}(\boldsymbol{x}) = \mu \Delta \boldsymbol{u}(\boldsymbol{x}) - \nabla p(\boldsymbol{x}) = 0 \\ \nabla \cdot \boldsymbol{u}(\boldsymbol{x}) = 0 \qquad \boldsymbol{x} \in \mathbb{R}^3 \end{cases} \tag{3.1}$$

The presence of the body generates a *disturbance flow* at the boundaries ∂D_b of the body, that we indicate as $\boldsymbol{w}^S(\boldsymbol{x})$, and thus, a disturbance flow $\boldsymbol{w}(\boldsymbol{x})$ in the whole domain of the fluid with associated pressure $q(\boldsymbol{x})$ and stress tensor $\boldsymbol{\tau}(\boldsymbol{x})$ that are solution of the Stokes equations

$$\begin{cases} -\nabla \cdot \boldsymbol{\tau}(\boldsymbol{x}) = \mu \Delta \boldsymbol{w}(\boldsymbol{x}) - \nabla q(\boldsymbol{x}) = 0 \\ \nabla \cdot \boldsymbol{w}(\boldsymbol{x}) = 0 \qquad \boldsymbol{x} \in D_f \\ \boldsymbol{w}(\boldsymbol{x}) = \boldsymbol{w}^S(\boldsymbol{x}),\ \boldsymbol{\tau}(\boldsymbol{x}) = \boldsymbol{\tau}^S(\boldsymbol{x}) \qquad \boldsymbol{x} \in \partial D_b \end{cases} \tag{3.2}$$

where $\boldsymbol{\tau}^S(\boldsymbol{x})$ is the stress tensor of the disturbance flow at the surface of the body.

The total field $(\boldsymbol{v}(\boldsymbol{x}), \boldsymbol{\sigma}(\boldsymbol{x})) = (\boldsymbol{u}(\boldsymbol{x}), \boldsymbol{\pi}(\boldsymbol{x})) + (\boldsymbol{w}(\boldsymbol{x}), \boldsymbol{\tau}(\boldsymbol{x}))$ is the solution of the Stokes equations

$$\begin{cases} -\nabla \cdot \boldsymbol{\sigma}(\boldsymbol{x}) = \mu \Delta \boldsymbol{v}(\boldsymbol{x}) - \nabla s(\boldsymbol{x}) = 0 \\ \nabla \cdot \boldsymbol{v}(\boldsymbol{x}) = 0 \qquad \boldsymbol{x} \in D_f \\ \boldsymbol{v}(\boldsymbol{x}) = \boldsymbol{v}^S(\boldsymbol{x}),\ \boldsymbol{\sigma}(\boldsymbol{x}) = \boldsymbol{\sigma}^S(\boldsymbol{x}) \qquad \boldsymbol{x} \in \partial D_b \\ \boldsymbol{v}(\boldsymbol{x}) = \boldsymbol{u}(\boldsymbol{x}) \qquad \boldsymbol{x} \to \infty \end{cases} \tag{3.3}$$

$s(\boldsymbol{x}) = p(\boldsymbol{x}) + q(\boldsymbol{x})$ being the total pressure field, $\boldsymbol{v}^S(\boldsymbol{x}) = \boldsymbol{w}^S(\boldsymbol{x}) + \boldsymbol{u}(\boldsymbol{x})$ and $\boldsymbol{\sigma}^S(\boldsymbol{x}) = \boldsymbol{\tau}^S(\boldsymbol{x}) + \boldsymbol{\pi}(\boldsymbol{x})$ the total velocity field and stress tensor, respectively, at the surface of the body.

As shown in Chapter 2, it is possible to express the disturbance flow as the solution of the non-homogeneous Stokes equations defined in the whole domain $\mathbb{R}^3$

$$\begin{cases} -\nabla \cdot \boldsymbol{\tau}(\boldsymbol{x}) = \mu \Delta \boldsymbol{w}(\boldsymbol{x}) - \nabla q(\boldsymbol{x}) = -\boldsymbol{\psi}(\boldsymbol{x}) \\ \nabla \cdot \boldsymbol{w}(\boldsymbol{x}) = 0 \qquad \boldsymbol{x} \in D_f \end{cases} \tag{3.4}$$

$\boldsymbol{\psi}(\boldsymbol{x})$ being any force field distribution, with compact support in D_b, satisfying the relation

$$\frac{1}{8\pi\mu} \int_{D_b} \psi_\alpha(\boldsymbol{\xi}) S_{a\,\alpha}(\boldsymbol{x}, \boldsymbol{\xi}) dV(\boldsymbol{\xi}) = w_a^S(\boldsymbol{x}) \qquad \boldsymbol{x} \in \partial D_b \tag{3.5}$$

where $dV(\boldsymbol{\xi})$ is the volume element at $\boldsymbol{\xi}$ and $S_{a\,\alpha}(\boldsymbol{x}, \boldsymbol{\xi})$ are the entries of the Oseen bitensor or Stokeslet and where the bitensorial formalism developed in the previous chapter is used.

Since we are analyzing bodies immersed in a unbounded fluid and since, for the sake of simplicity, we consider the poles of singularities located at a single point, it is always possible to express both source and field points in the same Cartesian coordinate system, and thus the parallel propagator [201, 190] is simply $g_{a\alpha}(\boldsymbol{x}, \boldsymbol{\xi}) = \delta_{a\alpha}$. However, behind the formal correctness in distinguishing entries at different points, the use of the bitensorial convention provides, apart from a higher notational clearness, some practical advantages. Specifically, i) it provides a direct extension of the results obtained in simple systems to more complex geometries, ii) the points where operators are applied are naturally specified, iii) different properties and symmetries between the entries are clearly highlighted.

As shown in the previous chapter, it is possible to express the disturbance velocity field by means of a differential operator applied at the pole point of the Stokeslet

$$w_a(\boldsymbol{x}) = \frac{1}{8\pi\mu} \sum_{n=0}^{\infty} \frac{M_{\alpha \boldsymbol{\alpha}_n}(\boldsymbol{\xi})}{n!} \nabla_{\boldsymbol{\alpha}_n} S_{a\,\alpha}(\boldsymbol{x}, \boldsymbol{\xi}) \tag{3.6}$$

and similarly for the pressure

$$q(\boldsymbol{x}) = \frac{1}{8\pi} \sum_{n=0}^{\infty} \frac{M_{\alpha \boldsymbol{\alpha}_n}(\boldsymbol{\xi})}{n!} \nabla_{\boldsymbol{\alpha}_n} P_\alpha(\boldsymbol{x}, \boldsymbol{\xi}) \tag{3.7}$$

and for the stress field

$$\tau_{ab}(\boldsymbol{x}) = \frac{1}{8\pi} \sum_{n=0}^{\infty} \frac{M_{\alpha \boldsymbol{\alpha}_n}(\boldsymbol{\xi})}{n!} \nabla_{\boldsymbol{\alpha}_n} \Sigma_{a\,b\,\alpha}(\boldsymbol{x}, \boldsymbol{\xi}) \tag{3.8}$$

where $\boldsymbol{\alpha}_n = \alpha_1 ... \alpha_n$ is a multi-index, $(\boldsymbol{x} - \boldsymbol{\xi})_{\boldsymbol{\alpha}_n} = (\boldsymbol{x} - \boldsymbol{\xi})_{\alpha_1} ... (\boldsymbol{x} - \boldsymbol{\xi})_{\alpha_n}$ and $\nabla_{\boldsymbol{\alpha}_n} = \nabla_{\alpha_1} ... \nabla_{\alpha_n}$. Where the n-th order moments are

$$M_{\alpha \boldsymbol{\alpha}_n}(\boldsymbol{\xi}) = \int_{D_b} (\boldsymbol{x} - \boldsymbol{\xi})_{\boldsymbol{\alpha}_n} \psi_\alpha(\boldsymbol{x}) dV(\boldsymbol{x}) \tag{3.9}$$

where, formally, $\psi_\alpha(\boldsymbol{x}) = \delta_{\alpha a} \psi_a(\boldsymbol{x})$ are the entries of the force field distribution at the point $\boldsymbol{x}$ expressed in the coordinate system of the point $\boldsymbol{\xi}$ and where $dV(\boldsymbol{x})$ is the volume element at the point $\boldsymbol{x}$.

In [201, Appendix B], it is shown that the moments defined by eq. (3.9) reduce to the surface moments defined by several authors [61, 115, 130] in the case no-slip boundary conditions are imposed at the surface of the body ∂D_b. However, the definition of moments in eq. (3.9) does not refer to any specific boundary condition, and therefore the expressions (3.6)-(3.8) are valid regardless of the boundary conditions imposed at the surface of the body. The evaluation of the moments directly from their definition is not an easy task since the distribution $\boldsymbol{\psi}(\boldsymbol{x})$ (in principle not unique) is not known. In the next section, we provide the surface integral expression valid for generic boundary conditions by resuming the same method.

3.3 Generalized geometrical moment expansion

Consider a n-th order unbounded polynomial ambient Stokes flow, singular at infinity and centered at a point $\boldsymbol{\xi} \in D_b$ (see the schematic representation in Fig. 3.1)

$$\begin{aligned} &u_a^{(n)}(\boldsymbol{x},\boldsymbol{\xi}) = A_{a\boldsymbol{a}_n}(\boldsymbol{x}-\boldsymbol{\xi})_{\boldsymbol{a}_n} \\ &A_{a\boldsymbol{a}_n}\nabla_a(\boldsymbol{x}-\boldsymbol{\xi})_{\boldsymbol{a}_n} = 0, \qquad \varepsilon_{abc}\, A_{b\,\boldsymbol{a}_n}\Delta\nabla_c(\boldsymbol{x}-\boldsymbol{\xi})_{\boldsymbol{a}_n} = 0 \end{aligned} \tag{3.10}$$

where hereafter the superscript (n) indicates any quantity referred to a n-th order ambient flow and ε_{abc} is the Ricci-Levi Civita symbol. The associated ambient pressure and stress tensor are, by linearity

$$\begin{aligned} &p^{(n)}(\boldsymbol{x},\boldsymbol{\xi}) = \mu A_{a\boldsymbol{a}_n}\, p_{a\boldsymbol{a}_n}(\boldsymbol{x},\boldsymbol{\xi}), \qquad \pi_{bc}^{(n)}(\boldsymbol{x},\boldsymbol{\xi}) = \mu A_{a\boldsymbol{a}_n}\pi_{bca\boldsymbol{a}_n}(\boldsymbol{x},\boldsymbol{\xi}) \\ &\pi_{bca\boldsymbol{a}_n}(\boldsymbol{x},\boldsymbol{\xi}) = [\delta_{bc}p_{a\boldsymbol{a}_n}(\boldsymbol{x},\boldsymbol{\xi}) - (\delta_{ac}\nabla_b(\boldsymbol{x}-\boldsymbol{\xi})_{\boldsymbol{a}_n} + \delta_{ab}\nabla_c(\boldsymbol{x}-\boldsymbol{\xi})_{\boldsymbol{a}_n})] \end{aligned} \tag{3.11}$$

so that the Stokes equation, expressed in terms of $\pi_{bca\boldsymbol{a}_n}(\boldsymbol{x},\boldsymbol{\xi})$, becomes

$$\mu A_{a\boldsymbol{a}_n}\nabla_b\pi_{bca\boldsymbol{a}_n}(\boldsymbol{x},\boldsymbol{\xi}) = 0 \tag{3.12}$$

Chwang and Wu introduced in [41] an external singularity, referred to as the *Stokeson*, which is a particular case of eq. (3.11) choosing $A_{aa_1a_2} = f_\alpha(\delta_{a\alpha}\delta_{a_1a_2} - \delta_{a_1\alpha}\delta_{aa_2})$, f_α being the intensity.

Consider a generic total velocity field for a body immersed in an ambient field $\boldsymbol{v}(\boldsymbol{x}) = \boldsymbol{u}(\boldsymbol{x}) + \boldsymbol{w}(\boldsymbol{x})$ in the non-homogeneous form defined in $\mathbb{R}^3$

$$\begin{cases} -\nabla\cdot\boldsymbol{\sigma}(\boldsymbol{x}) = \mu\Delta\boldsymbol{v}(\boldsymbol{x}) - \nabla s(\boldsymbol{x}) = -\boldsymbol{\psi}(\boldsymbol{x}) \\ \nabla\cdot\boldsymbol{v}(\boldsymbol{x}) = 0 \qquad \boldsymbol{x}\in\mathbb{R}^3 \\ \boldsymbol{v}(\boldsymbol{x}) = \boldsymbol{u}(\boldsymbol{x}) \qquad \boldsymbol{x}\to\infty \end{cases} \tag{3.13}$$

The application of the Lorentz reciprocal theorem in the differential form [194] to the fields $(\boldsymbol{u}^{(n)}(\boldsymbol{x},\boldsymbol{\xi}), \boldsymbol{\pi}^{(n)}(\boldsymbol{x},\boldsymbol{\xi}))$ and $(\boldsymbol{v}(\boldsymbol{x}),\boldsymbol{\sigma}(\boldsymbol{x}))$ provides

$$u_a^{(n)}(\boldsymbol{x},\boldsymbol{\xi})\nabla_b\sigma_{ab}(\boldsymbol{x}) - v_a(\boldsymbol{x})\nabla_b\pi_{ab}^{(n)}(\boldsymbol{x},\boldsymbol{\xi}) = \nabla_b\left[u_a^{(n)}(\boldsymbol{x},\boldsymbol{\xi})\sigma_{ab}(\boldsymbol{x}) - v_a(\boldsymbol{x})\pi_{ab}^{(n)}(\boldsymbol{x},\boldsymbol{\xi})\right] \tag{3.14}$$

From eq. (3.14), considering that $\nabla_b\pi_{bc}^{(n)}(\boldsymbol{x},\boldsymbol{\xi}) = 0$ and making use of (3.10)-(3.13), it follows that

$$\psi_a(\boldsymbol{x})(\boldsymbol{x}-\boldsymbol{\xi})_{\boldsymbol{a}_n} = \nabla_b\left[\sigma_{ab}(\boldsymbol{x})(\boldsymbol{x}-\boldsymbol{\xi})_{\boldsymbol{a}_n} - \mu v_c(\boldsymbol{x})\,\pi_{bca\boldsymbol{a}_n}(\boldsymbol{x},\boldsymbol{\xi})\right] \tag{3.15}$$

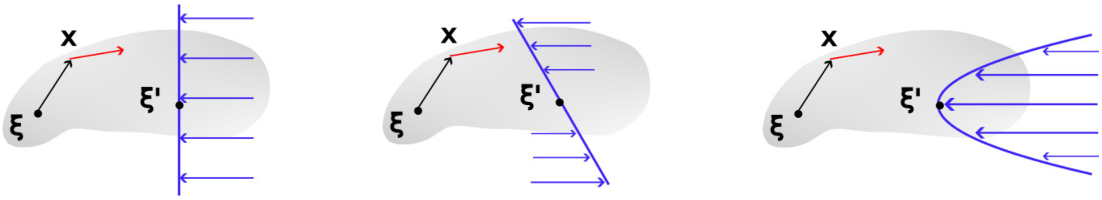

Figure 3.1. Schematic representation of a body immersed in an 0-th, 1-st and 2-nd order polynomial ambient flow centered at the point $\boldsymbol{\xi}'$ (blue arrows) as defined by eqs. (3.10)-(3.12). Black arrows represent the position vector with respect the point $\boldsymbol{\xi}$ of the force field $\boldsymbol{\psi}(\boldsymbol{x})$ (red arrows) by which geometrical moments, defined in eq. (3.18), are evaluated.

Integrating the latter equation over the volume of the body, using the Gauss theorem for the r.h.s of the resulting equation, and enforcing the definition eq. (3.9), the moments on volume forces $M_{\alpha\boldsymbol{\alpha}_n}(\boldsymbol{\xi})$ can be expressed as the surface integrals

$$M_{\alpha\boldsymbol{\alpha}_n}(\boldsymbol{\xi}) = \int_{\partial D_b} \left[\sigma_{\alpha b}(\boldsymbol{x})(\boldsymbol{x}-\boldsymbol{\xi})_{\boldsymbol{\alpha}_n} - \mu v_c(\boldsymbol{x})\, \pi_{bc\alpha\boldsymbol{\alpha}_n}(\boldsymbol{x},\boldsymbol{\xi})\right] n_b(\boldsymbol{x}) dS(\boldsymbol{x}) \tag{3.16}$$

where $n_b(\boldsymbol{x})$ are the entries of the outwardly oriented normal unit vector at point $\boldsymbol{x}$ of ∂D_b and $\sigma_{\alpha b}(\boldsymbol{x}) = \delta_{\alpha a}\sigma_{ab}(\boldsymbol{x})$. Therefore, by using the expression eq. (3.11) for $\pi_{bca\boldsymbol{a}_n}(\boldsymbol{x},\boldsymbol{\xi})$, the functional relation connecting the moments to the values of $\boldsymbol{v}(\boldsymbol{x})$ and $\boldsymbol{\sigma}(\boldsymbol{x})$ assigned at the boundary of the body follows

$$\begin{aligned} M_{\alpha\boldsymbol{\alpha}_n}(\boldsymbol{\xi}) &= \int_{\partial D_b} (\boldsymbol{x}-\boldsymbol{\xi})_{\boldsymbol{\alpha}_n} \sigma_{\alpha b}(\boldsymbol{x}) n_b(\boldsymbol{x}) dS(\boldsymbol{x}) - \mu \int_{\partial D_b} p_{\alpha\boldsymbol{\alpha}_n}(\boldsymbol{x},\boldsymbol{\xi}) v_b(\boldsymbol{x}) n_b(\boldsymbol{x}) dS(\boldsymbol{x}) \\ &+ \mu \int_{\partial D_b} \left[v_\alpha(\boldsymbol{x}) n_b(\boldsymbol{x}) \nabla_b (\boldsymbol{x}-\boldsymbol{\xi})_{\boldsymbol{\alpha}_n} + n_\alpha(\boldsymbol{x}) v_c(\boldsymbol{x}) \nabla_c (\boldsymbol{x}-\boldsymbol{\xi})_{\boldsymbol{\alpha}_n}\right] dS(\boldsymbol{x}) \end{aligned} \tag{3.17}$$

We can introduce the geometrical moments $m_{\alpha\boldsymbol{\alpha}_m\beta'\boldsymbol{\beta}'_n}(\boldsymbol{\xi},\boldsymbol{\xi}')$ as defined in [201] by the relation

$$M^{(n)}_{\alpha\boldsymbol{\alpha}_m}(\boldsymbol{\xi},\boldsymbol{\xi}') = 8\pi\mu A_{\beta'\boldsymbol{\beta}'_n}\, m_{\alpha\boldsymbol{\alpha}_m\beta'\boldsymbol{\beta}'_n}(\boldsymbol{\xi},\boldsymbol{\xi}') \tag{3.18}$$

where $M^{(n)}_{\alpha\boldsymbol{\alpha}_m}(\boldsymbol{\xi},\boldsymbol{\xi}')$ is the m-th order moments on the body with respect to the point $\boldsymbol{\xi}$ immersed in the n-th order ambient flow centered at the point $\boldsymbol{\xi}'$ and the index $\beta'\boldsymbol{\beta}'_n$ refers to the entries at the point $\boldsymbol{\xi}'$. A schematic representation of these special hydrodynamic systems is reported in Fig. 3.1, where a generic body is immersed in 0-th, 1-st and 2-nd order ambient flows.

The n-th order disturbance field $(\boldsymbol{w}^{(n)}(\boldsymbol{x},\boldsymbol{\xi}'), \boldsymbol{\tau}^{(n)}(\boldsymbol{x},\boldsymbol{\xi}'))$ of the ambient field $(\boldsymbol{u}^{(n)}(\boldsymbol{x},\boldsymbol{\xi}'), \boldsymbol{\pi}^{(n)}(\boldsymbol{x},\boldsymbol{\xi}'))$ centered at the point $\boldsymbol{\xi}' \in D_b$ is the solution of the Stokes equations

$$\begin{cases} -\nabla\cdot\boldsymbol{\tau}^{(n)}(\boldsymbol{x},\boldsymbol{\xi}') = \mu\Delta\boldsymbol{w}^{(n)}(\boldsymbol{x},\boldsymbol{\xi}') - \nabla q^{(n)}(\boldsymbol{x},\boldsymbol{\xi}') = 0 \\ \nabla\cdot\boldsymbol{w}^{(n)}(\boldsymbol{x},\boldsymbol{\xi}') = 0 \qquad \boldsymbol{x}\in D_f \\ \boldsymbol{w}^{(n)}(\boldsymbol{x},\boldsymbol{\xi}') = \boldsymbol{w}^{(S,n)}(\boldsymbol{x},\boldsymbol{\xi}'),\ \boldsymbol{\tau}^{(n)}(\boldsymbol{x},\boldsymbol{\xi}') = \boldsymbol{\tau}^{(S,n)}(\boldsymbol{x},\boldsymbol{\xi}') \qquad \boldsymbol{x}\in\partial D_b \end{cases} \tag{3.19}$$

where $\boldsymbol{w}^{(S,n)}(\boldsymbol{x},\boldsymbol{\xi}')$ and $\boldsymbol{\tau}^{(S,n)}(\boldsymbol{x},\boldsymbol{\xi}')$ are the n-th order disturbance velocity field and stress tensor at the surface of the body depending on the assigned boundary conditions. Introducing the singularity operator $\mathcal{F}_{\alpha\beta'\boldsymbol{\beta}'_n}$ defined starting from the hierarchy of the geometrical moments $m_{\alpha\boldsymbol{\alpha}_m\beta'\boldsymbol{\beta}'_n}(\boldsymbol{\xi},\boldsymbol{\xi}')$

$$\mathcal{F}_{\alpha\beta'\boldsymbol{\beta}'_n} = \sum_{m=0}^{\infty} \frac{m_{\alpha\boldsymbol{\alpha}_m\beta'\boldsymbol{\beta}'_n}(\boldsymbol{\xi},\boldsymbol{\xi}')}{m!} \nabla_{\boldsymbol{\alpha}_m} \tag{3.20}$$

it is possible to express the n-th order disturbance field $(\boldsymbol{w}^{(n)}(\boldsymbol{x},\boldsymbol{\xi}'),\boldsymbol{\tau}^{(n)}(\boldsymbol{x},\boldsymbol{\xi}'))$ in the form

$$w_a^{(n)}(\boldsymbol{x},\boldsymbol{\xi}') = A_{\beta'\boldsymbol{\beta}'_n}\mathcal{F}_{\alpha\beta'\boldsymbol{\beta}'_n}S_{a\alpha}(\boldsymbol{x},\boldsymbol{\xi}) \tag{3.21}$$

$$q^{(n)}(\boldsymbol{x},\boldsymbol{\xi}') = A_{\beta'\boldsymbol{\beta}'_n}\mathcal{F}_{\alpha\beta'\boldsymbol{\beta}'_n}P_{\alpha}(\boldsymbol{x},\boldsymbol{\xi}) \tag{3.22}$$

$$\tau_{ab}^{(n)}(\boldsymbol{x},\boldsymbol{\xi}') = A_{\beta'\boldsymbol{\beta}'_n}\mathcal{F}_{\alpha\beta'\boldsymbol{\beta}'_n}\Sigma_{ab\alpha}(\boldsymbol{x},\boldsymbol{\xi}) \tag{3.23}$$

The n-th order total velocity field is $(\boldsymbol{v}^{(n)}(\boldsymbol{x},\boldsymbol{\xi}'),\boldsymbol{\sigma}^{(n)}(\boldsymbol{x},\boldsymbol{\xi}')) = (\boldsymbol{u}^{(n)}(\boldsymbol{x},\boldsymbol{\xi}'),\boldsymbol{\pi}^{(n)}(\boldsymbol{x},\boldsymbol{\xi}'))+$ $(\boldsymbol{w}^{(n)}(\boldsymbol{x},\boldsymbol{\xi}'),\boldsymbol{\tau}^{(n)}(\boldsymbol{x},\boldsymbol{\xi}'))$ and its entries can be expressed by enforcing the linearity of the Stokes flow as $(v_a^{(n)}(\boldsymbol{x},\boldsymbol{\xi}'),\sigma_{ab}^{(n)}(\boldsymbol{x},\boldsymbol{\xi}')) = A_{\beta'\boldsymbol{\beta}'_n}(v_{a\beta'\boldsymbol{\beta}'_n}(\boldsymbol{x},\boldsymbol{\xi}'),\mu\sigma_{ab\beta'\boldsymbol{\beta}'_n}(\boldsymbol{x},\boldsymbol{\xi}'))$. Therefore, from eqs. (3.17) and (3.18), the geometrical moments can be evaluated as the following surface integrals

$$\begin{aligned} &8\pi\, m_{\alpha\boldsymbol{\alpha}_m\beta'\boldsymbol{\beta}'_n}(\boldsymbol{\xi},\boldsymbol{\xi}') = \\ &\int_{\partial D_b}(\boldsymbol{x}-\boldsymbol{\xi})_{\boldsymbol{\alpha}_m}\sigma_{\alpha b\beta'\boldsymbol{\beta}'_n}(\boldsymbol{x},\boldsymbol{\xi}')n_b(\boldsymbol{x})dS(\boldsymbol{x}) - \int_{\partial D_b} p_{\alpha\boldsymbol{\alpha}_m}(\boldsymbol{x},\boldsymbol{\xi})v_{b\beta'\boldsymbol{\beta}'_n}(\boldsymbol{x},\boldsymbol{\xi}')n_b(\boldsymbol{x})dS(\boldsymbol{x}) \\ &+\int_{\partial D_b}\left[v_{\alpha\beta'\boldsymbol{\beta}'_n}(\boldsymbol{x},\boldsymbol{\xi}')n_b(\boldsymbol{x})\nabla_b(\boldsymbol{x}-\boldsymbol{\xi})_{\boldsymbol{\alpha}_m} + n_\alpha(\boldsymbol{x})v_{c\beta'\boldsymbol{\beta}'_n}(\boldsymbol{x},\boldsymbol{\xi}')\nabla_c(\boldsymbol{x}-\boldsymbol{\xi})_{\boldsymbol{\alpha}_m}\right]dS(\boldsymbol{x}) \end{aligned} \tag{3.24}$$

Without loss of generality, we can always consider $\boldsymbol{\xi} = \boldsymbol{\xi}'$ in all the case addressed in the remainder since the distinction between these points is unnecessary. For example, as regards the geometrical moments $m_{\alpha\boldsymbol{\alpha}_m\beta\boldsymbol{\beta}_n}(\boldsymbol{\xi},\boldsymbol{\xi}) = m_{\alpha\boldsymbol{\alpha}_m\beta'\boldsymbol{\beta}'_n}(\boldsymbol{\xi},\boldsymbol{\xi}')|_{\boldsymbol{\xi}'=\boldsymbol{\xi}}$.

3.4 Generalized n-th order Faxén operator and the Hinch-Kim dualism theorem

Let us investigate the relations between the singularity operator $\mathcal{F}_{\alpha\beta\boldsymbol{\beta}_n}$ and the n-th order Faxén operator. For the sake of compactness, we indicate with the symbol $[\cdot,\cdot]$ the bi-linear operator acting on two generic Stokes flows $\mathbf{v}(\boldsymbol{x})$ and $\mathbf{v}'(\boldsymbol{x})$ corresponding to the surface integral on the body

$$[\mathbf{v},\mathbf{v}'] = \int_{\partial D_b}(\boldsymbol{\sigma}\{\mathbf{v}'(\boldsymbol{x})\}\cdot\mathbf{v}(\boldsymbol{x}) - \boldsymbol{\sigma}\{\mathbf{v}(\boldsymbol{x})\}\cdot\mathbf{v}'(\boldsymbol{x}))\cdot\boldsymbol{n}(\boldsymbol{x})dS(\boldsymbol{x}) \tag{3.25}$$

where $\boldsymbol{\sigma}\{\mathbf{v}(\boldsymbol{x})\}$ is the stress tensor related to the field $\mathbf{v}(\boldsymbol{x})$.

It is easy to verify that

$$[\mathbf{v},\mathbf{v}'] = -[\mathbf{v}',\mathbf{v}] \tag{3.26}$$

and therefore the operator $[\cdot,\cdot]$ admits odd parity. Since the ambient fields are regular homogeneous solutions of the Stokes equations in the domain of the body, given two ambient fields $\boldsymbol{u}(\boldsymbol{x})$ and $\boldsymbol{u}'(\boldsymbol{x})$ we have

$$[\boldsymbol{u},\boldsymbol{u}'] = 0 \tag{3.27}$$

In the case of two disturbance fields $\boldsymbol{w}(\boldsymbol{x})$ and $\boldsymbol{w}'(\boldsymbol{x})$, applying the Lorentz reciprocal theorem on the surface $\partial D_f \equiv \partial D_b \cup \partial D_\infty$ and considering that the disturbance fields vanish at ∂D_∞ we obtain

$$[\boldsymbol{w},\boldsymbol{w}'] = \int_{\partial D_\infty} (\boldsymbol{\sigma}\{\boldsymbol{w}'(\boldsymbol{x})\}\cdot\boldsymbol{w}(\boldsymbol{x}) - \boldsymbol{\sigma}\{\boldsymbol{w}(\boldsymbol{x})\}\cdot\boldsymbol{w}'(\boldsymbol{x}))\cdot\boldsymbol{n}(\boldsymbol{x})dS(\boldsymbol{x}) = 0 \tag{3.28}$$

On the other hand, given two total field $\boldsymbol{v}(\boldsymbol{x}) = \boldsymbol{u}(\boldsymbol{x})+\boldsymbol{w}(\boldsymbol{x})$ and $\boldsymbol{v}'(\boldsymbol{x}) = \boldsymbol{u}'(\boldsymbol{x})+\boldsymbol{w}'(\boldsymbol{x})$, the quantity $[\boldsymbol{v},\boldsymbol{v}']$ does not vanish in general, and the following identity holds

$$[\boldsymbol{v},\boldsymbol{v}'] = [\boldsymbol{u},\boldsymbol{w}'] - [\boldsymbol{u}',\boldsymbol{w}] \tag{3.29}$$

We call *reciprocal boundary conditions*, any boundary condition for which

$$[\boldsymbol{v},\boldsymbol{v}'] = 0, \qquad \forall\ \boldsymbol{v}(\boldsymbol{x}),\boldsymbol{v}'(\boldsymbol{x}) \tag{3.30}$$

Equivalently, eq. (3.30) is the mathematical definition of the property referred to as *Boundary-Condition reciprocity* (BC-reciprocity, for short).

It is possible to express the generic ambient field in the domain of the body by the Ladyzhenskaya boundary integrals [137]

$$u_\alpha(\boldsymbol{\xi}) = -\frac{[\boldsymbol{S}_\alpha(\boldsymbol{\xi}),\boldsymbol{u}]}{8\pi\mu} = -\int_{\partial D_b}\left[\pi_{ab}(\boldsymbol{x})\frac{S_{a\alpha}(\boldsymbol{x},\boldsymbol{\xi})}{8\pi\mu} - u_a(\boldsymbol{x})\frac{\Sigma_{ab\alpha}(\boldsymbol{x},\boldsymbol{\xi})}{8\pi}\right]n_b(\boldsymbol{x})dS(\boldsymbol{x}) \tag{3.31}$$

Applying the operator $A_{\beta\boldsymbol{\beta}_n}\mathcal{F}_{\alpha\beta\boldsymbol{\beta}_n}$ at both sides of eq. (3.31), and using the relations (3.21) one obtains

$$A_{\beta\boldsymbol{\beta}_n}\mathcal{F}_{\alpha\beta\boldsymbol{\beta}_n}u_\alpha(\boldsymbol{\xi}) = -\frac{[A_{\beta\boldsymbol{\beta}_n}\mathcal{F}_{\alpha\beta\boldsymbol{\beta}_n}\boldsymbol{S}_\alpha(\boldsymbol{\xi}),\boldsymbol{u}]}{8\pi\mu} = -\frac{[\boldsymbol{w}^{(n)}(\boldsymbol{\xi}),\boldsymbol{u}]}{8\pi\mu} \tag{3.32}$$

It is possible to add at the r.h.s. of eq. (3.32) the vanishing contribution $[\boldsymbol{w}^{(n)}(\boldsymbol{\xi}),\boldsymbol{w}]$ deriving from two disturbance fields, thus

$$A_{\beta\boldsymbol{\beta}_n}\mathcal{F}_{\alpha\beta\boldsymbol{\beta}_n}u_\alpha(\boldsymbol{\xi}) = -\frac{[\boldsymbol{w}^{(n)}(\boldsymbol{\xi}),\boldsymbol{u}] + [\boldsymbol{w}^{(n)}(\boldsymbol{\xi}),\boldsymbol{w}]}{8\pi\mu} = -\frac{[\boldsymbol{w}^{(n)}(\boldsymbol{\xi}),\boldsymbol{v}]}{8\pi\mu} \tag{3.33}$$

that can be expressed, replacing $\boldsymbol{w}^{(n)}(\boldsymbol{x},\boldsymbol{\xi}) = \boldsymbol{v}^{(n)}(\boldsymbol{x},\boldsymbol{\xi}) - \boldsymbol{u}^{(n)}(\boldsymbol{x},\boldsymbol{\xi})$, in the form

$$A_{\beta\boldsymbol{\beta}_n}\mathcal{F}_{\alpha\beta\boldsymbol{\beta}_n}u_\alpha(\boldsymbol{\xi}) = \frac{[\boldsymbol{u}^{(n)}(\boldsymbol{\xi}),\boldsymbol{v}] - [\boldsymbol{v}^{(n)}(\boldsymbol{\xi}),\boldsymbol{v}]}{8\pi\mu} \tag{3.34}$$

Comparing eq. (3.34) and eq. (3.16), we finally obtain

$$M_{\beta\boldsymbol{\beta}_n}(\boldsymbol{\xi}) = 8\pi\mu\mathcal{F}_{\alpha\beta\boldsymbol{\beta}_n}u_\alpha(\boldsymbol{\xi}) + [\boldsymbol{v}^{(n)}_{\beta\boldsymbol{\beta}_n}(\boldsymbol{\xi}),\boldsymbol{v}] \tag{3.35}$$

Eq. (3.35) is one of the main result of this chapter, connecting the Hinch-Kim duality to the condition of BC-reciprocity. From eq. (3.35) it is possible to state that the Hinch-Kim dualism holds whenever reciprocal boundary conditions are imposed on the surface of the body, i.e. whenever

$$[\boldsymbol{v}^{(n)}(\boldsymbol{\xi}), \boldsymbol{v}] = \int_{\partial D_b} [\sigma_{ab}(\boldsymbol{x}) v_a^{(n)}(\boldsymbol{x}, \boldsymbol{\xi}) - v_a(\boldsymbol{x}) \sigma_{ab}^{(n)}(\boldsymbol{x}, \boldsymbol{\xi})] n_b(\boldsymbol{x}) dS(\boldsymbol{x}) = 0 \tag{3.36}$$

This can be referred to as the Hinch-Kim dualism theorem. In the BC-reciprocal case, the n-th order singularity operator $\mathcal{F}_{\alpha\beta\boldsymbol{\beta}_n}$ defined by eq. (3.20) furnishes either the n-th order disturbance field if applied to the pole of the unbounded Green function according eqs. (3.21)-(3.23) or the n-th order moment on a particle immersed in an ambient field $\boldsymbol{u}(\boldsymbol{x})$ according to the relation

$$M_{\beta\boldsymbol{\beta}_n}(\boldsymbol{\xi}) = 8\pi\mu \mathcal{F}_{\alpha\beta\boldsymbol{\beta}_n} u_\alpha(\boldsymbol{\xi}) \tag{3.37}$$

Owing to the fact that the operator $\mathcal{F}_{\alpha\beta\boldsymbol{\beta}_n}$ returns the n-th order moments on the body if applied to an ambient flow, $\mathcal{F}_{\alpha\beta\boldsymbol{\beta}_n}$ is *sensu-stricto* a *n-th order generalized Faxén operator*.

Let us to show an interesting consequence of reciprocal boundary conditions. If BC-reciprocity holds, by using eq. (3.6), the disturbance field due to the inclusion of the body related to a generic ambient field $\boldsymbol{u}(\boldsymbol{x})$ can be expressed as

$$w_a(\boldsymbol{x}) = \frac{1}{8\pi\mu} \sum_{n=0}^{\infty} \frac{[\mathcal{F}_{\beta\alpha\boldsymbol{\alpha}_n} u_\beta(\boldsymbol{\xi})]}{n!} \nabla_{\boldsymbol{\alpha}_n} S_{a\,\alpha}(\boldsymbol{x}, \boldsymbol{\xi}) \tag{3.38}$$

and, as shown in [201] and briefly reviewed in Appendix 3.A, due to the following symmetry of the geometric moments

$$m_{\alpha\boldsymbol{\alpha}_m\beta'\boldsymbol{\beta}'_n}(\boldsymbol{\xi}, \boldsymbol{\xi}') = m_{\beta'\boldsymbol{\beta}'_n\alpha\boldsymbol{\alpha}_m}(\boldsymbol{\xi}', \boldsymbol{\xi}) \tag{3.39}$$

we obtain an expansion of a generic disturbance field in terms of the Faxén operators (i.e. in terms of the geometrical moments)

$$w_a(\boldsymbol{x}) = \sum_{n=0}^{\infty} \frac{\nabla_{\boldsymbol{\beta}_n} u_\beta(\boldsymbol{\xi})}{n!} \mathcal{F}_{\alpha\beta\boldsymbol{\beta}_n} S_{a\,\alpha}(\boldsymbol{x}, \boldsymbol{\xi}) \tag{3.40}$$

Gathering eqs. (3.37) and (3.40) a remarkable property follows, namely if BC-reciprocity holds, the hydromechanics (i.e. the motion of the body due to the interaction with the fluid and the motion of the fluid due to the interaction with the body) of a fluid-body system in the Stokes regime can be completely described by the knowledge of the entire set of (m, n)-th order geometrical moments of the body.

In the next Sections we analize typical hydrodynamic boundary conditions at the fluid-body interface in order to ascertain in which cases BC-reciprocity i.e. eq. (3.30) is fulfilled and $\mathcal{F}_{\alpha\beta\boldsymbol{\beta}_n}$ is a Faxén operator.

3.5 Boundary conditions at solid-fluid interfaces

BC-reciprocity i.e. $[\boldsymbol{v}, \boldsymbol{v}'] = 0$ is straightforwardly verified for no-slip conditions ($\boldsymbol{v}(\boldsymbol{x}) = 0$ for $\boldsymbol{x} \in \partial D_b$) or for complete slip conditions ($\boldsymbol{\sigma}(\boldsymbol{x}) \cdot \boldsymbol{n}(\boldsymbol{x}) = 0$ for $\boldsymbol{x} \in \partial D_b$) at the surface of the body.

Indeed, this property holds for any linear relation between velocity and traction at the boundary. In fact, consider the interfacial mobility matrix $\boldsymbol{\beta}(\boldsymbol{x})$ [10] defined by the relation

$$\boldsymbol{\beta}(\boldsymbol{x}) \cdot \boldsymbol{v}(\boldsymbol{x}) = \boldsymbol{\sigma}(\boldsymbol{x}) \cdot \boldsymbol{n}(\boldsymbol{x}), \qquad \boldsymbol{x} \in \partial D_b \tag{3.41}$$

Due to its symmetry, $\beta_{ab}(\boldsymbol{x}) = \beta_{ba}(\boldsymbol{x})$, we have that

$$\begin{aligned} [\boldsymbol{v}^{(n)}(\boldsymbol{\xi}), \boldsymbol{v}] = \int_{\partial D_b} [\sigma_{ab}(\boldsymbol{x}) n_b(\boldsymbol{x}) v_a^{(n)}(\boldsymbol{x}, \boldsymbol{\xi}) - v_a(\boldsymbol{x}) \sigma_{ab}^{(n)}(\boldsymbol{x}, \boldsymbol{\xi}) n_b(\boldsymbol{x})] dS(\boldsymbol{x}) &= \\ \int_{\partial D_b} [v_b(\boldsymbol{x}) \beta_{ab}(\boldsymbol{x}) v_a^{(n)}(\boldsymbol{x}, \boldsymbol{\xi}) - v_b^{(n)}(\boldsymbol{x}, \boldsymbol{\xi}) \beta_{ab}(\boldsymbol{x}) v_a(\boldsymbol{x})] dS(\boldsymbol{x}) &= 0 \end{aligned} \tag{3.42}$$

Consistently, in this case $\mathcal{F}_{\alpha\beta\boldsymbol{\beta}_n}$ is a Faxén operator.

Next, let us focus on the case of Navier-slip boundary conditions. Thus, given an ambient field $\boldsymbol{u}(\boldsymbol{x})$, the total field $\boldsymbol{v}(\boldsymbol{x}) = \boldsymbol{u}(\boldsymbol{x}) + \boldsymbol{w}(\boldsymbol{x})$ satisfies at the boundaries of the body the relations

$$\begin{cases} \boldsymbol{v}(\boldsymbol{x}) \cdot \boldsymbol{n}(\boldsymbol{x}) = 0 \\ \boldsymbol{v}(\boldsymbol{x}) \cdot \boldsymbol{t}(\boldsymbol{x}) = -\dfrac{\lambda}{\mu} \boldsymbol{h}(\boldsymbol{x}) \cdot \boldsymbol{t}(\boldsymbol{x}), \qquad \boldsymbol{x} \in \partial D_b \end{cases} \tag{3.43}$$

where λ is the slip length of the interface, $\boldsymbol{t}(\boldsymbol{x}) = \boldsymbol{I} - \boldsymbol{n}(\boldsymbol{x}) \otimes \boldsymbol{n}(\boldsymbol{x})$ the unit tangent matrix, and $\boldsymbol{h}(\boldsymbol{x}) = \boldsymbol{\sigma}(\boldsymbol{x}) \cdot \boldsymbol{n}(\boldsymbol{x})$ the surface traction of the total velocity field.

Navier-slip boundary conditions eq. (3.43) represent a particular case where the relation between velocity and traction at the boundary of the body is linear, and from what obtained above, BC-reciprocity applies, meaning that the Hinch-Kim dualism holds. Therefore, given a generic ambient field $\boldsymbol{u}(\boldsymbol{x})$, the moments on the body are given by eq. (3.37), and the disturbance field is expressed by eq. (3.40). The geometrical moments that are needed to explicit the Faxén operators can be obtained by substituting the boundary conditions eq. (3.43) into eq. (3.24), and by considering the geometrical surface traction of the body immersed in a n-th order ambient field $h_{\alpha\beta\boldsymbol{\beta}_n}(\boldsymbol{x}, \boldsymbol{\xi}) = \delta_{\alpha a} \sigma_{ab\beta\boldsymbol{\beta}_n}(\boldsymbol{x}, \boldsymbol{\xi}) n_b(\boldsymbol{x})$, thus

$$\begin{aligned} & m_{\alpha\boldsymbol{\alpha}_m\beta\boldsymbol{\beta}_n}(\boldsymbol{\xi}, \boldsymbol{\xi}) = \\ & \int_{\partial D_b} \frac{h_{\gamma\beta\boldsymbol{\beta}_n}(\boldsymbol{x}, \boldsymbol{\xi})}{8\pi} [\delta_{\alpha\gamma}(\boldsymbol{x} - \boldsymbol{\xi})_{\boldsymbol{\alpha}_m} - \lambda(t_{\alpha\gamma}(\boldsymbol{x}) n_b(\boldsymbol{x}) \nabla_b (\boldsymbol{x} - \boldsymbol{\xi})_{\boldsymbol{\alpha}_m} \\ & \qquad + n_\alpha(\boldsymbol{x}) t_{c\gamma}(\boldsymbol{x}) \nabla_c (\boldsymbol{x} - \boldsymbol{\xi})_{\boldsymbol{\alpha}_m})] dS(\boldsymbol{x}) \end{aligned} \tag{3.44}$$

The n-th order surface traction $h_{\alpha\beta\boldsymbol{\beta}_n}(\boldsymbol{x}, \boldsymbol{\xi})$ can be expressed as

$$h_{\alpha\beta\boldsymbol{\beta}_n}(\boldsymbol{x}, \boldsymbol{\xi}) = f_{\alpha\beta\boldsymbol{\beta}_n}(\boldsymbol{x}, \boldsymbol{\xi}) + n_\alpha(\boldsymbol{x}) p_{\beta\boldsymbol{\beta}_n}(\boldsymbol{x}, \boldsymbol{\xi}) - \Big(n_\beta(\boldsymbol{x}) \nabla_\alpha (\boldsymbol{x} - \boldsymbol{\xi})_{\boldsymbol{\beta}_n} + \delta_{\beta\alpha} n_\gamma(\boldsymbol{x}) \nabla_\gamma (\boldsymbol{x} - \boldsymbol{\xi})_{\boldsymbol{\beta}_n} \Big) \tag{3.45}$$

where $f_{\alpha\beta\boldsymbol{\beta}_n}(\boldsymbol{x}, \boldsymbol{\xi}) = \delta_{\alpha a} \tau_{ab\beta\boldsymbol{\beta}_n}(\boldsymbol{x}, \boldsymbol{\xi}) n_b(\boldsymbol{x})$ is the surface traction related to the n-th order disturbance field.

On the other hand, it is easy to see that $\mathcal{F}_{\alpha\beta\boldsymbol{\beta}_n}$ is not a Faxén operator for a deforming body. In fact, under the assumption that the body is a linear elastic material solid, the governing equations for the body deformation are [140]

$$\begin{cases} \nabla \cdot \boldsymbol{\sigma}^{[s]}(\boldsymbol{x}) = -\rho^{[s]} \ddot{\boldsymbol{u}}^{[s]}(\boldsymbol{x}) \\ \boldsymbol{\sigma}_{ab}^{[s]}(\boldsymbol{x}) = \delta_{ab} \lambda^{[s]} \nabla \cdot \boldsymbol{u}^{[s]}(\boldsymbol{x}) + \mu^{[s]} (\nabla_a u_b^{[s]}(\boldsymbol{x}) + \nabla_b u_a^{[s]}(\boldsymbol{x})), \qquad \boldsymbol{x} \in D_b \end{cases} \tag{3.46}$$

where $\boldsymbol{\sigma}^{[s]}(\boldsymbol{x})$ is the stress tensor field in the solid, $\boldsymbol{u}^{[s]}(\boldsymbol{x})$ the displacement field of the solid, $\rho^{[s]}$ the solid density, and $\lambda^{[s]}$ and $\mu^{[s]}$ the Lamé coefficients. In eq. (3.46) any upper "dot" indicates the derivative operation with respect to time. Enforcing continuity conditions at the solid-fluid interface [75]

$$\begin{cases} \boldsymbol{\sigma}(\boldsymbol{x}) \cdot \boldsymbol{n}(\boldsymbol{x}) = \boldsymbol{\sigma}^{[s]}(\boldsymbol{x}) \cdot \boldsymbol{n}(\boldsymbol{x}) \\ \boldsymbol{v}(\boldsymbol{x}) = \dot{\boldsymbol{u}}^{[s]}(\boldsymbol{x}) \qquad \boldsymbol{x} \in \partial D_b \end{cases} \tag{3.47}$$

and substituting eqs. (3.47) in the first integral in eq. (3.42), from the Maxwell-Betti theorem [168, 14] it follows that

$$\begin{aligned} [\boldsymbol{v}^{(n)}(\boldsymbol{\xi}), \boldsymbol{v}] &= \int_{\partial D_b} [\sigma_{ab}^{[s]}(\boldsymbol{x}) n_b(\boldsymbol{x}) \dot{u}_a^{[s](n)}(\boldsymbol{x}, \boldsymbol{\xi}) - \dot{u}_a^{[s]}(\boldsymbol{x}) \sigma_{ab}^{[s](n)}(\boldsymbol{x}, \boldsymbol{\xi}) n_b(\boldsymbol{x})] dS(\boldsymbol{x}) \\ &= -\rho^{[s]} \int_{D_b} [\ddot{u}_a^{[s]}(\boldsymbol{x})\, \dot{u}_a^{[s](n)}(\boldsymbol{x}, \boldsymbol{\xi}) - \dot{u}_a^{[s]}(\boldsymbol{x})\, \ddot{u}_a^{[s](n)}(\boldsymbol{x}, \boldsymbol{\xi})] dV(\boldsymbol{x}) \end{aligned} \tag{3.48}$$

which does not vanish in general for any flow $\boldsymbol{v}(\boldsymbol{x})$ and $\boldsymbol{v}^{(n)}(\boldsymbol{x}, \boldsymbol{\xi})$. BC-reciprocity is ensured only at the mechanical equilibrium of the body i.e. when $\ddot{\boldsymbol{u}}^{[s]}(\boldsymbol{x}) = 0$.

3.6 Boundary conditions at fluid-fluid interfaces

In the presence of a fluid body, the most common linear boundary conditions assumed at the fluid-fluid interface, considered incompressible and homogeneous, are [26, 208]

$$\begin{cases} \boldsymbol{v}(\boldsymbol{x}) = \boldsymbol{v}^{[i]}(\boldsymbol{x}) \\ \boldsymbol{v}(\boldsymbol{x}) \cdot \boldsymbol{n}(\boldsymbol{x}) = \dot{r}(\boldsymbol{x}, t) \\ \boldsymbol{\sigma}(\boldsymbol{x}) \cdot \boldsymbol{n}(\boldsymbol{x}) = \boldsymbol{\sigma}^{[i]}(\boldsymbol{x}) \cdot \boldsymbol{n}(\boldsymbol{x}) + \gamma\, \boldsymbol{n}(\boldsymbol{x})\, C(\boldsymbol{x}), \qquad \boldsymbol{x} \in \partial D_b \end{cases} \tag{3.49}$$

where $\boldsymbol{v}^{[i]}(\boldsymbol{x})$ and $\boldsymbol{\sigma}^{[i]}(\boldsymbol{x})$ are the velocity field and the stress tensor in the disturbing fluid (say a liquid drop or a gas bubble), $C(\boldsymbol{x})$ the trace of the curvature tensor of the surface and γ the surface tension.

Applying the reciprocity integral eq. (3.24) to the fields $\boldsymbol{v}(\boldsymbol{x})$ and $\boldsymbol{v}^{(n)}(\boldsymbol{x})$, it follows that

$$\begin{aligned} [\boldsymbol{v}^{(n)}(\boldsymbol{\xi}), \boldsymbol{v}] = \int_{\partial D_b} [\sigma_{ab}(\boldsymbol{x}) n_b(\boldsymbol{x}) v_a^{(n)}(\boldsymbol{x}, \boldsymbol{\xi}) - v_a(\boldsymbol{x}) \sigma_{ab}^{(n)}(\boldsymbol{x}, \boldsymbol{\xi}) n_b(\boldsymbol{x})] dS(\boldsymbol{x}) &= \\ \int_{\partial D_b} [\sigma_{ab}^{[i]}(\boldsymbol{x}) n_b(\boldsymbol{x}) v_a^{[i](n)}(\boldsymbol{x}, \boldsymbol{\xi}) - v_a^{[i]}(\boldsymbol{x}) \sigma_{ab}^{[i](n)}(\boldsymbol{x}, \boldsymbol{\xi}) n_b(\boldsymbol{x})] dS(\boldsymbol{x}) &+ \\ \gamma \int_{\partial D_b} (v_a^{[i](n)}(\boldsymbol{x}, \boldsymbol{\xi}) - v_a^{[i]}(\boldsymbol{x})) C(\boldsymbol{x}) n_a(\boldsymbol{x}) dS(\boldsymbol{x}) & \end{aligned} \tag{3.50}$$

Since the Lorentz reciprocal theorem is a peculiarity of Newtonian fluids (and, more generally, of continua characterized by linear relations between fluxes and thermodynamics forces), the first integral at the r.h.s of eq. (3.50) does not vanish, at least in principle, in the non-Newtonian case and consequently $\mathcal{F}_{\alpha\beta\boldsymbol{\beta}_n}$ cannot be a Faxén operator. In the case the disturbing fluid is Newtonian, the first integral at the r.h.s of eq. (3.50) vanishes due to the Lorentz reciprocal theorem for Newtonian fluids, but the second integral does not vanish until the interface shape does not reach the equilibrium state. In fact, the velocity at the interface $\boldsymbol{v}(\boldsymbol{x})|_{\boldsymbol{x}\in\partial D_b}$ is uniquely determined by the Rallison-Acrivos integral equations once the ambient field is assigned [209, 193]. Therefore, the second integral at the r.h.s of eq. (3.50) does not vanishes for any ambient flows, but solely in the trivial case of $\boldsymbol{u}(\boldsymbol{x}) = \boldsymbol{u}^{(n)}(\boldsymbol{x},\boldsymbol{\xi})$.

If the disturbing fluid is Newtonian and the shape of the body, say a drop or a bubble, is stationary ($\boldsymbol{v}(\boldsymbol{x}) \cdot \boldsymbol{n}(\boldsymbol{x})|_{\boldsymbol{x}\in\partial D_b} = 0$), the first integral at the r.h.s of eq. (3.50) vanishes due to Lorentz's reciprocity. Furthermore, since the normal velocity is assumed to be vanishing at the surface of the body, also the second integral at the r.h.s vanishes, independently of the shape of the body and of the surface tension. We obtain $[\boldsymbol{v}^{(n)}(\boldsymbol{\xi}), \boldsymbol{v}] = 0$ and consequently $\mathcal{F}_{\alpha\beta\boldsymbol{\beta}_n}$ is, in this case, a Faxén operator. This means that both the velocity field in the external fluid and the moments on the drop do not depend directly on the surface tension at the surface, as surface tension has only an indirect influence related to the geometry of the stationary shape of the drop.

In this case, in order to evaluate the geometrical moments providing the Faxén operator, the knowledge either of the set of n-th surface velocity fields $v_{ab\boldsymbol{b}_n}(\boldsymbol{x},\boldsymbol{\xi})$ or of n-th external surface traction $h_{ab\boldsymbol{b}_n}(\boldsymbol{x},\boldsymbol{\xi}) = \sigma_{acb\boldsymbol{b}_n}(\boldsymbol{x},\boldsymbol{\xi}) n_c(\boldsymbol{x})$ is required since

$$
\begin{aligned}
8\pi\, m_{\alpha\boldsymbol{\alpha}_m\beta\boldsymbol{\beta}_n}(\boldsymbol{\xi},\boldsymbol{\xi}) &= \int_{\partial D_b} (\boldsymbol{x}-\boldsymbol{\xi})_{\boldsymbol{\alpha}_m} h_{\alpha\beta\boldsymbol{\beta}_n}(\boldsymbol{x},\boldsymbol{\xi}) dS(\boldsymbol{x}) \\
&+ \int_{\partial D_b} \left[v_{\alpha\beta\boldsymbol{\beta}_n}(\boldsymbol{x},\boldsymbol{\xi}) n_b(\boldsymbol{x}) \nabla_b (\boldsymbol{x}-\boldsymbol{\xi})_{\boldsymbol{\alpha}_m} + n_\alpha(\boldsymbol{x}) v_{c\beta\boldsymbol{\beta}_n}(\boldsymbol{x},\boldsymbol{\xi}) \nabla_c (\boldsymbol{x}-\boldsymbol{\xi})_{\boldsymbol{\alpha}_m} \right] dS(\boldsymbol{x})
\end{aligned}
\tag{3.51}
$$

3.7 Boundary conditions at porous body-fluid interfaces

Next, consider the case the inner flow $(\boldsymbol{v}^{[i]}(\boldsymbol{x}), p^{[i]}(\boldsymbol{x}))$ inside a porous body is modeled by means of the Darcy equations [50, 240]

$$
\begin{cases}
\boldsymbol{v}^{[i]}(\boldsymbol{x}) = -\dfrac{k}{\mu} \nabla p^{[i]}(\boldsymbol{x}) \\
\nabla \cdot \boldsymbol{v}^{[i]}(\boldsymbol{x}) = 0, \qquad \boldsymbol{x} \in D_b
\end{cases}
\tag{3.52}
$$

where k is the permeability of the porous medium. The boundary condition to be imposed at the interface are the Beavers-Joseph-Saffman boundary conditions [214, 120], i.e.,

$$
\begin{cases}
(\boldsymbol{v}(\boldsymbol{x}) - \boldsymbol{v}^{[i]}(\boldsymbol{x})) \cdot (\boldsymbol{I} - \boldsymbol{n}(\boldsymbol{x}) \otimes \boldsymbol{n}(\boldsymbol{x})) = \dfrac{\sqrt{k}}{\alpha} \boldsymbol{\sigma}(\boldsymbol{x}) \cdot (\boldsymbol{I} - \boldsymbol{n}(\boldsymbol{x}) \otimes \boldsymbol{n}(\boldsymbol{x})) \\
\boldsymbol{v}(\boldsymbol{x}) \cdot \boldsymbol{n}(\boldsymbol{x}) = \boldsymbol{v}^{[i]}(\boldsymbol{x}) \cdot \boldsymbol{n}(\boldsymbol{x}) \\
p(\boldsymbol{x}) = p^{[i]}(\boldsymbol{x}), \qquad \boldsymbol{x} \in \partial D_b
\end{cases}
\tag{3.53}
$$

where $\alpha = \alpha_0\, \mu$ and α_0 is a nondimensional constant depending on the geometry and topology of the pore structure. In this case, BC-reciprocity is not satisfied because

$[\boldsymbol{v}, \boldsymbol{v}']$ does not vanish in general, since

$$[\boldsymbol{v}^{(n)}(\boldsymbol{\xi}), \boldsymbol{v}] = \int_{\partial D_b} [\sigma_{ab}(\boldsymbol{x}) n_b(\boldsymbol{x}) v_a^{(n)}(\boldsymbol{x}, \boldsymbol{\xi}) - v_a(\boldsymbol{x}) \sigma_{ab}^{(n)}(\boldsymbol{x}, \boldsymbol{\xi}) n_b(\boldsymbol{x})] dS(\boldsymbol{x}) \quad = \\ -2\mu \int_{\partial D_b} [e_{ab}\{\boldsymbol{v}(\boldsymbol{x})\} v_a^{[i](n)}(\boldsymbol{x}, \boldsymbol{\xi}) - e_{ab}\{\boldsymbol{v}^{(n)}(\boldsymbol{x}, \boldsymbol{\xi})\} v_a^{[i]}(\boldsymbol{x})] n_b(\boldsymbol{x}) dS(\boldsymbol{x}) \quad \neq \quad 0 \tag{3.54}$$

where

$$e_{ab}\{\boldsymbol{v}(\mathbf{x})\} = \frac{1}{2}(\nabla_a v_b(\boldsymbol{x}) + \nabla_b v_a(\boldsymbol{x}))$$

It is possible to check this result by identifying the singularities in the solution provided by Jones [120] for the simpler problem of a porous sphere with radius R_p in a constant flow with components U_β, comparing the solution with the Faxén theorem obtained by Palaniappan [188] for a Darcy porous sphere in a generic ambient flow. The disturbance field in the Jones solution is given by the operator applied at the pole of the Stokeslet centered at the center of the sphere $\boldsymbol{\xi}$

$$U_\beta \mathcal{F}_{\alpha\beta} = U_\beta \left[\frac{R_p A_D}{2} + \frac{R_p^3 B_D}{2} \Delta_\xi \right] \delta_{\alpha\beta} \tag{3.55}$$

where Δ_ξ is the Laplacian operator acting on the coordinate of the center of the sphere and where

$$A_D = -\frac{3R_p^2 \left(2\sqrt{k} + \alpha R_p\right)}{6k^{3/2} + 3\alpha k R_p + 6\sqrt{k} R_p^2 + 2\alpha R_p^3}$$
$$B_D = -\frac{\alpha R_p^3}{12k^{3/2} + 6\alpha k R_p + 12\sqrt{k} R_p^2 + 4\alpha R_p^3}$$

while the Faxén theorem obtained by Palaniappan [188] states that the force acting on a sphere in an ambient flow $\boldsymbol{u}(\boldsymbol{x})$ is

$$F_\alpha = -M_\alpha = -8\pi\mu \left[\frac{R_p A_D}{2} + \frac{R_p^3 B'_D}{2} \Delta_\xi \right] u_\alpha(\boldsymbol{\xi}_{(c)}) \tag{3.56}$$

where

$$B'_D = B_D - \frac{6k^{3/2} + 3\alpha k R_p}{6k^{3/2} + 3\alpha k R_p + 6\sqrt{k} R_p^2 + 2\alpha R_p^3}$$

The comparison of eqs. (3.55) an eq. (3.56) shows that the terms proportional to the Laplacian Δ_ξ are different in the two expressions (as $B_D \neq B'_D$), as it should be if the Hinch-Kim dualism would not apply. This result, follows almost immediately from the functional structure of the r.h.s. in eq. (3.54).

On the other hand, if the flow of the fluid in the porous medium is modeled by the Brinkman equations [31]

$$\begin{cases} \mu \Delta \boldsymbol{v}^{[i]}(\boldsymbol{x}) - \nabla p^{[i]}(\boldsymbol{x}) = \dfrac{\mu}{k} \boldsymbol{v}^{[i]}(\boldsymbol{x}) \\ \nabla \cdot \boldsymbol{v}^{[i]}(\boldsymbol{x}) = 0, \qquad \boldsymbol{x} \in D_b \end{cases} \tag{3.57}$$

with continuous boundary condition $(\boldsymbol{v}(\boldsymbol{x}), \boldsymbol{\sigma}(\boldsymbol{x})) = (\boldsymbol{v}^{[i]}(\boldsymbol{x}), \boldsymbol{\sigma}^{[i]}(\boldsymbol{x}))$ at the interface $\boldsymbol{x} \in \partial D_b$, the reciprocity of the boundary conditions is fulfilled, since

$$\begin{aligned}
[\boldsymbol{v}^{(n)}(\boldsymbol{\xi}), \boldsymbol{v}] = \int_{\partial D_b} [\sigma_{ab}(\boldsymbol{x}) n_b(\boldsymbol{x}) v_a^{(n)}(\boldsymbol{x}, \boldsymbol{\xi}) - v_a(\boldsymbol{x}) \sigma_{ab}^{(n)}(\boldsymbol{x}, \boldsymbol{\xi}) n_b(\boldsymbol{x})] dS(\boldsymbol{x}) &= \\
\int_{\partial D_b} [\sigma_{ab}^{[i]}(\boldsymbol{x}) n_b(\boldsymbol{x}) v_a^{[i](n)}(\boldsymbol{x}, \boldsymbol{\xi}) - v_a^{[i]}(\boldsymbol{x}) \sigma_{ab}^{[i](n)}(\boldsymbol{x}, \boldsymbol{\xi}) n_b(\boldsymbol{x})] dS(\boldsymbol{x}) &= \\
-\frac{\mu}{k} \int_{D_b} [v_a^{[i]}(\boldsymbol{x}) v_a^{[i](n)}(\boldsymbol{x}, \boldsymbol{\xi}) - v_a^{[i]}(\boldsymbol{x}) v_a^{[i](n)}(\boldsymbol{x}, \boldsymbol{\xi})] dV(\boldsymbol{x}) &= 0
\end{aligned} \tag{3.58}$$

thus for Brinkman porous bodies $\mathcal{F}_{\alpha\beta\boldsymbol{\beta}_n}$ is a Faxén operator.

The 0-th order Faxén operator for this case can be identified by the solutions given by Masliyah and al. [162] or by Yu and Kaloni [248] for a traslating Brinkman porous sphere in the Stokes flow. We observe that, in this case

$$U_\beta \mathcal{F}_{\alpha\beta} = U_\beta \left[\frac{R_p A_B}{2} + \frac{R_p^3 B_B}{2} \Delta_\xi \right] \delta_{\alpha\beta} \tag{3.59}$$

where

$$A_B = \frac{3R_p^2 \left(R_p \cosh\left(\frac{R_p}{\sqrt{k}}\right) - \sqrt{k} \sinh\left(\frac{R_p}{\sqrt{k}}\right) \right)}{6k^{3/2} \sinh\left(\frac{R_p}{\sqrt{k}}\right) - 6kR_p \cosh\left(\frac{R_p}{\sqrt{k}}\right) - 4R_p^3 \cosh\left(\frac{R_p}{\sqrt{k}}\right)}$$

$$B_B = \frac{6kR_p \cosh\left(\frac{R_p}{\sqrt{k}}\right) + R_p^3 \cosh\left(\frac{R_p}{\sqrt{k}}\right) - 6k^{3/2} \sinh\left(\frac{R_p}{\sqrt{k}}\right) - 3\sqrt{k} R_p^2 \sinh\left(\frac{R_p}{\sqrt{k}}\right)}{12k^{3/2} \sinh\left(\frac{R_p}{\sqrt{k}}\right) - 12kR_p \cosh\left(\frac{R_p}{\sqrt{k}}\right) - 8R_p^3 \cosh\left(\frac{R_p}{\sqrt{k}}\right)}$$

The same operator is identifiable in the Faxén theorem found by Padmavathi and al. [187, 71], according to which the force on a Brinkman porous sphere with center at $\boldsymbol{\xi}$ immersed in a generic ambient flow $\boldsymbol{u}(\boldsymbol{x})$ is, as expected,

$$F_\alpha = -M_\alpha = -8\pi\mu \left[\frac{R_p A_B}{2} + \frac{R_p^3 B_B}{2} \Delta_\xi \right] u_\alpha(\boldsymbol{\xi}) \tag{3.60}$$

In this case, in order to evaluate the geometrical moments we need to determine the surface traction and the velocity at the boundary, since

$$\begin{aligned}
&8\pi\, m_{\alpha\boldsymbol{\alpha}_m\beta\boldsymbol{\beta}_n}(\boldsymbol{\xi}, \boldsymbol{\xi}) = \int_{\partial D_b} (\boldsymbol{x} - \boldsymbol{\xi})_{\boldsymbol{\alpha}_m} h_{\alpha\beta\boldsymbol{\beta}_n}(\boldsymbol{x}, \boldsymbol{\xi}) dS(\boldsymbol{x}) \\
&- \int_{\partial D_b} p_{\alpha\boldsymbol{\alpha}_m}(\boldsymbol{x}, \boldsymbol{\xi}) v_{b\beta\boldsymbol{\beta}_n}(\boldsymbol{x}, \boldsymbol{\xi}) n_b(\boldsymbol{x}) dS(\boldsymbol{x}) \\
&+ \int_{\partial D_b} \left[v_{\alpha\beta\boldsymbol{\beta}_n}(\boldsymbol{x}, \boldsymbol{\xi}) n_b(\boldsymbol{x}) \nabla_b (\boldsymbol{x} - \boldsymbol{\xi})_{\boldsymbol{\alpha}_m} + n_\alpha(\boldsymbol{x}) v_{c\beta\boldsymbol{\beta}_n}(\boldsymbol{x}, \boldsymbol{\xi}) \nabla_c (\boldsymbol{x} - \boldsymbol{\xi})_{\boldsymbol{\alpha}_m} \right] dS(\boldsymbol{x})
\end{aligned} \tag{3.61}$$

3.8 Faxén operator for a sphere with Navier-slip boundary conditions

From eqs. (3.37), (3.40) and (3.44) it follows that the hydromechanics of a body in a Stokes fluid with Navier-slip boundary conditions can be determined if the complete set of surface traction is known. In this Section it is developed an analytic method, based on the Lorentz reciprocal theorem, for determining the surface tractions eq. (3.45) entering eq. (3.44), assuming Navier-slip boundary conditions on the surface of a spherical object. The method, here developed for a sphere with Navier-slip boundary conditions, can be employed systematically for obtaining analytic expressions of n-th order Faxén operators of spheres with different BC-reciprocal boundary conditions. To this aim consider, in the remainder, a Cartesian coordinate system for the point $\boldsymbol{x}$ with the origin at the center of the sphere. Also the entries at the source point $\boldsymbol{\xi}$ are expressed in the same Cartesian coordinate system, therefore there is no substantial distinction between Greek and Latin indexes.

0-th order Faxén operator

In order to determine the 0-th order surface traction on a sphere moving in the unbounded Stokes fluid with velocity $-\boldsymbol{U}$, consider the disturbance field $\boldsymbol{w}^{(0)}(\boldsymbol{x},\boldsymbol{\xi}) = \boldsymbol{w}^{(0)}(\boldsymbol{x})$ due to a sphere with Navier-slip boundary conditions in a constant field $\boldsymbol{u}^{(0)}(\boldsymbol{x},\boldsymbol{\xi}) = \boldsymbol{U}$, which is the solution of the Stokes problem

$$\begin{cases} \mu \Delta w_a^{(0)}(\boldsymbol{x}) - \nabla_a q^{(0)}(\boldsymbol{x}) = 0 \\ \nabla_a w_a^{(0)}(\boldsymbol{x}) = 0, \qquad \boldsymbol{x} \in D_f \\ w_a^{(0)}(\boldsymbol{x}) = -U_b \left(\delta_{ab} + \lambda h_{bc}(\boldsymbol{x}) t_{ac}(\boldsymbol{x})\right), \qquad \boldsymbol{x} \in \partial D_b \end{cases} \tag{3.62}$$

and the Stokeslet $(\boldsymbol{S}_\alpha(\boldsymbol{x},\boldsymbol{\xi}), \mu \boldsymbol{\Sigma}_\alpha(\boldsymbol{x},\boldsymbol{\xi}))$, explicitly reported in eq. (1.13) or in the monographs [194, 130]. Applying the Lorentz reciprocal theorem to the fields $(\boldsymbol{w}^{(0)}(\boldsymbol{x}), q^{(0)}(\boldsymbol{x}))$ solution of eqs. (3.62), and $(\boldsymbol{S}_\alpha(\boldsymbol{x},\boldsymbol{\xi}), \mu\boldsymbol{\Sigma}_\alpha(\boldsymbol{x},\boldsymbol{\xi}))$ within the domain of the fluid D_f, bounded by the surface $\partial D_b \cup \partial D_\infty$, and considering that both fields vanish at infinity i.e. on ∂D_∞, we have

$$[\boldsymbol{w}^{(0)}, \boldsymbol{S}_\alpha(\boldsymbol{\xi})] = 0 \tag{3.63}$$

At the surface of the sphere, a Stokeslet with pole at the center of the sphere (thus for $r = (\boldsymbol{x}-\boldsymbol{\xi})_a(\boldsymbol{x}-\boldsymbol{\xi})_a = R_p$ and $\boldsymbol{\xi} = (0,0,0)$) reads

$$S_{a\alpha}(\boldsymbol{x},\boldsymbol{\xi}) = \frac{\delta_{a\alpha} + n_{a\alpha}(\boldsymbol{x})}{R_p}$$

$$\Sigma_{ab\alpha}(\boldsymbol{x},\boldsymbol{\xi}) n_b(\boldsymbol{x}) = 6\frac{n_{a\alpha}(\boldsymbol{x})}{R_p^2}, \qquad r = R_p \tag{3.64}$$

where $n_{aa_1...a_n}(\boldsymbol{x}) = n_a(\boldsymbol{x}) n_{a_1}(\boldsymbol{x}) ... n_{a_n}(\boldsymbol{x})$ and $n_a(\boldsymbol{x}) = (\boldsymbol{x}-\boldsymbol{\xi})_a / R_p$.

Substituting eqs. (3.64) within eq. (3.63) and expliciting the $[\cdot,\cdot]$-operator in eq. (3.63) according to the definition eq. (3.25), we have the following relation between integrals

$$-\frac{6}{R_p}\int_{r=R_p} n_{a\alpha}(\boldsymbol{x})dS(\boldsymbol{x}) = \int_{r=R_p} f_{ab}(\boldsymbol{x})(\delta_{b\alpha} + n_{b\alpha}(\boldsymbol{x}))dS(\boldsymbol{x}) \tag{3.65}$$

where $f_{ab}(\boldsymbol{x})$ is the surface traction related to the disturbance field introduced in eq. (3.45). In order to satisfy eq. (3.65), the surface traction $f_{ab}(\boldsymbol{x})$ should have the generic form

$$f_{ab}(\boldsymbol{x}) = a\,\delta_{ab} + b\,n_{ab}(\boldsymbol{x}) \tag{3.66}$$

where a and b are constant to be determined. Alternatively, expressed in terms of normal and tangential components,

$$f_{ab}(\boldsymbol{x}) = f^n\,n_{ab}(\boldsymbol{x}) + f^t(\delta_{ab} - n_{ab}(\boldsymbol{x})) \tag{3.67}$$

where $f^n = a + b$ and $f^t = a$.

Substituting eq. (3.67) into eq. (3.65), a first relation between f^n and f^t is obtained

$$-\frac{6}{R_p}\int_{r=R_p} n_{a\alpha}(\boldsymbol{x})dS(\boldsymbol{x}) = 2f^n\int_{r=R_p} n_{a\alpha}(\boldsymbol{x})dS(\boldsymbol{x}) + f^t\int_{r=R_p}(\delta_{a\alpha} - n_{a\alpha}(\boldsymbol{x}))dS(\boldsymbol{x}) \tag{3.68}$$

that, solving the surface integrals, attains the simple form

$$f^n + f^t = -\frac{3}{R_p} \tag{3.69}$$

To determine f^n and f^t, a further independent relation between f^t and f^n is required. To this aim, we can consider the lowest order potential Stokes singularity, i.e. the so called source doublet $(-\Delta_\xi \boldsymbol{S}_\alpha(\boldsymbol{x},\boldsymbol{\xi})/2, -\mu\Delta_\xi\boldsymbol{\Sigma}_\alpha(\boldsymbol{x},\boldsymbol{\xi})/2)$. Also in this case, applying the Lorentz reciprocal theorem, we obtain

$$[\boldsymbol{w}^{(0)}, \Delta_\xi \boldsymbol{S}_\alpha(\boldsymbol{\xi})] = 0 \tag{3.70}$$

where Δ_ξ is the Laplacian operator acting on the coordinates of the pole. At the surface of the sphere, the Source Doublet with pole at the center of the sphere is

$$-\frac{\Delta_\xi\, S_{a\alpha}(\boldsymbol{x},\boldsymbol{\xi})}{2} = \frac{-\delta_{a\alpha} + 3\,n_{a\alpha}(\boldsymbol{x})}{R_p^3}$$

$$-\frac{(\Delta_\xi\, \Sigma_{ab\alpha}(\boldsymbol{x},\boldsymbol{\xi}))\,n_b(\boldsymbol{x})}{2} = 6\,\frac{-\delta_{a\alpha} + 3\,n_{a\alpha}(\boldsymbol{x})}{R_p^4}, \qquad r = R_p \tag{3.71}$$

Consequently, the second relation for f^n and f^t stemming from eq. (3.70) is

$$\begin{aligned}\frac{6}{R_p}\int_{r=R_p}(\delta_{a\alpha} - 3n_{a\alpha}(\boldsymbol{x}))dS(\boldsymbol{x}) \quad &+ \quad \frac{6\lambda f^t}{R_p}\int_{r=R_p}(\delta_{a\alpha} - n_{a\alpha}(\boldsymbol{x}))dS(\boldsymbol{x}) = \\ 2f^n\int_{r=R_p} n_{a\alpha}(\boldsymbol{x})dS(\boldsymbol{x}) \quad &- \quad f^t\int_{r=R_p}(\delta_{ab} - n_{ab}(\boldsymbol{x}))dS(\boldsymbol{x})\end{aligned} \tag{3.72}$$

that, upon explicit integration, simplifies as

$$\left(6\hat{\lambda} + 1\right) f^t - f^n = 0, \qquad \hat{\lambda} = \lambda/R_p \tag{3.73}$$

The solution of the linear system eqs. (3.69) and (3.73) provides

$$f^n = -\frac{3(1+6\hat{\lambda})}{2R_p(1+3\hat{\lambda})}, \qquad f^t = -\frac{3}{2R_p(1+3\hat{\lambda})} \tag{3.74}$$

and, thus, the total 0-th order geometrical surface traction is

$$h_{ab}(\boldsymbol{x}) = f_{ab}(\boldsymbol{x}) = -\frac{3}{2R_p}\left[\frac{\delta_{ab} + 6\hat{\lambda} n_{ab}(\boldsymbol{x})}{1+3\hat{\lambda}}\right] \tag{3.75}$$

In Appendix 3.B, we determine the analytical expression for the geometrical moments $m_{\alpha\boldsymbol{\alpha}_m\beta\boldsymbol{\beta}_n}(\boldsymbol{\xi},\boldsymbol{\xi})$ useful to evaluate the Faxén operators of the 0-th, 1-th and 2-nd order, by means of the surface traction obtained in this Section. To express the 0-th order Faxén operator according the eq. (3.20), we need the geometrical moments for $n=0$. Geometrical moments for $n=0$ and $m=0,1,2$ are obtained in eqs. (3.116)-(3.119). Due to the symmetry of the sphere, the moments for $n=0$ and $m=1$ in eq. (3.117) vanish, and equivalently also the moments for $n=0$ and $m=3,5,7,....$ It is easy to see that the moments for $n=0$ and $m=4,6,8,...$ contribute to the Faxén operator in eq. (3.68) by introducing terms proportional either to the divergence operators ∇_β and ∇_α or to the bilaplacian operator $\Delta_\xi\Delta_\xi$. Since Stokes fields are both divergence free and biharmonic, their action is immaterial. Therefore, in agreement with the result obtained in [197], the 0-th order Faxén operator for a sphere with Navier-slip boundary conditions is

$$\mathcal{F}_{\beta\alpha} = -\left(\frac{1+2\hat{\lambda}}{1+3\hat{\lambda}}\right)\left(\frac{3}{4}R_p + \frac{1}{8}\frac{R_p^3}{(1+2\hat{\lambda})}\Delta_\xi\right)\delta_{\alpha\beta} \tag{3.76}$$

where Δ_ξ is the Laplacian respect to the coordinates of the center of the sphere $\boldsymbol{\xi}$.

Since the force F_α exerted by the fluid on the particle is the 0-th order moment with reverse sign, for a sphere immersed in the ambient flow $\boldsymbol{u}(\boldsymbol{x})$ we have

$$F_\alpha = -M_\alpha(\boldsymbol{\xi}) = 8\pi\mu\left(\frac{1+2\hat{\lambda}}{1+3\hat{\lambda}}\right)\left(\frac{3}{4}R_p + \frac{1}{8}\frac{R_p^3}{(1+2\hat{\lambda})}\Delta_\xi\right)u_\alpha(\boldsymbol{\xi}) \tag{3.77}$$

1-st order Faxén operator

In order to evaluate the surface traction on a sphere immersed in a 1-st order ambient field, consider the disturbance field

$$\begin{cases} \mu\Delta w_a^{(1)}(\boldsymbol{x},\boldsymbol{\xi}) - \nabla_a q^{(1)}(\boldsymbol{x},\boldsymbol{\xi}) = 0 \\ \nabla_a w_a^{(1)}(\boldsymbol{x},\boldsymbol{\xi}) = 0, \qquad \boldsymbol{x}\in D_f \\ w_a^{(1)}(\boldsymbol{x},\boldsymbol{\xi}) = -A_{bb_1}\left((\boldsymbol{x}-\boldsymbol{\xi})_{b_1}\delta_{ab} + \lambda h_{cbb_1}(\boldsymbol{x},\boldsymbol{\xi})t_{ac}(\boldsymbol{x})\right), \qquad \boldsymbol{x}\in\partial D_b \end{cases} \tag{3.78}$$

with $\boldsymbol{\xi}=(0,0,0)$ at the center of the sphere. From eq. (3.45) we have

$$h_{abb_1}(\boldsymbol{x}) = f_{abb_1}(\boldsymbol{x}) - (n_b(\boldsymbol{x})\,\delta_{ab_1} + \delta_{ab}\,n_{b_1}(\boldsymbol{x})) \tag{3.79}$$

The procedure to obtain $f_{abb_1}(\boldsymbol{x})$ (and thus $h_{abb_1}(\boldsymbol{x})$) is equivalent to that followed in eqs. (3.63)-(3.75). In this case, the most general form for $f_{abb_1}(\boldsymbol{x})$ in order to satisfy reciprocity relations with singularities centered at the center of the sphere is

$$f_{abb_1}(\boldsymbol{x}) = a\,\delta_{ab}n_{b_1}(\boldsymbol{x}) + b\,\delta_{ab_1}n_b(\boldsymbol{x}) + c\,n_{abb_1}(\boldsymbol{x}) + d\,\delta_{bb_1}n_{a1}(\boldsymbol{x}) \tag{3.80}$$

where a, b, c and d are constant to be determined. Since, according to the definition eq. (3.10), $A_{bb_1} = 0$ due to the imcompressibility of the ambient flow, the last term in eq. (3.80) does not contribute to the surface traction, and we can set $d = 0$. If we apply the Lorentz reciprocal theorem to the solution $(\boldsymbol{w}^{(1)}(\boldsymbol{x},\boldsymbol{\xi}), \boldsymbol{\tau}^{(1)}(\boldsymbol{x},\boldsymbol{\xi}))$ of eqs. (3.78) and to the Stokeslet or the Source doublet, as in the previous paragraph, we obtain that all the integrals on the surface of the sphere vanish due to the spherical symmetry. For this reason, it is necessary to consider the Stokes doublet $(\nabla_\beta \boldsymbol{S}_\alpha(\boldsymbol{x},\boldsymbol{\xi}), \mu\nabla_\beta \boldsymbol{\Sigma}_\alpha(\boldsymbol{x},\boldsymbol{\xi}))$ with pole at the center of the sphere, and therefore

$$[\boldsymbol{w}^{(1)}(\boldsymbol{\xi}), \nabla_\beta \boldsymbol{S}_\alpha(\boldsymbol{\xi})] = 0 \tag{3.81}$$

from which one obtains a system of two linear equations in the coefficients a, b, c,

$$\begin{cases} -(8+6\hat{\lambda})a + (2+24\hat{\lambda})b - 3c = 24 + 18\hat{\lambda} \\ (2+24\hat{\lambda})a - (8+6\hat{\lambda})b - 3c = -6 + 18\hat{\lambda} \end{cases} \tag{3.82}$$

In order to solve the system we need another linearly independent equation. To this aim, it is possible to apply the Lorentz reciprocal theorem between the Source Quadrupole $(\Delta_\xi \nabla_\beta \boldsymbol{S}_\alpha(\boldsymbol{x},\boldsymbol{\xi}), \mu\, \Delta_\xi \nabla_\beta \boldsymbol{\Sigma}_\alpha(\boldsymbol{x},\boldsymbol{\xi}))$ and $(\boldsymbol{w}^{(1)}(\boldsymbol{x}), \boldsymbol{\tau}^{(1)}(\boldsymbol{x}))$. Thus, applying the relation

$$[\boldsymbol{w}^{(1)}(\boldsymbol{\xi}), \Delta_\xi \nabla_\beta \boldsymbol{S}_\alpha(\boldsymbol{\xi})] = 0 \tag{3.83}$$

one obtains another independent relation amongst a, b and c,

$$c - 8\hat{\lambda}(a+b) = -16\hat{\lambda} \tag{3.84}$$

Solving eqs. (3.82) and (3.84) one finally gets

$$a = \frac{-3 - 7\hat{\lambda} + 15\hat{\lambda}^2}{(1+5\hat{\lambda})(1+3\hat{\lambda})}, \qquad b = \frac{\hat{\lambda}(8+15\hat{\lambda})}{(1+5\hat{\lambda})(1+3\hat{\lambda})}, \qquad c = -\frac{40\hat{\lambda}}{1+5\hat{\lambda}} \tag{3.85}$$

The surface tensor in eq. (3.45) is obtained by substituting the constant defined by eq. (3.85) into eq. (3.80),

$$h_{abb_1}(\boldsymbol{x}) = -\frac{(4+15\hat{\lambda})\,\delta_{ab} n_{b_1}(\boldsymbol{x}) + \ \delta_{ab_1} n_b(\boldsymbol{x}) + 40\hat{\lambda}(1+3\hat{\lambda})\, n_{abb_1}(\boldsymbol{x})}{(1+5\hat{\lambda})(1+3\hat{\lambda})} \tag{3.86}$$

To determine the Faxén operator $\mathcal{F}_{\alpha\beta\beta_1}$, the moments $m_{\alpha\boldsymbol{\alpha}_m\beta\boldsymbol{\beta}_n}(\boldsymbol{\xi},\boldsymbol{\xi})$ at the center of the sphere for $n = 1$ should be evaluated using the surface traction defined by eq. (3.86). Since geometrical moments with even $m = 0, 2, ...$ vanish due to the symmetry of the sphere, only the geometrical moments for odd $m = 1, 3, ...$ are needed. Geometrical moments for $m = 1$ and $m = 3$ are given in eq. (3.120) and eq. (3.121) respectively. Higher order geometrical moments contribute to the Faxén operator by divergence and bilaplacian operators and thus, they can be neglected as their action is immaterial. Thus, according to eq. (3.68), the 1-st order Faxén operator is given by

$$\begin{aligned} \mathcal{F}_{\alpha\beta\beta_1} = &-\frac{R_p^3}{6(1+5\hat{\lambda})(1+3\hat{\lambda})} \Big\{ \Big[(4+20\hat{\lambda}+15\hat{\lambda}^2)\delta_{\alpha\beta}\nabla_{\beta_1} + (1+5\hat{\lambda}+15\hat{\lambda}^2)\delta_{\alpha\beta_1}\nabla_\beta \Big] \\ &+\frac{R_p^2}{10}\Big[(4+12\hat{\lambda}-15\hat{\lambda}^2)\Delta_\xi \nabla_{\beta_1}\delta_{\alpha\beta} + (1+3\hat{\lambda}+15\hat{\lambda}^2)\Delta_\xi \nabla_\beta \delta_{\alpha\beta_1} \Big] \Big\} \end{aligned} \tag{3.87}$$

The Faxén operator $\mathcal{T}_{\gamma\alpha}$, yielding the torque $T_\alpha = \varepsilon_{\alpha\beta\beta_1} M_{\beta\beta_1}(\boldsymbol{\xi})$ on the body if an ambient flow is applied, or the velocity field due to the body rotation if applied to the Stokeslet, can be defined by the antisymmetric part of the first order Faxén operator, i.e.,

$$\mathcal{T}_{\gamma\alpha} = \varepsilon_{\alpha\beta\beta_1} \mathcal{F}_{\gamma\beta\beta_1} \tag{3.88}$$

Considering that $\varepsilon_{\gamma\alpha\alpha_1} \Delta\nabla_{\alpha_1} u_\alpha(\boldsymbol{x}) = 0$ for any ambient flow, terms containing the third order derivatives in eq. (3.87) are immaterial and may be neglected, so we obtain

$$\mathcal{T}_{\gamma\alpha} = \frac{\varepsilon_{\alpha\gamma\gamma_1} R_p^3 \nabla_{\gamma_1}}{2(1+3\hat{\lambda})} \tag{3.89}$$

in agreement with [197].

Thus, the torque on the sphere in the ambient flow $u_\alpha(\boldsymbol{x})$ is give by

$$T_\alpha = \frac{4\pi\mu\, \varepsilon_{\alpha\gamma\gamma_1} R_p^3 \nabla_{\gamma_1} u_\gamma(\boldsymbol{\xi})}{(1+3\hat{\lambda})} \tag{3.90}$$

The symmetric part of the 1-th order Faxén operator, useful for evaluating stresses in suspensions, is given by

$$\mathcal{E}_{\alpha\beta\beta_1} = \frac{\mathcal{F}_{\alpha\beta\beta_1} + \mathcal{F}_{\alpha\beta_1\beta}}{2} = -\left(\frac{5+10\hat{\lambda}}{6+30\hat{\lambda}} + \frac{\Delta_\xi}{12(1+5\hat{\lambda})}\right)\left(\frac{\nabla_\beta \delta_{\alpha\beta_1} + \nabla_\beta \delta_{\alpha\beta_1}}{2}\right) \tag{3.91}$$

According to eq. (3.21), the Faxén operator in eq. (3.87) determines the flow around a sphere in the linear ambient flow $u_a(\boldsymbol{x}) = \delta_{a\,3}\,\delta_{b\,1}\,x_b = \delta_{a\,3}\,x_1$. In fact, by choosing $A_{\beta\beta_1} = \delta_{\beta\,3}\delta_{\beta_1\,1}$ in eq. (3.21) the disturbance field reads

$$w_a^{(1)}(\boldsymbol{x},\boldsymbol{\xi}) = -\frac{R_p^3}{6(1+5\hat{\lambda})(1+3\hat{\lambda})} \Big\{(4+20\hat{\lambda}+15\hat{\lambda}^2) S_{a\,3,1}(\boldsymbol{x},\boldsymbol{\xi}) + (1+5\hat{\lambda}+15\hat{\lambda}^2) S_{a\,1,3}(\boldsymbol{x},\boldsymbol{\xi}) \\ \frac{R_p^2}{10}\left[(4+12\hat{\lambda}-15\hat{\lambda}^2)\Delta_\xi S_{a\,3,1}(\boldsymbol{x},\boldsymbol{\xi}) + (1+3\hat{\lambda}+15\hat{\lambda}^2)\Delta_\xi S_{a\,1,3}(\boldsymbol{x},\boldsymbol{\xi})\right]\Big\} \tag{3.92}$$

Fig. 3.2 depicts the streamlines for the total flow in the case of no-slip, complete slip, and for two different values of $\hat{\lambda} = 1,\, 10$.

2-nd order Faxén operator

In order to evaluate the surface traction on a sphere immersed in a 2-nd order ambient field, consider the disturbance field

$$\begin{cases} \mu\Delta w_a^{(2)}(\boldsymbol{x},\boldsymbol{\xi}) - \nabla_a q^{(2)}(\boldsymbol{x},\boldsymbol{\xi}) = 0 \\ \nabla_a w_a^{(2)}(\boldsymbol{x},\boldsymbol{\xi}) = 0, \qquad \boldsymbol{x} \in D_f \\ w_a^{(2)}(\boldsymbol{x},\boldsymbol{\xi}) = -A_{bb_1b_2}\left((\boldsymbol{x}-\boldsymbol{\xi})_{b_1b_2}\delta_{ab} + \lambda h_{cbb_1b_2}(\boldsymbol{x},\boldsymbol{\xi}) t_{ac}(\boldsymbol{x})\right), \qquad \boldsymbol{x} \in \partial D_b \end{cases} \tag{3.93}$$

In this case, the ambient pressure is $p_{bb_1b_2}(\boldsymbol{x},\boldsymbol{\xi}) = (\boldsymbol{x}-\boldsymbol{\xi})_b \Delta(\boldsymbol{x}-\boldsymbol{\xi})_{b_1b_2}$. Therefore, from eq. (3.45) with $\boldsymbol{\xi} = (0,0,0)$ we can set

$$h_{abb_1b_2}(\boldsymbol{x}) = f_{abb_1b_2}(\boldsymbol{x}) - R_p\left(n_{bb_1}(\boldsymbol{x})\delta_{ab_2} + n_{bb_2}(\boldsymbol{x})\delta_{ab_1} + 2(\delta_{ab} n_{b_1b_2}(\boldsymbol{x}) - \delta_{b_1b_2} n_{ab}(\boldsymbol{x}))\right) \tag{3.94}$$

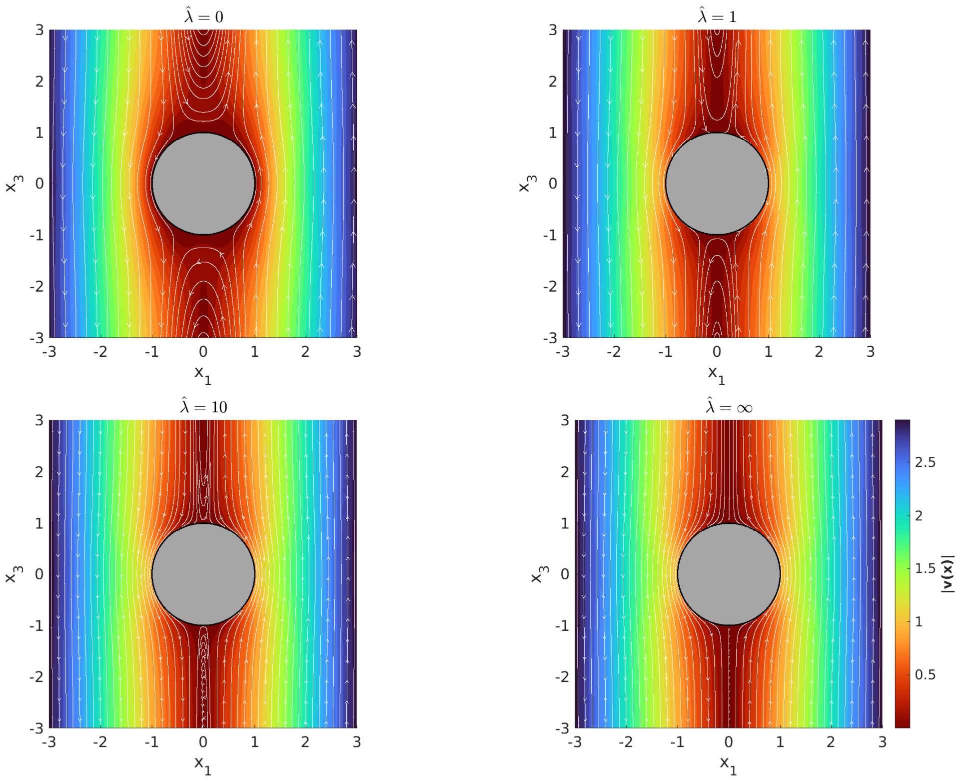

Figure 3.2. Streamlines on the plane $x_2 = 0$ of the fluid around a sphere in a linear ambient flow $u_a(\boldsymbol{x}) = \delta_{a\,3}\, x_1$ for different values of dimensionless slip length at the surface of the sphere.

Considering that $f_{abb_1b_2}(\boldsymbol{x})$ must be symmetric with respect to the indexes b_1 and b_2, and that $A_{bb} = 0$, the most general form for this traction is

$$f_{abb_1b_2}(\boldsymbol{x}) = a\,\delta_{ab}n_{b_1b_2}(\boldsymbol{x}) + b\,\delta_{ab}\delta_{b_1b_2} + c\,(\delta_{ab_1}n_{bb_2}(\boldsymbol{x}) + \delta_{ab_2}n_{bb_1}(\boldsymbol{x})) + d\,\delta_{b_1b_2}n_{ab}(\boldsymbol{x}) + e\,n_{abb_1b_2}(\boldsymbol{x}) \tag{3.95}$$

Following the same procedure used for the geometrical surface tractions of lower orders, we consider the Stokes Quadrupole $(\nabla_\gamma\nabla_\beta \boldsymbol{S}_\alpha(\boldsymbol{x},\boldsymbol{\xi}), \mu\nabla_\gamma\nabla_\beta\boldsymbol{\Sigma}_\alpha(\boldsymbol{x},\boldsymbol{\xi}))$. Applying the Lorentz reciprocal theorem, we have

$$[\boldsymbol{w}^{(2)}(\boldsymbol{\xi}), \nabla_\gamma\nabla_\beta\boldsymbol{S}_\alpha(\boldsymbol{\xi})] = 0 \tag{3.96}$$

Solving the integrals, we obtain four linear equations for the five unknown

$$\begin{cases} -2(3+4)a + 2(1+20\hat{\lambda})c - 2e = (25+24\hat{\lambda})R_p \\ (-5+12\hat{\lambda})a + 84\hat{\lambda}b - 3(1-8\hat{\lambda})c - 14d - 4e = 3(5+16\hat{\lambda})R_p \\ (1+20\hat{\lambda})a - (5-12\hat{\lambda})c - 2e = -(3-52\hat{\lambda})R_p \\ -4(1+6\hat{\lambda})a + 42\hat{\lambda}b + 6(1-\hat{\lambda})c - 7d + e = 6(2-9\hat{\lambda})R_p \end{cases} \tag{3.97}$$

out of which only three are linearly independent. In fact, by summing the fourth equation multiplied by 2 to the third equation multiplied by 3, we obtain the second equation. To obtain a further equation, we consider the Source Hexapole $(\Delta_\xi\nabla_\gamma\nabla_\beta\boldsymbol{S}_\alpha(\boldsymbol{x},\boldsymbol{\xi}), \mu\Delta_\xi\nabla_\gamma\nabla_\beta\boldsymbol{\Sigma}_\alpha(\boldsymbol{x},\boldsymbol{\xi}))$. As in the previous cases, the application of the the Lorentz reciprocal theorem provides

$$[\boldsymbol{w}^{(2)}(\boldsymbol{\xi}), \Delta_\xi\nabla_\gamma\nabla_\beta\boldsymbol{S}_\alpha(\boldsymbol{\xi})] = 0 \tag{3.98}$$

from which it follows that

$$-10\hat{\lambda}a - 20\hat{\lambda}c + e = -40\hat{\lambda} \tag{3.99}$$

We need another equation, linearly independent of eqs. (3.99) and of the three linearly independent eqs. (3.97) that can obtained by applying the Lorentz reciprocal theorem to the Stokeslet

$$[\boldsymbol{w}^{(2)}(\boldsymbol{\xi}), \boldsymbol{S}_\alpha(\boldsymbol{\xi})] = 0 \tag{3.100}$$

resulting the relation

$$3a + 10b + c + 5d + e = -3R_p \tag{3.101}$$

By solving the linear system formed by the first, third, and fourth equations in eq. (3.97), eq. (3.99) and eq. (3.101), that possesses a non-vanishing determinant for any $\hat{\lambda} \geq 0$, the constant a, b, c, d, e entering eq. (3.95) are determined

$$\frac{a}{R_p} = \frac{-17-52\hat{\lambda}+244\hat{\lambda}^2}{4(1+4\hat{\lambda})(1+7\hat{\lambda})} \qquad \frac{b}{R_p} = \frac{3+17\hat{\lambda}}{4(1+3\hat{\lambda})(1+4\hat{\lambda})(1+7\hat{\lambda})} \qquad \frac{e}{R_p} = -\frac{175\hat{\lambda}}{2+14\hat{\lambda}}$$

$$\frac{c}{R_p} = \frac{-1+44\hat{\lambda}+112\hat{\lambda}^2}{4(1+4\hat{\lambda})(1+7\hat{\lambda})} \qquad \frac{d}{R_p} = \frac{1+28\hat{\lambda}+127\hat{\lambda}^2+84\hat{\lambda}^3}{2(1+3\hat{\lambda})(1+4\hat{\lambda})(1+7\hat{\lambda})} \tag{3.102}$$

and therefore, the geometrical surface traction in eq. (3.94) is given by

$$h_{abb_1b_2}(\boldsymbol{x}) = \frac{R_p}{4(1+4\hat{\lambda})(1+7\hat{\lambda})} \Big[-5(5+28\hat{\lambda})\delta_{ab} n_{b_1b_2}(\boldsymbol{x}) \\
+ \frac{3+17\hat{\lambda}}{1+3\hat{\lambda}} \delta_{ab}\delta_{b_1b_2} - 5\left(\delta_{ab_1} n_{bb_2}(\boldsymbol{x}) + \delta_{ab_2} n_{bb_1}(\boldsymbol{x})\right) \\
+ \frac{2(5+84\lambda+371\lambda^2+420\lambda^3)}{1+3\hat{\lambda}} \delta_{b_1b_2} n_{ab}(\boldsymbol{x}) - 350\hat{\lambda}(1+4\hat{\lambda})\, n_{abb_1b_2}(\boldsymbol{x}))\Big] \tag{3.103}$$

through which it is possible to obtain the geometrical moments at the center of the sphere $m_{\alpha\beta\boldsymbol{\beta}_2}(\boldsymbol{\xi},\boldsymbol{\xi})$, $m_{\alpha\boldsymbol{\alpha}_2\beta\boldsymbol{\beta}_2}(\boldsymbol{\xi},\boldsymbol{\xi})$, $m_{\alpha\boldsymbol{\alpha}_4\beta\boldsymbol{\beta}_2}(\boldsymbol{\xi},\boldsymbol{\xi})$. Their analytic expression is reported in Appendix 3.B, eqs. (3.122), (3.123), (3.124). Using these results it is possible to express analytically the 2-nd order Faxén operator

$$\mathcal{F}_{\alpha\beta\beta_1\beta_2} = -\frac{R_p^3}{4(1+4\hat{\lambda})(1+7\hat{\lambda})} \Bigg\{ \frac{(1+4\hat{\lambda})(1+7\hat{\lambda})}{1+3\hat{\lambda}} \left[\delta_{\alpha\beta}\delta_{\beta_1\beta_2} + \hat{\lambda}(\delta_{\beta\beta_1}\delta_{\alpha\beta_2} + \delta_{\beta\beta_2}\delta_{\alpha\beta_1})\right] \\
+\frac{R_p^2}{6}\Bigg[-4\hat{\lambda}^2 \left(\frac{4+21\hat{\lambda}}{1+3\hat{\lambda}}\right) \Delta_\xi \delta_{\beta_1\beta_2}\delta_{\alpha\beta} + 5(1+6\hat{\lambda})\nabla_{\beta_1\beta_2}\delta_{\alpha\beta} + \\
(1+6\hat{\lambda}+28\hat{\lambda}^2)(\nabla_{\beta\beta_1}\delta_{\alpha\beta_2} + \nabla_{\beta\beta_2}\delta_{\alpha\beta_1}) + (1+12\hat{\lambda}+56\hat{\lambda}^2)(\delta_{\alpha\beta_1}\delta_{\beta\beta_2} + \delta_{\alpha\beta_2}\delta_{\beta\beta_1})\Delta_\xi\Bigg] \\
+\frac{R_p^4}{84}\left[(5+20\hat{\lambda}-56\hat{\lambda}^2)\nabla_{\beta_1\beta_2}\delta_{\alpha\beta} + (1+4\hat{\lambda}+28\hat{\lambda}^2)(\nabla_{\beta\beta_1}\delta_{\alpha\beta_2} + \nabla_{\beta\beta_2}\delta_{\alpha\beta_1})\right]\Delta_\xi \Bigg\} \tag{3.104}$$

The Faxén operator in eq. (3.104) can be used to obtain the flow around a sphere in the unbounded Poiseuille ambient flow

$$u_a^{(2)}(\boldsymbol{x}) = \delta_{a\,3}(\delta_{a_1a_2} - \delta_{a_1\,3}\delta_{a_2\,3})\,(\boldsymbol{x}-\boldsymbol{\xi})_{a_1a_2} = \delta_{a\,3}\left((\boldsymbol{x}-\boldsymbol{\xi})_1^2 + (\boldsymbol{x}-\boldsymbol{\xi})_2^2\right)$$

$\boldsymbol{\xi}$ being the center of the sphere. Choosing $A_{\beta\beta_1\beta_2} = \delta_{\beta\,3}(\delta_{\beta_1\beta_2} - \delta_{\beta_1\,3}\delta_{\beta_2\,3})$ in eq. (3.21) the disturbance field reads

$$w_a^{(2)}(\boldsymbol{x},\boldsymbol{\xi}) = -\frac{R_p^3}{24(1+7\hat{\lambda})} \Bigg\{ 12\left(\frac{1+7\hat{\lambda}}{1+3\hat{\lambda}}\right) S_{a\,3}(\boldsymbol{x},\boldsymbol{\xi}) + \\
R_p^2\left[\left(\frac{5+25\hat{\lambda}-42\hat{\lambda}^2}{1+3\hat{\lambda}}\right)\Delta_\xi S_{a\,3}(\boldsymbol{x},\boldsymbol{\xi}) - 7(1+2\hat{\lambda})S_{a\,3,3\,3}(\boldsymbol{x},\boldsymbol{\xi})\right] - R_p^4 \frac{\Delta_\xi S_{a\,3,3\,3}(\boldsymbol{x},\boldsymbol{\xi})}{2} \Bigg\} \tag{3.105}$$

The streamlines obtained using eq. (3.105) in the case of no-slip, complete slip, Navier-slip with $\hat{\lambda} = 1$ and $\hat{\lambda} = 10$ are reported in Fig. 3.3.

Appendix

3.A Symmetry of the geometrical moments

To show the symmetry in eq. (3.39), if BC-reciprocity applies, consider the moments $M^{(n)}_{\alpha\boldsymbol{\alpha}_m}(\boldsymbol{\xi},\boldsymbol{\xi}')$ and their expression eq. (3.16). Using the notation developed in Section

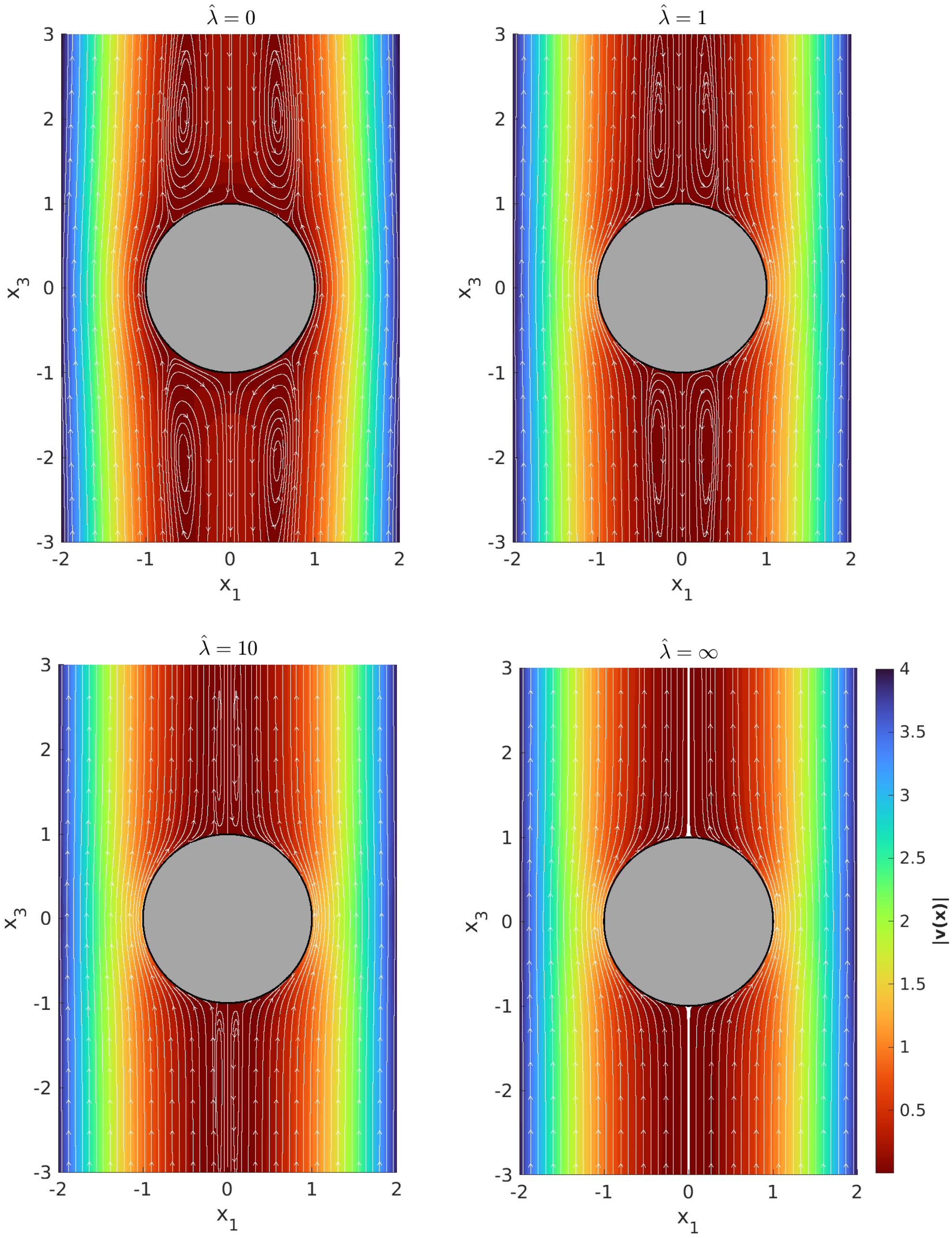

Figure 3.3. Streamlines on the plane $x_2 = 0$ of the fluid around a sphere in the unbounded Poiseuille ambient flow $u_a(\boldsymbol{x}) = \delta_{a\,3}\,(x_1^2 + x_2^2)$ for different values of dimensionless slip length, at the surface of the sphere.

3.4

$$A_{\alpha\boldsymbol{\alpha}_m} M^{(n)}_{\alpha\boldsymbol{\alpha}_m}(\boldsymbol{\xi},\boldsymbol{\xi}') = [\boldsymbol{u}^{(m)}(\boldsymbol{\xi}),\boldsymbol{v}^{(n)}(\boldsymbol{\xi}')] \tag{3.106}$$

and analogously

$$A_{\beta'\boldsymbol{\beta}'_n} M^{(m)}_{\beta'\boldsymbol{\beta}'_n}(\boldsymbol{\xi}',\boldsymbol{\xi}) = [\boldsymbol{u}^{(n)}(\boldsymbol{\xi}'),\boldsymbol{v}^{(m)}(\boldsymbol{\xi})] \tag{3.107}$$

Therefore, their difference can be expressed as

$$\begin{aligned} &A_{\alpha\boldsymbol{\alpha}_m} M^{(n)}_{\alpha\boldsymbol{\alpha}_m}(\boldsymbol{\xi},\boldsymbol{\xi}') - A_{\beta'\boldsymbol{\beta}'_n} M^{(m)}_{\beta'\boldsymbol{\beta}'_n}(\boldsymbol{\xi}',\boldsymbol{\xi}) = [\boldsymbol{u}^{(m)}(\boldsymbol{\xi}),\boldsymbol{v}^{(n)}(\boldsymbol{\xi}')] - [\boldsymbol{u}^{(n)}(\boldsymbol{\xi}'),\boldsymbol{v}^{(m)}(\boldsymbol{\xi})] \\ &= [\boldsymbol{u}^{(m)}(\boldsymbol{\xi}),\boldsymbol{u}^{(n)}(\boldsymbol{\xi}')] + [\boldsymbol{u}^{(m)}(\boldsymbol{\xi}),\boldsymbol{w}^{(n)}(\boldsymbol{\xi}')] - [\boldsymbol{u}^{(n)}(\boldsymbol{\xi}'),\boldsymbol{u}^{(m)}(\boldsymbol{\xi})] - [\boldsymbol{u}^{(n)}(\boldsymbol{\xi}'),\boldsymbol{w}^{(m)}(\boldsymbol{\xi})] \\ &= [\boldsymbol{u}^{(m)}(\boldsymbol{\xi}),\boldsymbol{w}^{(n)}(\boldsymbol{\xi}')] - [\boldsymbol{u}^{(n)}(\boldsymbol{\xi}'),\boldsymbol{w}^{(m)}(\boldsymbol{\xi})] \end{aligned} \tag{3.108}$$

Under the hypothesis of reciprocal boundary conditions, from the identity eq. (3.29) it follows that

$$[\boldsymbol{u}^{(m)}(\boldsymbol{\xi}),\boldsymbol{w}^{(n)}(\boldsymbol{\xi}')] - [\boldsymbol{u}^{(n)}(\boldsymbol{\xi}'),\boldsymbol{w}^{(m)}(\boldsymbol{\xi})] = [\boldsymbol{v}^{(m)}(\boldsymbol{\xi}),\boldsymbol{v}^{(n)}(\boldsymbol{\xi}')] = 0 \tag{3.109}$$

i.e.,

$$A_{\alpha\boldsymbol{\alpha}_m} M^{(n)}_{\alpha\boldsymbol{\alpha}_m}(\boldsymbol{\xi},\boldsymbol{\xi}') = A_{\beta'\boldsymbol{\beta}'_n} M^{(m)}_{\beta'\boldsymbol{\beta}'_n}(\boldsymbol{\xi}',\boldsymbol{\xi}) \tag{3.110}$$

Therefore, from the definition of geometrical moments eq. (3.18), since $A_{\beta'\boldsymbol{\beta}'_n}$ could be in principle arbitrary, we have

$$m_{\alpha\boldsymbol{\alpha}_m\beta'\boldsymbol{\beta}'_n}(\boldsymbol{\xi},\boldsymbol{\xi}') = m_{\beta'\boldsymbol{\beta}'_n\alpha\boldsymbol{\alpha}_m}(\boldsymbol{\xi}',\boldsymbol{\xi}) \tag{3.111}$$

corresponding to eq. (3.39). If the boundary conditions are not reciprocal, the r.h.s. of eq. (3.108) possesses the property

$$[\boldsymbol{u}^{(m)}(\boldsymbol{\xi}),\boldsymbol{w}^{(n)}(\boldsymbol{\xi}')] - [\boldsymbol{u}^{(n)}(\boldsymbol{\xi}'),\boldsymbol{w}^{(m)}(\boldsymbol{\xi})] \begin{cases} = 0, & n = m \\ \neq 0, & n \neq m \end{cases} \tag{3.112}$$

For $n = m = 0$ eq. (3.112) expresses the thermodynamic condition of symmetry of the resistance matrix, $m_{\alpha\beta} = m_{\beta\alpha}$, independently on the boundary conditions and on the nature of the immersed body [138]. This result represents a purely mechanical proof of the symmetry of the resistance matrix independently of the boundary conditions. The thermodynamic proof has been given by Landau [139, 138], while the mechanical proof by Brenner uses specific (no-slip) boundary conditions see [98, p. 166] and the discussion therein.

As seen in Section 3.3, a consequence of the symmetry of the geometrical moments, in the case the Hinch-Kim dualism holds, is the equivalence between eq. (3.6) and eq. (3.40). This equivalence can be proved by substituting the Hinch-Kim theorem expressed by eq. (3.37) in eq. (3.6), hence

$$w_a(\boldsymbol{x}) = \frac{1}{8\pi\mu}\sum_{m=0}^{\infty} \frac{M_{\alpha\,\boldsymbol{\alpha}_m}(\boldsymbol{\xi})}{m!} \nabla_{\boldsymbol{\alpha}_m} S_{a\,\alpha}(\boldsymbol{x},\boldsymbol{\xi}) = \sum_{m=0}^{\infty} \frac{\mathcal{F}_{\beta'\alpha\boldsymbol{\alpha}_m} u_{\beta'}(\boldsymbol{\xi}')}{m!} \nabla_{\boldsymbol{\alpha}_m} S_{a\,\alpha}(\boldsymbol{x},\boldsymbol{\xi}) \tag{3.113}$$

substituting the expression eq. (3.20) for the Faxén operator and using the symmetry eq. (3.111)

$$\begin{aligned} w_a(\boldsymbol{x}) &= \sum_{m=0}^{\infty}\sum_{n=0}^{\infty} \frac{m_{\beta'\boldsymbol{\beta}'_n\alpha\boldsymbol{\alpha}_m}(\boldsymbol{\xi}',\boldsymbol{\xi})\nabla_{\boldsymbol{\beta}'_n} u_{\beta'}(\boldsymbol{\xi}')}{m!n!}\nabla_{\boldsymbol{\alpha}_m} S_{a\,\alpha}(\boldsymbol{x},\boldsymbol{\xi}) \\ &= \sum_{m=0}^{\infty}\sum_{n=0}^{\infty} \frac{m_{\alpha\boldsymbol{\alpha}_m\beta'\boldsymbol{\beta}'_n}(\boldsymbol{\xi},\boldsymbol{\xi}')\nabla_{\boldsymbol{\beta}'_n} u_{\beta'}(\boldsymbol{\xi}')}{m!n!}\nabla_{\boldsymbol{\alpha}_m} S_{a\,\alpha}(\boldsymbol{x},\boldsymbol{\xi}) \end{aligned} \tag{3.114}$$

in which a new representation of the Faxén operator acting on the point $\boldsymbol{\xi}'$ is introduced

$$\mathcal{F}_{\alpha\beta'\boldsymbol{\beta}'_n} = \sum_{m=0}^{\infty} \frac{m_{\alpha\boldsymbol{\alpha}_m\beta'\boldsymbol{\beta}'_n}(\boldsymbol{\xi},\boldsymbol{\xi}')\nabla_{\boldsymbol{\alpha}_m}}{m!}$$

from which it follows that

$$w_a(\boldsymbol{x}) = \sum_{n=0}^{\infty} \frac{\nabla_{\boldsymbol{\beta}'_n} u_{\beta'}(\boldsymbol{\xi}')}{n!}\mathcal{F}_{\alpha\beta'\boldsymbol{\beta}'_n} S_{a\,\alpha}(\boldsymbol{x},\boldsymbol{\xi}) \tag{3.115}$$

that becomes eq. (3.40) for $\boldsymbol{\xi}' = \boldsymbol{\xi}$.

3.B Geometrical moments for a sphere with Navier-slip conditions

In this Appendix, we provide the analytical expression for the Cartesian entries $m_{\alpha\boldsymbol{\alpha}_m\beta\boldsymbol{\beta}_n}(\boldsymbol{\xi},\boldsymbol{\xi})$ of the geometrical moments, for a sphere with Navier-slip boundary conditions, $\boldsymbol{\xi}$ being the center of the sphere.

(m,n)-th order geometrical moments with $n=0$

In order to evaluate the geometrical moment with $n=0$, eqs. (3.44)-(3.45) can be applied using for the geometrical surface traction eq. (3.75).

In the case $m=0$ we obtain the well-known Basset term [4]

$$m_{\alpha\beta} = -\frac{3}{16\pi R_p}\int_{r=R_p}\left[\frac{\delta_{\alpha\beta}+6\hat{\lambda}n_{\alpha\beta}(\boldsymbol{x})}{1+3\hat{\lambda}}\right] dS(\boldsymbol{x}) = -\frac{3}{4}\left[\frac{1+2\hat{\lambda}}{1+3\hat{\lambda}}\right] R_p\,\delta_{\alpha\beta} \tag{3.116}$$

For $m=1$ the geometrical moments at the center of the sphere $\boldsymbol{\xi}=(0,0,0)$ vanish, in fact

$$m_{\alpha\alpha_1\beta} = m_{\beta\alpha\alpha_1} = \\ -\frac{3}{16\pi}\int_{r=R_p}\left[\frac{\delta_{\gamma\beta}+6\hat{\lambda}n_{\gamma\beta}(\boldsymbol{x})}{1+3\hat{\lambda}}\right]\left[\delta_{\alpha\gamma}n_{\alpha_1}(\boldsymbol{x}) - \hat{\lambda}(t_{\alpha\gamma}(\boldsymbol{x})n_{\alpha_1}(\boldsymbol{x}) + n_\alpha(\boldsymbol{x})t_{\alpha_1\gamma}(\boldsymbol{x}))\right] dS(\boldsymbol{x}) = 0 \tag{3.117}$$

and, due to the symmetry of the sphere,

$$m_{\alpha\boldsymbol{\alpha}_m\beta} = 0, \qquad m = 1,3,5\ldots \tag{3.118}$$

for any odd value of m. For $m = 2$

$$m_{\alpha\boldsymbol{\alpha}_2\beta} = m_{\beta\alpha\boldsymbol{\alpha}_2} = -\frac{3R_p}{16\pi}\int_{r=R_p}\left[\frac{\delta_{\gamma\beta} + 6\hat{\lambda} n_{\gamma\beta}(\boldsymbol{x})}{1+3\hat{\lambda}}\right] \times$$
$$\times \quad \left[\delta_{\alpha\gamma} n_{\alpha_1\alpha_2}(\boldsymbol{x}) - \hat{\lambda}(2t_{\alpha\gamma} n_{\alpha_1\alpha_2}(\boldsymbol{x}) + t_{\alpha_1\gamma} n_{\alpha\alpha_2}(\boldsymbol{x}) + t_{\alpha_2\gamma} n_{\alpha\alpha_1}(\boldsymbol{x}))\right] dS(\boldsymbol{x}) =$$
$$-\frac{R_p^3}{4(1+3\hat{\lambda})}\left[\delta_{\alpha\beta}\delta_{\alpha_1\alpha_2} + \hat{\lambda}(\delta_{\alpha\alpha_1}\delta_{\beta\alpha_2} + \delta_{\alpha\alpha_2}\delta_{\beta\alpha_1})\right] \tag{3.119}$$

(m,n)-th order geometrical moments with $n = 1$

For the geometrical moments with $n = 1$, eqs. (3.44)-(3.45) can be used with the geometrical surface traction expressed by eq. (3.103). By the symmetry expressed by eq. (3.117), the moment with $m = 0$ vanishes. For $m = 1$,

$$m_{\alpha\alpha_1\beta\beta_1} = m_{\beta\beta_1\alpha\alpha_1} = -R_p\int_{r=R_p}\left[\frac{(4+15\hat{\lambda})\,\delta_{\gamma\beta} n_{\beta_1}(\boldsymbol{x}) + \delta_{\gamma\beta_1} n_\beta(\boldsymbol{x}) + 40\hat{\lambda}(1+3\hat{\lambda})\, n_{\gamma\beta\beta_1}(\boldsymbol{x})}{8\pi(1+5\hat{\lambda})(1+3\hat{\lambda})}\right]$$
$$\times \quad \left[\delta_{\alpha\gamma} n_{\alpha_1}(\boldsymbol{x}) - \hat{\lambda}(t_{\alpha\gamma}(\boldsymbol{x}) n_{\alpha_1}(\boldsymbol{x}) + t_{\alpha_1\gamma}(\boldsymbol{x}) n_\alpha(\boldsymbol{x}))\right] dS(\boldsymbol{x}) =$$
$$-\frac{R_p^3}{6(1+5\hat{\lambda})(1+3\hat{\lambda})}\left[\left(4+20\hat{\lambda}+15\hat{\lambda}^2\right)\delta_{\alpha\beta}\delta_{\alpha_1\beta_1} + \left(1+5\hat{\lambda}+15\hat{\lambda}^2\right)\delta_{\alpha\beta_1}\delta_{\alpha_1\beta} + 10\hat{\lambda}(1+3\hat{\lambda})\delta_{\alpha\alpha_1}\delta_{\beta\beta_1}\right] \tag{3.120}$$

Due to symmetry of the sphere, for odd n and even m the geometrical moments vanish, therefore $m_{\alpha\boldsymbol{\alpha}_2\beta\beta_1} = m_{\beta\beta_1\alpha\boldsymbol{\alpha}_2} = 0$. For $m = 3$,

$$m_{\alpha\boldsymbol{\alpha}_3\beta\beta_1} = m_{\beta\beta_1\alpha\boldsymbol{\alpha}_3} =$$
$$- \quad R_p^3\int_{r=R_p}\left[\frac{(4+15\hat{\lambda})\,\delta_{\gamma\beta} n_{\beta_1}(\boldsymbol{x}) + \delta_{\gamma\beta_1} n_\beta(\boldsymbol{x}) + 40\hat{\lambda}(1+3\hat{\lambda})\, n_{\gamma\beta\beta_1}(\boldsymbol{x})}{8\pi(1+5\hat{\lambda})(1+3\hat{\lambda})}\right] \times$$
$$\left[\delta_{\alpha\gamma} n_{\alpha_1\alpha_2\alpha_3}(\boldsymbol{x}) - \hat{\lambda}(3t_{\alpha\gamma}(\boldsymbol{x}) n_{\alpha_1\alpha_2\alpha_3}(\boldsymbol{x}) + t_{\alpha_1\gamma}(\boldsymbol{x}) n_{\alpha\alpha_2\alpha_3}(\boldsymbol{x}) + t_{\alpha_2\gamma}(\boldsymbol{x}) n_{\alpha_1\alpha\alpha_3}(\boldsymbol{x})\right.$$
$$\left. + t_{\alpha_3\gamma}(\boldsymbol{x}) n_{\alpha_1\alpha_2\alpha}(\boldsymbol{x}))\right] dS(\boldsymbol{x})$$
$$= \quad -\frac{R_p^5}{30(1+5\hat{\lambda})(1+3\hat{\lambda})}\left[\left(4+12\hat{\lambda}-15\hat{\lambda}^2\right)\delta_{\alpha\beta}\eta_{\beta_1\boldsymbol{\alpha}_3} + \left(1+3\hat{\lambda}+15\hat{\lambda}^2\right)\delta_{\alpha\beta_1}\eta_{\beta\boldsymbol{\alpha}_3}\right.$$
$$\left. + 5\hat{\lambda}(1+3\hat{\lambda})(\delta_{\alpha\alpha_1}\eta_{\beta\alpha_2\alpha_3} + \delta_{\alpha\alpha_2}\eta_{\beta\alpha_1\alpha_3} + \delta_{\alpha\alpha_3}\eta_{\beta\alpha_1\alpha_2})\right] \tag{3.121}$$

where $\eta_{\alpha\beta\gamma\delta} = \delta_{\alpha\beta}\delta_{\gamma\delta} + \delta_{\alpha\delta}\delta_{\beta\gamma} + \delta_{\alpha\gamma}\delta_{\beta\delta}$.

(m,n)-th order geometrical moments with n=2

It is possible to obtain the geometrical moments for $n = 2$ and $m = 0$ by symmetry from eq. (3.119), thus

$$m_{\alpha\beta\boldsymbol{\beta}_2} = -\frac{R_p^3}{4(1+3\hat{\lambda})}\left[\delta_{\alpha\beta}\delta_{\beta_1\beta_2} + \hat{\lambda}(\delta_{\beta\beta_1}\delta_{\alpha\beta_2} + \delta_{\beta\beta_2}\delta_{\alpha\beta_1})\right] \tag{3.122}$$

For $m = 2$

$$m_{\alpha\boldsymbol{\alpha}_2\beta\boldsymbol{\beta}_2} = m_{\beta\boldsymbol{\beta}_2\alpha\boldsymbol{\alpha}_2} =$$
$$R_p^2 \int_{r=R_p} \frac{h_{\alpha\beta\boldsymbol{\beta}_2}(\boldsymbol{x})}{8\pi} \left[\delta_{\alpha\gamma} n_{\alpha_1\alpha_2}(\boldsymbol{x}) - \hat{\lambda}(2t_{\alpha\gamma} n_{\alpha_1\alpha_2}(\boldsymbol{x}) + t_{\alpha_1\gamma} n_{\alpha\alpha_2}(\boldsymbol{x}) + t_{\alpha_2\gamma} n_{\alpha\alpha_1}(\boldsymbol{x}))\right] dS(\boldsymbol{x}) =$$
$$-\frac{R_p^5}{24(1+4\hat{\lambda})(1+7\hat{\lambda})} \left\{ \delta_{\alpha\beta} \left[-8\hat{\lambda}^2 \left(\frac{4+21\hat{\lambda}}{1+3\hat{\lambda}} \right) \delta_{\alpha_1\alpha_2}\delta_{\beta_1\beta_2} + 5(1+6\hat{\lambda})(\delta_{\alpha_1\beta_2}\delta_{\beta_1\alpha_2} + \delta_{\alpha_1\beta_1}\delta_{\alpha_2\beta_2}) \right] \right.$$
$$+(1+6\hat{\lambda}+28\hat{\lambda}^2)(\delta_{\alpha\beta_1}(\delta_{\alpha_1\beta_2}\delta_{\alpha_2\beta} + \delta_{\alpha_1\beta}\delta_{\alpha_2\beta_2}) + \delta_{\alpha\beta_2}(\delta_{\alpha_1\beta_1}\delta_{\alpha_2\beta} + \delta_{\alpha_1\beta}\delta_{\alpha_2\beta_1}))$$
$$+(1+12\hat{\lambda}+56\hat{\lambda}^2)(\delta_{\alpha\beta_1}\delta_{\beta\beta_2} + \delta_{\alpha\beta_2}\delta_{\beta\beta_1})\delta_{\alpha_1\alpha_2} + (\text{terms giving vanishing contribution to}\, \mathcal{F}_{\alpha\beta\boldsymbol{\beta}_2}) \tag{3.123}$$

For $m = 4$

$$m_{\alpha\boldsymbol{\alpha}_4\beta\boldsymbol{\beta}_2} = m_{\beta\boldsymbol{\beta}_2\alpha\boldsymbol{\alpha}_4} =$$
$$R_p^4 \int_{r=R_p} \frac{h_{\alpha\beta\boldsymbol{\beta}_2}(\boldsymbol{x})}{8\pi} \left[\delta_{\alpha\gamma} n_{\boldsymbol{\alpha}_4}(\boldsymbol{x}) - \hat{\lambda}(4t_{\alpha\gamma} n_{\boldsymbol{\alpha}_4}(\boldsymbol{x}) + t_{\alpha_1\gamma} n_{\alpha\alpha_2\alpha_3\alpha_4}(\boldsymbol{x}) + t_{\alpha_2\gamma} n_{\alpha\alpha_1\alpha_3\alpha_4}(\boldsymbol{x})\right.$$
$$\left. + t_{\alpha_3\gamma} n_{\alpha\alpha_1\alpha_2\alpha_4}(\boldsymbol{x}) + t_{\alpha_4\gamma} n_{\alpha\alpha_1\alpha_2\alpha_3}(\boldsymbol{x}))\right] dS(\boldsymbol{x}) =$$
$$-\frac{R_p^7}{168(1+4\hat{\lambda})(1+7\hat{\lambda})} \left[(5+20\hat{\lambda}-56\hat{\lambda}^2)\delta_{\alpha\beta}\mathrm{H}_{\boldsymbol{\beta}_2\boldsymbol{\alpha}_4} + (1+4\hat{\lambda}+28\hat{\lambda}^2)(\delta_{\alpha\beta_1}\mathrm{H}_{\beta\beta_2\boldsymbol{\alpha}_4} + \delta_{\alpha\beta_2}\mathrm{H}_{\beta\beta_1\boldsymbol{\alpha}_4}) \right]$$
$$+(\text{terms giving vanishing contribution to}\, \mathcal{F}_{\alpha\beta\boldsymbol{\beta}_2}) \tag{3.124}$$

where

$$\mathrm{H}_{\boldsymbol{\beta}_2\boldsymbol{\alpha}_4} = \mathrm{H}_{\beta_1\beta_2\alpha_1\alpha_2\alpha_3\alpha_4} = \delta_{\beta_1\alpha_1}\eta_{\beta_2\alpha_2\alpha_3\alpha_4} + \delta_{\beta_1\alpha_2}\eta_{\beta_2\alpha_1\alpha_3\alpha_4} + \delta_{\beta_1\alpha_3}\eta_{\beta_2\alpha_1\alpha_2\alpha_4} + \delta_{\beta_1\alpha_4}\eta_{\beta_2\alpha_1\alpha_2\alpha_3}$$

Chapter 4

On the theory of body motion in confined Stokesian fluids

4.1 Introduction

The behavior of particles immersed in a viscous fluid in the low-Reynolds number regime is inevitably affected by hydrodynamic interactions with other nearby bodies, such as other particles, fluid interfaces and solid walls confining the fluid. These interactions, that are the origin of fundamental phenomena as the enhanced resistance on bodies [104], the intrinsic convection of suspensions [13], the Segre-Silberbeg effect [218], to quote just a few of them, arise whenever the characteristic length particle ℓ_b is comparable with the characteristic separation distance from the nearest boundary ℓ_d. Therefore, their accurate understanding is of great relevance in several areas of microfluidics such as separation devices [227, 114, 36], capillary transportation [87, 192, 232], dynamics of micro-swimmers [145] and active particles [170], etc., where, by definition, the characteristic dimension of the flow domain can be of the same order of magnitude of the particle size.

Microfluidics is typically characterized by low Reynolds numbers, apart from the specific applications referred to as *inertial microfluidics* [58, 250], so that, in most the cases, the fluid can be considered in the Stokes regime and, when the inertia of the fluid becomes significant ($Re \sim 1$) but not too large, it can be treated by perturbative methods with respect to the Stokes-flow solution [48, 107]. Although hydrodynamic problems related to particles in confined fluids can be approached by means of typical numerical methods for solving the Stokes equation (such as Finite Elements Method [235, 53] and Boundary Integral Method [194]), a deeper mathematical understanding of fluid-particle interactions can be beneficial in order to overcome, by means of explicit analytical solutions, the limits and shortcomings of the numerical approaches, to improve current numerical methods (such as Stokesian Dynamics [22]) and develop new ones, and to explain and predict the non-intuitive flow and transport phenomena that may occur at the microscale.

One of the main difficulties in the analytical approaches to multibody systems intrinsic geometric complexity induced by the presence of bodies and surfaces of different shapes where to impose the boundary conditions. This difficulty holds even when dealing with the most regular bodies (such as spheres or ellipsoids) and the simplest geometries of walls (for example planar or cylindrical), since the union of many bodies, in most cases, breaks down the original symmetries making it impossible to find a coordinate system that permits to express simultaneously all the boundary conditions in a simple mathematical way. This is the reason why the only exact solutions available in the literature concern axisymmetric systems (where this symmetry is defined with respect to a suitable orthogonal curvilinear coordinate system), thus enabling the definition of a stream function. This is the case of the resistance of a rigid sphere rigid close to a plane considering either no-slip [117, 23, 55, 183] or Navier-slip boundary conditions [90], and of the resistance of a sphere at the center of a cylindrical channel, translating parallelly to the symmetry axis assuming no-slip boundary conditions [94]. Whereas, for the majority of the confined systems considered in the literature, approximate analytical solutions have been obtained under the assumption of asymptotic approximations, by using mainly a lubrication method for short range ($\ell_d \ll \ell_b$), and a reflection method for long range interactions ($\ell_d \gg \ell_b$). In some cases, such as that of the resistance of two rigid moving spheres with no-slip boundary conditions [118], the solution has been approximated by matching the asymptotic solutions.

In the case of short range interaction, many specific solutions are available in the literature, such as the resistance for a sphere near a plane by considering both no-slip [47, 85] and Navier-slip [110] boundary conditions, and a general theory, regardless of the shape of the surface almost in contact, has been developed by [44] assuming no-slip boundary conditions.

On the other hand, in the case of long range interaction, the reflection method (in its multifaceted variations) is commonly employed to obtain the leading-order terms for the series expansion in powers of ℓ_b/ℓ_d of the particle transport parameters, such as resistance, mobility, and diffusivity. The reflection method, developed by [223] [98, p. 236] in order to match the boundary conditions of Stokes flows on a system of n spheres, consists in expressing the total flow (i. e. the solution of the Stokes equations with boundary condition assigned simultaneously on each sphere) as a series of an infinite number of flows satisfying Stokes equations with boundary conditions assigned separately on each body considered in a unbounded domain. For example, a simple version of this method, to obtain the exact flow in the case of two moving spheres, can be summarized as follows: the first term of the series is the flow due to the motion of the first sphere considered in the unbounded fluid, which generates in turn a flow on the domain occupied by the second sphere; the second term of the series corrects the flow on the surface of the second sphere generating a flow on the domain of the first sphere and so on. And a similar ping-pong correction at the boundaries of the two spheres proceeds iteratively. Although the Stokes equations and the boundary conditions of the global problem are formally satisfied, this procedure is affected by two main limitations: i) the solution of the infinity of Stokes problems involved is not an easy task even for the simplest geometries of the bodies involved, ii) the convergence of the series can be ensured only for some specific problems, and it is still an open question in the general case.

For example, as regards the second limitation, convergence has been proved heuristically for two equal spheres moving with the same velocity for all the separation distances [98, p. 259], but in the case of three equally separated spheres it has been shown that the reflection method does not converge if the distance between the centers of the spheres is smaller than 2.16 times the radius of the spheres [116]. In fact, as shown by [112], if particle velocities are imposed by Dirichlet boundary conditions, the method converges only for diluted systems enclosed in a finite volume; whereas, as proved by [157] using a variational method, in the case of suspensions with n particles enclosed in a finite volume, the convergence of the reflection method is ensured regardless of the concentration of the particles if particle velocities are not assigned, i.e. if they move under the action of an external force as in the case of sedimentation phenomena.

Therefore, given that the convergence is ensured only for $\ell_d \gg \ell_b$ and that the exact evaluation of the terms in the series is feasible only for the first ones, i.e. the first corrections to the unbounded approximation, reflection methods are widely employed to model very long range interactions between particles. The main field of application is in the analysis of suspensions, indirectly applied in Stokesian dynamics [61, 22] under the form of inverting the particle-particle interactions mobility matrix [116], and in the analysis of confined systems, mainly considering the interaction between a single particle with the walls of the confinement, such as a sphere or a spheroid near planar [228, 229, 171] or cylindrical [86, 225, 100] walls.

However, the convergence of the method even for touching body such as in the case of two translating spheres or in the case of Luke's suspensions and the relatively small breakdown gap ($\sim 0.16\,\ell_b$) computed by [116] for three translating spheres suggest that, if all the terms of the series were exactly evaluated, reflection method should be a valid approach to provide exact solutions not only in the asymptotic limit $\ell_d \gg \ell_b$, but also in a closer region $\ell_d \sim \ell_b$, albeit external to the lubrication range $\ell_d \ll \ell_b$. A general theory, furnishing the reflection solution regardless of the geometry of the bodies involved, has been developed by [24, 25] and [46] for obtaining the resistance on an arbitrary body immersed in an arbitrarily confined Stokesian fluid, that can be also regarded as a second fixed body. In [24, 25] it is provided the first order correction with respect to the unbounded approximation of the hydrodynamics resistance (force and torque) on a body rigidly moving (translating and rotating) in terms of the resistance matrix of the body in the unbounded fluid and the Stokes's Green function of the domain of the confined fluid without the body inclusion; while in [46] a formal expression for the exact reflection resistance is derived, considering also an arbitrary ambient flow, in terms of generic tensors depending separately on the geometry of the body and the geometry of the confinement. The formal approach by [46] is not easily amenable to a simple practical implementation as regards the higher-order terms in the expansion, and for this reason, it has remained as a beautiful formal development disjoint from practical implementation in confined flows.

In this chapter, it is furnished a novel contribution, amenable to practical implementation, to the theory of the hydrodynamic interactions between a body in a confined fluid and the walls of the confinement by providing exact reflection solutions for the flow of the fluid in the system and for the grand-resistance on the body (force, torque and higher moments). The global solution is expressed in terms of well defined tensors depending separately on the geometry of the body and on the geometry of the confinement: moments on the body in the unbounded fluid (or the Faxén operators of the body) and multi-poles of the domain of the confinement (hence derivatives of the Green function). Unlike the tensors appearing in the expressions for the resistance on the body provided by [46], these tensors, when not yet available in the literature, can be directly evaluated by classical analytical or numerical methods. Furthermore, there are considered boundary conditions on the body different from the no-slip boundary conditions, requiring only the assumption that these boundary conditions satisfy the principle of BC-reciprocity as defined in the previous chapter. For instance, Navier-slip, and many other fluid-fluid boundary conditions of common hydrodynamic practice fall in this class.

To this aim, the bitensorial formulation of the Stokes singularities developed in Chapter 2 is enforced in dealing with the entries of the two-point dependent tensorial field (in hydrodynamics these fields depend simultaneously on the position of fluid element and on the position of the body in the confinement). Furthermore, the results derived in Chapter 3 are used in order to express the hydrodynamics of a body with arbitrary boundary conditions (requiring solely BC-reciprocity) in the ambient flows generated by the walls of the confinement, which can be complex even in the simplest case of translation motion.

The Chapter is organized as follows. Section 4.2 states the problem and briefly reviews the definition of the two simpler sub-problems, the solution of which permits obtaining the analytic expression for the global confined hydrodynamics: (i) the Faxén operators of the body and (ii) the multi-poles in the domain of the confinement. In Sections 4.3 the exact expression for the terms entering in the reflection expansion is derived, showing that they can be expressed as the product of suitable tensorial quantities depends on the moments on the body immersed in the ambient field associated with the regular parts of the bounded multi-poles. In Section 4.4 a generalized matrix notation is introduced for tensorial systems more compact than the notation in terms of the entries of each individual tensor, and the compact expression of the global velocity field is obtained. Moreover, by using the properties of infinite matrices [43], it is shown in Appendix 4.A that the convergence of the method is ensured for $\ell_d \gtrsim 2.65\,\ell_b$. This does not mean that the series expansion could not converge under more general conditions, although it is reasonable to hypothesize that there exist a constant $\Gamma > 0$, depending on the geometry of the problem, such that the reflection solution converges only for $\ell_d > \Gamma\,\ell_b$. In Section 4.5, the exact reflection formulae for force, torque and higher order moments on the body are provided. The estimate of the error resulting in truncating the exact solutions by considering only lower order multi-pole (or Faxén operators) is addressed in Section 4.6. It is also analyzed the truncation error made in preceding literature works, specifically in [24, 25] and in [228, 229]. Finally, in Section 4.7.1 the reflection solution obtained with the present theory (using Faxén operators and bounded multi-pole available in the literature), approximated to the order $O\left((\ell_b/\ell_d)^5\right)$, are compared and contrasted with the exact solution of a sphere near a planar wall, and the expressions for forces considering the more general situation of Navier-slip boundary conditions on the body are provided.

4.2 Statement of the problem

Consider a rigid body immersed in a stationary, Newtonian fluid with viscosity μ at vanishing Reynolds number. Let $V_b \subset \mathbb{R}^3$ be the domain representing the

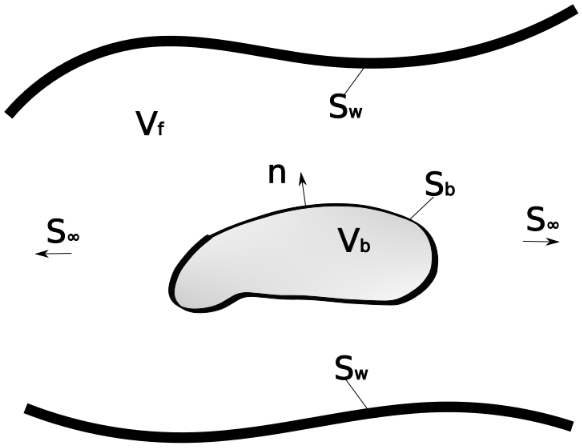

Figure 4.1. Schematic representation of geometry of the system.

space occupied by the body, S_b the boundary of the body and V_f the flow domain, bounded by the surface $S_b \cup S_w \cup S_\infty$, where S_w is the surface bounding externally the fluid, and considered in the proximity of the body, and S_∞ the boundary at infinity, infinitely far from the body. See the schematic representation of the system geometry in Fig. 4.1.

An *ambient flow* in the confined fluid $(\boldsymbol{u}(\boldsymbol{x}), \boldsymbol{\pi}(\boldsymbol{x}))$ is any flow, regular at the surface of the body S_b, and satisfying the Stokes equations with no-slip boundary conditions on the surface of the walls S_w. Thus, representing the solution of the system of equations

$$\begin{cases} -\nabla \cdot \boldsymbol{\pi}(\boldsymbol{x}) = \mu\Delta\, \boldsymbol{u}(\boldsymbol{x}) - \nabla p(\boldsymbol{x}) = 0 \\ \nabla \cdot \boldsymbol{u}(\boldsymbol{x}) = 0 \qquad \boldsymbol{x} \in V_f \cup V_b \\ \boldsymbol{u}(\boldsymbol{x}) = 0 \qquad \boldsymbol{x} \in S_w \end{cases} \tag{4.1}$$

Assuming linear homogeneous boundary conditions given by a generic operator $\mathcal{L}[\,]$ acting on the velocity at the surface of the body and no-slip boundary conditions at the surface of the confinement, the total flow (or *disturbed flow*) in the system $(\boldsymbol{v}(\boldsymbol{x}), \boldsymbol{\sigma}(\boldsymbol{x}))$ is

$$\begin{cases} -\nabla \cdot \boldsymbol{\sigma}(\boldsymbol{x}) = \mu\Delta\, \boldsymbol{v}(\boldsymbol{x}) - \nabla s(\boldsymbol{x}) = 0 \\ \nabla \cdot \boldsymbol{v}(\boldsymbol{x}) = 0 \qquad \boldsymbol{x} \in V_f \\ \mathcal{L}[\boldsymbol{v}(\boldsymbol{x})] = 0 \qquad \boldsymbol{x} \in S_b \\ \boldsymbol{v}(\boldsymbol{x}) = 0 \qquad \boldsymbol{x} \in S_w \end{cases} \tag{4.2}$$

Henceforth, we require that the boundary conditions represented by by the linear operator $\mathcal{L}[\,]$, satisfy the *reciprocity* condition defined in the Chapter 3. As it will become clear in the remainder, the assumption of validity of BC-reciprocity, together with the linearity of boundary conditions given by an operator $\mathcal{L}$, are necessary prerequisites in the development of the present theory.

In the next section, the solution of the problem eq. (4.2) is expressed in terms of the hydrodynamic solutions of two simpler problems: i) the Green function of the Stokes equations in the domain of the confinement $V_f \cup V_b$ and ii) the geometrical moments of the body in the unbounded fluid. For this reason, it is useful to define these solutions, discuss briefly their formal properties, introducing and clarifying in this way the notation that we use throughout this Chapter.

4.2.1 Summary of useful results obtained in the previous chapters

As discussed in Chapter 2, the Green function in the confined domain $V_f \cup V_b$ is a bitensorial field, hence a field depending on two points (called *field* and *source points*) with entries at both points expressed, in principle, in different coordinate systems. For the sake of simplicity, we consider Cartesian entries both at field and source points.

The Green function $G_{a\alpha}(\boldsymbol{x},\boldsymbol{\xi})$ of the confined flow is the solution of the equations

$$\begin{cases} -\nabla_b \Sigma_{ab\alpha}(\boldsymbol{x},\boldsymbol{\xi}) = \mu\Delta\, G_{a\alpha}(\boldsymbol{x},\boldsymbol{\xi}) - \nabla_a P_\alpha(\boldsymbol{x},\boldsymbol{\xi}) = -8\pi\delta_{a\alpha}\delta(\boldsymbol{x}-\boldsymbol{\xi}) \\ \nabla_a G_{a\alpha}(\boldsymbol{x},\boldsymbol{\xi}) = 0 \qquad \boldsymbol{x},\boldsymbol{\xi} \in V_f \cup V_b \\ G_{a\alpha}(\boldsymbol{x},\boldsymbol{\xi}) = 0 \qquad \boldsymbol{x} \in S_w \cup S_\infty \end{cases} \tag{4.3}$$

where $G_{a\alpha}(\boldsymbol{x},\boldsymbol{\xi})$, $P_\alpha(\boldsymbol{x},\boldsymbol{\xi})$, $\Sigma_{ab\alpha}(\boldsymbol{x},\boldsymbol{\xi})$ are the associated velocity, pressure and stress tensor field.

It is useful to define also the *regular part of the Green function* $(W_{a\alpha}(\boldsymbol{x},\boldsymbol{\xi}), Q_\alpha(\boldsymbol{x},\boldsymbol{\xi}))$ as the bitensorial fields solving the problem

$$\begin{cases} -\nabla_b T_{ab\alpha}(\boldsymbol{x},\boldsymbol{\xi}) = \mu\Delta W_{a\alpha}(\boldsymbol{x},\boldsymbol{\xi}) - \nabla_a Q_\alpha(\boldsymbol{x},\boldsymbol{\xi}) = 0 \\ \nabla_a W_{a\alpha}(\boldsymbol{x},\boldsymbol{\xi}) = 0 \qquad \boldsymbol{x},\boldsymbol{\xi} \in V_f \cup V_b \\ W_{a\alpha}(\boldsymbol{x},\boldsymbol{\xi}) = -S_{a\alpha}(\boldsymbol{x}-\boldsymbol{\xi}) \qquad \boldsymbol{x} \in S_w \cup S_\infty \end{cases} \tag{4.4}$$

where $S_{a\alpha}(\boldsymbol{x}-\boldsymbol{\xi})$ is the Stokeslet. Therefore, the bounded Green function can be written as sum of a a regular field $W_{a\alpha}(\boldsymbol{x},\boldsymbol{\xi})$ and a singular field given by the Stokeslet

$$G_{a\alpha}(\boldsymbol{x},\boldsymbol{\xi}) = S_{a\alpha}(\boldsymbol{x}-\boldsymbol{\xi}) + W_{a\alpha}(\boldsymbol{x},\boldsymbol{\xi}) \tag{4.5}$$

By differentiating eq. (4.5) at the pole, higher order singularities in the domain $V_b \cup V_f$ are obtained. For example, the n-th order multipole is obtained by

$$\nabla_{\boldsymbol{\alpha}_n} G_{a\alpha}(\boldsymbol{x},\boldsymbol{\xi}) = \nabla_{\boldsymbol{\alpha}_n} S_{a\alpha}(\boldsymbol{x}-\boldsymbol{\xi}) + \nabla_{\boldsymbol{\alpha}_n} W_{a\alpha}(\boldsymbol{x},\boldsymbol{\xi}) \tag{4.6}$$

Consider a body immersed in an ambient flow $(\boldsymbol{u}(\boldsymbol{x}), \boldsymbol{\pi}(\boldsymbol{x}))$ in the unbounded domain. The *disturbance flow* $(\boldsymbol{w}(\boldsymbol{x}), \boldsymbol{\tau}(\boldsymbol{x}))$ generated by the body immersed in the ambient flow is solution of

$$\begin{cases} -\nabla \cdot \boldsymbol{\tau}(\boldsymbol{x}) = \mu\Delta\, \boldsymbol{w}(\boldsymbol{x}) - \nabla q(\boldsymbol{x}) = 0 \\ \nabla \cdot \boldsymbol{w}(\boldsymbol{x}) = 0 \qquad \boldsymbol{x} \in V_f \\ \mathcal{L}[\boldsymbol{w}(\boldsymbol{x})] = -\mathcal{L}[\boldsymbol{u}(\boldsymbol{x})] \qquad \boldsymbol{x} \in S_b \\ \boldsymbol{w}(\boldsymbol{x}) = 0 \qquad \boldsymbol{x} \to \infty \end{cases} \tag{4.7}$$

where $\boldsymbol{w}(\boldsymbol{x})$, $q(\boldsymbol{x})$, $\boldsymbol{\tau}(\boldsymbol{x})$ are the associated disturbance velocity, pressure and stress tensor fields representing the the velocity field at the surface of the rigid body due to the interaction of the ambient flow $\boldsymbol{u}(\boldsymbol{x})$ with S_b.

In Chapter 3, based on the hierarchy of the geometrical moments, the operator

$$\mathcal{F}_{\alpha\beta'\boldsymbol{\beta}'_n} = \sum_{m=0}^{\infty} \frac{m_{\alpha\boldsymbol{\alpha}_m\beta'\boldsymbol{\beta}'_n}(\boldsymbol{\xi},\boldsymbol{\xi}')\nabla_{\boldsymbol{\alpha}_m}}{m!} \tag{4.8}$$

has been introduced. As shown has been shown, if BC-reciprocity holds, $\mathcal{F}_{\alpha\beta'\boldsymbol{\beta}'_n}$ represents a n-th order Faxén operator of the body. Assuming that the operator $\mathcal{L}[\boldsymbol{v}(\boldsymbol{x})]$ in the total Stokes system eq. (4.2) belongs to the class of linear homogeneous reciprocal boundary conditions, the following relations for the body in the unbounded domain hold

$$M_{\alpha\boldsymbol{\alpha}_n}(\boldsymbol{\xi}) = 8\pi\mu\mathcal{F}_{\beta'\alpha\boldsymbol{\alpha}_n}u_{\beta'}(\boldsymbol{\xi}') \tag{4.9}$$

and

$$w_a(\boldsymbol{x}) = \sum_{n=0}^{\infty} \frac{\nabla_{\boldsymbol{\beta}'_n}u_{\beta'}(\boldsymbol{\xi}')}{n!}\mathcal{F}_{\alpha\beta'\boldsymbol{\beta}'_n}S_{a\alpha}(\boldsymbol{x}-\boldsymbol{\xi}) \tag{4.10}$$

Furthermore, owing to the property that $\mathcal{F}_{\alpha\beta'\boldsymbol{\beta}'_n}$ is a Faxén operator, the disturbance field can be expressed by

$$\begin{aligned} w_a(\boldsymbol{x}) &= \sum_{m=0}^{\infty} \frac{\mathcal{F}_{\beta'\alpha\boldsymbol{\alpha}_m}u_{\beta'}(\boldsymbol{\xi}')}{m!}\nabla_{\boldsymbol{\alpha}_m}S_{a\alpha}(\boldsymbol{x}-\boldsymbol{\xi}) \\ &= \frac{1}{8\pi\mu}\sum_{m=0}^{\infty} \frac{M_{\alpha\boldsymbol{\alpha}_m}(\boldsymbol{\xi})}{m!}\nabla_{\boldsymbol{\alpha}_m}S_{a\alpha}(\boldsymbol{x}-\boldsymbol{\xi}) \end{aligned} \tag{4.11}$$

Finally, it is useful to remark that the force exerted by the fluid on the body is $F_\alpha = -M_\alpha(\boldsymbol{\xi})$, thus, by eq. (4.9)

$$F_\alpha = -8\pi\mu\mathcal{F}_{\beta\alpha}u_\beta(\boldsymbol{\xi}) \tag{4.12}$$

while the torque $T_\alpha = \varepsilon_{\alpha\beta\beta_1}M_{\beta\beta_1}(\boldsymbol{\xi})$, is given by

$$T_\alpha = 8\pi\mu\mathcal{T}_{\beta\alpha}u_\beta(\boldsymbol{\xi}) \tag{4.13}$$

where $\mathcal{T}_{\gamma\alpha} = \varepsilon_{\alpha\beta\beta_1}\mathcal{F}_{\gamma\beta\beta_1}$ and $\varepsilon_{\alpha\beta\beta_1}$ the Levi-Civita symbol.

4.3 The flow due to a body in a confined fluid

4.3.1 The reflection method

Consider the problem defined by eq. (4.2) providing the total flow in the system in the case of no-slip conditions both on the body surface and on the confinement walls, thus considering the identity matrix as operator $\mathcal{L}[] = I$. Owing to the linearity of the equations and of the boundary conditions, we can apply the reflection method [98,] to express the solution $(v_a(\boldsymbol{x}), \sigma_{ab}(\boldsymbol{x}))$ as the superposition of a countable system of fields $(v_a^{[k]}(\boldsymbol{x}), \sigma_{ab}^{[k]}(\boldsymbol{x}))$, with $k = 0, 1, 2, ...$,

$$\begin{aligned} v_a(\boldsymbol{x}) &= v_a^{[0]}(\boldsymbol{x}) + v_a^{[1]}(\boldsymbol{x}) + ... + v_a^{[k]}(\boldsymbol{x}) + ... \\ \sigma_{ab}(\boldsymbol{x}) &= \sigma_{ab}^{[0]}(\boldsymbol{x}) + \sigma_{ab}^{[1]}(\boldsymbol{x}) + ... + \sigma_{ab}^{[k]}(\boldsymbol{x}) + ... \end{aligned} \tag{4.14}$$

where

$$\sigma_{ab}^{[k]}(\boldsymbol{x}) = s^{[k]}(\boldsymbol{x})\delta_{ab} - \mu(\nabla_a v_b^{[k]}(\boldsymbol{x}) + \nabla_b v_a^{[k]}(\boldsymbol{x})) \tag{4.15}$$

$s^{[k]}(\boldsymbol{x})$ being the associated pressure, each of which is the solution of the Stokes equations equipped with the following system of boundary conditions

$$v_a^{[2k+1]}(\boldsymbol{x}) = -v_a^{[2k]}(\boldsymbol{x}), \qquad \boldsymbol{x} \in S_b \tag{4.16}$$

$$v_a^{[2k+2]}(\boldsymbol{x}) = -v_a^{[2k+1]}(\boldsymbol{x}), \qquad \boldsymbol{x} \in S_w$$

For $k = 0$

$$v_a^{[0]}(\boldsymbol{x}) = u_a(\boldsymbol{x}), \quad \boldsymbol{x} \in V_b \cup V_f \tag{4.17}$$

As can be sen from eqs. (4.16), for odd k the condition involves the boundary of the body, for even k the walls of the confinement.

4.3.2 The velocity fields $\boldsymbol{v}^{[1]}$ and $\boldsymbol{v}^{[2]}$

Let us start by expressing the first velocity fields $v_a^{[1]}(\boldsymbol{x})$ and $v_a^{[2]}(\boldsymbol{x})$ in terms of the Green function of the confinement and the Faxén operator of the body. Either the confinement Green function or the body Faxén operator are supposed to be known.

Comparing eqs. (4.16) with eqs. (4.7) it is easy to recognize that $\boldsymbol{v}^{[1]}(\boldsymbol{x})$ is the disturbance field of the ambient field $\boldsymbol{u}(\boldsymbol{x})$. Therefore, by using eq. (4.10), it is possible to explicit the velocity field with $k = 1$ as

$$v_a^{[1]}(\boldsymbol{x}) = \sum_{n=0}^{\infty} \frac{\nabla_{\boldsymbol{\beta}_n} u_\beta(\boldsymbol{\xi})}{n!} \mathcal{F}_{\alpha\beta\boldsymbol{\beta}_n} S_{a\alpha}(\boldsymbol{x} - \boldsymbol{\xi}) \tag{4.18}$$

Alternatively, from eq. (4.11), the first velocity field can be expressed alternatively as

$$v_a^{[1]}(\boldsymbol{x}) = \frac{1}{8\pi\mu} \sum_{m=0}^{\infty} \frac{M_{\alpha\boldsymbol{\alpha}_m}(\boldsymbol{\xi})}{m!} \nabla_{\boldsymbol{\alpha}_m} S_{a\alpha}(\boldsymbol{x} - \boldsymbol{\xi}) \tag{4.19}$$

Since, by linearity, any $\boldsymbol{v}^{[k]}(\boldsymbol{x})$ is solution of the Stokes equations, equipped with the boundary conditions eq. (4.16), the flow with $k = 2$ is the solution of the problem

$$\begin{cases} \mu\Delta\, v_a^{[2]}(\boldsymbol{x}) - \nabla_a\, s^{[2]}(\boldsymbol{x}) = 0 \\ \nabla_a\, v_a^{[2]}(\boldsymbol{x}) = 0 \qquad \boldsymbol{x} \in V_b \cup V_f \\ v_a^{[2]}(\boldsymbol{x}) = -v_a^{[1]}(\boldsymbol{x}) \qquad \boldsymbol{x} \in S_w \end{cases} \tag{4.20}$$

By applying the operator

$$\sum_{n=0}^{\infty} \frac{\nabla_{\boldsymbol{\beta}_n} u_\beta(\boldsymbol{\xi})}{n!} \mathcal{F}_{\alpha\beta\boldsymbol{\beta}_n}$$

at a source point $\boldsymbol{\xi} \in V_b$ of the regular part of the Green function defined by the eq. (4.4), and comparing the resulting problem with eq. (4.20), it is easy to conclude, by the uniqueness of the solution of Stokes equations, that

$$v_a^{[2]}(\boldsymbol{x}) = \sum_{n=0}^{\infty} \frac{\nabla_{\boldsymbol{\beta}_n} u_\beta(\boldsymbol{\xi})}{n!} \mathcal{F}_{\alpha\beta\boldsymbol{\beta}_n} W_{a\alpha}(\boldsymbol{x}, \boldsymbol{\xi}) \tag{4.21}$$

or, alternatively, by applying the operator

$$\frac{1}{8\pi\mu}\sum_{m=0}^{\infty}\frac{M_{\alpha\boldsymbol{\alpha}_m}(\boldsymbol{\xi})}{m!}\nabla_{\boldsymbol{\alpha}_m}$$

we obtain the representation

$$v_a^{[2]}(\boldsymbol{x}) = \frac{1}{8\pi\mu}\sum_{m=0}^{\infty}\frac{M_{\alpha\boldsymbol{\alpha}_m}(\boldsymbol{\xi})}{m!}\nabla_{\boldsymbol{\alpha}_m}W_{a\alpha}(\boldsymbol{x},\boldsymbol{\xi}) \tag{4.22}$$

and thus

$$\begin{aligned} v_a^{[1]}(\boldsymbol{x}) + v_a^{[2]}(\boldsymbol{x}) &= \sum_{n=0}^{\infty}\frac{\nabla_{\boldsymbol{\beta}_n}u_\beta(\boldsymbol{\xi})}{n!}\mathcal{F}_{\alpha\beta\boldsymbol{\beta}_n}G_{a\alpha}(\boldsymbol{x},\boldsymbol{\xi}) \\ &= \frac{1}{8\pi\mu}\sum_{m=0}^{\infty}\frac{M_{\alpha\boldsymbol{\alpha}_m}(\boldsymbol{\xi})}{m!}\nabla_{\boldsymbol{\alpha}_m}G_{a\alpha}(\boldsymbol{x},\boldsymbol{\xi}) \end{aligned} \tag{4.23}$$

4.3.3 The velocity fields $\boldsymbol{v}^{[3]}$ and $\boldsymbol{v}^{[4]}$

From the boundary conditions eq. (4.16), the velocity field for $k = 3$ is the disturbance field of $v_a^{[2]}(\boldsymbol{x})$ and therefore, by eq. (4.10)

$$v_a^{[3]}(\boldsymbol{x}) = \sum_{\ell=0}^{\infty}\frac{\nabla_{\boldsymbol{\gamma}'_\ell}v_{\gamma'}^{[2]}(\boldsymbol{\xi}')}{\ell!}\mathcal{F}_{\beta\gamma'\boldsymbol{\gamma}'_\ell}S_{a\beta}(\boldsymbol{x}-\boldsymbol{\xi}) \tag{4.24}$$

Substituting eq. (4.22) into eq. (4.24) one obtains

$$v_a^{[3]}(\boldsymbol{x}) = \frac{1}{8\pi\mu}\sum_{m=0}^{\infty}\frac{M_{\alpha\boldsymbol{\alpha}_m}(\boldsymbol{\xi})}{m!}\sum_{\ell=0}^{\infty}\frac{\nabla_{\boldsymbol{\gamma}'_\ell}\nabla_{\boldsymbol{\alpha}_m}W_{\gamma'\alpha}(\boldsymbol{\xi}',\boldsymbol{\xi})}{\ell!}\mathcal{F}^{(ns)}_{\beta\gamma'\boldsymbol{\gamma}'_\ell}S_{a\beta}(\boldsymbol{x}-\boldsymbol{\xi}) \tag{4.25}$$

By the equivalence between the two expressions eq. (4.10) and eq. (4.11)

$$\sum_{\ell=0}^{\infty}\frac{\nabla_{\boldsymbol{\gamma}'_\ell}\nabla_{\boldsymbol{\alpha}_m}W_{\gamma'\alpha}(\boldsymbol{\xi}',\boldsymbol{\xi})}{\ell!}\mathcal{F}_{\beta\gamma'\boldsymbol{\gamma}'_\ell}S_{a\beta}(\boldsymbol{x}-\boldsymbol{\xi}) = \sum_{n=0}^{\infty}\frac{\mathcal{F}_{\gamma'\beta\boldsymbol{\beta}_n}\nabla_{\boldsymbol{\alpha}_m}W_{\gamma'\alpha}(\boldsymbol{\xi}',\boldsymbol{\xi})}{n!}\nabla_{\boldsymbol{\beta}_n}S_{a\beta}(\boldsymbol{x}-\boldsymbol{\xi}) \tag{4.26}$$

It is useful introduce the tensor $N_{\alpha\boldsymbol{\alpha}_m\beta\boldsymbol{\beta}_n}(\boldsymbol{\xi})$ as

$$N_{\alpha\boldsymbol{\alpha}_m\beta\boldsymbol{\beta}_n}(\boldsymbol{\xi}) = \mathcal{F}^{(ns)}_{\gamma'\beta\boldsymbol{\beta}_n}\nabla_{\boldsymbol{\alpha}_m}W_{\gamma'\alpha}(\boldsymbol{\xi}',\boldsymbol{\xi})\Big|_{\boldsymbol{\xi}'=\boldsymbol{\xi}} \tag{4.27}$$

which corresponds to the n-th order moment on the body immersed in an ambient field consisting in the regular part of the m-th derivative of the Green function. Thus, using the identity eq. (4.26) and the definition eq. (4.27), eq. (4.25) can be expressed as

$$v_a^{[3]}(\boldsymbol{x}) = \frac{1}{8\pi\mu}\sum_{m=0}^{\infty}\frac{M_{\alpha\boldsymbol{\alpha}_m}(\boldsymbol{\xi})}{m!}\sum_{n=0}^{\infty}\frac{N_{\alpha\boldsymbol{\alpha}_m\beta\boldsymbol{\beta}_n}(\boldsymbol{\xi})}{n!}\nabla_{\boldsymbol{\beta}_n}S_{a\beta}(\boldsymbol{x}-\boldsymbol{\xi}) \tag{4.28}$$

and, enforcing the same argument applied above to obtain eqs. (4.20)-(4.22) we have

$$v_a^{[4]}(\boldsymbol{x}) = \frac{1}{8\pi\mu}\sum_{m=0}^{\infty}\frac{M_{\alpha\boldsymbol{\alpha}_m}(\boldsymbol{\xi})}{m!}\sum_{n=0}^{\infty}\frac{N_{\alpha\boldsymbol{\alpha}_m\beta\boldsymbol{\beta}_n}(\boldsymbol{\xi})}{n!}\nabla_{\boldsymbol{\beta}_n}W_{a\beta}(\boldsymbol{x},\boldsymbol{\xi}) \tag{4.29}$$

so that

$$v_a^{[3]}(\boldsymbol{x}) + v_a^{[4]}(\boldsymbol{x}) = \frac{1}{8\pi\mu}\sum_{m=0}^{\infty}\frac{M_{\alpha\boldsymbol{\alpha}_m}(\boldsymbol{\xi})}{m!}\sum_{n=0}^{\infty}\frac{N_{\alpha\boldsymbol{\alpha}_m\beta\boldsymbol{\beta}_n}(\boldsymbol{\xi})}{n!}\nabla_{\boldsymbol{\beta}_n}G_{a\beta}(\boldsymbol{x},\boldsymbol{\xi}) \tag{4.30}$$

4.3.4 The velocity fields $\boldsymbol{v}^{[5]}$ and $\boldsymbol{v}^{[6]}$

The subsequent velocity fields can be determined following the same procedure used for $\boldsymbol{v}^{[3]}(\boldsymbol{x})$ and $\boldsymbol{v}^{[4]}(\boldsymbol{x})$. In fact, $\boldsymbol{v}^{[5]}(\boldsymbol{x})$ can be considered as the disturbance field of $\boldsymbol{v}^4(\boldsymbol{x})$, and thus

$$v_a^{[5]}(\boldsymbol{x}) = \sum_{\ell=0}^{\infty}\frac{\nabla_{\boldsymbol{\beta}'_\ell}v_{\beta'}^{[4]}(\boldsymbol{\xi}')}{\ell!}\mathcal{F}^{(ns)}_{\gamma\beta'\boldsymbol{\beta}'_\ell}S_{a\gamma}(\boldsymbol{x}-\boldsymbol{\xi}) \tag{4.31}$$

Enforcing the same argument used above for $v_a^{[3]}(\boldsymbol{x})$ and $v_a^{[4]}(\boldsymbol{x})$, eqs. (4.25)-(4.30) we obtain

$$v_a^{[5]}(\boldsymbol{x}) = \frac{1}{8\pi\mu}\sum_{m=0}^{\infty}\frac{M_{\alpha\boldsymbol{\alpha}_m}(\boldsymbol{\xi})}{m!}\sum_{n=0}^{\infty}\frac{N_{\alpha\boldsymbol{\alpha}_m\beta\boldsymbol{\beta}_n}(\boldsymbol{\xi})}{n!}\sum_{\ell=0}^{\infty}\frac{N_{\beta\boldsymbol{\beta}_n\gamma\boldsymbol{\gamma}_\ell}(\boldsymbol{\xi})}{\ell!}\nabla_{\boldsymbol{\gamma}_\ell}S_{a\gamma}(\boldsymbol{x}-\boldsymbol{\xi}) \tag{4.32}$$

$$v_a^{[6]}(\boldsymbol{x}) = \frac{1}{8\pi\mu}\sum_{m=0}^{\infty}\frac{M_{\alpha\boldsymbol{\alpha}_m}(\boldsymbol{\xi})}{m!}\sum_{n=0}^{\infty}\frac{N_{\alpha\boldsymbol{\alpha}_m\beta\boldsymbol{\beta}_n}(\boldsymbol{\xi})}{n!}\sum_{\ell=0}^{\infty}\frac{N_{\beta\boldsymbol{\beta}_n\gamma\boldsymbol{\gamma}_\ell}(\boldsymbol{\xi})}{\ell!}\nabla_{\boldsymbol{\gamma}_\ell}W_{a\gamma}(\boldsymbol{x},\boldsymbol{\xi}) \tag{4.33}$$

so that

$$v_a^{[5]}(\boldsymbol{x}) + v_a^{[6]}(\boldsymbol{x}) = \frac{1}{8\pi\mu}\sum_{m=0}^{\infty}\frac{M_{\alpha\boldsymbol{\alpha}_m}(\boldsymbol{\xi})}{m!}\sum_{n=0}^{\infty}\frac{N_{\alpha\boldsymbol{\alpha}_m\beta\boldsymbol{\beta}_n}(\boldsymbol{\xi})}{n!}\sum_{\ell=0}^{\infty}\frac{N_{\beta\boldsymbol{\beta}_n\gamma\boldsymbol{\gamma}_\ell}(\boldsymbol{\xi})}{\ell!}\nabla_{\boldsymbol{\gamma}_\ell}G_{a\gamma}(\boldsymbol{x},\boldsymbol{\xi}) \tag{4.34}$$

4.3.5 The total velocity field

Iterating the same procedure for any k, it is possible to generalize the above results in the form

$$v_a^{[2k+1]}(\boldsymbol{x}) = \frac{1}{8\pi\mu}\sum_{m=0}^{\infty}\frac{M_{\alpha\boldsymbol{\alpha}_m}(\boldsymbol{\xi})}{m!}\sum_{m_1=0}^{\infty}\frac{N_{\alpha\boldsymbol{\alpha}_m\beta\boldsymbol{\beta}_{m_1}}(\boldsymbol{\xi})}{m_1!}\dots\sum_{m_k=0}^{\infty}\frac{N_{\gamma\boldsymbol{\gamma}_{m_{k-1}}\delta\boldsymbol{\delta}_{m_k}}(\boldsymbol{\xi})}{m_k!}\nabla_{\boldsymbol{\delta}_{m_k}}S_{a\delta}(\boldsymbol{x}-\boldsymbol{\xi}) \tag{4.35}$$

and

$$v_a^{[k+2]}(\boldsymbol{x}) = \frac{1}{8\pi\mu}\sum_{m=0}^{\infty}\frac{M_{\alpha\boldsymbol{\alpha}_m}(\boldsymbol{\xi})}{m!}\sum_{m_1=0}^{\infty}\frac{N_{\alpha\boldsymbol{\alpha}_m\beta\boldsymbol{\beta}_{m_1}}(\boldsymbol{\xi})}{m_1!}\dots\sum_{m_k=0}^{\infty}\frac{N_{\gamma\boldsymbol{\gamma}_{m_{k-1}}\delta\boldsymbol{\delta}_{m_k}}(\boldsymbol{\xi})}{m_k!}\nabla_{\boldsymbol{\delta}_{m_k}}W_{a\delta}(\boldsymbol{x},\boldsymbol{\xi}) \tag{4.36}$$

so that

$$v_a^{[2k+1]}(\boldsymbol{x}) + v_a^{[2k+2]}(\boldsymbol{x}) =$$
$$\frac{1}{8\pi\mu}\sum_{m=0}^{\infty}\frac{M_{\alpha\boldsymbol{\alpha}_m}(\boldsymbol{\xi})}{m!}\sum_{m_1=0}^{\infty}\frac{N_{\alpha\boldsymbol{\alpha}_m\beta\boldsymbol{\beta}_{m_1}}(\boldsymbol{\xi})}{m_1!}\dots\sum_{m_k=0}^{\infty}\frac{N_{\gamma\boldsymbol{\gamma}_{m_{k-1}}\delta\boldsymbol{\delta}_{m_k}}(\boldsymbol{\xi})}{m_k!}\nabla_{\boldsymbol{\delta}_{m_k}}G_{a\delta}(\boldsymbol{x},\boldsymbol{\xi}) \tag{4.37}$$

Summing all the fields according to eq. (4.14), the total velocity field can be expressed as

$$v_a(\boldsymbol{x}) - u_a(\boldsymbol{x}) = \sum_{k=0}^{\infty} v_a^{[2k+1]}(\boldsymbol{x}) + v_a^{[2k+2]}(\boldsymbol{x}) =$$
$$\frac{1}{8\pi\mu}\sum_{m=0}^{\infty}\frac{M_{\alpha\boldsymbol{\alpha}_m}(\boldsymbol{\xi})}{m!}\sum_{k=0}^{\infty}\sum_{m_1=0}^{\infty}\frac{N_{\alpha\boldsymbol{\alpha}_m\beta\boldsymbol{\beta}_{m_1}}(\boldsymbol{\xi})}{m_1!}\dots\sum_{m_k=0}^{\infty}\frac{N_{\gamma\boldsymbol{\gamma}_{m_{k-1}}\delta\boldsymbol{\delta}_{m_k}}(\boldsymbol{\xi})}{m_k!}\nabla_{\boldsymbol{\delta}_{m_k}}G_{a\delta}(\boldsymbol{x},\boldsymbol{\xi}) \tag{4.38}$$

4.3.6 Extension to Linear and BC-reciprocal boundary conditions on the body

The extension to more general linear homogeneous BC-reciprocal boundary conditions is straightforward considering the total field

$$\begin{aligned} v_a(\boldsymbol{x}) &= v_a^{[0]}(\boldsymbol{x}) + v_a^{[1]}(\boldsymbol{x}) + \dots + v_a^{[k]}(\boldsymbol{x}) + \dots \\ \sigma_{ab}(\boldsymbol{x}) &= \sigma_{ab}^{[0]}(\boldsymbol{x}) + \sigma_{ab}^{[1]}(\boldsymbol{x}) + \dots + \sigma_{ab}^{[k]}(\boldsymbol{x}) + \dots \end{aligned} \tag{4.39}$$

constituted by fields satisfying the conditions at the boundary

$$\mathcal{L}[v_a^{[2k+1]}(\boldsymbol{x})] = -\mathcal{L}[v_a^{[2k]}(\boldsymbol{x})], \qquad \boldsymbol{x} \in S_b \tag{4.40}$$

$$v_a^{[2k+2]}(\boldsymbol{x}) = -v_a^{[2k+1]}(\boldsymbol{x}), \qquad \boldsymbol{x} \in S_w$$

For $k = 0$

$$v_a^{[0]}(\boldsymbol{x}) = u_a(\boldsymbol{x}), \quad \boldsymbol{x} \in V_b \cup V_f \tag{4.41}$$

In fact, by applying the operator $\mathcal{L}[\,]$ to the total field in eq. (4.39) at the surface of the body and using the linear property, we have

$$\begin{aligned} &\mathcal{L}[v_a(\boldsymbol{x})] = \mathcal{L}[v_a^{[0]}(\boldsymbol{x}) + v_a^{[1]}(\boldsymbol{x}) + v_a^{[2]}(\boldsymbol{x}) + v_a^{[3]}(\boldsymbol{x}) + \dots] = \\ &\mathcal{L}[v_a^{[0]}(\boldsymbol{x})] + \mathcal{L}[v_a^{[1]}(\boldsymbol{x})] + \mathcal{L}[v_a^{[2]}(\boldsymbol{x})] + \mathcal{L}[v_a^{[3]}(\boldsymbol{x})] + \dots = 0, \qquad \boldsymbol{x} \in S_b \end{aligned} \tag{4.42}$$

Since, the procedure developed in the previous paragraph eqs. (4.18)-(4.38), is independent of the boundary conditions at the surface of the body, with the only constraint for the use of the Faxén operators of the BC-reciprocity of $\mathcal{L}[\,]$, we can conclude that eq. (4.38) is still valid considering the Faxén operators associated with the boundary conditions assumed on the body surface.

i	1	2	3	4	5	6	7	8	9	10	11	12	13	...
$(\alpha\,\alpha_1\,\alpha_2\,...\,\alpha_m)$	(1)	(2)	(3)	(11)	(12)	(13)	(21)	(22)	(23)	(31)	(32)	(33)	(111)	...

Table 4.1. Conversion between the index i for the entries of the vector $[M]_i$ and the multi-index $\alpha\,\boldsymbol{\alpha}_m$ for the entries of the $(m+1)$-order tensors $M_{\alpha\boldsymbol{\alpha}_m}(\boldsymbol{\xi})$.

4.4 Matrix representation of the velocity field

In this Section, a compact and useful matrix representation of the equations obtained in the Section 4.3 is developed. To this aim, collect the entries of the system of moments $M_{\alpha\boldsymbol{\alpha}_m}(\boldsymbol{\xi})$ in an infinite-dimensional vector [43]

$$[M] = \begin{bmatrix} \boldsymbol{M}_{(0)} \\ \boldsymbol{M}_{(1)} \\ \dfrac{\bar{\boldsymbol{M}}_{(2)}}{2} \\ \vdots \\ \dfrac{\boldsymbol{M}_{(m)}}{m!} \\ \vdots \end{bmatrix} \tag{4.43}$$

where $\boldsymbol{M}_{(m)}$ are 3^{m+1} dimensional vectors obtained by the vectorization of the $(m+1)$-order tensors $M_{\alpha\boldsymbol{\alpha}_m}(\boldsymbol{\xi})$ so that any entry $[M]_i$ corresponds to the entry $M_{\alpha\boldsymbol{\alpha}_m}(\boldsymbol{\xi})$ according the conversion $i \leftrightarrow \alpha\,\boldsymbol{\alpha}_m$ shown in Table 4.1. We use the notation $[M_{(n:m)}]$ to indicate the part of the array (4.43) collecting the entries of the tensors with orders going from n to m ($m > n$), i.e.,

$$[M_{(n:m)}] = \begin{bmatrix} \dfrac{\boldsymbol{M}_{(n)}}{n!} \\ \vdots \\ \dfrac{\boldsymbol{M}_{(m)}}{m!} \end{bmatrix} \tag{4.44}$$

In the same way, the entries of the entries of $\nabla_{\boldsymbol{\alpha}_m} G_{a\alpha}(\boldsymbol{x},\boldsymbol{\xi})$ can be collected in the $3^{m+1} \times 3$ matrices $\boldsymbol{G}_{(0)}, \boldsymbol{G}_{(1)}, ..., \boldsymbol{G}_{(m)}, ...$ (with row indexes corresponding to the Latin field point index) to build the $\infty \times 3$ matrix $[G]$ defined by

$$[G] = \begin{bmatrix} \boldsymbol{G}_{(0)} \\ \boldsymbol{G}_{(1)} \\ \vdots \\ \boldsymbol{G}_{(m)} \\ \vdots \end{bmatrix} \tag{4.45}$$

By using this representation, eq. (4.23) can be compactly expressed as

$$\boldsymbol{v}^{[1]}(\boldsymbol{x}) + \boldsymbol{v}^{[2]}(\boldsymbol{x}) = \frac{[M]^t[G]}{8\pi\mu} \tag{4.46}$$

$[M]^t$ being the transpose of $[M]$.

It is also possible to define the infinite matrix [43]

$$[N] = \begin{bmatrix} \boldsymbol{N}_{(0,0)} & \boldsymbol{N}_{(0,1)} & \cdots & \dfrac{\boldsymbol{N}_{(0,n)}}{n!} & \cdots \\ \boldsymbol{N}_{(1,0)} & \ddots & & \vdots & \\ \vdots & & \ddots & \vdots & \\ \boldsymbol{N}_{(m,0)} & \cdots & \cdots & \dfrac{\boldsymbol{N}_{(m,n)}}{n!} & \cdots \\ \vdots & & & \vdots & \ddots \end{bmatrix} \tag{4.47}$$

where $\boldsymbol{N}_{(m,n)}$ are $3^{m+1} \times 3^{n+1}$ matrices obtained unfolding the $(m+n+2)$-order tensors $N_{\alpha\boldsymbol{\alpha}_m\beta\boldsymbol{\beta}_n}(\boldsymbol{\xi})$ so that the entries $[N]_{i,j}$ are obtained by converting both $i \leftrightarrow \alpha\,\boldsymbol{\alpha}_m$ and $j \leftrightarrow \beta\,\boldsymbol{\beta}_m$ according to Table 4.1.

Using this representation, eq. (4.30) becomes

$$\boldsymbol{v}^{[3]}(\boldsymbol{x}) + \boldsymbol{v}^{[4]}(\boldsymbol{x}) = \frac{[M]^t[N][G]}{8\pi\mu} \tag{4.48}$$

while eq. (4.34) takes the form

$$\boldsymbol{v}^{[5]}(\boldsymbol{x}) + \boldsymbol{v}^{[6]}(\boldsymbol{x}) = \frac{[M]^t[N]^2[G]}{8\pi\mu} \tag{4.49}$$

where $[N]^2 = [N][N]$. Defining the power of $[N]$ by induction as $[N]^3 = [N]^2[N]$, $[N]^k = [N]^{k-1}[N]$ and $[N]^0 = [I]$, $[I]$ being the infinite identity matrix, the total velocity field expressed by eq. (4.38) can be compactly represented as

$$\boldsymbol{v}(\boldsymbol{x}) - \boldsymbol{u}(\boldsymbol{x}) = \frac{1}{8\pi\mu}\sum_{k=0}^{\infty}[M]^t[N]^k[G] \tag{4.50}$$

Let us consider the sum entering eq. (4.50) truncated up to $k = K$ and multiply it by $([I] - [N])$. It is straightforward to show that

$$([I] - [N])\sum_{k=0}^{K}[N]^k = [I] - [N]^K \tag{4.51}$$

as for the truncated geometric series defined over a scalar field. As shown in Appendix 4.A, for characteristic distances ℓ_d of the body from the nearest walls greater enough than the characteristic length of the body itself ℓ_b, the series in eq. (4.51) converges, since

$$\lim_{K\to\infty}[N]^K = 0, \qquad \text{for } \ell_d > \Gamma\,\ell_b \tag{4.52}$$

where the constant $\Gamma > 0$ depends on the geometry of the system. As a consequence

$$([I]-[N])\sum_{k=0}^{\infty}[N]^k = [I], \qquad \ell_d > \Gamma \ell_b \tag{4.53}$$

and multiplying by $([I]-[N])^{-1}$

$$\sum_{k=0}^{\infty}[N]^k = ([I]-[N])^{-1}, \qquad \ell_d > \Gamma\,\ell_b \tag{4.54}$$

$([I]-[N])^{-1}$ being the inverse matrix of $([I]-[N])$ [43].

Therefore, the velocity field attains the simple expression

$$\boldsymbol{v}(\boldsymbol{x}) - \boldsymbol{u}(\boldsymbol{x}) = \frac{[M]^t([I]-[N])^{-1}[G]}{8\pi\mu}, \qquad \ell_d > \Gamma\,\ell_b \tag{4.55}$$

or alternatively,

$$\boldsymbol{v}(\boldsymbol{x}) - \boldsymbol{u}(\boldsymbol{x}) = \frac{[M]^t[X]}{8\pi\mu}, \qquad \ell_d > \Gamma\,\ell_b \tag{4.56}$$

where $[X]$ is the solution of the infinite-matrix equation of

$$([I]-[N])[X] = [G] \tag{4.57}$$

In the remainder we consider exclusively the situation $\ell_d > \Gamma\,\ell_b$, for which eq. (4.55) holds.

4.5 Force and torque on the particle

By linearity, the force and the torque acting on the particle due to the hydrodynamic interactions with the fluid, are given by the summation of all the forces and torques associated with the terms in (4.14), i.e.,

$$\begin{aligned} \boldsymbol{F} &= \boldsymbol{F}^{[0]} + \boldsymbol{F}^{[1]} + \boldsymbol{F}^{[2]} + \ldots \\ \boldsymbol{T} &= \boldsymbol{T}^{[0]} + \boldsymbol{T}^{[1]} + \boldsymbol{T}^{[2]} + \ldots \end{aligned} \tag{4.58}$$

where

$$\begin{aligned} \boldsymbol{F}^{[k]} &= -\int_{S_p} \boldsymbol{\sigma}^{[k]}(\boldsymbol{x})\cdot\boldsymbol{n}dS, \qquad k = 0,1,2,\ldots \\ \boldsymbol{T}^{[k]} &= -\int_{S_p} (\boldsymbol{x}-\boldsymbol{\xi})\times\boldsymbol{\sigma}^{[k]}(\boldsymbol{x})\cdot\boldsymbol{n}dS, \qquad k = 0,1,2,\ldots \end{aligned} \tag{4.59}$$

Since $\nabla\cdot\boldsymbol{\sigma}^{[k]}(\boldsymbol{x}) = 0$, and due to the symmetry of the stress tensors $\boldsymbol{\sigma}^{[k]}(\boldsymbol{x})$, the forces and torques associated to even values of k (i.e. the forces due to regular fields on the boundary of the particle) vanish for the Gauss-Green theorem. The only terms contributing to the total force and torque are the terms corresponding to odd value of $k = 1, 3, 5, ...$

$$\boldsymbol{F} = \boldsymbol{F}^{[1]} + \boldsymbol{F}^{[3]} + \boldsymbol{F}^{[5]} + ...$$
$$\boldsymbol{T} = \boldsymbol{T}^{[1]} + \boldsymbol{T}^{[3]} + \boldsymbol{T}^{[5]} + ... \tag{4.60}$$

The first contribution $\boldsymbol{F}^{[1]}$ in the sum eq. (4.60) is the force experienced by the body immersed in the unbounded ambient flow $\boldsymbol{u}(\boldsymbol{x})$, therefore it can be obtained by applying the 0-th order Faxén operator according eq. (4.12)

$$F_\alpha^{[1]} = F_\alpha^{[\infty]} = -M_\alpha(\boldsymbol{\xi}) = -8\pi\mu\mathcal{F}_{\beta\alpha}u_\beta(\boldsymbol{\xi}) \tag{4.61}$$

where, with the notation $F_\alpha^{[\infty]}$, we want to remark that the force $F_\alpha^{[1]}$ is exactly that experienced by the body if the fluid were unbounded.

The other contribution $\boldsymbol{F}^{[3]} + \boldsymbol{F}^{[5]} + ...$ in eq. (4.60) is the force experienced by the body immersed in the ambient flow $\boldsymbol{v}^{[2]}(\boldsymbol{x}) + \boldsymbol{v}^{[4]}(\boldsymbol{x}) + ...$ Therefore,

$$F_\alpha^{[3]} + F_\alpha^{[5]} + ... = -8\pi\mu\mathcal{F}_{\beta\alpha}(v_\beta^{[2]}(\boldsymbol{\xi}) + v_\beta^{[4]}(\boldsymbol{\xi}) + ...) \tag{4.62}$$

Indicating with $[S]$ the $\infty \times 3$ dimensional matrix collecting all the derivatives of the Stokeslet $\nabla_{\boldsymbol{\alpha}_m} S_{a\alpha}(\boldsymbol{x} - \boldsymbol{\xi})$ (equivalently to the definition eq. (4.45) given for $[G]$) and with $[W]$ the $\infty \times 3$ dimensional matrix collecting all the derivatives of the regular part of the Green function $\nabla_{\boldsymbol{\alpha}_m} W_{a\alpha}(\boldsymbol{x}, \boldsymbol{\xi})$, the matrix $[G]$ can be decomposed as

$$[G] = [S] + [W] \tag{4.63}$$

and the sum of the fields $v_\alpha^{[2]}(\boldsymbol{\xi}) + v_\alpha^{[4]}(\boldsymbol{\xi}) + ...$ with even values of k, eq. (4.50), takes the form

$$\sum_{k=0}^{\infty} \boldsymbol{v}^{[2k+2]}(\boldsymbol{x}) = \frac{[M]^t([I] - [N])^{-1}[W]}{8\pi\mu} \tag{4.64}$$

while the sum of all the fields corresponding to odd values of k, associated with the disturbance field due to the body, is given by

$$\sum_{k=0}^{\infty} \boldsymbol{v}^{[2k+1]}(\boldsymbol{x}) = \frac{[M]^t([I] - [N])^{-1}[S]}{8\pi\mu} \tag{4.65}$$

Substituting eqs. (4.61), (4.62) and (4.64) into eq. (4.60), we arrive to a compact representation of the force

$$\boldsymbol{F} = \boldsymbol{F}^{[\infty]} - [M]^t([I] - [N])^{-1}[N_{(:,0)}] \tag{4.66}$$

where the matrix

$$[N_{(:,0)}] = \begin{bmatrix} \boldsymbol{N}_{(0,0)} \\ \boldsymbol{N}_{(1,0)} \\ \vdots \\ \boldsymbol{N}_{(m,0)} \\ \vdots \end{bmatrix} \tag{4.67}$$

collecting the entries $N_{\alpha\boldsymbol{\alpha}_m\beta\boldsymbol{\beta}_n}(\boldsymbol{\xi})$ for $n=0$, is exactly the $\infty\times 3$ matrix corresponding to the first three columns of the matrix $[N]$.

The same procedure can be applied to obtain an analogous relation for the torque acting on the body. By eq. (4.13), the torque $\boldsymbol{T}^{[1]}=\boldsymbol{T}^{[\infty]}$ is provided by the operator $\mathcal{T}_{\gamma\alpha}=\varepsilon_{\gamma\beta\beta_1}\mathcal{F}_{\alpha\beta\beta_1}$ applied at the ambient flow $\boldsymbol{u}(\boldsymbol{x})$, i.e.,

$$T_\alpha^{[1]}=T_\alpha^{[\infty]}=\varepsilon_{\alpha\beta\beta_1}M_{\beta\beta_1}(\boldsymbol{\xi})=8\pi\mu\mathcal{T}_{\beta\alpha}u_\beta(\boldsymbol{\xi}) \tag{4.68}$$

and the remaining term in eq. (4.60) is equal to

$$T_\alpha^{[3]}+T_\alpha^{[5]}+\ldots=8\pi\mu\mathcal{T}_{\beta\alpha}^{(ns)}(v_\beta^{[2]}(\boldsymbol{\xi})+v_\beta^{[4]}(\boldsymbol{\xi})+\ldots) \tag{4.69}$$

Therefore, the total torque is compactly expressed by the equation by

$$\boldsymbol{T}=\boldsymbol{T}^{[\infty]}+[M]^t([I]-[N])^{-1}[L] \tag{4.70}$$

with

$$[L]=\begin{bmatrix}\boldsymbol{L}_{(0)}\\ \boldsymbol{L}_{(1)}\\ \vdots\\ \boldsymbol{L}_{(m)}\\ \vdots\end{bmatrix} \tag{4.71}$$

where $\boldsymbol{L}_{(m)}$ are the $3^{m+1}\times 3$ dimensional matrices with entries $\varepsilon_{\gamma\beta\beta_1}N_{\alpha\boldsymbol{\alpha}_m\beta\beta_1}(\boldsymbol{\xi})$.

This result can be generalized to the moments: the n-th order moment $\overline{\boldsymbol{M}}_{(n)}(\boldsymbol{\xi})$ on the particle in a confined fluid is given by

$$\overline{\boldsymbol{M}}_{(n)}^t(\boldsymbol{\xi})=\boldsymbol{M}_{(n)}^t(\boldsymbol{\xi})+[M]^t([I]-[N])^{-1}[N_{(:,n)}] \tag{4.72}$$

where

$$[N_{(:,n)}]=\begin{bmatrix}\boldsymbol{N}_{(0,n)}\\ \boldsymbol{N}_{(1,n)}\\ \vdots\\ \boldsymbol{N}_{(m,n)}\\ \vdots\end{bmatrix} \tag{4.73}$$

4.6 Error estimation in truncation

The exact results obtained for velocity field, force, torque in eqs (4.55), (4.66) and (4.70) are expressed in terms of infinite matrices. It is evident that, in practical application, it is not possible to take all the entries of the matrices into account. In fact, in most of the practical applications, analytical expressions for Faxén operators and multi-poles singularities are available only for lower-order and there is no recursive relations able to predict them even for the simplest geometries involved. In addition, for more complex geometries, a finite set of geometrical moments of the body and the multi-poles in the domain can be computed by only numerically, by enforcing approximations or series truncation. It is therefore useful to determine the error deriving by considering only the first K-th order moments and K-th order multipole in the analytical expressions derived in the previous paragraphs, substituting in the exact expressions eqs. (4.55), (4.66) and (4.70) involving an infinite matrix $[M]$ its truncated counterpart $[M_{(0:K)}]$, where, according the notation introduced in eq. (4.44), $[M_{(0:K)}]$ is the vector collecting all the unbounded moments from the 0-th to the K-th order, and similarly for the other infinite matrices, $[N] \to [N_{(0:K,0:K)}]$, $[G] \to [G_{(0:K)}]$. In other words, it is important to determine the order of magnitude of the difference between the exact result and the truncated approximation for the velocity field,

$$\left| \boldsymbol{v}(\boldsymbol{x}) - \boldsymbol{u}(\boldsymbol{x}) - \frac{[M_{(0:K)}]^t([I_{(0:K,0:K)}] - [N_{(0:K,0:K)}])^{-1}[G_{(0:K)}]}{8\pi\mu} \right| \tag{4.74}$$

To this aim, consider the eq. (4.46) written in the form

$$v_a^{[1]}(\boldsymbol{x}) + v_a^{[2]}(\boldsymbol{x}) = \frac{[M_{(0:K)}]^t[G_{(0:K)}]}{8\pi\mu} + \frac{1}{8\pi\mu} \sum_{m=K+1}^{\infty} \frac{\left(\boldsymbol{M}_{(m)}\right)^t \boldsymbol{G}_{(m)}}{m!} \tag{4.75}$$

Enforcing the dimensional analysis developed in the Appendix, and specifically eqs.(4.157) and (4.159) the leading term in the series at the r.h.s of eq. (4.75) is

$$|\boldsymbol{M}^t_{(K+1)} \boldsymbol{G}_{(K+1)}| = \mu U_c O \left(\frac{\ell_b}{\ell_f} \right)^{K+2} \tag{4.76}$$

U_c being the characteristic magnitude of the ambient velocity field. Therefore, truncating the series

$$v_a^{[1]}(\boldsymbol{x}) + v_a^{[2]}(\boldsymbol{x}) = \frac{[M_{(0:K)}]^t[G_{(0:K)}]}{8\pi\mu} + U_c O \left(\frac{\ell_b}{\ell_f} \right)^{K+2} \tag{4.77}$$

The velocity fields due to the next reflections, hence for $k = 1$, can be written as

$$\begin{aligned} v_a^{[3]}(\boldsymbol{x}) + v_a^{[4]}(\boldsymbol{x}) &= \frac{[M_{(0:K)}]^t[N_{(0:K,0:K)}][G_{(0:K)}]}{8\pi\mu} \\ &+ \frac{1}{8\pi\mu} \sum_{m=K+1}^{\infty} \sum_{n=K+1}^{\infty} \frac{\left(\boldsymbol{M}_{(m)}\right)^t \boldsymbol{N}_{(m,n)} \boldsymbol{G}_{(n)}}{m!} \end{aligned} \tag{4.78}$$

where the leading term in the series, estimated by using eqs. (4.157), (4.159) and (4.164), is

$$|\boldsymbol{M}^t_{(K+1)} \boldsymbol{N}_{(K+1,K+1)} \boldsymbol{G}_{(K+1)}| = \mu U_c O \left(\frac{\ell_b}{\ell_f} \frac{\ell_b}{2\ell_d} \right)^{K+2} \tag{4.79}$$

since $\ell_b/(2\ell_d) < 1$, the term in eq. (4.79) is always smaller than the term in eq. (4.76), and thus

$$|\boldsymbol{M}^t_{(K+1)} \boldsymbol{N}_{(K+1,K+1)} \boldsymbol{G}_{(K+1)}| = \mu U_c \, o \left(\frac{\ell_b}{\ell_f} \right)^{K+2} \tag{4.80}$$

The corresponding velocity fields are

$$v_a^{[3]}(\boldsymbol{x}) + v_a^{[4]}(\boldsymbol{x}) = \frac{[M_{(0:K)}]^t [N_{(0:K,0:K)}][G_{(0:K)}]}{8\pi\mu} + U_c\, o\left(\frac{\ell_b}{\ell_f}\right)^{K+2} \tag{4.81}$$

By reiterating the procedure for higher order reflected velocity fields, hence for $k > 1$,

$$v_a^{[2k+1]}(\boldsymbol{x}) + v_a^{[2k+2]}(\boldsymbol{x}) = \frac{[M_{(0:K)}]^t [N_{(0:K,0:K)}]^k [G_{(0:K)}]}{8\pi\mu} + U_c\, o\left(\frac{\ell_b}{\ell_f}\right)^{K+2}, \qquad k = 1, 2, ... \tag{4.82}$$

Finally, summing all the velocity fields, the leading neglected term is that furnished by the truncation of the first reflected fields $\boldsymbol{v}^{[1]}(\boldsymbol{x}) + \boldsymbol{v}^{[2]}(\boldsymbol{x})$ in eq. (4.77), and therefore

$$\boldsymbol{v}(\boldsymbol{x}) - \boldsymbol{u}(\boldsymbol{x}) = \frac{[M_{(0:K)}]^t ([I_{(0:K,0:K)}] - [N_{(0:K,0:K)}])^{-1} [G_{(0:K)}]}{8\pi\mu} + U_c O\left(\frac{\ell_b}{\ell_f}\right)^{K+2} \tag{4.83}$$

A similar analysis can be extended to forces and torques, obtaining

$$\boldsymbol{F} - \boldsymbol{F}^{[\infty]} = -[M_{(0:K)}]^t ([I_{(0:K,0:K)}] - [N_{(0:K,0:K)}])^{-1} [N_{(0:K,0)}] + F_c O\left(\frac{\ell_b}{\ell_d}\right)^{K+2} \tag{4.84}$$

and

$$\boldsymbol{T} - \boldsymbol{T}^{[\infty]} = [M_{(0:K)}]^t ([I_{(0:K,0:K)}] - [N_{(0:K,0:K)}])^{-1} [L_{(0:K)}] + T_c O\left(\frac{\ell_b}{\ell_d}\right)^{K+2} \tag{4.85}$$

where $F_c = \mu\, \ell_b\, U_c$ and $T_c = \mu\, \ell_b^2\, U_c$.

The scaling analysis of the truncation error addressed above can be applied to the approximations of the hydromechanical properties addressed in the literature. Therefore, let us analyze and discuss, under the point of view of the theory developed in this thesis, the main expressions regarding body in confined Stokes flow present in literature.

4.6.1 The approximation for $K = 0$ and Brenner's formula

An explicit approximation for the force acting on an arbitrary body translating in a confined fluid has been derived by [25] in terms of the resistance matrix of the body in the unbounded fluid and the value of the regular part of the Green function at a position of the body. In the present formalism this corresponds to the truncation of the $[M]$, $[N]$ and $[G]$ matrices to the 0-th order. In fact, for $K = 0$ explicating the matrices entering eq. (4.83), according to eqs. (4.43)-(4.47), and substituting $\boldsymbol{M}_{(0)}^t = -\boldsymbol{F}^{[\infty]}$, we have

$$\boldsymbol{v}(\boldsymbol{x}) = \boldsymbol{u}(\boldsymbol{x}) - \frac{\boldsymbol{F}^{[\infty]}(I - \boldsymbol{N}_{(0,0)})^{-1} \boldsymbol{G}_{(0)}}{8\pi\mu} + U_c O\left(\frac{\ell_b}{\ell_f}\right)^2 \tag{4.86}$$

I being the 3×3 identity matrix.

By eqs. (4.27) and (4.8), the entries of $\boldsymbol{N}_{(0,0)}$ are

$$N_{\alpha\beta}(\boldsymbol{\xi}) = \mathcal{F}_{\gamma'\beta} W_{\gamma'\alpha}(\boldsymbol{\xi}', \boldsymbol{\xi})\Big|_{\boldsymbol{\xi}'=\boldsymbol{\xi}} = \sum_{n=0}^{\infty} \frac{m_{\gamma'\boldsymbol{\gamma}'_n\beta}(\boldsymbol{\xi}', \boldsymbol{\xi}) \nabla_{\boldsymbol{\gamma}'_n} W_{\gamma'\alpha}(\boldsymbol{\xi}', \boldsymbol{\xi})}{n!}\Big|_{\boldsymbol{\xi}'=\boldsymbol{\xi}} \tag{4.87}$$

In order to identify terms in eq. (4.87) that can be neglected in eq (4.86), let us, briefly, perform a dimensional analysis of geometrical moments. By defining a "geometrical" volume force field $\psi_{\alpha\beta'\boldsymbol{\beta}'_n}(\boldsymbol{x}, \boldsymbol{\xi}')$ such that

$$\psi^{(n)}_{\alpha}(\boldsymbol{x}, \boldsymbol{\xi}') = 8\pi\mu A_{\beta'\boldsymbol{\beta}'_n} \psi_{\alpha\beta'\boldsymbol{\beta}'_n}(\boldsymbol{x}, \boldsymbol{\xi}')$$

it is possible to express geometrical moments by the integral

$$m_{\alpha\boldsymbol{\alpha}_m\beta\boldsymbol{\beta}_n}(\boldsymbol{\xi}, \boldsymbol{\xi}') = \int (\boldsymbol{x} - \boldsymbol{\xi})_{\boldsymbol{\alpha}_m} \psi_{\alpha\beta'\boldsymbol{\beta}'_n}(\boldsymbol{x}, \boldsymbol{\xi}') dV(\boldsymbol{x}) \qquad \boldsymbol{\xi}, \boldsymbol{\xi}' \in V_b \tag{4.88}$$

Considering that

$$\psi^{(n)}_{\alpha}(\boldsymbol{x}, \boldsymbol{\xi}') \sim \frac{\mu U_c}{\ell_b^2}, \qquad A_{\beta'\boldsymbol{\beta}'_n} \sim \frac{U_c}{\ell_b^n}$$

and then

$$\psi_{\alpha\beta'\boldsymbol{\beta}'_n}(\boldsymbol{x}, \boldsymbol{\xi}') = O(\ell_b)^{n-2}$$

it easy to estimate, by eq. (4.88), geometrical moments

$$m_{\alpha\boldsymbol{\alpha}_m\beta\boldsymbol{\beta}_n}(\boldsymbol{\xi}, \boldsymbol{\xi}) = O(\ell_b)^{m+n+1} \tag{4.89}$$

Therefore, neglecting in eq. (4.87) the order of $\boldsymbol{N}_{(0,0)}$ higher than $O(\ell_b/\ell_d)$, and denoting the resistance matrix by $R_{\alpha\beta} = -8\pi\mu\, m_{\alpha\beta}$, we obtain

$$N_{\alpha\beta}(\boldsymbol{\xi}) = -\frac{R_{\gamma\beta} W_{\gamma\alpha}(\boldsymbol{\xi}, \boldsymbol{\xi})}{8\pi\mu} + O\left(\frac{\ell_b}{\ell_d}\right)^2 \tag{4.90}$$

and therefore

$$\boldsymbol{v}(\boldsymbol{x}) = \boldsymbol{u}(\boldsymbol{x}) - \frac{\boldsymbol{F}^{[\infty]}}{8\pi\mu}\left(I + \frac{\boldsymbol{R}\boldsymbol{W}_{(0)}}{8\pi\mu}\right)^{-1} \boldsymbol{G}_{(0)} + U_c O\left(\frac{\ell_b}{\ell_f}\right)^2 \tag{4.91}$$

Considering the force on the body approximated to $K = 0$, eq. (4.84) becomes

$$\boldsymbol{F} - \boldsymbol{F}^{[\infty]} = \boldsymbol{F}^{[\infty]}(I - \boldsymbol{N}_{(0,0)})^{-1} \boldsymbol{N}_{(0,0)} + F_c O\left(\frac{\ell_b}{\ell_d}\right)^2 \tag{4.92}$$

By simple matrix manipulations, and using eq. (4.90), we obtain the approximation furnished by [25]

$$\boldsymbol{F} = \boldsymbol{F}^{[\infty]}\left(I + \frac{\boldsymbol{R}\boldsymbol{W}_{(0)}}{8\pi\mu}\right)^{-1} + F_c O\left(\frac{\ell_b}{\ell_d}\right)^2 \tag{4.93}$$

By assuming $K = 0$ in eq. (4.85), the torque is approximated as

$$\boldsymbol{T} - \boldsymbol{T}^{[\infty]} = -\boldsymbol{F}^{[\infty]}(I - \boldsymbol{N}_{(0,0)})^{-1} \boldsymbol{L}_{(0)} + T_c O\left(\frac{\ell_b}{\ell_d}\right)^2 \tag{4.94}$$

The entries of $\boldsymbol{L}_{(0)}$ are, by definition eq. (4.71)

$$L_{\alpha\beta} = \mathcal{T}_{\gamma'\beta} W_{\gamma'\alpha}(\boldsymbol{\xi}', \boldsymbol{\xi})\Big|_{\boldsymbol{\xi}'=\boldsymbol{\xi}} = \varepsilon_{\beta\delta\delta_1} \mathcal{F}_{\gamma'\delta\delta_1} W_{\gamma'\alpha}(\boldsymbol{\xi}', \boldsymbol{\xi})\Big|_{\boldsymbol{\xi}'=\boldsymbol{\xi}}$$
$$= \varepsilon_{\beta\delta\delta_1} \sum_{n=0}^{\infty} \frac{m_{\gamma'\boldsymbol{\gamma}'_n\delta\delta_1}(\boldsymbol{\xi}', \boldsymbol{\xi}) \nabla_{\boldsymbol{\gamma}'_n} W_{\gamma'\alpha}(\boldsymbol{\xi}', \boldsymbol{\xi})}{n!}\Bigg|_{\boldsymbol{\xi}'=\boldsymbol{\xi}} \tag{4.95}$$

By the same dimensional analysis provided in eqs. (4.88)-(4.90) and identifying the coupling resistance matrix in the unbounded fluid as $C_{\beta\gamma} = 8\pi\mu\, \varepsilon_{\beta\delta\delta_1}\, m_{\gamma\delta\delta_1}(\boldsymbol{\xi}, \boldsymbol{\xi})$

$$L_{\alpha\beta} = \frac{C_{\beta\gamma} W_{\gamma\alpha}(\boldsymbol{\xi}, \boldsymbol{\xi})}{8\pi\mu} + O\left(\frac{\ell_b^3}{\ell_d^2}\right)$$

and therefore, considering that $\boldsymbol{W}_{(0)}$ is a symmetric matrix [194], we have the first order term

$$\boldsymbol{T} = \boldsymbol{T}^{[\infty]} - \boldsymbol{F}^{[\infty]} \left(I + \frac{\boldsymbol{R}\boldsymbol{W}_{(0)}}{8\pi\mu}\right)^{-1} \frac{\boldsymbol{W}_{(0)}\boldsymbol{C}^t}{8\pi\mu} + T_c O\left(\frac{\ell_b}{\ell_d}\right)^2 \tag{4.96}$$

In the case that the body translate with velocity $\boldsymbol{U}$ in a quiescent fluid, the velocity field is the same of a disturbance field due to an ambient field $\boldsymbol{u}(\boldsymbol{x}) = -\boldsymbol{U}$ past the still body. Therefore, from eq. (4.91) and considering $\boldsymbol{F}^{[\infty]} = -\boldsymbol{U}\boldsymbol{R}$, the velocity field around the translating body is

$$\boldsymbol{w}(\boldsymbol{x}) = \frac{\boldsymbol{U}\boldsymbol{R}}{8\pi\mu} \left(I + \frac{\boldsymbol{R}\boldsymbol{W}_{(0)}}{8\pi\mu}\right)^{-1} \boldsymbol{G}_{(0)} + U_c O\left(\frac{\ell_b}{\ell_f}\right)^2 \tag{4.97}$$

By eq. (4.93), the force is

$$\boldsymbol{F} = -\boldsymbol{U}\boldsymbol{R} \left(I + \frac{\boldsymbol{R}\boldsymbol{W}_{(0)}}{8\pi\mu}\right)^{-1} + F_c O\left(\frac{\ell_b}{\ell_d}\right)^2 \tag{4.98}$$

while, by considering $\boldsymbol{T}^{[\infty]} = -\boldsymbol{U}\boldsymbol{C}^t$, from eq. (4.102) the torque is

$$\boldsymbol{T} = -\boldsymbol{U} \left(I + \frac{\boldsymbol{R}\boldsymbol{W}_{(0)}}{8\pi\mu}\right)^{-1} \boldsymbol{C}^t + T_c O\left(\frac{\ell_b}{\ell_d}\right)^2 \tag{4.99}$$

If the particle rotate (without translating) with angular velocity $\boldsymbol{\omega}$, the force on the particle in the unbounded fluid is given by $\boldsymbol{F}^{[\infty]} = -\boldsymbol{\omega}\,\boldsymbol{C}$ [98] and therefore, following the same procedure, the velocity field is

$$\boldsymbol{w}(\boldsymbol{x}) = \frac{\boldsymbol{\omega}\,\boldsymbol{C}}{8\pi\mu} \left(I + \frac{\boldsymbol{R}\boldsymbol{W}_{(0)}}{8\pi\mu}\right)^{-1} \boldsymbol{G}_{(0)} + U_c O\left(\frac{\ell_b}{\ell_f}\right)^2 \tag{4.100}$$

the force

$$\boldsymbol{F} = -\boldsymbol{\omega} \left(I + \frac{\boldsymbol{R}\boldsymbol{W}_{(0)}}{8\pi\mu}\right)^{-1} \boldsymbol{C} + F_c O\left(\frac{\ell_b}{\ell_d}\right)^2 \tag{4.101}$$

and the torque, considering $\boldsymbol{T}^{[\infty]} = -\boldsymbol{\omega}\,\boldsymbol{\Omega}$,

$$\boldsymbol{T} = -\boldsymbol{\omega}\left[\boldsymbol{\Omega} - \boldsymbol{C}\left(I + \frac{\boldsymbol{R}\boldsymbol{W}_{(0)}}{8\pi\mu}\right)^{-1}\frac{\boldsymbol{W}_{(0)}\boldsymbol{C}^t}{8\pi\mu}\right] + T_c O\left(\frac{\ell_b}{\ell_d}\right)^2 \tag{4.102}$$

after some algebra

$$\boldsymbol{T} = -\boldsymbol{\omega}\,\boldsymbol{\Omega}\left(I + \frac{(\boldsymbol{R} - \boldsymbol{\Omega}^{-1}\boldsymbol{C}\boldsymbol{C}^t)\boldsymbol{W}_{(0)}}{8\pi\mu}\right)\left(I + \frac{\boldsymbol{R}\boldsymbol{W}_{(0)}}{8\pi\mu}\right)^{-1} + T_c O\left(\frac{\ell_b}{\ell_d}\right)^2 \tag{4.103}$$

where $\boldsymbol{\Omega}$, having entries $\Omega_{\alpha\beta} = -8\pi\mu\,\varepsilon_{\alpha\gamma\gamma_1}\varepsilon_{\beta\delta\delta_1}m_{\gamma\gamma_1\delta\delta_1}(\boldsymbol{\xi},\boldsymbol{\xi})$, is the angular resistance matrix.

Eqs. (4.97)-(4.103), requiring solely the Green function of the confinement and the grand-resistance matrix of the body, provide the first order of the correction due to the confinement to the unbounded hydrodynamics of the body. However, many geometries of bodies of great interest (such as the sphere) have symmetries which make it so that most of the entries of the coupling matrix $\boldsymbol{C}$ vanishes. This means that eqs. (4.99)-(4.103) are not able to express any correction term for these bodies, independently of the confinement. Therefore, in this case, to obtain first correction terms due to the confinement, it is necessary to consider higher order terms of the $[N]$-matrix (thus $K > 0$), as shown for the case of a sphere near a plane wall in Section 4.7.1. Otherwise, a convenient approach is to use the [228, 229] approximate expressions, which are obtained and discussed according the present formalism in the next sub-section.

4.6.2 Extended Swan and Brady's approximation for rigid motion

In obtaining the approximate expressions eqs. (4.93) and (4.102), valid to the order (ℓ_b/ℓ_d), we have neglected the higher order terms in the 0-th order Faxén operator for the force and in the 1-st order Faxén operator for the torque. Supposing that these Faxén operators are exactly known, it is possible to obtain expressions for the force and the torque on a rigid moving body accurate to $(\ell_b/\ell_d)^2$ or to $(\ell_b/\ell_d)^3$ for the axisymmetric motion of the body, by exploiting all the higher order terms in the lower order Faxén operators. It is shown below that this procedure provides exactly the extension to arbitrary geometries and reciprocal boundary conditions of the relations found by [228, 229] in the case of confined spherical bodies with no-slip boundary conditions. To begin with, let us suppose that the body translates without rotation with velocity $\boldsymbol{U}$ (therefore $\boldsymbol{u}(\boldsymbol{x}) = -\boldsymbol{U}$). By equation (4.21), the velocity field $\boldsymbol{v}^{[2]}(\boldsymbol{x})$, of the order of magnitude $O(U\ell_b/\ell_d)$, at the pole $\boldsymbol{\xi}$ can be obtained exactly by the 0-th order Faxén operator

$$v_\alpha^{[2]}(\boldsymbol{\xi}) = -U_\beta \mathcal{F}_{\alpha'\beta} W_{\alpha\alpha'}(\boldsymbol{\xi},\boldsymbol{\xi}')\Big|_{\boldsymbol{\xi}'=\boldsymbol{\xi}} \tag{4.104}$$

and hence the force is exactly given by

$$F_\gamma^{[3]} = -8\pi\mu\mathcal{F}_{\alpha\gamma}v_\alpha^{[2]}(\boldsymbol{\xi}) = 8\pi\mu U_\beta \mathcal{F}_{\alpha\gamma}\mathcal{F}_{\alpha'\beta}W_{\alpha\alpha'}(\boldsymbol{\xi},\boldsymbol{\xi}')\Big|_{\boldsymbol{\xi}'=\boldsymbol{\xi}} \tag{4.105}$$

while for the torque we have

$$T_\gamma^{[3]} = 8\pi\mu\mathcal{T}_{\alpha\gamma}v_\alpha^{[2]}(\boldsymbol{\xi}) = -8\pi\mu U_\beta \mathcal{T}_{\alpha\gamma}\mathcal{F}_{\alpha'\beta}W_{\alpha\alpha'}(\boldsymbol{\xi},\boldsymbol{\xi}')\Big|_{\boldsymbol{\xi}'=\boldsymbol{\xi}} \tag{4.106}$$

To obtain the contributions $\boldsymbol{F}^{[5]}$ and $\boldsymbol{T}^{[5]}$ to the force and the torque it is necessary to have an explicit expression for the velocity field $\boldsymbol{v}^{[4]}(\boldsymbol{x})$, which in turn implies the knowledge of the higher order Faxén operators. From eq. (4.89) and (4.104), we have

$$v_\alpha^{[2]}(\boldsymbol{\xi}) = U_c O\left(\frac{\ell_b}{\ell_d}\right), \qquad \nabla_{\boldsymbol{\beta}_n} v_\beta^{[2]}(\boldsymbol{\xi}) = U_c O\left(\frac{\ell_b}{\ell_d^{1+n}}\right) \tag{4.107}$$

By which it is possible to estimate the error committed in approximating the field $v^{[4]}(\boldsymbol{\xi})$ to the 0-th order Faxén operator, thus

$$v_\alpha^{[4]}(\boldsymbol{\xi}) = \sum_{n=0}^{\infty} \frac{\nabla_{\boldsymbol{\beta}_n} v_\beta^{[2]}(\boldsymbol{\xi})}{n!}\mathcal{F}_{\alpha'\beta\boldsymbol{\beta}_n}W_{\alpha\alpha'}(\boldsymbol{\xi},\boldsymbol{\xi}') = v_\beta^{[2]}(\boldsymbol{\xi})\mathcal{F}_{\alpha'\beta}W_{\alpha\alpha'}(\boldsymbol{\xi},\boldsymbol{\xi}')\Big|_{\boldsymbol{\xi}'=\boldsymbol{\xi}} + O\left(\frac{\ell_b}{\ell_d}\right)^3 \tag{4.108}$$

by which we obtain the force

$$F_\gamma^{[5]} = -8\pi\mu\mathcal{F}_{\alpha\gamma}v_\alpha^{[4]}(\boldsymbol{\xi}) = -8\pi\mu\, v_\beta^{[2]}(\boldsymbol{\xi})\mathcal{F}_{\alpha\gamma}\mathcal{F}_{\alpha'\beta}W_{\alpha\alpha'}(\boldsymbol{\xi},\boldsymbol{\xi}')\Big|_{\boldsymbol{\xi}'=\boldsymbol{\xi}} + O\left(\frac{\ell_b}{\ell_d}\right)^3 \tag{4.109}$$

and the torque

$$T_\gamma^{[5]} = 8\pi\mu\mathcal{T}_{\alpha\gamma}v_\alpha^{[4]}(\boldsymbol{\xi}) = 8\pi\mu\, v_\beta^{[2]}(\boldsymbol{\xi})\mathcal{T}_{\alpha\gamma}\mathcal{F}_{\alpha'\beta}W_{\alpha\alpha'}(\boldsymbol{\xi},\boldsymbol{\xi}')\Big|_{\boldsymbol{\xi}'=\boldsymbol{\xi}} + O\left(\frac{\ell_b}{\ell_d}\right)^3 \tag{4.110}$$

By eq. (4.105) and the definition of the resistance matrix $\boldsymbol{R}$

$$F_\gamma^{[3]} = R_{\gamma\alpha}v_\alpha^{[2]}(\boldsymbol{\xi}) + O\left(\frac{\ell_b}{\ell_d}\right)^2, \qquad v_\alpha^{[2]}(\boldsymbol{\xi}) = (R^{-1})_{\alpha\gamma}F_\gamma^{[3]} + O\left(\frac{\ell_b}{\ell_d}\right)^2 \tag{4.111}$$

while by eq. (4.106) and the definition of the coupling resistance matrix $\boldsymbol{C}$

$$T_\gamma^{[3]} = C_{\gamma\alpha}v_\alpha^{[2]}(\boldsymbol{\xi}) + O\left(\frac{\ell_b}{\ell_d}\right)^2, \qquad v_\alpha^{[2]}(\boldsymbol{\xi}) = (C^{-1})_{\alpha\gamma}T_\gamma^{[3]} + O\left(\frac{\ell_b}{\ell_d}\right)^2 \tag{4.112}$$

Let us call with $\boldsymbol{X}$ and $\boldsymbol{Y}$ the matrices with entries

$$X_{\alpha\beta} = -8\pi\mu\mathcal{F}_{\gamma\beta}\mathcal{F}_{\gamma'\alpha}W_{\gamma\gamma'}(\boldsymbol{\xi},\boldsymbol{\xi}')\Big|_{\boldsymbol{\xi}'=\boldsymbol{\xi}} \tag{4.113}$$

and $\boldsymbol{Y}$

$$Y_{\alpha\beta} = 8\pi\mu\mathcal{T}_{\gamma\beta}\mathcal{F}_{\alpha'\delta}W_{\gamma\alpha'}(\boldsymbol{\xi},\boldsymbol{\xi}')\Big|_{\boldsymbol{\xi}'=\boldsymbol{\xi}} \tag{4.114}$$

respectively. Substituting eq. (4.111) into eq. (4.109) and eq. (4.112) into eq. (4.110) it follows that

$$\boldsymbol{F}^{[5]} = \boldsymbol{F}^{[3]}\,\boldsymbol{R}^{-1}\,\boldsymbol{X} + O\left(\frac{\ell_b}{\ell_d}\right)^3 \tag{4.115}$$

and

$$\boldsymbol{T}^{[5]} = \boldsymbol{T}^{[3]}(\boldsymbol{C}^t)^{-1}\boldsymbol{Y} + O\left(\frac{\ell_b}{\ell_d}\right)^3 \tag{4.116}$$

Using the same approach, these results can be generalized for $k = 2, 3, ...$, obtaining

$$\boldsymbol{F}^{[2k+3]} = \boldsymbol{F}^{[2k+1]}\boldsymbol{R}^{-1}\boldsymbol{X} + o\left(\frac{\ell_b}{\ell_d}\right)^3 \tag{4.117}$$

$$\boldsymbol{T}^{[2k+3]} = \boldsymbol{T}^{[2k+1]}(\boldsymbol{C}^{-1})^t\boldsymbol{Y} + o\left(\frac{\ell_b}{\ell_d}\right)^3 \tag{4.118}$$

and thus

$$\boldsymbol{F} = \boldsymbol{F}^{[\infty]} + \sum_{k=0}^{\infty}\boldsymbol{F}^{[2k+3]} = \boldsymbol{F}^{[\infty]}\sum_{k=0}^{\infty}(\boldsymbol{R}^{-1}\boldsymbol{X})^k + O\left(\frac{\ell_b}{\ell_d}\right)^3 = \boldsymbol{F}^{[\infty]}(\boldsymbol{I} - \boldsymbol{R}^{-1}\boldsymbol{X})^{-1} + O\left(\frac{\ell_b}{\ell_d}\right)^3 \tag{4.119}$$

$$\boldsymbol{T} = \boldsymbol{T}^{[\infty]} + \sum_{k=0}^{\infty}\boldsymbol{T}^{[2k+3]} = \boldsymbol{T}^{[\infty]}\sum_{k=0}^{\infty}((\boldsymbol{C}^t)^{-1}\boldsymbol{Y})^k + O\left(\frac{\ell_b}{\ell_d}\right)^3 = \boldsymbol{T}^{[\infty]}(\boldsymbol{I} - (\boldsymbol{C}^t)^{-1}\boldsymbol{Y})^{-1} + O\left(\frac{\ell_b}{\ell_d}\right)^3 \tag{4.120}$$

Finally

$$\boldsymbol{F} = -\boldsymbol{U}\,\boldsymbol{R}\,(\boldsymbol{I} - \boldsymbol{R}^{-1}\boldsymbol{X})^{-1} + O\left(\frac{\ell_b}{\ell_d}\right)^3 \tag{4.121}$$

and

$$\boldsymbol{T} = -\boldsymbol{U}\,\boldsymbol{C}^t\,(\boldsymbol{I} - (\boldsymbol{C}^t)^{-1}\boldsymbol{Y})^{-1} + O\left(\frac{\ell_b}{\ell_d}\right)^3 \tag{4.122}$$

Eqs. (4.121) and (4.122) can be expressed equivalently by

$$\boldsymbol{F} = -\boldsymbol{U}\,(\boldsymbol{R} + \boldsymbol{X}(\boldsymbol{I} - \boldsymbol{R}^{-1}\boldsymbol{X})^{-1}) + O\left(\frac{\ell_b}{\ell_d}\right)^3 \tag{4.123}$$

$$\boldsymbol{T} = -\boldsymbol{U}\,(\boldsymbol{C}^t + \boldsymbol{Y}(\boldsymbol{I} - (\boldsymbol{C}^t)^{-1}\boldsymbol{Y})^{-1}) + O\left(\frac{\ell_b}{\ell_d}\right)^3 \tag{4.124}$$

The same procedure (reported explicitly in Appendix 4.B for a spherical body) can be applied to the case the body is rotating with velocity $\boldsymbol{\omega}$ in the absence of translation, obtaining

$$\boldsymbol{F} = -\boldsymbol{\omega}\,(\boldsymbol{C} + \boldsymbol{Y}^t(\boldsymbol{I} - \boldsymbol{R}^{-1}\boldsymbol{X})^{-1}) + O\left(\frac{\ell_b}{\ell_d}\right)^3 \tag{4.125}$$

$$\boldsymbol{T} = -\boldsymbol{\omega}\,(\boldsymbol{\Omega} + \boldsymbol{Z}(\boldsymbol{I} - (\boldsymbol{C}^t)^{-1}\boldsymbol{Y})^{-1}) + O\left(\frac{\ell_b}{\ell_d}\right)^3 \tag{4.126}$$

where $\boldsymbol{Z}$ is the matrix with entries

$$Z_{\beta\alpha} = -8\pi\mu\mathcal{T}_{\gamma\beta}\mathcal{T}_{\alpha'\delta}W_{\gamma\alpha'}(\boldsymbol{\xi}, \boldsymbol{\xi}')\Big|_{\boldsymbol{\xi}'=\boldsymbol{\xi}} \tag{4.127}$$

As it is well known [98], the resistance coupling matrix in eq. (4.125) should be the transpose matrix of the resistance coupling matrix in eq. (4.124). The disagreement with the expected result is only apparent and it is due to the neglecting terms. In fact, approximating $\boldsymbol{Y} = \boldsymbol{C}^t \boldsymbol{R}^{-1} \boldsymbol{X} + O(\ell_b/\ell_d)^2$ and substituting in eq. (4.124), the expected symmetry is returned without modifying the great order of the error in the approximation.

If the body is a sphere, the (m, n)-th order geometrical moments $m_{\alpha \boldsymbol{\alpha}_m \beta \boldsymbol{\beta}_n}(\boldsymbol{\xi}, \boldsymbol{\xi})$ vanish if $m + n$ is odd, which means that m and n are neither both even or odd. Therefore, the 1-st order Faxén operator contributes to the force $\boldsymbol{F}^{[5]}$ with a term of the order of magnitude $O(\ell_b/\ell_d)^4$ smaller than the leading term in the remainder entering eq. (4.109). Therefore, it easy to see, that the error in the estimate of the global force is of the same order $O(\ell_b/\ell_f)^4$ instead of $O(\ell_b/\ell_f)^3$. Furthermore, since the coupling resistance matrix vanishes $\boldsymbol{T}^{[\infty]} = 0$, the higher order contribution is provided by $\boldsymbol{T}^{[3]}$, which can be written in term of the resistance matrix

$$\boldsymbol{T}^{[3]} = \boldsymbol{F}^{[\infty]} \boldsymbol{R}^{-1} \boldsymbol{Y} \tag{4.128}$$

The next contribution $\boldsymbol{T}^{[5]}$ can be evaluated as in eq. (4.110) considering that the first term in the Faxén operator for the torque vanishes, thus

$$\boldsymbol{T}^{[5]} = \boldsymbol{F}^{[3]} \boldsymbol{R}^{-1} \boldsymbol{Y} + O\left(\frac{\ell_b}{\ell_d}\right)^5 \tag{4.129}$$

Following the same procedure of eqs. (4.117)-(4.126), we obtain for the spherical body (or more generally problems where unbounded coupling terms vanish)

$$\boldsymbol{F} = -\boldsymbol{U}\,\boldsymbol{R}\,(\boldsymbol{I} - \boldsymbol{R}^{-1}\boldsymbol{X})^{-1} + O\left(\frac{\ell_b}{\ell_d}\right)^4 \tag{4.130}$$

and

$$\boldsymbol{T} = -\boldsymbol{U}\,(\boldsymbol{I} - \boldsymbol{R}^{-1}\boldsymbol{X})^{-1}\,\boldsymbol{Y} + O\left(\frac{\ell_b}{\ell_d}\right)^5 \tag{4.131}$$

while for rotations (see Appendix 4.B for the proof)

$$\boldsymbol{F} = -\boldsymbol{\omega}\,(\boldsymbol{I} - \boldsymbol{R}^{-1}\boldsymbol{X})^{-1}\,\boldsymbol{Y}^t + O\left(\frac{\ell_b}{\ell_d}\right)^5 \tag{4.132}$$

and

$$\boldsymbol{T} = -\boldsymbol{\omega}(\boldsymbol{\Omega} + \boldsymbol{Z} + (\boldsymbol{I} - \boldsymbol{R}^{-1}\boldsymbol{X})^{-1}\,(\boldsymbol{Y}^t \boldsymbol{R}^{-1} \boldsymbol{Y})) + O\left(\frac{\ell_b}{\ell_d}\right)^6 \tag{4.133}$$

Relations (4.121)-(4.126) and (4.130)-(4.133) are useful because they permits to obtain a good approximation of the resistance on bodies (especially spheres) in confined systems by the knowledge solely of the 0-th and 1-st order (for torque) Faxén operators. However, although these corrections improve the approximate solution, the above scaling analysis indicates that the $O(\ell_b/\ell_d)^5$ order reported by [228, 229] cannot not obtained by these relations because the contribution of order $O(\ell_b/\ell_d)^4$ does not vanishes, as found by Faxén [98], and further derived in Section 4.7.1 by considering all the terms in the matrix $[N]$.

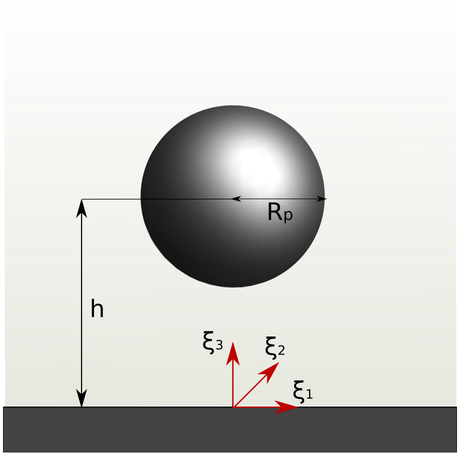

Figure 4.2. Schematic representation of a sphere near a plane wall

4.7 A sphere near a plane wall

4.7.1 Resistance on a translating particle near a plane wall

Consider a spherical body with radius R_p translating with velocity $\boldsymbol{U}$ at a distance h from a plane wall and consider the force given by eq. (4.84) assuming $K = 3$ in the form

$$\boldsymbol{F} = \boldsymbol{F}^{[\infty]} - [M_{(0:3)}]^t [X_{(0:3,0)}] + O\left(\frac{R_p}{h}\right)^5 \tag{4.134}$$

where the matrix $[X_{(0:3,0)}] = [\boldsymbol{X}_{(0,0)}, \boldsymbol{X}_{(1,0)}, \boldsymbol{X}_{(2,0)}, \boldsymbol{X}_{(3,0)}]^t$ is given by

$$[X_{(0:3,0)}] = \sum_{k=0}^{\infty} [N_{(0:3,0:3)}]^k [N_{(0:3,0)}] \tag{4.135}$$

and, thus

$$\boldsymbol{X}_{(m,0)} = \boldsymbol{N}_{(m,0)} + [N_{(m,0:3)}] \sum_{k=0}^{\infty} [N_{(0:3,0:3)}]^k [N_{(0:3,0)}], \qquad m = 0, 1, 2, 3 \tag{4.136}$$

Since in the unbounded fluid the first and third order moments on the translating sphere vanish, $\boldsymbol{M}_{(1)} = 0$, $\boldsymbol{M}_{(3)} = 0$, while $\boldsymbol{M}^t_{(0)} = -\boldsymbol{F}^{[\infty]}$ where,

$$\boldsymbol{F}^{[\infty]} = -6\pi\mu R_p \left(\frac{1 + 2\hat{\lambda}}{1 + 3\hat{\lambda}}\right) \boldsymbol{U} \tag{4.137}$$

eq. (4.134) becomes

$$\boldsymbol{F} = \boldsymbol{F}^{[\infty]} + \boldsymbol{F}^{[\infty]} \boldsymbol{X}_{(0,0)} - \frac{\boldsymbol{M}^t_{(2)} \boldsymbol{X}_{(2,0)}}{2!} + O\left(\frac{R_p}{h}\right)^5 \tag{4.138}$$

The entries of the vector $\boldsymbol{M}^t_{(2)}$ corresponds to the vectorization according Table 4.1 of the tensor

$$-8\pi\mu \mathcal{F}_{\gamma\alpha\alpha_1\alpha_2} U_\gamma = -\frac{R_p^2}{3(1 + 2\hat{\lambda})} \left(F^{[\infty]}_\alpha \delta_{\alpha_1\alpha_2} + \hat{\lambda}(F^{[\infty]}_{\alpha_1} \delta_{\alpha\alpha_2} + F^{[\infty]}_{\alpha_2} \delta_{\alpha\alpha_1})\right) + O(R_p)^5 \tag{4.139}$$

where $\mathcal{F}_{\gamma\alpha\alpha_1\alpha_2}$, evaluated in 3 eq. (3.104). Since the the second term within parentheses at the r.h.s of eq. (4.139) yields a vanishing contribution to the total force, the vector $\boldsymbol{M}_{(2)}$ can be expressed in matrix form as

$$\boldsymbol{M}^t_{(2)} = -\frac{R_p^2}{3(1+2\hat{\lambda})}\boldsymbol{F}^{[\infty]}\boldsymbol{I}_{(0,2)} + O(R_p)^5 \tag{4.140}$$

where $(\boldsymbol{I}_{(0,2)})_{ij}$, following the notation developed in Section 4.3, is the matrix collecting the entries of the tensor $\delta_{\beta\alpha}\delta_{\alpha_1\alpha_2}$ by the conversion $i \leftrightarrow \beta\alpha$ and $j \leftrightarrow \alpha_1\alpha_2$ according to Table 4.1, thus

$$\boldsymbol{I}_{(0,2)} =$$
$$\begin{pmatrix} 1&0&0&0&1&0&0&0&1&0&0&0&0&0&0&0&0&0&0&0&0&0&0&0&0&0&0 \\ 0&0&0&0&0&0&0&0&0&1&0&0&0&1&0&0&0&1&0&0&0&0&0&0&0&0&0 \\ 0&0&0&0&0&0&0&0&0&0&0&0&0&0&0&0&0&0&1&0&0&0&1&0&0&0&1 \end{pmatrix}$$

Therefore, eq. (4.138) becomes

$$\boldsymbol{F} = \boldsymbol{F}^{[\infty]}\left(I + \boldsymbol{X}_{(0,0)} + \frac{R_p^2}{6(1+2\hat{\lambda})}\boldsymbol{I}_{(0,2)}\boldsymbol{X}_{(2,0)}\right) + O\left(\frac{R_p}{h}\right)^5 \tag{4.141}$$

By eq. (4.136) and by the dimensional analysis explicited in eq. (4.165)

$$\begin{aligned} \boldsymbol{X}_{(0,0)} \quad = \quad & \boldsymbol{N}_{(0,0)} + \boldsymbol{N}^2_{(0,0)} + \boldsymbol{N}_{(0,1)}\boldsymbol{N}_{(1,0)} + \frac{1}{2}\boldsymbol{N}_{(0,2)}\boldsymbol{N}_{(2,0)} + \boldsymbol{N}^3_{(0,0)} + \\ & \boldsymbol{N}_{(0,0)}\boldsymbol{N}_{(0,1)}\boldsymbol{N}_{(1,0)} + \boldsymbol{N}_{(0,1)}\boldsymbol{N}_{(1,0)}\boldsymbol{N}_{(0,0)} + \boldsymbol{N}^4_{(0,0)} + O\left(\frac{R_p}{h}\right)^5 \end{aligned} \tag{4.142}$$

while

$$\boldsymbol{X}_{(2,0)} = \boldsymbol{N}_{(2,0)} + \boldsymbol{N}_{(2,0)}\boldsymbol{N}_{(0,0)} + O\left(\frac{R_p}{h}\right)^5 \tag{4.143}$$

Eqs. (4.141)-(4.143), can be equivalently written as

$$\begin{aligned} \boldsymbol{F} = \boldsymbol{F}^{[\infty]} & \Bigg((I - \boldsymbol{N}_{(0,0)})^{-1} + \boldsymbol{N}_{(0,1)}\boldsymbol{N}_{(1,0)} + \frac{1}{2}\boldsymbol{N}_{(0,2)}\boldsymbol{N}_{(2,0)} + \boldsymbol{N}_{(0,0)}\boldsymbol{N}_{(0,1)}\boldsymbol{N}_{(1,0)} + \\ & \boldsymbol{N}_{(0,1)}\boldsymbol{N}_{(1,0)}\boldsymbol{N}_{(0,0)} + \frac{R_p^2}{6(1+2\hat{\lambda})}\boldsymbol{I}_{(0,2)}(\boldsymbol{N}_{(2,0)} + \boldsymbol{N}_{(2,0)}\boldsymbol{N}_{(0,0)})\Bigg) + O\left(\frac{R_p}{h}\right)^5 \end{aligned} \tag{4.144}$$

The entries of the matrices $\boldsymbol{N}_{(m,n)}$ entering eq. (4.144) can be evaluated from the definition of the matrix $[N]$ eq. (4.47), and from the expression for its entries in eq. (4.27). For example, the entries $\mathcal{F}_{\gamma'\beta}W_{\gamma'\alpha}(\boldsymbol{\xi}', \boldsymbol{\xi})|_{\boldsymbol{\xi}'=\boldsymbol{\xi}}$ of the matrix $\boldsymbol{N}_{(0,0)}$ are obtained by applying the 0-th Faxén operator in eq. (3.76) to the regular part of the Green function in eq. (2.89). Considering a Cartesian system (ξ_1, ξ_2, ξ_3) with ξ_3 perpendicular to the plane as in Figure 4.2

$$\boldsymbol{N}_{(0,0)} = \begin{pmatrix} \alpha_\parallel & 0 & 0 \\ 0 & \alpha_\parallel & 0 \\ 0 & 0 & \alpha_\perp \end{pmatrix} \tag{4.145}$$

with

$$\alpha_{\|} = \frac{9R_p(1+2\hat{\lambda})}{16h(1+3\hat{\lambda})} - \frac{{R_p}^3}{16h^3(1+3\hat{\lambda})}, \qquad \alpha_{\perp} = \frac{9R_p(1+2\hat{\lambda})}{8h(1+3\hat{\lambda})} - \frac{\mathrm{Rp}^3}{4h^3(1+3\hat{\lambda})} \tag{4.146}$$

and thus

$$(I - \boldsymbol{N}_{(0,0)})^{-1} = \begin{pmatrix} \frac{1}{1-\alpha_{\|}} & 0 & 0 \\ 0 & \frac{1}{1-\alpha_{\|}} & 0 \\ 0 & 0 & \frac{1}{1-\alpha_{\perp}} \end{pmatrix} \tag{4.147}$$

From the application of the Faxén operators reported in Chapter 3 to the multipole of the regular part of the Green function reported in Chapter 2 we evaluated the significant entries of the matrix $\boldsymbol{N}_{(0,1)}$, $\boldsymbol{N}_{(1,0)}$, $\boldsymbol{N}_{(0,2)}$, $\boldsymbol{N}_{(2,0)}$ as for $\boldsymbol{N}_{(0,0)}$. By substituting all these matrices into eq. (4.141), we obtain

$$\left(\begin{pmatrix} \frac{1}{1-\alpha_{\|}} & 0 & 0 \\ 0 & \frac{1}{1-\alpha_{\|}} & 0 \\ 0 & 0 & \frac{1}{1-\alpha_{\perp}} \end{pmatrix} - \begin{pmatrix} \frac{{R_p}^3}{16h^3(1+3\hat{\lambda})} & 0 & 0 \\ 0 & \frac{{R_p}^3}{16h^3(1+3\hat{\lambda})} & 0 \\ 0 & 0 & \frac{{R_p}^3}{4h^3(1+3\hat{\lambda})} \end{pmatrix}\right.$$
$$\left. + \begin{pmatrix} \frac{27{R_p}^4\left(1+7\hat{\lambda}+20\hat{\lambda}^2+20\hat{\lambda}^3\right)}{256h^4(1+3\hat{\lambda})^2(1+5\hat{\lambda})} & 0 & 0 \\ 0 & \frac{27{R_p}^4\left(1+7\hat{\lambda}+20\hat{\lambda}^2+20\hat{\lambda}^3\right)}{256h^4(1+3\hat{\lambda})^2(1+5\hat{\lambda})} & 0 \\ 0 & 0 & -\frac{9{R_p}^4\left(1+7\hat{\lambda}-80\hat{\lambda}^2-180\hat{\lambda}^3\right)}{256h^4(1+3\hat{\lambda})^2(1+5\hat{\lambda})} \end{pmatrix}\right) + O\left(\frac{R_p}{h}\right)^5 \tag{4.148}$$

After some algebra, the latter expression can be simplified as

$$\boldsymbol{F} = \boldsymbol{F}^{[\infty]} \begin{pmatrix} \frac{1}{1-\beta_{\|}} & 0 & 0 \\ 0 & \frac{1}{1-\beta_{\|}} & 0 \\ 0 & 0 & \frac{1}{1-\beta_{\perp}} \end{pmatrix} + O\left(\frac{R_p}{h}\right)^5 \tag{4.149}$$

where

$$\beta_{\|} = \frac{9R_p}{16h}\left(\frac{1+2\hat{\lambda}}{1+3\hat{\lambda}}\right) - \frac{R_p^3}{8h^3(1+3\hat{\lambda})} + \frac{45R_p^4}{256h^4}\left(\frac{(1+2\hat{\lambda})^2}{(1+3\hat{\lambda})(1+5\hat{\lambda})}\right) \tag{4.150}$$

and

$$\beta_{\perp} = \frac{9R_p}{8h}\left(\frac{1+2\hat{\lambda}}{1+3\hat{\lambda}}\right) - \frac{R_p^3}{2h^3(1+3\hat{\lambda})} + \frac{135R_p^4}{256h^4}\left(\frac{(1+2\hat{\lambda})^2}{(1+3\hat{\lambda})(1+5\hat{\lambda})}\right) \tag{4.151}$$

For $\hat{\lambda} = 0$ (i.e. in the no-slip case), existing literature results can be recovered. In fact, the force on the sphere translating perpendicularly to the wall is in perfect agreement with the Taylor series expansion of the exact solution obtained by [23]

$$\frac{F_\perp}{6\pi\mu R_p U} = 1 + \frac{9R_p}{8h} + \frac{81{R_p}^2}{64h^2} + \frac{473{R_p}^3}{512h^3} + \frac{4113{R_p}^4}{4096h^4} + O\left(\frac{R_p}{h}\right)^5 \tag{4.152}$$

and $\beta_\|$ reduces to the same factor obtained by Faxén [98, p. 327].

Figure 4.3 and 4.4 depict the results obtained by applying eqs. (4.149)-(4.151) compared to the exact results (such as those deriving by solving the [90] equations) and to Finite Element Method (FEM) simulations (in those cases the exact result are not available). Considering all the terms in $\beta_\|$ and $\beta_\perp$, eq. (4.149) provides the force on a spherical body valid for gaps $\delta = (h - R_p) \gtrsim R_p$ or even smaller. Further improvements of the expansion, taking into account higher order Faxén operators, could increase tha range of validity of the theoretical expressions to smaller values of the gap. However, apart from the specific interest of exhibiting explicit expressions for forces in the case $\hat{\lambda} \neq 0$, the strength of the theory is that it provides a systematic procedure which does not depend on the geometrical symmetries of the particle-confinement system and on the nature of the boundary conditions. In fact, both the Faxén and the Brenner's expressions, corresponding to eq. (4.150) and (4.151) for $\hat{\lambda} = 0$ have been obtained enforcing specific symmetries of the problem (in order to transform the solution in the Fourier space, or expressing it in a suitable coordinate system, represented in this case by bispherical coordinates). Once the matrix $[N]$ is known the same procedure can be applied for evaluating the force and torque in any geometrical configuration of the particle-confinement problem.

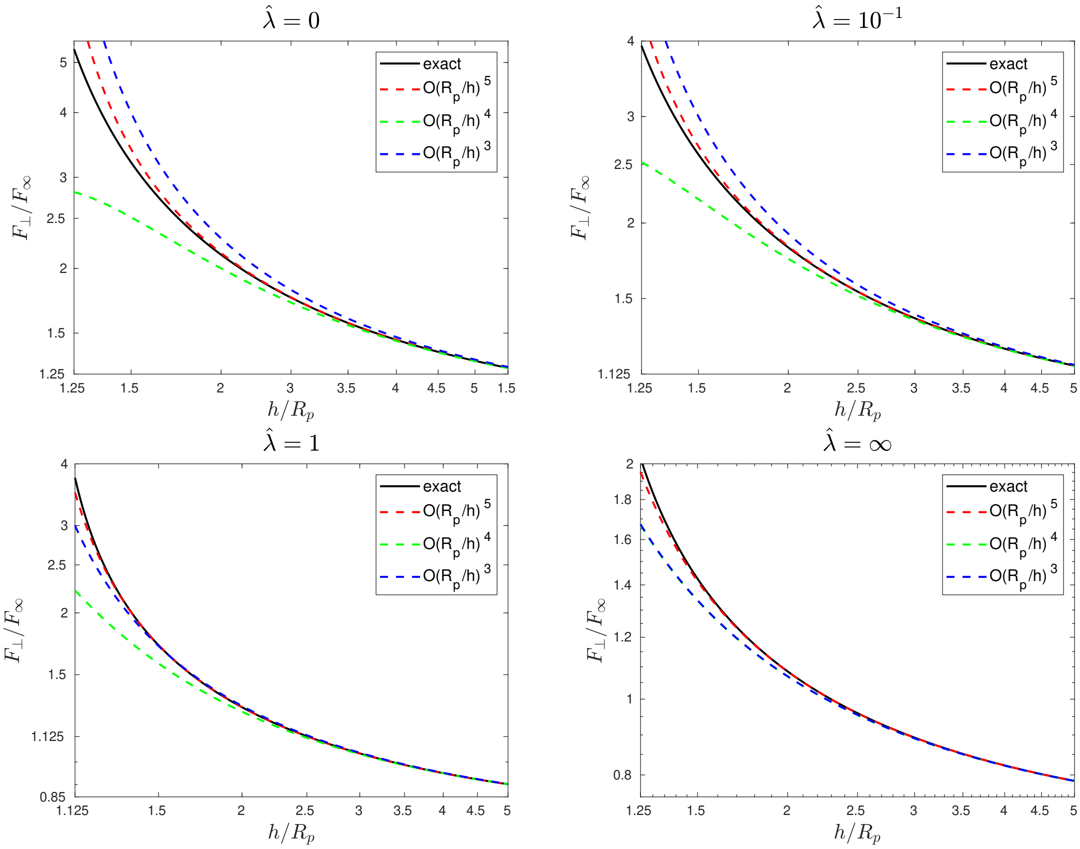

Figure 4.3. Force on a spherical body translating perpendicularly to a planar wall for different slip lengths on the sphere. Solid black lines represent exact results obtained by solving the Goren's equation [90], dashed lines are obtained by eq. (4.149) taking into account all the terms (red dashed line), neglecting the term $O(R_p//h)^4$ (green dashed line) and neglecting terms $O(R_p/h)^3$ (blue dashed line). For complete slip ($\hat{\lambda} = \infty$) blue and green dashed lines are practically coincident.

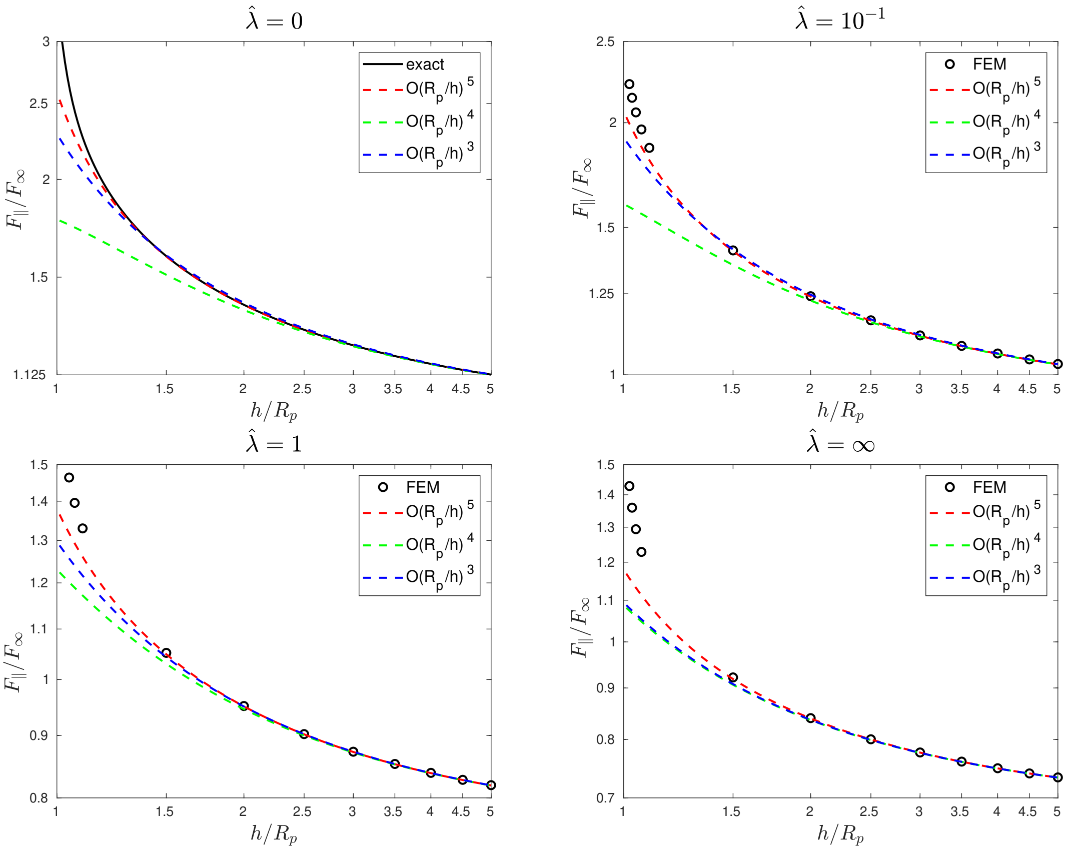

Figure 4.4. Force on a spherical body translating parallel to aplane wall for different slip lengths on the sphere. The solid black line represents the exact no-slip result obtained by solving the O'Neill's equations [184], black circles are the results of FEM simulations, dashed lines are results obtained by eq. (4.149) taking into account all the terms (red dashed line), neglecting the term $O(R_p//h)^4$ (green dashed line) and neglecting terms $O(R_p/h)^3$ (blue dashed line). For complete slip ($\hat{\lambda} = \infty$), blue and green dashed lines are practically coincident.

Appendix

4.A Analysis of the convergence of series

In this Appendix the convergence of the series introduced in Chapters 4.3 and 4.4 is investigated.

To begin with, let us consider the convergence of the series eq. (4.23) yielding the first two terms $\boldsymbol{v}^{[1]}(\boldsymbol{x})+\boldsymbol{v}^{[2]}(\boldsymbol{x})$ in the the reflection formula (4.14), that expressed in compact matrix form, according to eq. (4.49), read

$$\boldsymbol{v}^{[1]}(\boldsymbol{x})+\boldsymbol{v}^{[2]}(\boldsymbol{x})=\frac{[M]^t[G]}{8\pi\mu} \tag{4.153}$$

It is easy to verify that the row by column multiplication $[M]^t[G]$ corresponds to the sum of of products between the elements $\boldsymbol{M}_{(m)}$ and $\boldsymbol{G}_{(m)}$, i.e.,

$$[M]^t[G]=\sum_m^\infty \frac{\left(\boldsymbol{M}_{(m)}\right)^t \boldsymbol{G}_{(m)}}{m!} \tag{4.154}$$

and using the Cauchy–Schwarz inequality we have

$$|[M]^t[G]|=\left|\sum_m^\infty \frac{\left(\boldsymbol{M}_{(m)}\right)^t \boldsymbol{G}_{(m)}}{m!}\right| \leq \sum_m^\infty \frac{\left|\left(\boldsymbol{M}_{(m)}\right)^t \boldsymbol{G}_{(m)}\right|}{m!} \leq \sum_m^\infty \frac{\left\|\boldsymbol{M}_{(m)}\right\| \left\|\boldsymbol{G}_{(m)}\right\|}{m!} \tag{4.155}$$

where $\|.\|$ represents the norm of a matrix.

In order to estimate an upper bound for the rightmost term in eq. 4.155), an estimate for the norms $\left\|\boldsymbol{M}_{(m)}\right\|$ and $\left\|\boldsymbol{G}_{(m)}\right\|$ is required. According to the reflection procedure followed in Section 4.3, the moments $M_{\alpha\boldsymbol{\alpha}_m}(\boldsymbol{\xi})$ refer to a body, with characteristic length ℓ_b, immersed in an unbounded ambient flow $\boldsymbol{u}(\boldsymbol{x})$, with characteristic velocity U_c. Therefore, by dimensional analysis, the force field distribution $\boldsymbol{\psi}(\boldsymbol{x})$ and the position vector $(\boldsymbol{x}-\boldsymbol{\xi})$ can be normalized as follows

$$(\hat{\boldsymbol{x}}-\hat{\boldsymbol{\xi}})=\frac{(\boldsymbol{x}-\boldsymbol{\xi})}{\ell_b}, \quad \hat{\boldsymbol{\psi}}(\boldsymbol{x})=\frac{\boldsymbol{\psi}(\boldsymbol{x})}{\frac{\mu U_c}{\ell_b^2}} \tag{4.156}$$

By the definition, the entries of the moments can be normalized by

$$\widehat{M}_{\alpha\boldsymbol{\alpha}_m}(\boldsymbol{\xi})=\frac{M_{\alpha\boldsymbol{\alpha}_m}(\boldsymbol{\xi})}{\mu U_c \ell_b^{m+1}} \tag{4.157}$$

so that $\widehat{M}_{\alpha\boldsymbol{\alpha}_m}(\boldsymbol{\xi}) \sim O(1)$, and we can define the characteristic velocity U_c such that $|\widehat{M}_{\alpha\boldsymbol{\alpha}_m}(\boldsymbol{\xi})| \leq 1$, strictly. Therefore, if $\widehat{\boldsymbol{M}}_{(m)}$ is the $(m+1)$-dimensional vector with $\widehat{M}_{\alpha\boldsymbol{\alpha}_m}(\boldsymbol{\xi})$ as its entries, we have

$$\left\|\boldsymbol{M}_{(m)}\right\|=\left\|\hat{\boldsymbol{M}}_{(m)}\right\| \mu U_c \ell_b^{m+1} \leq 3^{\frac{m+1}{2}} \mu U_c \ell_b^{m+1} \tag{4.158}$$

On the other hand, since the leading term in the Green function derivatives eq. (4.6), is the derivative of the Stokeslet, we can normalize the entries of the m-th order derivative of the Green function evaluated at the field point by a characteristic distance ℓ_f between the body and the field point as

$$\widehat{\nabla}_{\boldsymbol{\alpha}_m} \widehat{G}_{a\alpha}(\boldsymbol{x}, \boldsymbol{\xi}) = \ell_f^{m+1} \nabla_{\boldsymbol{\alpha}_m} G_{a\alpha}(\boldsymbol{x}, \boldsymbol{\xi}) \tag{4.159}$$

with $\ell_f > \ell_b$ defined so that

$$\left\|\boldsymbol{G}_{(m)}\right\| = \frac{\left\|\widehat{\boldsymbol{G}}_{(m)}\right\|}{\ell_f^{m+1}} \leq \frac{3^{\frac{m+1}{2}}}{\ell_f^{m+1}} \tag{4.160}$$

$\widehat{\boldsymbol{G}}_{(m)}$ being the vector admitting $\widehat{\nabla}_{\boldsymbol{\alpha}_m} \widehat{G}_{a\alpha}(\boldsymbol{x}, \boldsymbol{\xi})$ as its entries.

Therefore, since $\ell_f > \ell_b$, the velocity field $\boldsymbol{v}^{[1]}(\boldsymbol{x}) + \boldsymbol{v}^{[2]}(\boldsymbol{x})$ is bounded by

$$\left|\boldsymbol{v}^{[1]}(\boldsymbol{x}) + \boldsymbol{v}^{[2]}(\boldsymbol{x})\right| = \frac{\left|[M]^t [G]\right|}{8\pi\mu} \leq \frac{U_c}{8\pi} \sum_m^\infty \frac{3^{m+1}}{m!} \left(\frac{\ell_b^{m+1}}{\ell_f^{m+1}}\right) = \frac{U_c}{8\pi} \left(3 \frac{\ell_b}{\ell_f}\right) e^{\left(\frac{3\ell_b}{\ell_f}\right)} \tag{4.161}$$

Next, consider the velocity field $\boldsymbol{v}^{[3]}(\boldsymbol{x}) + \boldsymbol{v}^{[4]}(\boldsymbol{x})$, given in matrix form by eq. (4.49)

$$\boldsymbol{v}^{[3]}(\boldsymbol{x}) + \boldsymbol{v}^{[4]}(\boldsymbol{x}) = \frac{[M]^t [N][G]}{8\pi\mu} \tag{4.162}$$

for which, analogously to the inequalities eq. (4.155), we have

$$\begin{aligned} \left|[M']^t [N][G]\right| &= \left|\sum_m^\infty \sum_n^\infty \frac{\left(\boldsymbol{M}_{(m)}\right)^t \boldsymbol{N}_{(m,n)} \boldsymbol{G}_{(n)}}{m!n!}\right| \leq \sum_m^\infty \sum_n^\infty \frac{\left|\left(\boldsymbol{M}_{(m)}\right)^t \boldsymbol{N}_{(m,n)} \boldsymbol{G}_{(n)}\right|}{m!n!} \\ &\leq \sum_m^\infty \sum_n^\infty \frac{\left\|\boldsymbol{M}_{(m)}\right\| \left\|\boldsymbol{N}_{(m,n)}\right\| \left\|\boldsymbol{G}_{(n)}\right\|}{m!n!} \end{aligned} \tag{4.163}$$

By the definition eq. (4.27), the entries of the matrices $\boldsymbol{N}_{(m,n)}$ are n-th order moments evaluated for a body immersed in an ambient flow corresponding to the regular part of the m-th derivative of the Green function. Since the regular part of the Green function is a disturbance field for the Stokeslet with pole in the body generated by the walls of the confinement, its characteristic magnitude can be considered as that of a Stokeslet with pole at distance $2\ell_d$, ℓ_d being the characteristic distance between the body and the nearest walls from the body. Thus, the characteristic magnitude of its m-th order derivatives can be estimated as $W_c^{(m)} = 1/(2\ell_d)^{m+1}$, hence, by the same arguments used for $M_{\alpha\boldsymbol{\alpha}_m}$, we have

$$\widehat{N}_{\alpha\boldsymbol{\alpha}_m\beta\boldsymbol{\beta}_n}(\boldsymbol{\xi}) = \frac{N_{\alpha\boldsymbol{\alpha}_m\beta\boldsymbol{\beta}_n}(\boldsymbol{\xi})}{\mu W_c^{(m)} \ell_b^{n+1}} = \frac{N_{\alpha\boldsymbol{\alpha}_m\beta\boldsymbol{\beta}_n}(\boldsymbol{\xi})}{\dfrac{\mu \ell_b^{n+1}}{(2\ell_d)^{m+1}}} \tag{4.164}$$

Therefore, given that $\left\|\widehat{\boldsymbol{N}}_{(m,n)}\right\| \sim O(1)$ is the norm of the matrix with normalized entries $\widehat{N}_{\alpha\boldsymbol{\alpha}_m\beta\boldsymbol{\beta}_n}(\boldsymbol{\xi})$, there exists a constant $C_{m,n}^{(1)} \sim O(1)$, such that $|\left\|\widehat{\boldsymbol{N}}_{(m,n)}\right\|| \leq$

$C^{(1)}_{m,n}$, and

$$\left\|\boldsymbol{N}_{(m,n)}\right\| = \left\|\widehat{\boldsymbol{N}}_{(m,n)}\right\| \frac{(\ell_b)^{n+1}}{(2\ell_d)^{m+1}} \leq C^{(1)}_{m,n}\, 3^{\frac{m+n+2}{2}} \frac{(\ell_b)^{n+1}}{(2\ell_d)^{m+1}} \tag{4.165}$$

By considering the inequalities eqs. (4.158), (4.160) and (4.165), the velocity field $\boldsymbol{v}^{[3]}(\boldsymbol{x}) + \boldsymbol{v}^{[4]}(\boldsymbol{x})$ is bounded by

$$\begin{aligned}
\left|\boldsymbol{v}^{[3]}(\boldsymbol{x}) + \boldsymbol{v}^{[4]}(\boldsymbol{x})\right| &= \frac{\left|[M]^t[N][G]\right|}{8\pi\mu} \\
&\leq C^{(1)}_{m,n} \frac{U_c}{8\pi}\left(\frac{3\ell_b}{\ell_f}\right)\left(\frac{3\ell_b}{2\ell_d}\right)\sum_m^\infty\sum_n^\infty \frac{1}{m!n!}\left(\frac{3\ell_b}{\ell_f}\right)^m\left(\frac{3\ell_b}{2\ell_d}\right)^n \\
&= C^{(1)} \frac{U_c}{8\pi}\left(\frac{3\ell_b}{\ell_f}\right) e^{\frac{3\ell_b}{\ell_f}} \left(\frac{3\ell_b}{2\ell_d}\right) e^{\frac{3\ell_b}{2\ell_d}}
\end{aligned} \tag{4.166}$$

where $C^{(1)} = \sup_{m,n} C^{(1)}_{m,n} \sim O(1)$. Iterating the same procedure for all $k = 0, 1, 2, 3...$, we have

$$\begin{aligned}
\left|\boldsymbol{v}^{[2k+1]}(\boldsymbol{x}) + \boldsymbol{v}^{[2k+2]}(\boldsymbol{x})\right| &= \frac{\left|[M]^t[N]^k[G]\right|}{8\pi\mu} \\
&\leq C^{(k)} \frac{U_c}{8\pi}\left(\frac{3\ell_b}{\ell_f}\right) e^{\frac{3\ell_b}{\ell_f}} \left[\left(\frac{3\ell_b}{2\ell_d}\right) e^{\frac{3\ell_b}{2\ell_d}}\right]^k
\end{aligned} \tag{4.167}$$

with $C^{(k)} \sim O(1)$, and because of it, there exists a constant $C > 0$, such that $C^{(k)} < C$ for any k. Therefore, for $k \to \infty$, the contribution given by $\boldsymbol{v}^{[2k+1]}(\boldsymbol{x}) + \boldsymbol{v}^{[2k+2]}(\boldsymbol{x})$ to the total velocity field in eq. (4.49) vanishes only if

$$\left(\frac{3\ell_b}{2\ell_d}\right) e^{\frac{3\ell_b}{2\ell_d}} \leq 1 \tag{4.168}$$

i.e. for

$$\ell_d \gtrsim 2.65\,\ell_b \tag{4.169}$$

Therefore, if $\ell_d = \ell_b + \delta$, where δ is characteristic length of the gap between the surface of the particle and the walls of the confinement, the convergence of the method is ensured for

$$\delta \gtrsim 1.65\,\ell_b \tag{4.170}$$

The convergence analysis developed above establishes a sufficient condition $\ell_d \gg \ell_b$, regardless the geometry of the system, for the convergence of the reflection method developed in Section 4.3. However, the convergence is not excluded even for smaller distances and eq. (4.169) suggests that it holds for $\ell_d \sim \ell_b$. Extending this argument we can state that there exist a constant $\Gamma > 0$, depending on the geometry of the system and in principle smaller then the value 2.65 eq. (4.169), such that, for

$$\ell_d > \Gamma\,\ell_b \tag{4.171}$$

the reflection method developed in Section (4.3) converges and the velocity field can be represented in terms of the Faxén operator of the body and the Green function of the confinement by eq. (4.54).

4.B Derivation of extended Swan and Brady's approximations for rotating sphere

In this appendix, the approximate eqs. (4.132) and (4.133) for force and torque acting on a sphere rotating with angular velocity $\boldsymbol{\omega}$ in a bounded fluid are derived.

By considering in eq. (4.21) a purely rotational field

$$u_a(\boldsymbol{x}) = -\varepsilon_{abc}\,\omega_b(\boldsymbol{x}-\boldsymbol{\xi}')_c$$

we obtain the second order reflected field

$$v^{[2]}_{\alpha}(\boldsymbol{\xi}) = \omega_\beta \mathcal{T}_{\alpha'\beta} W_{\alpha\alpha'}(\boldsymbol{\xi},\boldsymbol{\xi}')\Big|_{\boldsymbol{\xi}'=\boldsymbol{\xi}} \tag{4.172}$$

exerting a force and a torque on the spherical body

$$\boldsymbol{F}^{[3]} = -\boldsymbol{\omega}\,\boldsymbol{Y}^t \tag{4.173}$$

and

$$\boldsymbol{T}^{[3]} = -\boldsymbol{\omega}\,\boldsymbol{Z} \tag{4.174}$$

Since, for the symmetries of the sphere, $m_{\alpha\beta\beta_1}(\boldsymbol{\xi},\boldsymbol{\xi})$ vanishes in the 1-st order Faxén operator

$$v^{[2]}_{\alpha}(\boldsymbol{\xi}) = U_c O\left(\frac{\ell_b}{\ell_d}\right)^2, \qquad \nabla_{\boldsymbol{\beta}_n} v^{[2]}_{\beta}(\boldsymbol{\xi}) = U_c O\left(\frac{\ell_b^2}{\ell_d^{2+n}}\right) \tag{4.175}$$

Also the leading neglected term in eq. (4.108) is smaller

$$v^{[4]}_{\alpha}(\boldsymbol{\xi}) = v^{[2]}_{\beta}(\boldsymbol{\xi})\mathcal{F}_{\alpha'\beta} W_{\alpha\alpha'}(\boldsymbol{\xi},\boldsymbol{\xi}')\Big|_{\boldsymbol{\xi}'=\boldsymbol{\xi}} + O\left(\frac{\ell_b}{\ell_d}\right)^5 \tag{4.176}$$

therefore

$$\boldsymbol{F}^{[5]} = \boldsymbol{v}^{[2]}\,\boldsymbol{X} + O\left(\frac{\ell_b}{\ell_d}\right)^5 \tag{4.177}$$

and

$$\boldsymbol{T}^{[5]} = \boldsymbol{v}^{[2]}\,\boldsymbol{Y} + O\left(\frac{\ell_b}{\ell_d}\right)^5 \tag{4.178}$$

By approximating the second velocity field as constant

$$\boldsymbol{v}^{[2]} = \boldsymbol{F}^{[3]}\boldsymbol{R}^{-1} + O\left(\frac{\ell_b}{\ell_d}\right)^4 \tag{4.179}$$

thus

$$\boldsymbol{F}^{[5]} = \boldsymbol{F}^{[3]}\boldsymbol{R}^{-1}\,\boldsymbol{X} + O\left(\frac{\ell_b}{\ell_d}\right)^5 \tag{4.180}$$

and

$$\boldsymbol{T}^{[5]} = \boldsymbol{F}^{[3]}\boldsymbol{R}^{-1}\,\boldsymbol{Y} + O\left(\frac{\ell_b}{\ell_d}\right)^5 \tag{4.181}$$

while higher order reflected fields

$$\boldsymbol{F}^{[2k+3]} = \boldsymbol{F}^{[2k+1]}\boldsymbol{R}^{-1}\,\boldsymbol{X} + o\left(\frac{\ell_b}{\ell_d}\right)^5 \tag{4.182}$$

and

$$\boldsymbol{T}^{[2k+3]} = \boldsymbol{F}^{[2k+1]}\boldsymbol{R}^{-1}\boldsymbol{Y} + o\left(\frac{\ell_b}{\ell_d}\right)^5 \tag{4.183}$$

Summing all the reflected forces

$$\boldsymbol{F} = \boldsymbol{F}^{[3]}(I - \boldsymbol{R}^{-1}\boldsymbol{X})^{-1} + O\left(\frac{\ell_b}{\ell_d}\right)^5 \tag{4.184}$$

and torques

$$\boldsymbol{T} = \boldsymbol{T}^{[\infty]} + \boldsymbol{T}^{[3]} + \boldsymbol{F}^{[3]}\boldsymbol{R}^{-1}\boldsymbol{Y}(1 - \boldsymbol{R}^{-1}\boldsymbol{X})^{-1} + O\left(\frac{\ell_b}{\ell_d}\right)^5 \tag{4.185}$$

substituting eq. (4.173),(4.174) and $\boldsymbol{T}^{[\infty]} = -\boldsymbol{\omega}\,\boldsymbol{\Omega}$ we obtain the relations eqs. (4.132) and (4.133)

$$\boldsymbol{F} = \boldsymbol{\omega}\boldsymbol{Y}^t(I - \boldsymbol{R}^{-1}\boldsymbol{X})^{-1} + O\left(\frac{\ell_b}{\ell_d}\right)^5 \tag{4.186}$$

and torques

$$\boldsymbol{T} = -\boldsymbol{\omega}(\boldsymbol{\Omega} + \boldsymbol{Z} + \boldsymbol{Y}^t\boldsymbol{R}^{-1}\boldsymbol{Y}(1 - \boldsymbol{R}^{-1}\boldsymbol{X})^{-1}) + O\left(\frac{\ell_b}{\ell_d}\right)^5 \tag{4.187}$$

Chapter 5

Particle transport in confined geometries

5.1 Introduction

The main legacy of the Einsteinian theory of Brownian motion to modern physics lies in the confirmation of the atomistic nature of matter and in the equivalence between random molecular motion at the microscopic level and the macroscopic phenomenon of diffusion [67, 38].

Thanks also to the contributions by Langevin, Smoluchowski and many others [141, 224, 37], it is now common knowledge in applied transport theory [236] that any transport equation, expressed in the form of an advection-diffusion equation for the concentration field $c(\boldsymbol{x}, t)$ of some solute diffusing in a fluid phase,

$$\frac{\partial c(\boldsymbol{x}, t)}{\partial t} = -\nabla \cdot \left[\boldsymbol{u}^{(p)}(\boldsymbol{x})\, c(\boldsymbol{x}, t)\right] + D\, \nabla^2 c(\boldsymbol{x}, t) \tag{5.1}$$

where $\boldsymbol{u}^{(p)}(\boldsymbol{x})$ is the macroscopic velocity field experienced by the solute (coinciding in most of the applications with the fluid phase velocity $\boldsymbol{u}(\boldsymbol{x})$), and D its isotropic diffusivity, can be represented in terms of the microscopic motion of the solute particles by means of a Langevin equation of the form

$$d\boldsymbol{x}(t) = \boldsymbol{u}^{(p)}(\boldsymbol{x}(t))\, dt + \sqrt{2\, D}\, d\boldsymbol{w}(t) \tag{5.2}$$

where $d\boldsymbol{w}(t) = (dw_1(t), dw_2(t), dw_3(t))$ is the increment of a three-dimensional Wiener process in the time interval $(t, t + dt)$. This equivalence is also computationally important as it enables to solve parabolic transport equations in complex geometries by means of stochastic simulations of the Langevin equation (5.2) [91, 35, 158, 29].

The description of physical processes in terms of stochastic Langevin equations, both in equilibrium and in out-of equilibrium conditions, has become one of the strongest and more fruitful research lines in modern statistical physics, providing useful insights in all the fields of physical investigation, including quantum and particle physics [131, 42, 251].

The Langevin equation (5.2), expressed exclusively with respect to the particle position $\boldsymbol{x}(t)$, can be derived from a stochastic dynamics (stochastic Newton equation) of the form

$$\begin{aligned} \frac{d\boldsymbol{x}}{dt} &= \boldsymbol{v} \\ m\,\frac{d\boldsymbol{v}}{dt} &= -\eta\,\left[\boldsymbol{v}-\boldsymbol{u}^{(p)}(\boldsymbol{x})\right]+\boldsymbol{F}_{\text{stocha}}(t) \end{aligned} \tag{5.3}$$

where $\boldsymbol{F}_{\text{stocha}}(t)\,dt=\alpha\,d\boldsymbol{w}(t)$, $\alpha=\sqrt{2\,k_b\,T\,\eta}$, m is the particle mass, η the friction factor, T the absolute temperature and k_B the Boltzmann constant, in the limit for $m/\eta \ll 1$, i.e., in the case particle inertia could be neglected. This simplification is not only important in transport theory, but also in the thermodynamics of fluctuations as it implies the simplest form of fluctuation-dissipation relation [133, 134],

$$D\,\eta = \,k_B\,T \tag{5.4}$$

that, in the case of spherical particles for which $\eta=6\,\pi\,\mu\,R_p$ is referred to as the Stokes-Einstein relation. Equation (5.4) connects a transport parameter, related to the intensity of fluctuations (the diffusivity D) to a hydrodynamic quantity, related to dissipation (the friction factor η) at constant temperature T.

For timescales much larger than the dissipation time $t_{\text{diss}}=m/\eta$, the instantaneous Stokes equations (1.1), here expressed by

$$\begin{cases}\mu\nabla^2\boldsymbol{u}(\boldsymbol{x})-\nabla p(\boldsymbol{x})=-\nabla\cdot\boldsymbol{\tau}(\boldsymbol{x})=0\\ \nabla\cdot\boldsymbol{u}(\boldsymbol{x})=0\end{cases} \tag{5.5}$$

where $(\boldsymbol{u},p,\boldsymbol{\tau})$ are the velocity, the pressure and the stress tensor of the fluid respectively, provides a good approximation for modeling fluid-particle interactions, and the no-slip boundary conditions at the particle surface (S_p)

$$\boldsymbol{u}(\boldsymbol{x})=\boldsymbol{v}+(\boldsymbol{x}-\boldsymbol{x}_0)\times\boldsymbol{\omega} \qquad \boldsymbol{x}\in S_p \tag{5.6}$$

where $(\boldsymbol{v},\boldsymbol{\omega})$ is the velocity and the angular velocity of the particle, and $\boldsymbol{x}_0$ a reference point, say the center of mass of the particle, describe with sufficient accuracy fluid-particle interactions.

Therefore, the hydrodynamic resistance law in the more general position-dependent and tensorial character is

$$\begin{pmatrix}\boldsymbol{F}\\ \boldsymbol{T}\end{pmatrix}=-\boldsymbol{H}(\boldsymbol{x})\begin{pmatrix}\boldsymbol{v}\\ \boldsymbol{\omega}\end{pmatrix} \tag{5.7}$$

where $\boldsymbol{H}(\boldsymbol{x})$ is the 6×6 overall resistance matrix of the hydrodynamic interactions, possessing a block structure

$$\boldsymbol{H}=\begin{pmatrix}\boldsymbol{\eta}(\boldsymbol{x}) & \boldsymbol{C}^{(1)}(\boldsymbol{x})\\ \boldsymbol{C}^{(2)}(\boldsymbol{x}) & \boldsymbol{\eta}^{\omega}(\boldsymbol{x})\end{pmatrix} \tag{5.8}$$

where (i) $\boldsymbol{\eta}$, and $\boldsymbol{\eta}^{\omega}$ are the translational and rotational friction matrices, respectively, (ii) $\boldsymbol{C}^{(1)}$, and $\boldsymbol{C}^{(2)}$ are the roto-translational coupling matrices. As seen in Chapter 3, by the Lorentz's reciprocal theorem it is possible to prove (see also [98]) that $\boldsymbol{\eta}$ and $\boldsymbol{\eta}^{\omega}$ are symmetric matrices, while $\boldsymbol{C}^{(1)}$ and $\boldsymbol{C}^{(2)}$ satisfy the property $\boldsymbol{C}^{(2)}=\left[\boldsymbol{C}^{(1)}\right]^t$.

Correspondingly, the overall resistance matrix $\boldsymbol{H}(\boldsymbol{x})$ is symmetric and positive definite.

This automatically implies, due to the fluctuation-dissipation relation (5.4), a tensorial and position-dependent diffusivity. The latter two properties have deep and non trivial implications whenever a stochastic equation of motion, in the form of eq. (5.3) is considered, due to the highly singular nature of the Wiener description of the thermal/hydrodynamic fluctuations. For the sake of completeness, it should be also mentioned that a position dependent effective diffusivity arises in modeling solute transport in microchannels with undulated walls, in the case the transport problem is referred exclusively to the channel axial coordinate [32, 15]. This is referred to as the Fick-Jacobs approximation and it is essentially a geometrical effect within an approximate transport model unrelated to any hydrodynamic interactions.

The scope of this chapter is to analyze in detail the problems and the peculiarities of particle transport in microfluidic systems, originated by the confined nature of the flow, starting from the stochastic description of the microscopic particle motion, in a way that may also be useful for researchers in microfluidics that are not fully familiar with stochastic differential equations. While stochastic modeling of particle transport involving constant effective diffusivities is widely used in the analysis of microfluidic devices, the inclusion of hydrodynamic effects, deriving from fluid confinement, represents a completely new and unexplored field of theoretical and numerical investigation. This chapter attempts to fill this gap, providing a methodological bridge between hydrodynamic theory and the stochastic formulation of transport phenomena in confined geometries, addressing also in a clear and critical way the complexities and the difficulties of this approach. The chapter addresses also novel original derivations as regards specific topics, such as the use of the overdamped approximation in non-equilibrium conditions and the effect of slippage as regards transport phenomena involving surface effects (such as surface chemical reactions).

In order to illustrate the physical concepts and the resulting analytical approaches, the hydrodynamics of a spherical particle near an infinite planar solid surface is explicitly considered, as a prototypical and paradigmatic case study of the hydrodynamic problems occurring in microfluidic channels. Throughout this chapter, rigid particles and Newtonian fluids are considered.

The chapter is organized as follows. Section 5.2 addresses the formulation of fluctuation dissipation relations in confined systems, and the computational problems associated with it. Section 5.3 analyzes the reduction of the equation of motion in the form of a Langevin equation (5.3), discussing also the case of non-equilibrium thermal conditions (thermophoresis). Section 5.4 discusses the problems arising from the non-integrable singularity of the friction factor near a solid no-slip wall, as regards diffusional problems in the presence of superficial phenomena (surface chemical reactions). A way for overcoming these problems lies in relaxing the no-slip assumption, as discussed in Section 5.5, where it is shown the necessity of considering slippage effects both at the particle external surface and at the walls of the fluid domain. Finally, Section 5.6 discusses in a succinct way the role of the fluid inertial effects in the formulation of the stochastic equations for particle motion.

5.2 Fluctuation-dissipation relations in confined geometries

Consider the motion of a rigid spherical particle, of mass m and momentum of inertia I, in a microfluidic device. Let $\boldsymbol{v}$ and $\boldsymbol{\omega}$ be its velocity and angular velocity, respectively. Assume that the particle is dispersed in a fluid flow, characterized by the fluid velocity $\boldsymbol{u}(\boldsymbol{x})$ and that the particle is also subjected to the action of an external potential field $\Phi(\boldsymbol{x})$. The particle equations of motion read

$$\begin{aligned} m\, d\boldsymbol{v} &= (\boldsymbol{F}_{\text{flow}} + \boldsymbol{F}_{\text{hydro}})\, dt - \nabla\Phi\, dt + \boldsymbol{F}_{\text{stocha}}\, dt \\ I\, d\boldsymbol{\omega} &= (\boldsymbol{T}_{\text{flow}} + \boldsymbol{T}_{\text{hydro}})\, dt + \boldsymbol{T}_{\text{stocha}}\, dt \end{aligned} \tag{5.9}$$

where $\boldsymbol{F}_{\text{flow}}$ and $\boldsymbol{T}_{\text{flow}}$ are the force and the torque deriving from the action of the external flow field $\boldsymbol{u}(\boldsymbol{x})$ (assuming that the particle velocity and angular velocity are vanishing), $\boldsymbol{F}_{\text{hydro}}$ and $\boldsymbol{T}_{\text{hydro}}$ are the force and the torque due to the hydrodynamic interactions (described by means of eq. (5.7) in the case the external flow velocity is vanishing and the particle possesses a velocity $\boldsymbol{v}$ and an angular velocity $\boldsymbol{\omega}$), and $\boldsymbol{F}_{\text{stocha}}$, $\boldsymbol{T}_{\text{stocha}}$ represent the the stochastic force and the torque deriving from to thermal fluctuations. This decomposition is made possible because the hydrodynamic equations for the fluid are assumed to be linear. The basic problem in the statistical physics of microparticle motion resides in the determination of the contributions of the thermal perturbations $\boldsymbol{F}_{\text{stocha}}$ and $\boldsymbol{T}_{\text{stocha}}$, since all the other terms in eq. (5.9) stem from a classical hydrodynamic analysis.

Following the original approach due to Einstein and Langevin [134], in the case the fluid is described by means of an instantaneous response (Stoke's regime), it is natural to represent $\boldsymbol{F}_{\text{stocha}}$ and $\boldsymbol{T}_{\text{stocha}}$ in the form of a linear superposition of vector-valued Wiener processes, i.e. as

$$\begin{aligned} \boldsymbol{F}_{\text{stocha}}(\boldsymbol{x}) dt &= \boldsymbol{\alpha}(\boldsymbol{x})\, d\boldsymbol{w}(t) + \boldsymbol{\gamma}(\boldsymbol{x})\, d\boldsymbol{w}^{\omega}(t) \\ \boldsymbol{T}_{\text{stocha}}(\boldsymbol{x}) dt &= \boldsymbol{\varepsilon}(\boldsymbol{x})\, d\boldsymbol{w}(t) + \boldsymbol{\beta}(\boldsymbol{x})\, d\boldsymbol{w}^{\omega}(t) \end{aligned} \tag{5.10}$$

where $d\boldsymbol{w}(t) = (dw_1(t),\, d_2(t),\, dw_3(t))$ and $d\boldsymbol{w}^{\omega}(t) = (dw_1^{\omega}(t),\, dw_2^{\omega}(t),\, dw_3^{\omega}(t))$ are the increments in the time interval $(t, t+dt)$ of two mutually independent vector-valued Wiener processes. This observation is a consequence of the fact that Wiener processes are also memoryless, in the meaning that if one defines $\boldsymbol{\xi}(t) = d\boldsymbol{w}(t)/dt = (\xi_1(t), \xi_2(t), \xi_3(t))$, interpreted in a distributional meaning, than the correlation function $\langle \xi_i(t_0, +t)\, \xi_j(t_0)\rangle = \delta(t)\, \delta_{i,j}$ is impulsive (here $\langle\cdot\rangle$ indicates indifferently either ensemble or temporal averages, and $t_0 > 0$ is any time instant) [77].

Henceforth, in order to simplify the notation, the explicit dependence of the matrices $\boldsymbol{\alpha}$, $\boldsymbol{\gamma}$, $\boldsymbol{\varepsilon}$, $\boldsymbol{\beta}$ on the position $\boldsymbol{x}$ will be omitted. While the determination of $\boldsymbol{F}_{\text{flow}}$, $\boldsymbol{F}_{\text{hydro}}$ and $\boldsymbol{T}_{\text{flow}}$, $\boldsymbol{T}_{\text{hydro}}$ follows for the simple application of the Stokesian hydrodynamics, the estimate of the matrices entering eq. (5.10) and defining the thermal perturbations requires a statistical physical ansatz that, at constant temperature T, the thermal fluctuations described by eq. (5.10) would provide the known result of equilibrium statistical physics [133]. This is the essence of the fluctuation-dissipation ansatz, and for this reason, owing to linearity, it is sufficient to consider the statistical properties for the particle dynamics in the absence of external forcings, i.e. for $\boldsymbol{F}_{\mathrm{flow}} = \nabla\Phi = 0$, $\boldsymbol{T}_{\mathrm{flow}} = 0$. Under these conditions, by substituting eqs. (5.7)-(5.8) and (5.10) into the equations of motion (5.9) one obtains,

$$\begin{aligned} d\boldsymbol{v}(t) &= -\frac{\boldsymbol{\eta}}{m}\boldsymbol{v}(t)\,dt - \frac{\boldsymbol{C}^{(1)}}{m}\boldsymbol{\omega}(t)\,dt + \frac{\boldsymbol{\alpha}}{m}\,d\boldsymbol{w}(t) + \frac{\boldsymbol{\gamma}}{m}\,d\boldsymbol{w}^{\omega}(t) \\ d\boldsymbol{\omega}(t) &= -\frac{\boldsymbol{C}^{(2)}}{I}\boldsymbol{v}(t)\,dt - \frac{\boldsymbol{\eta}^{\omega}}{I}\boldsymbol{\omega}(t)\,dt + \frac{\boldsymbol{\varepsilon}}{I}\,d\boldsymbol{w}(t) + \frac{\boldsymbol{\beta}}{I}\,d\boldsymbol{w}^{\omega}(t) \end{aligned} \tag{5.11}$$

where also for $\boldsymbol{\eta}$, $\boldsymbol{C}^{(1)}$, $\boldsymbol{C}^{(2)}$, $\boldsymbol{\eta}^{\omega}$ the explicit dependence on the position has been omitted.

The matrices $\boldsymbol{\alpha}$, $\boldsymbol{\beta}$, $\boldsymbol{\gamma}$, $\boldsymbol{\varepsilon}$ are the stochastic amplitude matrices, and the final goal of fluctuation-dissipation analysis is their determination from physical principles enforcing equilibrium properties. Let $\boldsymbol{\Delta}$ be the overall 6×6 stochastic amplitude matrix entering eq. (5.11),

$$\boldsymbol{\Delta} = \begin{pmatrix} \frac{\boldsymbol{\alpha}}{m} & \frac{\boldsymbol{\gamma}}{m} \\ \frac{\boldsymbol{\varepsilon}}{I} & \frac{\boldsymbol{\beta}}{I} \end{pmatrix} \tag{5.12}$$

and define the 6×6 matrix $\boldsymbol{\sigma}$, the entries of which are $\sigma_{i,j}$ as

$$\sigma_{i,j} = \frac{1}{2}\sum_{h=1}^{6}\Delta_{i,h}\,\Delta_{j,h} \tag{5.13}$$

In matrix form,

$$\boldsymbol{\sigma} = \frac{1}{2}\boldsymbol{\Delta}\,\boldsymbol{\Delta}^T = \begin{pmatrix} \frac{\boldsymbol{\alpha}\,\boldsymbol{\alpha}^T + \boldsymbol{\gamma}\,\boldsymbol{\gamma}^T}{2\,m^2} & \frac{\boldsymbol{\alpha}\,\boldsymbol{\varepsilon}^T + \boldsymbol{\gamma}\,\boldsymbol{\beta}^T}{2\,m\,I} \\ \frac{\boldsymbol{\varepsilon}\,\boldsymbol{\alpha}^T + \boldsymbol{\beta}\,\boldsymbol{\gamma}^T}{2\,m\,I} & \frac{\boldsymbol{\beta}\,\boldsymbol{\beta}^T + \boldsymbol{\varepsilon}\,\boldsymbol{\varepsilon}^T}{2\,I^2} \end{pmatrix} = \begin{pmatrix} \frac{\boldsymbol{a}}{2\,m^2} & \frac{\boldsymbol{c}}{2\,m\,I} \\ \frac{\boldsymbol{d}}{2\,m\,I} & \frac{\boldsymbol{b}}{2\,I^2} \end{pmatrix} \tag{5.14}$$

which is, by definition, symmetric. Expressing eq. (5.11) componentwise

$$\begin{aligned} dv_i &= -\left(\frac{1}{m}\sum_{j=1}^{3}\eta_{i,j}\,v_j + \frac{1}{m}\sum_{j=1}^{3}C^{(1)}_{i,j}\,\omega_j\right) + \frac{1}{m}\sum_{j=1}^{3}\alpha_{i,j}\,dw_j + \frac{1}{m}\sum_{j=1}^{3}\gamma_{i,j}\,dw^{\omega}_j \\ d\omega_i &= -\left(\frac{1}{I}\sum_{j=1}^{3}C^{(2)}_{i,j}\,v_j + \frac{1}{I}\sum_{j=1}^{3}\eta^{\omega}_{i,j}\,\omega_j\right) + \frac{1}{I}\sum_{j=1}^{3}\varepsilon_{i,j}\,dw_j + \frac{1}{m}\sum_{j=1}^{3}\beta_{i,j}\,dw^{\omega}_j \end{aligned} \tag{5.15}$$

so that the associated Fokker-Planck equation for the probability density function $p(\boldsymbol{v},\boldsymbol{\omega},t)$ attains the form [77]

$$\begin{aligned} \frac{\partial p}{\partial t} &= \sum_{i=1}^{3}\frac{\partial}{\partial v_i}\left[\left(\frac{1}{m}\sum_{j=1}^{3}\eta_{i,j}\,v_j + \frac{1}{m}\sum_{j=1}^{3}C^{(1)}_{i,j}\,\omega_j\right)\,p\right] \\ &+ \sum_{i=1}^{3}\frac{\partial}{\partial \omega_i}\left[\left(\frac{1}{I}\sum_{j=1}^{3}C^{(2)}_{i,j}\,v_j + \frac{1}{I}\sum_{j=1}^{3}\eta^{\omega}_{i,j}\,\omega_j\right)\,p\right] \\ &+ \sum_{i,j=1}^{3}\frac{\partial^2}{\partial v_i\partial v_j}\left(\frac{a_{i,j}\,p}{2\,m^2}\right) + \sum_{i,j=1}^{3}\frac{\partial^2}{\partial v_i\partial \omega_j}\left(\frac{c_{i,j}\,p}{2\,m\,I}\right) \\ &+ \sum_{i,j=1}^{3}\frac{\partial^2}{\partial \omega_i\partial v_j}\left(\frac{d_{i,j}\,p}{2\,m\,I}\right) + \sum_{i,j=1}^{3}\frac{\partial^2}{\partial \omega_i\partial \omega_j}\left(\frac{b_{i,j}\,p}{2\,I^2}\right) \end{aligned} \tag{5.16}$$

The statistical equilibrium properties can be ascertained from the analysis of the lower-order (first and second) moments of $p(\boldsymbol{v},\boldsymbol{\omega},t)$. The first-order moments relax to zero in the long-term regime, as a consequence of the fact that the hydrodynamic interaction matrix $\boldsymbol{H}$ is positive definite. It is therefore sufficient to consider the second-order moments for the translational/angular velocities,

$$\begin{aligned} M_{i,j}^{v,v}(t) &= \int_{\mathbb{R}^3} d\boldsymbol{\omega} \int_{\mathbb{R}^3} v_i\, v_j\, p(\boldsymbol{v},\boldsymbol{\omega},t)\, d\boldsymbol{v} \\ M_{i,j}^{v,\omega}(t) &= \int_{\mathbb{R}^3} \omega_j d\boldsymbol{\omega} \int_{\mathbb{R}^3} v_i\, p(\boldsymbol{v},\boldsymbol{\omega},t)\, d\boldsymbol{v} \\ M_{i,j}^{\omega,\omega}(t) &= \int_{\mathbb{R}^3} d\boldsymbol{v} \int_{\mathbb{R}^3} \omega_i\, \omega_j\, p(\boldsymbol{v},\boldsymbol{\omega},t)\, d\boldsymbol{\omega} \end{aligned} \tag{5.17}$$

To begin with, consider $\boldsymbol{M}^{v,v}$. From the Fokker-Planck equation (5.16) one obtains

$$\begin{aligned} \frac{dM_{h,k}^{v,v}}{dt} &= -\frac{1}{m}\sum_{j=1}^{3}\eta_{h,j}M_{j,k}^{v,v} - \frac{1}{m}\sum_{j=1}^{3}\eta_{k,j}M_{j,h}^{v,v} - \frac{1}{m}\sum_{j=1}^{3}C_{h,j}^{(1)}M_{k,j}^{v,\omega} - \frac{1}{m}\sum_{j=1}^{3}C_{k,j}^{(1)}M_{h,j}^{v,\omega} \\ &+ \frac{a_{h,k}+a_{k,h}}{2\,m^2} \end{aligned} \tag{5.18}$$

In the long-term limit (equilibrium), it follows from eq. (5.18) that

$$[\boldsymbol{\eta}\,\boldsymbol{M}^{v,v} + \boldsymbol{M}^{v,v}\,\boldsymbol{\eta}] + \left[\boldsymbol{C}^{(1)}\,(\boldsymbol{M}^{v,\omega})^T + \boldsymbol{M}^{v,\omega}\left(\boldsymbol{C}^{(1)}\right)^T\right] = \frac{1}{2\,m}\left(\boldsymbol{a}+\boldsymbol{a}^T\right) \tag{5.19}$$

Next, consider $\boldsymbol{M}^{\omega,\omega}$, the entries of which satisfy the equations

$$\begin{aligned} \frac{dM_{h,k}^{\omega,\omega}}{dt} &= -\frac{1}{I}\sum_{j=1}^{3}C_{h,j}^{(2)}M_{j,k}^{v,\omega} - \frac{1}{I}\sum_{j=1}^{3}C_{k,j}^{(2)}M_{j,h}^{v,\omega} - \frac{1}{I}\sum_{j=1}^{3}\eta_{h,j}^{\omega}M_{j,k}^{\omega,\omega} - \frac{1}{I}\sum_{j=1}^{3}\eta_{k,j}^{\omega}M_{j,h}^{\omega,\omega} \\ &+ \frac{b_{h,k}+b_{k,h}}{2\,I^2} \end{aligned} \tag{5.20}$$

so that the value attained at equilibrium is

$$[\boldsymbol{\eta}^{\omega}\,\boldsymbol{M}^{\omega,\omega} + \boldsymbol{M}^{\omega,\omega}\,\boldsymbol{\eta}^{\omega}] + \left[\boldsymbol{C}^{(2)}\boldsymbol{M}^{v,\omega} + (\boldsymbol{M}^{v,\omega})^T\left(\boldsymbol{C}^{(2)}\right)^T\right] = \frac{1}{2\,I}\left(\boldsymbol{b}+\boldsymbol{b}^T\right) \tag{5.21}$$

Finally, consider the mixed second-order roto-translational moments

$$\begin{aligned} \frac{dM_{h,k}^{v,\omega}}{dt} &= -\frac{1}{m}\sum_{j=1}^{3}\eta_{h,j}M_{j,k}^{v,\omega} - \frac{1}{m}C_{h,j}^{(1)}M_{j,k}^{\omega,\omega} - \frac{1}{I}\sum_{j=1}^{3}\eta_{k,j}^{\omega}M_{h,j}^{v,\omega} - \frac{1}{I}\sum_{j=1}^{3}C_{k,j}^{(2)}M_{j,h}^{v,v} \\ &+ \frac{c_{h,k}+d_{k,h}}{2\,m\,I} \end{aligned} \tag{5.22}$$

admitting the equilibrium condition

$$\frac{1}{m}\left[\boldsymbol{\eta}\boldsymbol{M}^{v,\omega} + \boldsymbol{C}^{(1)}\boldsymbol{M}^{\omega,\omega}\right] + \frac{1}{I}\left[\boldsymbol{M}^{v,\omega}\boldsymbol{\eta}^{\omega} + \boldsymbol{M}^{v,v}\left(\boldsymbol{C}^{(2)}\right)^T\right] = \frac{\boldsymbol{c}+\boldsymbol{d}^T}{2\,m\,I} \tag{5.23}$$

Fluctuation-dissipation conditions, and the explicit expression for the stochastic amplitude matrices follow by enforcing the equilibrium properties [133]

$$\boldsymbol{M}^{v,v} = \frac{k_B\,T}{m}\,\boldsymbol{I}\,, \qquad \boldsymbol{M}^{\omega,\omega} = \frac{k_B\,T}{I}\,\boldsymbol{I}\,, \qquad \boldsymbol{M}^{v,\omega} = 0 \tag{5.24}$$

where I is the moment of inertia, and $\boldsymbol{I}$ the identity matrix. These conditions stem from the Maxwellian equilibrium velocity distribution, and from the energy equipartition theorem applied to a rigid particle, admitting 6 degrees of freedom. Making use of eq. (5.24) and of the equilibrium expression eq. (5.19) for $\boldsymbol{M}^{v,v}$, one obtains that the matrix $\boldsymbol{a}$ should be symmetric and

$$\boldsymbol{a} = 2\,k_B\,T\,\boldsymbol{\eta} \tag{5.25}$$

A similar analysis for $\boldsymbol{M}^{\omega,\omega}$ eq. (5.21) at equilibrium provides

$$\boldsymbol{b} = 2\,k_B\,T\,\boldsymbol{\eta}^{\omega} \tag{5.26}$$

The equilibrium results deriving from the analysis of the mixed roto-translational moments yield

$$k_B\,T\,\left[\boldsymbol{C}^{(1)} + \left(\boldsymbol{C}^{(2)}\right)^T\right] = \frac{\boldsymbol{c}+\boldsymbol{d}^T}{2} \tag{5.27}$$

a solution of which is $\boldsymbol{d}^T = \boldsymbol{c}$ and

$$\boldsymbol{c} = 2\,k_B\,T\,\boldsymbol{C}^{(1)}\,, \qquad \boldsymbol{d} = 2\,k_B\,T\,\boldsymbol{C}^{(2)} \tag{5.28}$$

Once the “diffusional" matrices $\boldsymbol{a}$, $\boldsymbol{b}$, $\boldsymbol{c}$, $\boldsymbol{d}$ have been expressed in terms of the hydrodynamic resistance matrices, the next step is to derive the expression for the stochastic amplitude matrices $\boldsymbol{\alpha}$, $\boldsymbol{\beta}$, $\boldsymbol{\gamma}$, $\boldsymbol{\varepsilon}$.

Because of eq. (5.28), the 6×6 matrix $\boldsymbol{\Delta}$ defined by eq. (5.12) is symmetric, and satisfies the algebraic matrix equation

$$\frac{\boldsymbol{\Delta}^2}{2} = k_B\,T \begin{pmatrix} \frac{\boldsymbol{\eta}}{m^2} & \frac{\boldsymbol{C}^{(1)}}{m\,I} \\ \frac{\boldsymbol{C}^{(2)}}{m\,I} & \frac{\boldsymbol{\eta}^{\omega}}{I^2} \end{pmatrix} = \boldsymbol{\sigma} \tag{5.29}$$

Mutuating this property from the symmetry of hydrodynamic matrices, the matrix $\boldsymbol{\sigma}$ is symmetric and positive definite, and it is known from matrix theory [89] that there exists a unique, symmetric, and positive definite matrix $\boldsymbol{\Delta}$ solution of eq. (5.29), formally

$$\boldsymbol{\Delta} = \sqrt{2}\,\boldsymbol{\sigma}^{1/2} \tag{5.30}$$

In order to determine the explicit expression for the matrix $\boldsymbol{\Delta}$, it is convenient to normalize its entries, expressing the force/torque and the velocity/angular velocity in the same physical dimensions. If ℓ_p is the characteristic particle length, $\ell_p = R_p$ for spherical particle of radius R_p, set $\widehat{\boldsymbol{T}} = \boldsymbol{T}/\ell_p$, $\widehat{\boldsymbol{\omega}} = \ell_p\,\boldsymbol{\omega}$. In this way, $\widehat{\boldsymbol{T}}$ has the dimension of a force, and $\widehat{\boldsymbol{\omega}}$ the dimension of a velocity, so that eqs. (5.7)-(5.8) become

$$\begin{pmatrix} \boldsymbol{F} \\ \widehat{\boldsymbol{T}} \end{pmatrix} = -\widehat{\boldsymbol{H}}(\boldsymbol{x}) \begin{pmatrix} \boldsymbol{v} \\ \widehat{\boldsymbol{\omega}} \end{pmatrix} \tag{5.31}$$

where $\widehat{\boldsymbol{H}}(\boldsymbol{x})$ is the normalized overall resistance matrix possessing the block structure

$$\widehat{\boldsymbol{H}}(\boldsymbol{x}) = \begin{pmatrix} \widehat{\boldsymbol{\eta}}(\boldsymbol{x}) & \widehat{\boldsymbol{C}}^{(1)}(\boldsymbol{x}) \\ \widehat{\boldsymbol{C}}^{(2)}(\boldsymbol{x}) & \widehat{\boldsymbol{\eta}}^{\omega}(\boldsymbol{x}) \end{pmatrix} = \begin{pmatrix} \boldsymbol{\eta}(\boldsymbol{x}) & \boldsymbol{C}^{(1)}(\boldsymbol{x})/\ell_p \\ \boldsymbol{C}^{(2)}(\boldsymbol{x})/\ell_p & \boldsymbol{\eta}^{\omega}(\boldsymbol{x})/\ell_p^2 \end{pmatrix} \tag{5.32}$$

and the normalized moment of inertia is given by $\widehat{I} = I/\ell_p^2$. In this way, eq. (5.11) attains the normalized representation

$$\begin{aligned} d\boldsymbol{v}(t) &= -\frac{\boldsymbol{\eta}}{m}\boldsymbol{v}(t)\,dt - \frac{\widehat{\boldsymbol{C}}^{(1)}}{m}\widehat{\boldsymbol{\omega}}(t)\,dt + \frac{\widehat{\boldsymbol{\alpha}}}{m}\,d\boldsymbol{w}(t) + \frac{\widehat{\boldsymbol{\gamma}}}{m}\,d\boldsymbol{w}^{\omega}(t) \\ d\widehat{\boldsymbol{\omega}}(t) &= -\frac{\widehat{\boldsymbol{C}}^{(2)}}{\widehat{I}}\boldsymbol{v}(t)\,dt - \frac{\widehat{\boldsymbol{\eta}}^{\omega}}{\widehat{I}}\widehat{\boldsymbol{\omega}}(t)\,dt + \frac{\widehat{\boldsymbol{\varepsilon}}}{\widehat{I}}\,d\boldsymbol{w}(t) + \frac{\widehat{\boldsymbol{\beta}}}{\widehat{I}}\,d\boldsymbol{w}^{\omega}(t) \end{aligned} \tag{5.33}$$

with $\widehat{\boldsymbol{\alpha}} = \boldsymbol{\alpha}$, $\widehat{\boldsymbol{\gamma}} = \boldsymbol{\gamma}/\ell_p$, $\widehat{\boldsymbol{\varepsilon}} = \boldsymbol{\varepsilon}/\ell_p$, $\widehat{\boldsymbol{\beta}} = \boldsymbol{\beta}/\ell_p^2$. The normalized matrix eq. (5.29) thus becomes

$$\frac{\widehat{\boldsymbol{\Delta}}^2}{2} = k_B T \begin{pmatrix} \frac{\boldsymbol{\eta}}{m^2} & \frac{\widehat{\boldsymbol{C}}^{(1)}}{m\widehat{I}} \\ \frac{\widehat{\boldsymbol{C}}^{(2)}}{m\widehat{I}} & \frac{\widehat{\boldsymbol{\eta}}^{\omega}}{\widehat{I}^2} \end{pmatrix} = \widehat{\boldsymbol{\sigma}} \tag{5.34}$$

and $\widehat{\boldsymbol{\Delta}} = \sqrt{2}\,\widehat{\boldsymbol{\sigma}}^{1/2}$.

For symmetric and positive definite matrices $\widehat{\boldsymbol{\sigma}}$, the estimate of their square root $\widehat{\boldsymbol{\sigma}}^{1/2}$ reduces to an eigenvalue problem [89]. Let $\lambda_i > 0$, $i = 1, \dots, 6$, be the eigenvalues of $\widehat{\boldsymbol{\sigma}}$, and $\boldsymbol{V}^{(i)} = (V_1^{(i)}, \dots, V_6^{(i)})$ the corresponding unit eigenvectors. The solution of eq. (5.34) can be expressed as

$$\widehat{\boldsymbol{\Delta}} = \sqrt{2}\boldsymbol{V}\,\mathrm{diag}(\lambda_1^{1/2}, \dots, \lambda_6^{1/2})\boldsymbol{V}^{-1} \tag{5.35}$$

where $\boldsymbol{V}$ is the eigenbasis transformation matrix, the column of which are orderly the eigevectors of $\widehat{\boldsymbol{\sigma}}$, i.e.,

$$\boldsymbol{V} = \begin{pmatrix} V_1^{(1)} & \dots & V_1^{(6)} \\ \dots & \dots & \dots \\ V_6^{(1)} & \dots & V_6^{(6)} \end{pmatrix} \tag{5.36}$$

and $\mathrm{diag}(\lambda_1^{1/2}, \dots, \lambda_6^{1/2})$ is a diagonal matrix, the diagonal entries of which are the square roots of the eigenvalues λ_i, $i = 1, \dots, 6$.

5.2.1 An example: systems with axialsymmetric geometry

As an application of the previous analysis, consider a system with axialsymmetric geometry. Typical axisymmetric systems in microfluidics are spherical particles moving in a slit channel or near an infinitely extended planar wall. The symmetries of the problem reduces the 21 independent coefficients of the hydrodynamic resistance matrix to 5. By taking a Cartesian coordinate system (x_1, x_2, x_3) with x_3 lying on

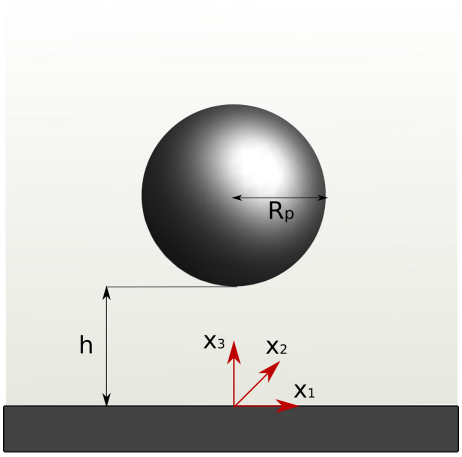

Figure 5.1. Schematic rapresentation of a spherical particle near an infinitely extended planar wall.

the axis of symmetry as in Fig. 5.1, the resistance matrix takes the form [98]

$$\boldsymbol{H} = \begin{pmatrix} \eta_{1,1} & 0 & 0 & 0 & C & 0 \\ 0 & \eta_{1,1} & 0 & -C & 0 & 0 \\ 0 & 0 & \eta_{3,3} & 0 & 0 & 0 \\ 0 & -C & 0 & \eta^{\omega}_{1,1} & 0 & 0 \\ C & 0 & 0 & 0 & \eta^{\omega}_{1,1} & 0 \\ 0 & 0 & 0 & 0 & 0 & \eta^{\omega}_{3,3} \end{pmatrix} \tag{5.37}$$

Therefore, the matrix $\widehat{\boldsymbol{\sigma}}$, chosing $\ell_p = R_p$, becomes

$$\widehat{\boldsymbol{\sigma}} = \begin{pmatrix} \widehat{\sigma}_1 & 0 & 0 & 0 & \widehat{\sigma}_c & 0 \\ 0 & \widehat{\sigma}_1 & 0 & -\widehat{\sigma}_c & 0 & 0 \\ 0 & 0 & \widehat{\sigma}_3 & 0 & 0 & 0 \\ 0 & -\widehat{\sigma}_c & 0 & \widehat{\sigma}_4 & 0 & 0 \\ \widehat{\sigma}_c & 0 & 0 & 0 & \widehat{\sigma}_4 & 0 \\ 0 & 0 & 0 & 0 & 0 & \widehat{\sigma}_6 \end{pmatrix} \tag{5.38}$$

where

$$\begin{aligned} \widehat{\sigma}_1 &= \widehat{\sigma}_2 = \eta_{1,1}\,\frac{k_B\,T}{m^2}\,, \quad \widehat{\sigma}_3 = \eta_{3,3}\,\frac{k_B\,T}{m^2}\,, \quad \widehat{\sigma}_4 = \widehat{\sigma}_5 = \eta^{\omega}_{1,1}\,\frac{k_B\,T}{I^2}\,R_p^2 \qquad (5.39) \\ \widehat{\sigma}_6 &= \eta^{\omega}_{3,3}\,\frac{k_B\,T}{I^2}\,R_p^2\,, \quad \widehat{\sigma}_c = C\,\frac{k_B\,T}{m\,I}\,R_p \end{aligned}$$

The eigenvalues of $\widehat{\boldsymbol{\sigma}}$ are

$$\lambda_1 = \lambda_2 = \frac{\widehat{\sigma}_1 + \widehat{\sigma}_4 - r}{2}\,, \quad \lambda_3 = \widehat{\sigma}_3\,, \quad \lambda_4 = \lambda_5 = \frac{\widehat{\sigma}_1 + \widehat{\sigma}_4 + r}{2}\,, \quad \lambda_6 = \widehat{\sigma}_6 \tag{5.40}$$

where $r = \sqrt{(\widehat{\sigma}_4 - \widehat{\sigma}_1)^2 + 4\widehat{\sigma}_c^2}$. The eigenvector matrix $\boldsymbol{V}$ entering eq. (5.36) takes in this case the expression

$$\boldsymbol{V} = \begin{pmatrix} -\frac{-\widehat{\sigma}_1+\widehat{\sigma}_4+r}{2\widehat{\sigma}_c} & 0 & 0 & -\frac{-\widehat{\sigma}_1+\widehat{\sigma}_4-r}{2\widehat{\sigma}_c} & 0 & 0 \\ 0 & -\frac{\widehat{\sigma}_1-\widehat{\sigma}_4-r}{2\widehat{\sigma}_c} & 0 & 0 & -\frac{\widehat{\sigma}_1-\widehat{\sigma}_4+r}{2\widehat{\sigma}_c} & 0 \\ 0 & 0 & 1 & 0 & 0 & 0 \\ 0 & 1 & 0 & 0 & 1 & 0 \\ 1 & 0 & 0 & 1 & 0 & 0 \\ 0 & 0 & 0 & 0 & 0 & 1 \end{pmatrix} \tag{5.41}$$

By applying eqs. (5.36), (5.38), one obtains for $\widehat{\boldsymbol{\Delta}}$

$$\widehat{\boldsymbol{\Delta}} = \begin{pmatrix} \widehat{\Delta}_1 & 0 & 0 & 0 & \widehat{\Delta}_c & 0 \\ 0 & \widehat{\Delta}_1 & 0 & -\widehat{\Delta}_c & 0 & 0 \\ 0 & 0 & \widehat{\Delta}_3 & 0 & 0 & 0 \\ 0 & -\widehat{\Delta}_c & 0 & \widehat{\Delta}_4 & 0 & 0 \\ \widehat{\Delta}_c & 0 & 0 & 0 & \widehat{\Delta}_4 & 0 \\ 0 & 0 & 0 & 0 & 0 & \widehat{\Delta}_6 \end{pmatrix} \tag{5.42}$$

where

$$\begin{aligned} \widehat{\Delta}_1 &= \widehat{\Delta}_2 = \frac{(\widehat{\sigma}_1 - \lambda_1)\sqrt{\lambda_4} - (\widehat{\sigma}_1 - \lambda_4)\sqrt{\lambda_1}}{r}, \quad \widehat{\Delta}_3 = \sqrt{2\,\widehat{\sigma}_3} \\ \widehat{\Delta}_4 &= \widehat{\Delta}_5 = \frac{(\widehat{\sigma}_4 - \lambda_4)\sqrt{\lambda_1} - (\widehat{\sigma}_4 - \lambda_1)\sqrt{\lambda_4}}{r}, \quad \widehat{\Delta}_6 = \sqrt{2\,\widehat{\sigma}_6}\,, \quad \widehat{\Delta}_c = \frac{\widehat{\sigma}_c(\sqrt{\lambda_4} - \sqrt{\lambda_1})}{r} \end{aligned} \tag{5.43}$$

As $h \to \infty$, i.e., far away from the wall, the coupling term $\widehat{\boldsymbol{\sigma}}_c \to 0$, and the quantity r take the limit form

$$r = \sqrt{(\widehat{\boldsymbol{\sigma}}_4 - \widehat{\boldsymbol{\sigma}}_1)^2} = \frac{\pi\,\mu\,R_p\,k_B\,T}{m^2}\sqrt{\left(\frac{\bar{\eta}^{\omega}_{1,1}}{\bar{I}^2} - \bar{\eta}_{1,1}\right)^2} \tag{5.44}$$

where

$$\bar{\eta}^{\omega}_{1,1} = \frac{\eta^{\omega}_{11}}{\pi\,\mu\,R_p^3} = 8\,, \qquad \bar{\eta}_{1,1} = \frac{\eta_{11}}{\pi\,\mu\,R_p} = 6, \qquad \bar{I} = \frac{I}{mR_p^2} = \frac{2}{5} \tag{5.45}$$

Substituting these values into eq. (5.44), the expected results in the free space are obtained

$$\hat{\Delta}_i = \sqrt{2\,\hat{\sigma}_i}\,, \qquad i = 1, \ldots, 6 \tag{5.46}$$

and therefore

$$\boldsymbol{\alpha} = \sqrt{2k_BT\eta_\infty}\,\boldsymbol{I}\,, \qquad \boldsymbol{\beta} = \sqrt{2k_BT\eta^{\omega}_\infty}\,\boldsymbol{I}\,, \qquad \boldsymbol{\gamma} = \boldsymbol{\varepsilon} = 0 \tag{5.47}$$

where $\boldsymbol{I}$ is the 3×3 identity matrix. In order to recover the Stokesian limit values in the free space η_∞, η^{ω}_∞, the argument of the square root in eq. (5.44) should be positive, i.e.,

$$\frac{\bar{\eta}^{\omega}_{1,1}}{\bar{\eta}_{1,1}} > \bar{I}^2 \tag{5.48}$$

Inequality (5.48) is fulfilled in the free space as follows from eq. (5.45).

5.3 Adiabatic elimination of the velocity variables

In this Section, the formulation of the overdamped approximation for micrometric rigid particles in confined geometries is considered. The overdamped approximation consists in expressing the equations of motion in the form of a kinematic equation for the mechanical degrees of freedom associated with translational and rotational motions. This is made possible due to the fact that velocity variables are customarily characterized by a faster relaxation dynamics than position and orientational variables. This is certainly true for micrometric particles if one considers their transport properties at time scales much larger than the characteristic dissipation timescale $t_{\text{diss}} = m/\eta_\infty$, the order of magnitude of which falls between 10^{-6}-10^{-7} s for micrometric particles in water at room temperature. For this reason, the overdamped approximation is often referred to as the adiabatic elimination of the fast velocity variables, and this follows by imposing the condition

$$m\, d\boldsymbol{v} \simeq 0\,, \quad I\, d\boldsymbol{\omega} \simeq 0 \tag{5.49}$$

and extracting out of eqs. (5.49) the expression for $\boldsymbol{v}$ and $\boldsymbol{\omega}$, entering the kinematic equation

$$d\boldsymbol{x} = \boldsymbol{v}\, dt\,, \qquad d\boldsymbol{\phi} = \boldsymbol{\omega}\, dt \tag{5.50}$$

where $\boldsymbol{\phi} = (\phi_1, \phi_2, \phi_3)$ is the vector-valued angular variable accounting for the particle orientation.

The overdamped approximation in confined geometries presents intrinsic peculiarities, just because the hydrodynamic resistance matrix depends on the position $\boldsymbol{x}$, and in general of the orientation $\boldsymbol{\phi}$, and this raises delicate issues when the thermal fluctuations are expressed as linear superposition of increments of Wiener processes, owing to their highly singular local structure [77]. This problem in the physical literature is usually referred to as the Ito-Stratonovich dilemma [234, 161]. The most convenient and simple approach to perform the adiabatic elimination of the fast velocity variable is due to Sancho et al. [215]. The starting point in this derivation is that the configurational coordinates of a particle driven by Wiener fluctuations still represent a locally smooth, and almost everywhere differentiable continuous stochastic process with probability 1, and this property determines the way eq. (5.49) is interpreted. Without loss of generality, let us suppose that the particle is subjected to an external potential $\Phi(\boldsymbol{x})$, and that no additional flow contribution are present. The latter can be added at the end of the adiabatic elimination process.

In order to perform this analysis in the simplest formal way, it is convenient to group together configurational and velocity variables, thus introducing the 6-dimensional configurational and velocity variables, $\boldsymbol{z}$ and $\boldsymbol{U}$, respectively, and the overall stochastic forcing $d\boldsymbol{W}(t)$

$$\boldsymbol{z} = \begin{pmatrix} \boldsymbol{x} \\ \boldsymbol{\phi} \end{pmatrix}, \quad \boldsymbol{U} = \begin{pmatrix} \boldsymbol{v} \\ \boldsymbol{\omega} \end{pmatrix}, \quad d\boldsymbol{W}(t) = \begin{pmatrix} d\boldsymbol{w}(t) \\ d\boldsymbol{w}^\omega(t) \end{pmatrix} \tag{5.51}$$

so that the equations of motion can be compactly expressed as

$$d\boldsymbol{z} = \boldsymbol{U}\, dt\,, \quad \boldsymbol{m}_{mI}\, d\boldsymbol{z} = -\boldsymbol{H}(\boldsymbol{z})\, \boldsymbol{U}\, dt - \nabla_z \Phi(\boldsymbol{z})\, dt + \boldsymbol{\nu}(\boldsymbol{z})\, d\boldsymbol{W}(t) \tag{5.52}$$

where $\boldsymbol{m}_{mI}$ is the mass/moment-of inertial tensor, $\boldsymbol{m}_{mI} = \mathrm{diag}(m, m, m, I, I, I)$ for a spherical particle, $\boldsymbol{H}(\boldsymbol{z})$ the hydrodynamic resistance matrix, ∇_z the nabla operator with respect to the $\boldsymbol{z}$-variable and $\boldsymbol{\nu}$ is the matrix of thermal fluctuation intensity satisfying, as discussed in the previous Section, the condition at thermal equilibrium,

$$\boldsymbol{\nu}(\boldsymbol{z})\,\boldsymbol{\nu}^T(\boldsymbol{z}) = 2\,k_B\,T\,\boldsymbol{H}(\boldsymbol{z}) \tag{5.53}$$

The overdamped approximation corresponds to the limit for mass and momentum of inertia tending to zero. In performing this limit, upon correct physical grounds, it should be ensured that the configurational variable $\boldsymbol{z}(t)$ is a smooth stochastic process. To this end, the Wong-Zakai theorem can be enforced [243, 244], implying that the stochastic differential equation describing particle dynamics should be interpreted in a Stratonovich way [132], Technically, this means that, in performing the limit process, the quantity $\boldsymbol{H}(\boldsymbol{z})\,\boldsymbol{U}\,dt$ should be interpreted as

$$\boldsymbol{H}(\boldsymbol{z})\,\boldsymbol{U}\,dt = \boldsymbol{H}(\boldsymbol{z}) \circ d\boldsymbol{z} = \boldsymbol{H}(\boldsymbol{z} + d\boldsymbol{z}/2)\,d\boldsymbol{z} \tag{5.54}$$

where "∘" indicates the Stratonovich rule in the definition of stochastic integrals and differentials. It is also convenient to recall a known result, deriving from the Ito lemma, namely that [77]

$$dW_i(t)\,dW_j(t) = \delta_{i,j}\,dt + o(dt) \tag{5.55}$$

where $\delta_{i,j}$ are the Kronecker's symbols (entries of the identity matrix), and $o(dt)$ is a quantity going to zero for $dt \to 0$ faster than dt.

The final goal of this analysis is to derive a kinematic equation for the configurational particle degrees of freedom (Langevin equation) expressed in the Ito way and, out of it, the transport equation for particle density, corresponding to the Fokker-Planck equation for the statistical characterization of the so-obtained Langevin equation.

Making use of the Wong-Zakai result, expressed by eq. (5.54), the overdamped approximation of eq. (5.52) is thus given componentwise by

$$0 = \sum_{j=1}^{6} H_{i,j}\left(\boldsymbol{z} + \frac{\boldsymbol{d}z}{2}\right)\,dz_j - \frac{\partial \Phi}{\partial z_i}\,dt + \sum_{j=1}^{6} \nu_{i,j}(\boldsymbol{z})\,dW_j(t) \tag{5.56}$$

Expanding the first term at the r.h.s. of eq. (5.56) in Taylor series to the leading order,

$$\sum_{j=1}^{6} H_{i,j}\left(\boldsymbol{z} + \frac{\boldsymbol{d}z}{2}\right)\,dz_j = \sum_{j=1}^{6} H_{i,j}(\boldsymbol{z})\,dz_j + \frac{1}{2}\sum_{j,k=1}^{6} \frac{\partial H_{i,j}(\boldsymbol{z})}{\partial z_k}\,dz_j\,dz_k + o(dt) \tag{5.57}$$

The quantity $dz_j\,dz_k$ can be evaluated from eq. (5.56), by considering for the first term at the r.h.s. of eq. (5.56) its Ito interpretation, namely $\sum_{j=1}^{6} H_{i,j}(\boldsymbol{z})\,dz_j$ that provides the leading order contribution as the remainder in this approximation is order of $o(dt)$. Thus, enforcing also eq. (5.55), one obtains

$$\begin{aligned}
dz_j\, dz_k &= \left(-\sum_{p=1}^{6} H^{-1}_{j,p} \frac{\partial \Phi}{\partial z_p} dt + \sum_{p,m=1}^{6} H^{-1}_{j,p}\, \nu_{p,m}\, dW_m(t) \right) \\
&\times \left(-\sum_{q=1}^{6} H^{-1}_{k,q} \frac{\partial \Phi}{\partial z_q} dt + \sum_{q,n}^{6} H^{-1}_{k,q}\, \nu_{q,n}\, dW_n(t) \right) \\
&= \sum_{p,m,q,n=1}^{6} H^{-1}_{j,p}\, H^{-1}_{k,q}\, \nu_{p,m}\, \nu_{q,n}\, dW_m(t)\, dW_n(t) \\
&= \sum_{p,m,q,n=1}^{6} H^{-1}_{j,p}\, H^{-1}_{k,q}\, \nu_{p,m}\, \nu_{q,n} \delta_{m,n}\, dt = \sum_{p,q,m=1}^{6} H^{-1}_{j,p}\, H^{-1}_{k,q}\, \nu_{p,m}\, \nu_{q,m}\, dt \\
&= \sum_{p,q=1}^{6} H^{-1}_{j,p}\, H^{-1}_{k,q}\, k_B\, T\, H_{q,p}\, dt = 2\, k_B\, T\, H^{-1}_{j,k}\, dt + o(dt) \qquad (5.58)
\end{aligned}$$

where $H^{-1}_{j,p} = (\boldsymbol{H}^{-1})_{j,p}$, and in deriving the last relation eq. (5.53) has been used. Substituting eqs. (5.57), (5.58) into eq. (5.56) it follows that

$$\sum_{j=1}^{6} H_{i,j}\, dz_j = -k_B\, T \sum_{j,k=1}^{6} \frac{\partial H_{i,j}}{\partial z_k} H^{-1}_{k,j}\, dt - \frac{\partial \Phi}{\partial z_i} dt + \sum_{j=1}^{6} \nu_{i,j}\, dW_j(t) \qquad (5.59)$$

where the $o(dt)$-terms have been neglected. Correspondingly, the Langevin equation in the configuration $(\boldsymbol{x}, \boldsymbol{\phi})$-space becomes

$$dz_i = -\sum_{j=1}^{6} H^{-1}_{i,j} \frac{\partial \Phi}{\partial z_j} dt - f_i\, dt + \sum_{j,h=1}^{6} H^{-1}_{i,j} \nu_{j,h}\, dW_h(t) \qquad (5.60)$$

where

$$f_i = k_B\, T \sum_{j,h,k=1}^{6} H^{-1}_{i,j} \frac{\partial H_{j,h}}{\partial z_k} H^{-1}_{k,h} \qquad (5.61)$$

The Fokker-Planck equation for the probability density $p(\boldsymbol{z}, t)$ associated with eq. (5.61) is thus given by

$$\frac{\partial p}{\partial t} = \nabla_z \cdot \left(\boldsymbol{H}^{-1}\, \nabla_z \Phi\, p \right) + \nabla_z \cdot (\boldsymbol{f}\, p) + \sum_{i,j=1}^{6} \frac{\partial^2}{\partial z_i \partial z_j} (D_{i,j}\, p) \qquad (5.62)$$

where $\boldsymbol{f} = (f_i)_{i=1}^6$ and the generalized diffusivity tensor $D_{i,j}$ takes the form

$$\begin{aligned}
D_{i,j} &= \frac{1}{2} \sum_{p,k,q=1}^{6} H^{-1}_{i,p}\, \nu_{p,k}\, H^{-1}_{j,q}\, \nu_{q,k} = \frac{1}{2} \sum_{p,q=1}^{6} H^{-1}_{i,p}\, H^{-1}_{j,q}\, 2\, k_B\, T\, H_{p,q} \\
&= k_B\, T\, H^{-1}_{i,j} \qquad (5.63)
\end{aligned}$$

i.e., the generalized diffusivity tensor $\boldsymbol{D}(\boldsymbol{z}) = (D_{i,j}(\boldsymbol{z}))_{i,j=1}^6$ is related to the resistance matrix $\boldsymbol{H}(\boldsymbol{z})$ by the relation

$$\boldsymbol{D}(\boldsymbol{z})\, \boldsymbol{H}(\boldsymbol{z}) = k_B\, T \qquad (5.64)$$

generalizing the fluctuation-dissipation relation eq. (5.4). Next, consider the contribution of the vector field $\boldsymbol{f}$ entering the Fokker-Planck equation (5.62). From the identity $\boldsymbol{H}^{-1}\boldsymbol{H} = \boldsymbol{I}$, it follows componentwise, for any $k = 1, \dots, 6$,

$$\sum_{j=1}^{6} \frac{\partial H^{-1}_{i,j}}{\partial z_k} H_{j,h} + \sum_{j=1}^{6} H^{-1}_{i,j} \frac{\partial H_{j,h}}{\partial z_k} = 0 \tag{5.65}$$

and thus,

$$\frac{\partial H^{-1}_{j,h}}{\partial z_k} = - \sum_{m,j=1}^{6} H^{-1}_{i,m} \frac{\partial H_{m,j}}{\partial z_k} H^{-1}_{j,h} \tag{5.66}$$

The latter expression implies that the entries f_i of $\boldsymbol{f}$ defined by eq. (5.61) reduce to

$$f_i = -k_B T \sum_{h=1}^{6} \frac{\partial H^{-1}_{i,h}}{\partial z_h} \tag{5.67}$$

Substituting eqs. (5.63), (5.67) into eq. (5.62), the Fokker-Planck equation for $p(\boldsymbol{z}, t)$ attains the simpler form

$$\frac{\partial p}{\partial t} = \sum_{i,j=1}^{6} \frac{\partial}{\partial z_i} \left(H^{-1}_{i,j} \frac{\partial \Phi}{\partial z_j} p \right) - k_B T \sum_{i=1}^{6} \frac{\partial}{\partial z_i} \left(\sum_{j=1}^{6} \frac{\partial H^{-1}_{i,j}}{\partial z_j} p \right) + k_B T \sum_{i,j=1}^{6} \frac{\partial}{\partial z_i \partial z_j} \left(H^{-1}_{i,j}\, p \right) \tag{5.68}$$

that can be rewritten in a more compact way as

$$\frac{\partial p}{\partial t} = \sum_{i,j=1}^{6} \frac{\partial}{\partial z_i} \left(H^{-1}_{i,j} \frac{\partial \Phi}{\partial z_j} p \right) + \sum_{i,j=1}^{6} \frac{\partial}{\partial z_i} \left(D_{i,j} \frac{\partial p}{\partial z_j} \right) \tag{5.69}$$

The latter corresponds to an advection-diffusion equation in the configuration space in the presence of the effective velocity $\boldsymbol{v}_{\text{eff}} = \boldsymbol{H}^{-1} \nabla_z \Phi$, stemming from the potential $\Phi(\boldsymbol{z})$ and of the tensor diffusivity $\boldsymbol{D}$. Conversely, eq. (5.68) represents the classical formulation of the Fokker-Planck equation associated with a Langevin dynamics interpreted in the Ito way, attaining the following expression

$$dz_i = -\sum_{j=1}^{6} H^{-1}_{i,j} \frac{\partial \Phi}{\partial z_j} dt + \sum_{j=1}^{6} \frac{\partial D_{i,h}}{\partial z_h} dt + \sqrt{2} \sum_{j=1}^{6} (\boldsymbol{D}^{1/2})_{i,j}\, dW_j(t) \tag{5.70}$$

where $(\boldsymbol{D}^{1/2})_{i,j}$ are the entries of the square root matrix $\boldsymbol{D}^{1/2}$ of the diffusivity tensor $\boldsymbol{D}$, $\boldsymbol{D}^{1/2}\boldsymbol{D}^{1/2} = \boldsymbol{D}$. It is also clear from the Ito representation of the Langevin eq. (5.70) the occurrence of an additional convective contribution depending on the divergence of the diffusivity tensor. This term admits a physical meaning as, even for $\Phi(\boldsymbol{z}) = 0$, it provides a biasing average velocity $U_i^{(\text{bias})}(\boldsymbol{z})$,

$$U_i^{(\text{bias})}(\boldsymbol{z}^*) = \left. \frac{d\langle z_i \rangle}{dt} \right|_{\boldsymbol{z}=\boldsymbol{z}^*} \tag{5.71}$$

where $d\langle z_i \rangle / dt|_{\boldsymbol{z}=\boldsymbol{z}^*}$ is the average value of the particle velocity evaluated when the particle configuration is at $\boldsymbol{z} = \boldsymbol{z}^*$ [143, 144].

In the case of a spherical particle, the hydrodynamic matrices depends solely on $\boldsymbol{x}$ and not on $\boldsymbol{\phi}$. Consequently it is easy to obtain the evolution equation for the marginal distribution $p_x(\boldsymbol{x},t) = \int_{S_3} p(\boldsymbol{z},t)\, d\boldsymbol{\phi}$, where $S_3 = [0, 2\pi)^3$. Assume also that the spherical particles are immersed in a flow, and that the force exterted by the flow onto a generic particle located at $\boldsymbol{x}$ is $\boldsymbol{F}_{\text{flow}}(\boldsymbol{x}) = \boldsymbol{\eta}(\boldsymbol{x})\, \boldsymbol{u}^{(p)}(\boldsymbol{x})$. In this case, the spatial particle density function $p_x(\boldsymbol{x},t)$ satisfies the balance equation

$$\frac{\partial p_x}{\partial t} = \sum_{i=1}^{3} \frac{\partial}{\partial x_i} \left[\left(u_i^{(p)} - \sum_{j=1}^{3} \eta_{i,j}^{-1} \frac{\partial \Phi}{\partial x_j} \right) p_x \right] + \sum_{i,j=1}^{3} \frac{\partial}{\partial x_i} \left(D_{i,j}^x \frac{\partial p_x}{\partial x_j} \right) \tag{5.72}$$

where $D_{i,j}^x(\boldsymbol{x})$, is the 3×3 diffusivity tensor, $\sum_{h=1}^{3} D_{i,h}^x(\boldsymbol{x})\, \eta_{h,j}(\boldsymbol{x}) = k_B\, T\, \delta_{i,j}$.

5.3.1 An application

As a simple application of the overdamped theory, consider the vertical motion of a spherical particle in the upper half-plane delimited by a planar wall at $x_3 = 0$ in isothermal conditions at temperature T. Indicate with $x = h$ the distance of the particle from the wall, and assume that the particle is subjected to an external potential $\Phi(x)$, as in [237, 30], where $\Phi(x)$ stems from gravity and from a local double-layer repulsive potential near the wall. In this case the problem is spatially one-dimensional, since $\eta(x) = \eta_{3,3}(x)$, and $D(x) = k_B\, T/\eta(x)$ depends solely from the distance x from the wall. Setting $\Phi'(x) = d\Phi(x)/dx$, and similarly for $D'(x)$, the Fokker-Planck equation for the density function $p_x(x,t)$ reads

$$\frac{\partial p_x(x,t)}{\partial t} = \frac{\partial}{\partial x} \left(\frac{\Phi'(x)}{\eta(x)}\, p_x(x,t) \right) + \frac{\partial}{\partial x} \left(D(x)\, \frac{\partial p_x(x,t)}{\partial x} \right) \tag{5.73}$$

and this equation corresponds to the Langevin-Ito equation

$$dx(t) = -\eta^{-1}(x(t))\, \Phi'(x(t))\, dt + D'(x(t))\, dt + \sqrt{2\, D(x(t))}\, dw(t) \tag{5.74}$$

where $dw(t)$ is the increment of a one-dimensional Wiener process. Assuming that the potential is attractive towards $x = 0$ at large distances, so that $\int_0^\infty e^{-\Phi(x)/k_B\, T}\, dx < \infty$, it follows from eq. (5.73) that in the limit for $t \to \infty$, the density $p_x(x,t)$ converges towards a stationary density $p_x^*(x)$, solution of the equation

$$\eta^{-1}(x)\, \Phi'(x)\, p_x^*(x) + D(x)\, \frac{dp_x^*(x)}{dx} = 0 \tag{5.75}$$

corresponding, as expected, to the Boltzmann distribution

$$p_x^*(x) = A\, e^{-\Phi(x)/k_B\, T} \tag{5.76}$$

This is a classical result, starting from which, micrometric particles may be used as Brownian probes, upon recording their statistical properties i.e. their stationary density function $p_x^*(x)$, in order to investigate and measure surface properties of materials [237, 30].

It is instructive to analyze in greater detail the mathematical properties of eq. (5.73). This is a one-dimensional parabolic equation for $p_x(x,t)$, and as the wall at $x = 0$ is impermeable to particle transport, $\int_0^\infty p_x(x,t)\,dx = 1$ for any $t \geq 0$. To solve eq. (5.73), it should be equipped with initial and boundary conditions. As regards the initial condition, $p_x(x,0) = p_{x,0}(x)$, with $\int_0^\infty p_{x,0}(x)\,dx = 1$. The boundary condition at infinity, $x \to \infty$ is the classical regularity condition, namely

$$\lim_{x\to\infty} x^n\, p_x(x,t) = \lim_{x\to\infty} x^n \frac{\partial p_x(x,t)}{\partial x} = 0\,, \qquad \text{for } t > 0\,,\;\; n = 0,1,\ldots \tag{5.77}$$

meaning that $p_x(x,t)$ and $\partial p_x(x,t)/\partial x$ should decay faster than any power x^n of x for $x \to \infty$. At $x = 0$, the zero-flux boundary condition applies, implying in the present case

$$-\frac{\Phi'(x)}{\eta(x)}\, p_x(x,t) - D(x)\, \frac{\partial p_x(x,t)}{\partial x}\bigg|_{x=0} = 0 \tag{5.78}$$

Two cases should be discussed. If, (i) $\lim_{x\to 0} |\Phi'(x)| < \infty$, since $D(0) = k_B\,T/\eta(0) = 0$, the wall boundary condition at $x = 0$ blows up, reducing eq. (5.78) to a trivial identity that does not provide any condition on the local behavior of $p_x(x,t)$ near $x = 0$. Conversely, if (ii) $\lim_{x\to 0} |\Phi'(x)| = \infty$, and moreover $\lim_{x\to 0} \Phi'(x)/\eta(x) = C \neq 0$, where the constant C may even diverge to ∞, the boundary condition (5.78) reduces to a homogeneous Dirichlet condition,

$$p_x(0,t) = 0 \tag{5.79}$$

As in principle, the condition on the potential Φ leading to eq. (5.79) could not be verified in a physical systems, as for the case analyzed in [237, 30], it follows from the above analysis that the simple transport model eq. (5.73) displays a singular behavior as regards the wall boundary conditions. This singular phenomenon is a peculiar feature of the transport equations involving a hydrodynamic Stokesian description of the fluid-particle interactions in confined geometries, deriving from the singularity of some entries of the resistance matrix near a solid wall.

5.3.2 Thermophoresis from the overdamped approximation

An interesting byproduct of the overdamped analysis discussed above is the derivation of thermophoretic effects from the stochastic equations of motion. For simplicity, let us consider the case of a spherical particle in its translational motion, neglecting rotational effects and in the absence of any external or fluid forcing. It has been shown in [60] (see also [113]) that even in the presence of a non-equilibrium steady temperature profile $T(\boldsymbol{x})$ the fluctuation-dissipation relation can be applied, so that the equations of motion in the present case read

$$\begin{aligned} d\boldsymbol{x} &= \boldsymbol{v}\,dt \\ m\,d\boldsymbol{v} &= -\boldsymbol{\eta}(\boldsymbol{x})\,\boldsymbol{v}\,dt + \sqrt{2\,k_B\,T(\boldsymbol{x})}\,\boldsymbol{\eta}^{1/2}(\boldsymbol{x})\,d\boldsymbol{w}(t) \end{aligned} \tag{5.80}$$

Within the overdamped approximation, enforcing the same Stratonovich-approach developed in Section 5.2 to the term $\boldsymbol{\eta}(\boldsymbol{x})\,\boldsymbol{v}\,dt = \boldsymbol{\eta}(\boldsymbol{x}) \circ d\boldsymbol{x}$, one obtains

$$-\sum_{j=1}^{3} \eta_{i,j}\,dx_j - \frac{1}{2}\sum_{j,k=1}^{3} \frac{\partial \eta_{i,j}}{\partial x_k}\,dx_j\,dx_k + \sqrt{2\,k_B\,T(\boldsymbol{x})}\,(\boldsymbol{\eta}^{1/2})_{i,j}\,dw_j(t) = 0 \tag{5.81}$$

Since,

$$\begin{aligned} dx_j\, dx_k &= 2\, k_B\, T(\boldsymbol{x}) \sum_{p,q=1}^{3} (\boldsymbol{\eta}^{1/2})_{j,p}\, (\boldsymbol{\eta}^{1/2})_{k,q}\, dw_p(t)\, dw_q(t) + o(dt) \\ &= 2\, k_B\, T(\boldsymbol{x}) \sum_{p,q=1}^{3} (\boldsymbol{\eta}^{1/2})_{j,p}\, (\boldsymbol{\eta}^{1/2})_{k,p}\, dt + o(dt) = 2\, k_B\, T(\boldsymbol{x}) \eta_{j,k}^{-1}\, dt + o(dt) \end{aligned} \tag{5.82}$$

This leads to the following Langevin equation

$$dx_i = -k_B\, T(\boldsymbol{x}) \sum_{j,h,k=1}^{3} \eta_{i,j}^{-1}\, \frac{\partial \eta_{j,h}}{\partial x_k}\, \eta_{h,k}^{-1}\, dt + \sqrt{2\, k_B\, T(\boldsymbol{x})}\, (\boldsymbol{\eta}^{1/2})_{i,j}\, dw_j(t) \tag{5.83}$$

From the fluctuation-dissipation relation extended to non-equilibrium steady thermal conditions, $\sum_{h=1}^{3} D_{i,h}\, \eta_{h,j} = k_B\, T(\boldsymbol{x})\, \delta_{i,j}$, it follows, for any $k = 1, 2, 3$, that

$$\begin{aligned} \sum_{h=1}^{3} \frac{\partial D_{i,h}}{\partial x_k}\, \eta_{h,j} + \sum_{h=1}^{3} D_{i,h}\, \frac{\partial \eta_{h,j}}{\partial x_k} &= k_B\, \frac{\partial T}{\partial x_k}\, \delta_{i,j} \\ \sum_{h=1}^{3} \frac{\partial D_{i,h}}{\partial x_k}\, \eta_{h,j} + k_B\, T(\boldsymbol{x}) \sum_{h=1}^{3} \eta_{i,h}^{-1}\, \frac{\partial \eta_{h,j}}{\partial x_k} &= k_B\, \frac{\partial T}{\partial x_k}\, \delta_{i,j} \end{aligned} \tag{5.84}$$

which implies

$$-k_B\, T(\boldsymbol{x}) \sum_{h,j=1}^{3} \eta_{i,h}^{-1}\, \frac{\partial \eta_{h,j}}{\partial x_k}\, \eta_{j,m} = \frac{\partial D_{i,m}}{\partial x_k} - k_B\, \frac{\partial T}{\partial x_k}\, \eta_{i,m}^{-1} \tag{5.85}$$

From the latter expression it follows that

$$-k_B\, T(\boldsymbol{x}) \sum_{h,j,k=1}^{3} \eta_{i,h}^{-1}\, \frac{\partial \eta_{h,j}}{\partial x_k}\, \eta_{j,k} = \sum_{k=1}^{3} \frac{\partial D_{i,k}}{\partial x_k} - \frac{1}{T(\boldsymbol{x})}\, \frac{\partial T}{\partial x_k}\, D_{i,k} \tag{5.86}$$

Therefore, eq. (5.82) becomes

$$dx_i = \left(\sum_{k=1}^{3} \frac{\partial D_{i,k}}{\partial x_k} \right) dt - \sum_{k=1}^{3} \frac{D_{i,k}}{T(\boldsymbol{x})}\, \frac{\partial T}{\partial x_k}\, dt + \sum_{k=1}^{3} \sqrt{2} (\boldsymbol{D}^{1/2})_{i,k}\, dw_k(t) \tag{5.87}$$

and the corresponding Fokker-Planck equations reads

$$\frac{\partial p_x}{\partial t} = \sum_{i,j=1}^{3} \frac{\partial}{\partial x_i} \left(\frac{D_{i,j}}{T}\, \frac{\partial T}{\partial x_j}\, p_x \right) + \sum_{i,j=1}^{3} \frac{\partial}{\partial x_i} \left(D_{i,j}\, \frac{\partial p_x}{\partial x_j} \right) \tag{5.88}$$

providing the occurrence of an additional convective contribution to the flux, depending on the temperature gradient, and equal to

$$\boldsymbol{J}_{\text{thermo}} = -\frac{\boldsymbol{D}}{T}\, \nabla T\, p_x \tag{5.89}$$

providing a thermophoretic velocity $\boldsymbol{v}_{\text{thermo}}$ equal to $-\boldsymbol{D}\, \nabla T / T$ [54]. This result shows that thermophoretic effects naturally follow from the accurate description of stochastic particle motion in thermal non-equilibrium conditions.

5.4 Wall singularities: superficial phenomena

In the previous Section, the physical problems associated with the setting of boundary conditions for transport equations in confined geometries due to the singularities of the entries of the resistance matrix has been outlined. The asymptotic trends of all the entries of $\boldsymbol{H}(\boldsymbol{x})$ of two smooth no-slip surfaces almost in contact, such as the case of a particle very close to a solid surface, has been studied by Cox [45] for any value of the walls' curvatures. From the Cox's lubrication analysis, it results that the drag force on a particle moving towards the wall is inversely proportional to gap between the surfaces (particle and wall surfaces). To simplify the analysis, let us focus on a spherical particle of radius R_p.

By considering a Cartesian reference system $(\hat{\boldsymbol{x}}_1, \hat{\boldsymbol{x}}_2, \hat{\boldsymbol{x}}_3)$ with the origin on the wall and with $\hat{\boldsymbol{x}}_3$ collinear to the axis passing between the two contact points of the two surfaces, the asymptotic trend of the resistance on the particle is $\eta_{3,3}(\boldsymbol{x}) \sim O(R_p/h)$ as $h/R_p \to 0$.

For example, the drag force on a sphere moving towards a planar wall can be expressed to the leading order by the Taylor approximation [47]

$$\eta_{3,3}(\boldsymbol{x}) = \frac{6\,\pi\,\mu\,R_p^2}{h} + O(1) \tag{5.90}$$

for small gaps h between sphere and planar wall. At larger distances, as seen in Chapter 4, the Lorentz friction [156] is

$$\eta_{3,3}(\boldsymbol{x}) = 6\,\pi\,\mu\,R_p \left(1 + \frac{9}{8}\frac{R_p}{h}\right) \tag{5.91}$$

and, since $9/8 \approx 1$, a reasonable approximation over the whole range of h values is given by

$$\eta_{3,3}(\boldsymbol{x}) = 6\,\pi\,\mu\,R_p \left(1 + \frac{R_p}{h}\right) \tag{5.92}$$

The singularity of $\eta_{3,3}(\boldsymbol{x})$ at the wall implies that a particle, initially at $h = h_0$ and moving towards the solid surface due to the action of a constant force F_g, say gravity, reaches the surface in an infinity time t_{surf}, being the integral

$$t_{\text{surf}} = \int_{h_0}^{0} \frac{\eta_{3,3}(h)}{F_g} dh \to \infty \tag{5.93}$$

divergent to infinity. The characteristic time t_{surf} is referred to as the wall touching time. This result poses severe problems in predicting the kinetics of coalescence and deposition of dispersed particles from hydrodynamic theories based on the Stokes model eq. (5.5). To complete the picture, let us consider the scaling behavior of the remaining resistance coefficients. As regards the other coefficients, they are all logarithmically singular as $O(\log(h))$ with the exception of the rotational resistance around the normal axis to the surfaces attaining a finite value close to the wall, i.e., $\eta_{6,6}(h) = O(1)$ as $h \to 0$. Singularities at a contact point between surfaces are typical of Stoke's flows due to the no-slip conditions at solid boundaries. For example, in contact line motions [64] and for flows near a corner [175] it has be found that unphysical singularities can be eliminated or mollified by introducing slippage at solid boundaries [63, 238]. Before addressing the effect of slip boundary conditions, it is useful to investigate further the pathologies arising from the classical no-slip hydrodynamic description in dealing with surface phenomena.

5.4.1 Surface phenomena and hydrodynamic singularities

All the surface phenomena (particle coalescence, surface aggregation, adsorption, surface chemical reactions) depending on a transfer mechanism of molecules and particles from the fluid phase onto the surface are deeply influenced by the spatial dependence of the entries of the hydrodynamic resistance matrix. Paradoxes arise due to the singularities of these entries at the solid walls (for incompressible flows, assuming no-slip boundary conditions at the solid boundaries).

In order to highlight these phenomena, it is sufficient to consider a simple problem, namely the pure diffusional motion of solute particles (nanoparticles) in the neighborhood of a solid wall (located at $x_3 = x = 0$), undergoing at the solid wall a surface chemical reaction characterized by a linear, first-order kinetics. To simplify the analysis, let us assume that far away from the wall, say at $x = L$, the particle concentration is kept fixed, and equal to c_0. The problem is thus specified by the parabolic diffusion equation for the particle concentration $c(x, t)$,

$$\frac{\partial c(x,t)}{\partial t} = \frac{\partial}{\partial x} \left(D(x) \, \frac{\partial c(x,t)}{\partial x} \right) \tag{5.94}$$

equipped with the boundary conditions

$$D(x) \, \frac{\partial c(x,t)}{\partial x} = k \, c(x,t) \bigg|_{x=0} \,, \quad c(L,t) = c_0 \tag{5.95}$$

Consider the steady-state solution $c^*(x)$ of eq. (5.94). From eq. (5.94) it follows that,

$$\frac{dc^*(x)}{dx} = \frac{B}{D(x)} \tag{5.96}$$

where B is a constant, and thus

$$c^*(x) = A + B \int_0^x \frac{d\xi}{D(\xi)} \tag{5.97}$$

where A is a second constant to be determined from the boundary conditions. From eq. (5.97) it follows that a solution exists provided that $1/D(x)$ is locally integrable near $x = 0$. But this is not the case when the hydrodynamic modeling deriving from incompressible Stokes equations imposing no-slip boundary conditions at the solid walls, as $1/D(x) \sim 1/x$.

On the other hand, in the case $1/D(x)$ would be locally integrable near $x = 0$, the steady-state solution $c^*(x)$ would attain the expression

$$c^*(x) = c_0 \, \frac{1 + k \, \Psi(x)}{1 + k \, \Psi(L)} \,, \qquad \Psi(x) = \int_0^x \frac{d\xi}{D(\xi)} \tag{5.98}$$

It is clear from the above problem that Stokes' hydrodynamics applied to transport phenomena coupled to any form of superficial chemical physical processes determines unphysical paradoxes. In the present case, the paradox can be resolved within a classical hydrodynamic formulation by deriving, from more general hydrodynamic conditions, a diffusion coefficient $D(x)$ that is integrable near $x = 0$, i.e., such that $D(x) \leq C/x^\alpha$, with $C > 0$ and $\alpha < 1$. Indeed, this property can be recovered by relaxing the no-slip boundary conditions as addressed in the next Section.

5.5 Effect of slip boundary conditions

Although the no-slip assumption, $\boldsymbol{u} = 0$, at the interface between a Newtonian fluid and a solid boundary is largely accepted due to its capability of predicting mechanical and hydrodynamical properties involving macroscopic bodies and large-scale systems, the nature of the proper boundary conditions for the tangential velocity at a solid interface has been a long-debated issue over more than two centuries of hydrodynamic research [88]. As an alternative to the no-slip hypothesis, Navier [179] proposed that the tangential stresses at any point on the solid surface should be the same as the stresses at a neighboring internal point of the fluid, providing the boundary condition

$$\beta\,(\boldsymbol{u} - \boldsymbol{v}) \cdot (I - \boldsymbol{n} \otimes \boldsymbol{n}) = -\boldsymbol{n} \cdot \boldsymbol{\tau} \cdot (I - \boldsymbol{n} \otimes \boldsymbol{n}) \tag{5.99}$$

where I is the identity matrix, $\boldsymbol{n}$, the unit normal vector to the surface of the solid, β a friction constant and "$\otimes$" indicates dyadic composition, $(\boldsymbol{n} \otimes \boldsymbol{n})_{i,j} = n_i\, n_j$. Since the isotropic pressure contribution entering $\boldsymbol{\tau}$ vanishes at the r.h.s of eq. (5.99), the Navier's boundary condition (5.99) can be written as

$$(\boldsymbol{u} - \boldsymbol{v}) \cdot (\boldsymbol{I} - \boldsymbol{n} \otimes \boldsymbol{n}) = \lambda \boldsymbol{n} \cdot (\nabla \boldsymbol{u} + \nabla \boldsymbol{u}^T) \cdot (\boldsymbol{I} - \boldsymbol{n} \otimes \boldsymbol{n}) \tag{5.100}$$

where $\lambda = \mu/\beta$, having the dimension of a length, is the so called slip length. It is evident that the slip length represents a new parameter in modeling Stokes flow. In fact, while the no-slip model describes an idealized fluid/solid interface, the slip model introduces an additional parameter related to the chemical physical interactions at the solid-liquid interface.

Slip phenomena can be distinguished in two main classes: intrinsic slip and apparent slip [145]. The first one is due exclusively to the molecular dynamics at the solid-liquid interface. The second one is due to artifacts at the surfaces that can increase or decrease the slippage, such as the presence of gas bubbles or the surface roughness. However, these artifacts have necessarily a characteristic length below which no-slip conditions applies. In addition, as shown by Cox [45], the nature of the singularity does not depend on the curvature of the approaching surfaces. In considering very small gaps between the surfaces ($h \to 0$), the apparent slip vanishes. Therefore, in the remainder, solely to the intrinsic (molecular) slip will be taking into account. The occurrence of slippage depends in principle, either on hydrodynamic conditions or on the gap length. In fact, as shown by molecular dynamic simulations [68], the slip length for the system (PA-6,6 oligomer)-graphene increases by increasing the shear rate and by reducing the gap between the solid walls. Being such behavior, due to the molecular rearrangement of the fluid, it is appreciable solely when the gap is small enough to be comparable with the characteristic size of the molecular structure of the fluid. However, at this lengthscale scale, it is not possible to mark a clear distinction between the solid surface and the domain of the fluid used in continuous hydrodynamic models, due to solvation and diffusive phenomena. Therefore, a constant slip length, used in hydrodynamic theories (and in the remainder), should be considered as a parameter emerging from the complexity of the molecular system. A review of typical slip lengths for several fluid-surface systems obtained experimentally is given in [145]. Non vanishing values of the slip length are in the range $\lambda = 1 \div 100nm$, whereas typical characteristic lengthscales of colloids are $R_p = 10 \div 10^4 nm$. Correspondingly, the dimensionless slip length for a colloid attains values in the range $\hat{\lambda} = 10^{-4} \div 10$.

Either the problems of translating or rotating sphere in an unbounded fluid have been solved by Basset [4] in the presence of the Navier's slip obtaining the following expressions for the force and the torque acting on the sphere

$$\boldsymbol{F}_{\text{hydro}} = -6\pi\mu R_p \left(\frac{1+2\hat{\lambda}}{1+3\hat{\lambda}}\right)\boldsymbol{v} \tag{5.101}$$

$$\boldsymbol{T}_{\text{hydro}} = -8\pi\mu R_p^3 \left(\frac{1}{1+3\hat{\lambda}}\right)\boldsymbol{\omega} \tag{5.102}$$

Being $\hat{\lambda} = 10^{-4} \div 10$, larger spherical particles experience the force and the torque corresponding to no-slip boundary conditions $\boldsymbol{F}_{\text{hydro}} \approx -6\,\pi\,\mu R_p \boldsymbol{v}$ and $\boldsymbol{T}_{\text{hydro}} \approx -8\,\pi\,\mu\,R_p^3\,\boldsymbol{\omega}$, whereas for smaller colloids the Basset's correction becomes necessary. For a particle in a confined geometry, the slip boundary conditions can be considered either at the surface of the particle (S_p), with a slip length λ_p, or at the surface of the walls (S_w) with a slip length λ_w. Therefore, the boundary conditions for the flow become

$$\begin{cases} (\boldsymbol{u}-\boldsymbol{v})\cdot(\boldsymbol{I}-\boldsymbol{n}\otimes\boldsymbol{n}) = \lambda_p \boldsymbol{n}\cdot(\nabla\boldsymbol{u}+\nabla\boldsymbol{u}^T)\cdot(\boldsymbol{I}-\boldsymbol{n}\otimes\boldsymbol{n}), & \boldsymbol{x}\in S_p \\ (\boldsymbol{u}-\boldsymbol{v})\cdot(\boldsymbol{I}-\boldsymbol{n}\otimes\boldsymbol{n}) = \lambda_w \boldsymbol{n}\cdot(\nabla\boldsymbol{u}+\nabla\boldsymbol{u}^T)\cdot(\boldsymbol{I}-\boldsymbol{n}\otimes\boldsymbol{n}), & \boldsymbol{x}\in S_w \end{cases} \tag{5.103}$$

5.5.1 Spherical particle moving perpendicular to a planar wall

Let us consider the problem of a spherical particle near a planar wall as depicted in Fig. 5.1. Hocking has shown [110] that, in the presence of the same slip on both the surfaces ($\lambda_p = \lambda_w = \lambda$), the touching time in eq. (5.93) becomes finite although the singularity of the transversal resistance at the wall still remains [110] . The functional dependence of the resistance to perpendicular translations on h in the limit $h \to 0$, derived by Hocking using lubrication methods, attains the form

$$\frac{\eta_{3,3}(\hat{h},\hat{\lambda})}{\eta_\infty} = \frac{1}{3\hat{\lambda}}\left[\left(1+\frac{\hat{h}}{6\hat{\lambda}}\right)\log\left(1+\frac{6\hat{\lambda}}{\hat{h}}\right)-1\right]+O(1) \tag{5.104}$$

where $\hat{h} = h/R_p$. Consequently, the drag force is logarithmically singular at the wall, eq. (5.91) becomes integrable and the touching time attains a finite value.

A seminalytical expression for the drag force over a sphere translating perpendicularly to a plane has been obtained by Goren [90] over the entire range of positions and for any values of λ_w and λ_p using a bispherical coordinate system. However, the author [90] has provided only few numerical values for $\hat{\eta}_{3,3}(\hat{h},\hat{\lambda})$ corresponding

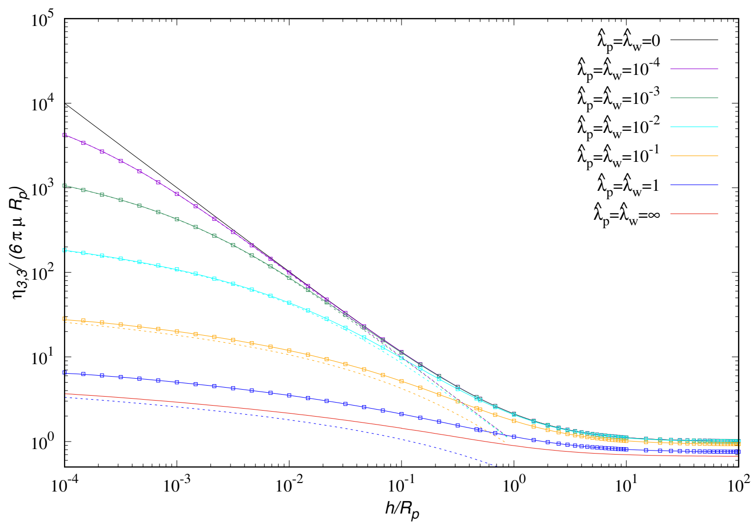

Figure 5.2. Dimensionless hydrodynamics resistance coefficient $\eta_{3,3}/(6\,\pi\,\mu\,R_p)$ vs h/R_p for equal slip lengths on the particle surface and on the wall. Each color in the figure corresponds to a different slip length as described in the inner legend. Continuous lines represent the results of the Goren's equations, dashed lines the values obtained by the Hocking's equation eq. (5.104), and symbols the results of FEM simulations.

to relatively large gaps and slip lengths, and considering solely the case $\lambda_w = \lambda_p$. In point of fact, in order to obtain the numeric values for the transversal resistance from the Goren's solution is in principle necessary to solve an infinite dimensional linear system of equations for any position of the sphere. On the other hand, the infinite linear system, truncated to a finite number N of equations, provides approximate but accurate values for the force experienced by the particle with an error that decreases as N increases, while the number of the equations from a fixed accuracy increases as $\hat{h} \to 0$ and the slip lengths increase.

In order to obtain the values of $\eta_{3,3}(\hat{h}, \hat{\lambda}_p, \hat{\lambda}_w)$ for different slip lengths and at any distance from the wall, it has been either performed FEM simulations, the detail of which are reported in the Appendix 5.6, or solved the Goren's equations up to $N = 500$. The data depicted in Fig. 5.2 show that the Hocking asymptotic equation (5.104) matches accurately the FEM simulations and the Goren solution in the range of $\hat{\lambda} = 0 \div 10^{-1}$ and that the predicted logarithmic scaling starts to appear for gaps smaller then the slip length ($\hat{h} \lesssim \hat{\lambda}$), after a transition zone, where $\eta_{3,3} \sim 1/\hat{h}$.

On the other hand, as depicted in Fig. 5.3, if the no-slip boundary condition is imposed on solely one of the surfaces, the singular scaling $\eta_{3,3} \sim 1/\hat{h}$ remains no matter the value of the slip length imposed on the other surface. In the latter conditions, three different regimes can be distinguished: (i) the scaling $\eta_{3,3} \sim 1/\hat{h}$ for $\hat{\lambda} \lesssim \hat{h} \lesssim 10^{-1}$, (ii) an apparent logarithmic behavior for $10^{-2}\hat{\lambda} \lesssim \hat{h} \lesssim \hat{\lambda}$ and (iii) the asymptotic regime where $\eta_{3,3} \sim 1/\hat{h}$ for $\hat{h} \lesssim 10^{-2}\hat{\lambda}$.

To complete the analysis the data in Fig. 5.4 show that, keeping fixed the slip length at one of the surfaces ($\hat{\lambda}_i = 10^{-3}$, $i = w, p$) and increasing the slip length on the other $\hat{\lambda}_j$, $j = p, w$, the logarithmic scaling occurs for $\hat{h} \lesssim \hat{\lambda}_j$. This means that an arbirarily small slip on both the surfaces is sufficient to determine an asymptotic

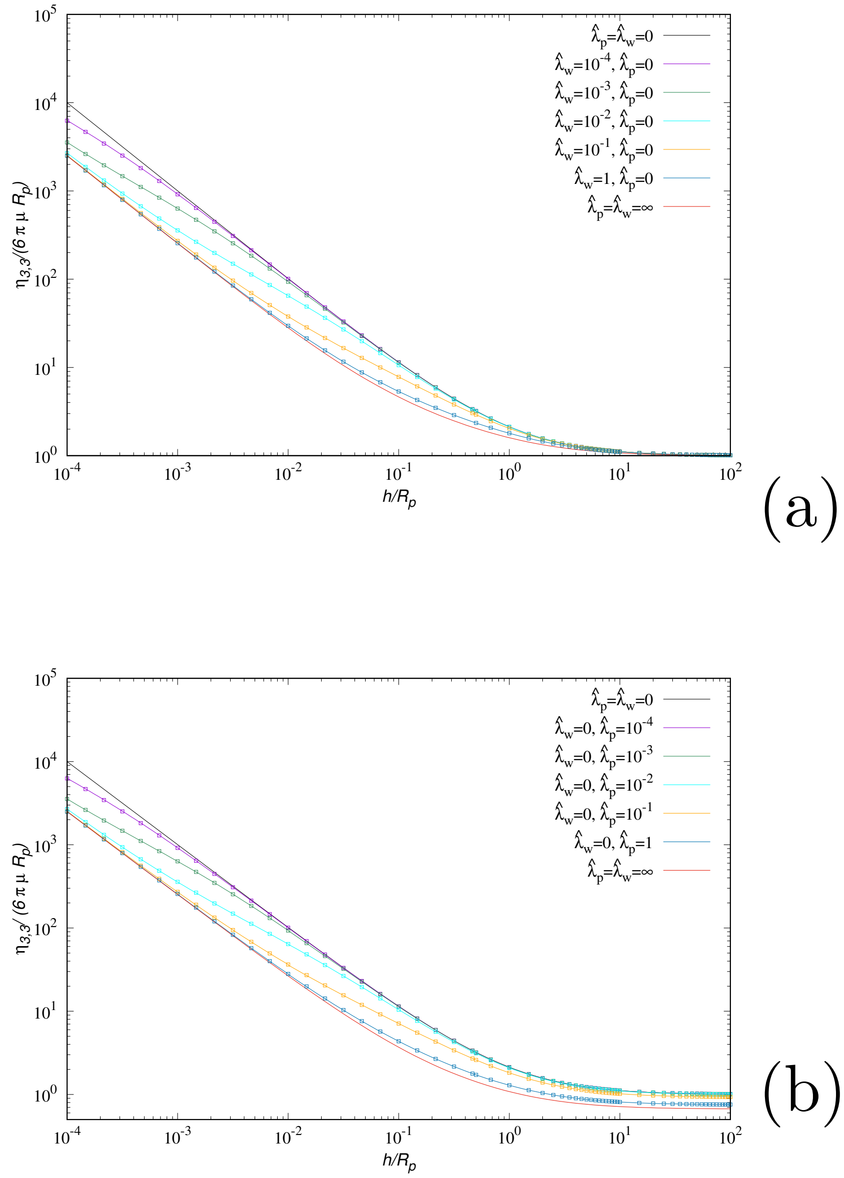

Figure 5.3. Dimensionless hydrodynamics resistance coefficient $\eta_{3,3}/(6\,\pi\,\mu\,R_p)$ vs h/R_p in the case no-slip boundary conditions are imposed at the surface of the sphere (panel a) or at the wall (panel b). Each color in the panels corresponds to a different combination of slip lengths λ_p, λ_w as described in the inner legends. Continuous lines represent the results of the Goren's equations, symbols the results of FEM simulations.

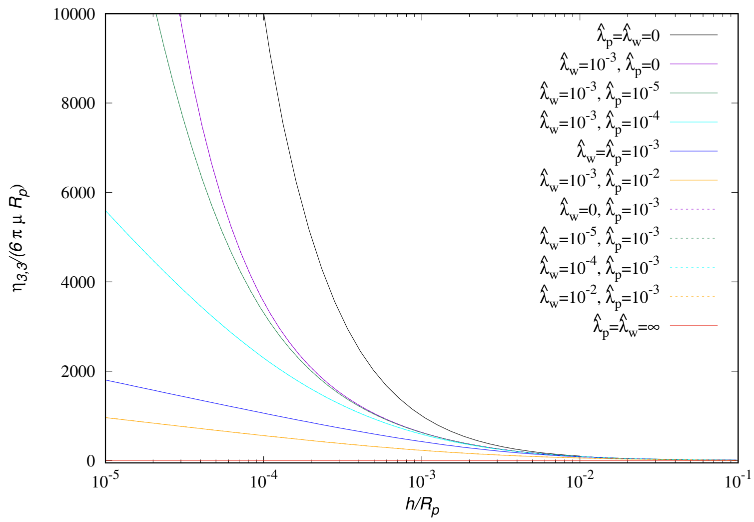

Figure 5.4. Dimensionless hydrodynamics resistance coefficient $\eta_{3,3}/(6\,\pi\,\mu\,R_p)$ vs h/R_p obtained by keeping fixed the slip length $\hat{\lambda}_i = \lambda_i/R_p = 10^{-3}$ on the i-th surface $(i = w, p)$ and varying the slip length on the other obtained by solving the Goren's equations. Observe that the curves corresponding to $i = w$ and $i = p$ practically overlap in this range of parameter values.

logarithmic scaling of the transversal resistance and thus the occurrence of a finite value of the touching time.

5.6 Fluid inertial effects

So far fluid-particle interaction within the instantaneous Stokes regime has been considered, neglecting fluid inertia. In point of fact, while the Reynolds number is smaller that 1 in most of the microfluidic applications, this is not the case of the product of the Reynolds number times the Strouhal number, which is order of 1 or higher due to the high frequency of the thermal fluctuations. This means that a more accurate description of particle motion at short time and length scales would involve a hydrodynamic description of fluid inertia, that in the present case corresponds to the time-dependent Stokes regime [138],

$$\rho \frac{\partial \boldsymbol{u}}{\partial t} = \mu \nabla^2 \boldsymbol{u} - \nabla p \tag{5.105}$$

with $\nabla \cdot \boldsymbol{u} = 0$.

It is well known that the force $\boldsymbol{F}_{\text{hydro}}(t)$ exerted by a fluid with density ρ and viscosity μ on a spherical particle of radius R_p moving with velocity $\boldsymbol{v}$ in a still fluid, can be expressed in the Laplace domain $\widehat{\boldsymbol{F}}_{\text{hydro}}(s) = L[\boldsymbol{F}_{\text{hydro}}(t)] = \int_0^\infty e^{-s\,t} \boldsymbol{F}_{\text{hydro}}(t)\, dt$ as [130]

$$\widehat{\boldsymbol{F}}_{\text{hydro}}(s) = -6\,\pi\,\mu\,R_p\,\widehat{\boldsymbol{v}}(s) - 6\,\pi\sqrt{\mu\,\rho}\,R_p^2\,\frac{1}{\sqrt{s}}\,(s\,\widehat{\boldsymbol{v}}(s)) - \frac{2}{3}\,\pi\,R_p^3\,\rho\,(s\,\widehat{\boldsymbol{v}}(s)) \tag{5.106}$$

The first term at the r.h.s of eq. (5.106) is the Stokesian friction factor, the second one corresponds in the time domain to the convolutional Basset force

$$\boldsymbol{F}_{\text{Basset}}(t) = -6\,\sqrt{\pi\,\mu\,\rho}\,R_p^2 \int_0^t \frac{1}{\sqrt{t-\tau}} \left(\frac{d\boldsymbol{v}(\tau)}{d\tau} + \boldsymbol{v}(0)\,\delta(\tau) \right) d\tau \tag{5.107}$$

and the third term is the added-mass contribution

$$\boldsymbol{F}_{\text{am}}(t) = -m_a \left(\frac{d\boldsymbol{v}(t)}{dt} + \boldsymbol{v}(0)\,\delta(t) \right), \qquad m_a = \frac{V_p\,\rho}{2} \tag{5.108}$$

where V_p is the particle volume, equal to half the mass of the fluid occupying the particle volume. Physically, the added mass contribution corresponds to the back action on the particle of the correlated motion of nearby fluid elements originated by the particle movement within the fluid [51]. In confined geometries, the added mass $\boldsymbol{m}_a(\boldsymbol{x})$ becomes a tensorial quantity dependent on particle position. For instance, for a spherical particle near a solid planar wall,

$$\boldsymbol{m}_a(\boldsymbol{x}) = \begin{pmatrix} m_1(h) & 0 & 0 \\ 0 & m_1(h) & 0 \\ 0 & 0 & m_2(h) \end{pmatrix} \tag{5.109}$$

where $m_1(h)$, and $m_2(h)$, corresponding to the parallel and transversal added masses, are smooth functions of the particle distance from the wall, as depicted in Fig. 5.5 attaining a finite value for $h = 0$. Similarly, the Basset contribution attains in confined geometries a tensorial, position-dependent character,

$$\boldsymbol{F}_{\text{Basset}} = \int_0^t \boldsymbol{B}(t-\tau, \boldsymbol{x})\, \frac{d\boldsymbol{v}(\tau)}{d\tau}\, d\tau \tag{5.110}$$

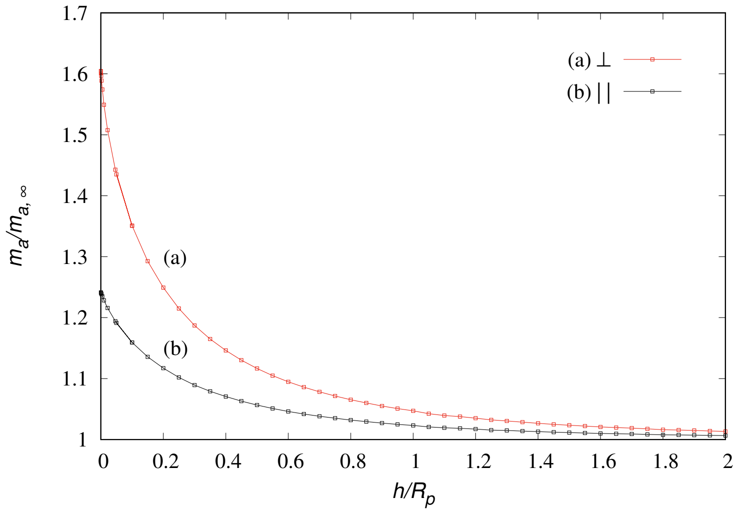

Figure 5.5. Ratio of the added mass m_a of a sphere moving perpendicular (m_2, red line) and parallel (m_1, black line) to a planar wall to that in an unbounded fluid $m_{a,\infty} = (2/3)\pi\rho R_p^3$ obtained by FEM simulations.

where $\boldsymbol{B}(t, \boldsymbol{x}) = (B_{i,j}(t, \boldsymbol{x}))_{i,j=1}^3$ and $\boldsymbol{x} = \boldsymbol{x}(t)$. There are very few works on the characterization of the Basset force in confined geometries [221], and the detailed study of fluid inertial effects in microchannels and in the presence of solid walls represents an almost virgin field of theoretical and experimental investigation.

Gathering these contributions, and considering also the action of a potential $\Phi(\boldsymbol{x})$ and of a flow force $\boldsymbol{F}_{\text{flow}} = \boldsymbol{\eta}(\boldsymbol{x})\,\boldsymbol{u}^{(p)}(\boldsymbol{x})$, deriving e.g. by a (pressure-drive) flow in the fluid, the equations of motion for a microparticle become,

$$
\begin{aligned}
\frac{d\boldsymbol{x}}{dt} &= \boldsymbol{v} \\
(m + \boldsymbol{m}_a(\boldsymbol{x}))\,\frac{d\boldsymbol{v}}{dt} &= -\boldsymbol{\eta}(\boldsymbol{x})\,(\boldsymbol{v} - \boldsymbol{u}^{(p)}(\boldsymbol{x})) - \nabla\Phi(\boldsymbol{x}) \\
&- \int_0^t \boldsymbol{B}(t-\tau, \boldsymbol{x}) \left(\frac{d\boldsymbol{v}(\tau)}{d\tau} - \frac{d\boldsymbol{u}^{(p)}(\boldsymbol{x}(\tau))}{d\tau} \right) + \boldsymbol{F}_{\text{stocha}}(\boldsymbol{x}, t)
\end{aligned}
\tag{5.111}
$$

where $\boldsymbol{F}_{\text{stocha}}(\boldsymbol{x}, t)$ is the stochastic fluctuational contributions, to be determined by enforcing fluctuation-dissipation relations. But also this aspect, owing to the explicit dependence of $\boldsymbol{F}_{\text{stocha}}(\boldsymbol{x}, t)$ on the position $\boldsymbol{x}$, represents a challenging problem in statistical physics, especially if one is interested in determining the velocity autocorrelation function.

Fortunately, for $t \gg t_{\text{diss}}$, corresponding to typical conditions in microfluidic applications, the fluid inertia can be neglected, and the stochastic description of particle motion can be based on the theory addressed in Sections 5.2,5.3.

In the next Chapter, the Basset contribution to the dynamic of a particle in a Newtonian and non-Newtonian fluid will be addressed in more detail, investigating the mathematical form of the kernel in eq. (5.110) and developing a modal representation able to simplify computation and theoretical analysis.

Appendix - Details on the FEM simulations

The software COMSOL Multiphysics 5.4 has been used to perform FEM simulations. To take computational advantage from the axial symmetry of the problem of a sphere translating perpendicularly to a planar wall, for obtaining the coefficient $\eta_{3,3}$ in eq. (5.33), cylindrical coordinates (r, ϕ, z) have been used in a two dimensional (r, z) square domain representing the fluid domain, with an empty disk, representing the spherical particle, possessing unit radius placed at distance h from planar wall.

The length of the sides of the square has been chosen much larger than the characteristic length of the physical problem ($L \geqslant \max(10^3 h, 10R_p)$), so that their presence does not affect the resistance on the sphere, and a no-slip boundary condition has been imposed on these sides. Conversely, on the perimeter of the disk and on the nearest side (representing the planar wall), Navier's slip conditions eq. (5.103) have been imposed to solve the Stokes' problem eq. (5.5).

A finer mesh has been set on the perimeter of the disk representing the sphere, and the maximal length of the elements has been imposed to be less than $0.1R_p$. A quadratic shape order has been set to model the curvature of the circle and a double boundary layer with thickness about $0.005\,R_p$ has been built around the circle, representing the surface of the sphere. The mesh in the square (fluid domain) has been modeled by imposing two different zones: a nearest zone of linear size $10R_p$ with a maximum growth rate of the finite elements equal to 1.1, and an exterior zone with a higher growth rate of about 2. Both P2P1 and P3P2 finite elements have been used depending on the position of the particle. Figure 5.6 reports the data of the error analysis. The reference data for checking the numerical simulations are those of a no-slip particle moving parallel to a slip plane wall reported by Kezirian [125], obtained by the author solving the Stokes' equations in bi-spherical coordinates. These data, to the best of our knowledge, are the only exact results regarding this kind of problem available in the literature. The percentage error has been evaluated by the relation

$$\%error = 100\left|\frac{\eta_{1,1}^{Com} - \eta_{1,1}^{Kez}}{\eta_{1,1}^{Kez}}\right| \tag{5.112}$$

where $\eta_{1,1}^{Com}$ refers to numerical simulations and $\eta_{1,1}^{Kez}$ to the data by [125]. Fig. 5.6 reports this comparison in three different cases. The data obtained by P2P1 element are accurate ($\%error < 1$) for gaps larger than the radius of the particle. For smaller gaps, the dimension of the box can be considerably reduced since the total force depend principally on the hydrodynamic field in the gap. In this near field zone, pressure field is the leading term in the evaluation of the stress tensor [110]. Correspondingly, an improvement of the evaluation of the pressure field, obtained by non linear elements P3P2, yields accurate results with a percentage error less then 1%.

The same parameters have been used for building both the geometry and the mesh for evaluating the added mass of a sphere moving near a plane wall. In this case, the fluid model used is a potential flow,

$$\nabla \cdot \boldsymbol{u}(\boldsymbol{x}) = 0, \qquad \boldsymbol{u}(\boldsymbol{x}) = \nabla\phi(\boldsymbol{x}), \qquad \boldsymbol{x} \in D_f \tag{5.113}$$

Therefore, for a given position of the sphere, three Laplace equations (one for each

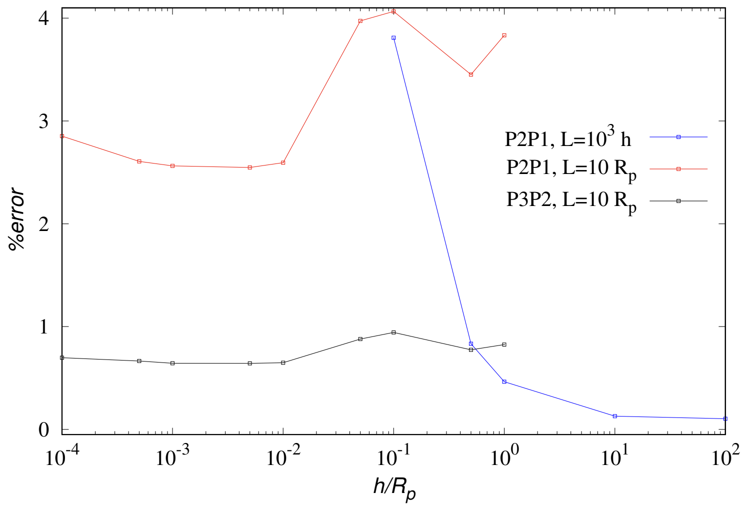

Figure 5.6. Percentage error (5.112) of the FEM results for $\eta_{1,1}$ with respect to the data obtained by Kezirian [125] for a no-slip sphere translating parallel to a planar wall with slip length $\lambda_w/R_p = 10^4$.

Cartesian axis $i = 1, 2, 3$)

$$\nabla^2 \phi_{(i)}(\boldsymbol{x}) = 0 \tag{5.114}$$

has been solved by using Lagrangian quadratic elements, with the impermeability boundary conditions

$$\boldsymbol{n} \cdot \nabla \phi_{(i)}(\boldsymbol{x}) = \boldsymbol{n} \cdot \boldsymbol{v}_{(i)}, \qquad \boldsymbol{x} \in S_p \tag{5.115}$$

where $\boldsymbol{n}$ is the normal unit vector to the sphere and $\boldsymbol{v}_{(i)}$ the velocity of the particle in the i-th direction. The entries of the added-mass matrix have been evaluated as [80],

$$\frac{m_{a,ij}}{m_{a,\infty}} = \frac{\int_{S_p} \phi_{(i)} n_j dS}{\frac{2}{3}\pi R_p^3} \tag{5.116}$$

Chapter 6

Complex flows and modal representation of the intertial kernels

6.1 Introduction

Microfluidics and the study of fluid–particle interactions at a microscale represent not only a vast area of practical engineering applications [213, 93] as they provide the opportunity of addressing fundamental physical questions in fluid dynamics [27, 107, 200], such as the relevance of acoustic propagation in liquid hydrodynamics [255, 39, 83], the nature of the boundary conditions and the occurrence of slip effects [146, 147, 174], as well as the role of the finite propagation velocity in the evolution of internal stresses [83, 82].

A significant role in this research is played by the study, both theoretical and experimental, of Brownian motion, i.e., of the motion of micrometric particles in a quiescent fluid. This is due to the fact that Brownian motion is a central problem in statistical physics, from the early age of Einstein, Langevin, Smoluchowski, Perrin, [67, 141, 224, 37] up to now [17, 74], providing a direct way of quantifying the influence of thermal fluctuations and of studying the interactions between a fluid and a particle, thus permitting the investigation of the role and the relative relevance of different hydrodynamic effects. In this sense, Brownian motion represents an invaluable probe to verify experimentally fundamental fluid dynamic properties at short time and length scales [172, 174].

The last two decades have seen an increasing attention on the experimental analysis of Brownian motion at short time scales in different fluids (gases and liquids) [206, 127, 73, 205], with different rheological properties (Newtonian, viscoelastic) [92]. The experimental results have confirmed many predictions of the hydrodynamic theory of Brownian motion [254, 242, 34], and in some cases have raised fundamental questions involving basic principles of statistical mechanics [173].

The analysis of the velocity autocorrelation function of a micrometric particle in a liquid phase has shown the importance of fluid inertial contributions, expressed by the occurrence of the Basset force and of the added-mass term [51] in the expression of the force exerted by a fluid on a rigid object [73, 205]. These terms arise in the low-Reynolds number hydrodynamics, using the time-dependent Stokes equations, and provide a power-law decay of the particle velocity autocorrelation function [92], to be compared with the exponential decay occurring if solely the Stokesian drag is considered [134]. Indeed, the use of the time-dependent Stokes equation, instead of the instantaneous Stokes formulation, is well justified and appropriate when addressing micrometric particle motion in liquids at short time scale, due to the high frequencies characterizing thermal fluctuations. Consequently, while the Reynolds number is extremely small in these systems, the product of the Reynolds number times the Strouhal numbers is order of unity, justifying the inclusion of the inertial contribution expressed as the time derivative of the velocity in the hydrodynamic equations. In the case of viscoelastic fluids, characterized by time-dependent constitutive equations, this statement is a fortiori valid.

The rheological modeling of complex viscoelastic fluids is well consolidated as regards the quantitative description of viscoelastic properties [159]. As regards the dynamics of a microparticle, this corresponds to the formulation of a generalized Langevin equation with a dissipative memory kernel [252, 177, 253]. This class of equations has been introduced by Zwanzig in connection with the interaction of a physical system with a heat bath, and the fluctuation–dissipation theorem for this class of systems has been obtained by Kubo [133]. On the other hand, the hydrodynamic analysis of Brownian motion and the numerical simulation experiments by Alder and Wainwright [1] have clearly indicated that fluid inertial contributions are of paramount importance in order to correctly predict particle dynamics.

The current approach to particle motion in complex fluids is essentially based on the direct hydrodynamic simulation of particle motion [65, 52]. What is missing is a physically consistent and computationally tractable formulation of particle dynamics in viscoelastic fluids, analogous to the corresponding equation of motion (which includes Stokes friction, the Basset force and the added mass effect) that apply for Newtonian ones. These equations can be derived into two steps: (i) via the detailed characterization of the fluid inertial contribution to particle motion in a complex fluid, expressing it in a computationally effective representation, and (ii) by generalizing the Kubo fluctuation–dissipation theory in order to include fluid-inertial contributions. In this thesis, the focus is essentially on the first issue.

Albeit the present analysis is focused on the hydrodynamic theory of particle motion, its application to microfluidic engineering for particle separation and nanoparticle production and optimization is significant. Indeed, the obtained result could be directly applied to the design of microfluidic systems enforcing the rheological properties of complex fluids in the limit of Stokesian hydrodynamics. In point of fact, the importance of inertial effects and rheological properties in separation devices is well known, e.g., in connection with the Segré-Silberberg effect [218, 52], although this effect involves flows at non-vanishing Reynolds numbers [107, 108].

The aim of this contribution is two-fold. A first goal involves the development of the modal representation of the fluid inertial contributions in the expression of the particle equation of motion in a fluid phase. This naturally leads to a simple field-theoretical representation of these effects. The second goal involves the mathematical structure of the inertial memory kernels entering the convolutional representation of the Basset forces, and their basic qualitative properties derived from fundamental physical principles. Specifically, it is shown that for any viscoelastic fluid (and all the liquids fall in this category, even if their characteristic relaxation times could be extremely small), the inertial memory kernel accounting for the generalized Basset contribution is bounded and non-singular near time $t = 0$.

The chapter is organized as follows. Section 6.2 introduces the hydrodynamic problem, the representation of fluid inertial effects and their implications in microparticle dynamics. Section 6.3 analyzes the modal representation of the Basset force, and its compact description in terms of a simple field equation. Moreover, it is shown in Section 6.3.2 that the modal representation also provides an efficient computational tool to study inertial particle motion. This is an important topic that recently emerged in the fluid-dynamic literature [142, 189, 195] in connection with the numerical solution of the Maxey–Riley equation [167] (see also [95] and references therein). Specifically, the modal expansion transforms the integro-differential equations of motion into a system of ordinary differential equations. Section 6.4 addresses the boundedness of the resulting memory kernels in the presence of viscoelastic constitutive equations, outlining the physical and computational relevance of this result. For a simple Maxwell fluid, the expression of this kernel is obtained in closed form, and a general method for approximating it for generic complex viscoelastic fluids is proposed. Finally, Section 6.4.3 describes the connection between the present theory and the generalization of the Kubo fluctuation–dissipation theory to include fluid inertial effects in the stochastic equations of motion for a microparticle in a heat bath at constant temperature.

6.2 Fluid–Particle Interactions and Inertial Effects

Consider the motion of a micrometric rigid spherical particle of radius R in a unbounded incompressible fluid. Assume that the fluid is Newtonian, and ρ and μ represent its density and viscosity, respectively. Let D_b be the domain representing the space occupied by the particle, ∂D_b its boundary and $\boldsymbol{U}_p(t)$ its translational velocity. Since it is considered the motion of a Brownian particle in a still liquid (the liquid is referred to be still if its velocity field originates exclusively from thermal motion of the immersed Brownian particle), the momentum balance equation for the particle reads

$$m\,\frac{d\boldsymbol{U}_p(t)}{dt} = \boldsymbol{F}_{f\to p}[\boldsymbol{U}_p(t)] + \boldsymbol{S}(t) \tag{6.1}$$

where $\boldsymbol{F}_{f\to p}[\boldsymbol{U}_p(t)]$ represents the force exerted by the fluid on the particle, and is a functional of the particle velocity, expressed by the surface integral over ∂D_b,

$$\boldsymbol{F}_{f\to p}[\boldsymbol{U}_p(t)] = -\int_{\partial D_b} (\boldsymbol{\tau}(\boldsymbol{x},t) + p(\boldsymbol{x},t)\,\boldsymbol{I})\cdot \boldsymbol{n}(\boldsymbol{x})\,dS \tag{6.2}$$

where, in this Chapter, $\boldsymbol{\tau}$ is the shear stress tensor, p the pressure, $\boldsymbol{I}$ the identity matrix and $\boldsymbol{n}(\boldsymbol{x})$ is the unit normal vector (considering a reference system with the origin at the center of the spherical particle) and $\boldsymbol{S}(t)$ is a stochastic contribution describing the thermal force fluctuation.

Indicating with $\boldsymbol{v}(\boldsymbol{x},t)$ the fluid velocity field, in the low-Reynolds number regime it is the solution of the time-dependent Stokes equations

$$\rho \, \frac{\partial \boldsymbol{v}(\boldsymbol{x},t)}{\partial t} = -\nabla \cdot \boldsymbol{\tau} - \nabla p(\boldsymbol{x},t) \,, \qquad \nabla \cdot \boldsymbol{v}(\boldsymbol{x},t) = 0 \,, \;\; \boldsymbol{x} \in \mathbb{R}^3/D_b \tag{6.3}$$

equipped with the no-slip boundary and initial conditions,

$$\boldsymbol{v}(\boldsymbol{x},t)|_{\boldsymbol{x}\in\partial D_b} = \boldsymbol{U}_p(t) \,, \qquad \boldsymbol{v}(\boldsymbol{x},t)|_{t=0} = 0 \tag{6.4}$$

Equation (6.4) corresponds to the no-slip assumption. For an incompressible Newtonian fluid,

$$\boldsymbol{\tau}(\boldsymbol{x},t) = -\mu \left(\nabla \boldsymbol{v}(\boldsymbol{x},t) + \nabla \boldsymbol{v}^t(\boldsymbol{x},t) \right) \tag{6.5}$$

so that eq. (6.3) is a linear partial differential equation for $\boldsymbol{v}(\boldsymbol{x},t)$ (the time-dependent Stokes equation)

$$\rho \, \frac{\partial \boldsymbol{v}(\boldsymbol{x},t)}{\partial t} = \mu \, \nabla^2 \boldsymbol{v}(\boldsymbol{x},t) - \nabla p(\boldsymbol{x},t) \tag{6.6}$$

where, from eq. (6.3), the velocity field $\boldsymbol{v}(\boldsymbol{x},t)$ is incompressible. Owing to the linearity of eqs. (6.5) and (6.6), the functional $\boldsymbol{F}_{f\to p}[\boldsymbol{U}_p(t)]$ is a linear and causal functional of the particle velocity $\boldsymbol{U}_p(t)$. Causality means that $\boldsymbol{F}_{f\to p}[\boldsymbol{U}_p(t)]$ depends solely on the velocity history in the interval $[0,t)$.

Under these conditions, the force exerted by the fluid onto the rigid spherical particle can be expressed analytically. Let us indicate with $\widehat{\boldsymbol{F}}_{f\to p}(s)$ the Laplace transform of $\boldsymbol{F}_{f\to p}[\boldsymbol{U}_p(t)]$ (henceforth, $\widehat{f}(s) = \int_0^\infty e^{-s\,t} f(t)\, dt$ indicates the Laplace transform of any function $f(t)$ of time t, and s the complex-valued Laplace variable), $\widehat{\boldsymbol{F}}_{f\to p}(s)$ attains the expression [130, 98]

$$-\widehat{\boldsymbol{F}}_{f\to p}(s) = 6\,\pi\,\mu\,R_p\,\widehat{\boldsymbol{U}}_p(s) + 6\,\pi \sqrt{\frac{\rho\,\mu}{s}}\, R_p^2 \left(s\,\widehat{\boldsymbol{U}}_p(s) \right) + \frac{2}{3}\,\rho\,\pi\,R_p^3 \left(s\,\widehat{\boldsymbol{U}}_p(s) \right) \tag{6.7}$$

Transforming Equation (6.7) back into the time domain, one obtains

$$\begin{aligned} \boldsymbol{F}_{f\to p}[\boldsymbol{U}_p(t)] &= -6\,\pi\,\mu\,R_p\,\boldsymbol{U}_p(t) \\ &-6\,\sqrt{\pi\,\rho\,\mu}\,R_p^2 \int_0^t \frac{1}{\sqrt{t-\tau}} \left(\frac{d\boldsymbol{U}_p(\tau)}{d\tau} + \boldsymbol{U}_p(0)\,\delta(\tau) \right) d\tau - \frac{2}{3}\,\rho\,\pi\,R_p^3\,\frac{d\boldsymbol{U}_p(t)}{dt} \end{aligned} \tag{6.8}$$

where $\boldsymbol{U}_p(0)$ is the initial condition for the particle velocity at $t=0$. The first term at the r.h.s. of eq. (6.8) is the Stokes resistance addressed in detail in the previous Chapters of this thesis, with the factor for a sphere $\eta = 6\,\pi\,\mu\,R$, corresponding to the only dissipative term occurring also in the case of the instantaneous Stokes regime. The two other contributions at the r.h.s. stem from fluid inertial effects, and depend on the history of particle acceleration up to time t. The first of these terms is the convolutional integral of $d\boldsymbol{U}_p(t)/dt$ with the kernel $k(t)$ given by

$$k(t) = \frac{6\,\sqrt{\pi\,\rho\,\mu}\,R_p^2}{\sqrt{t}} \tag{6.9}$$

and it is usually referred to as the Basset force. Let us observe that kernel $k(t)$ is singular at $t=0$. This property will be thoroughly analyzed in Section 6.4. The last term at the r.h.s. of eq. (6.8) is an instantaneous inertial contribution proportional to the actual value (i.e., at time t) of the acceleration $d\boldsymbol{U}_p(t)/dt$ of the particle, and it defines the hydrodynamic added mass $m_a = 2\rho\pi R_p^3/3$, equal to half of the mass of the fluid displaced by the particle [138]. Let us observe within the Basset term the occurrence of a contribution proportional to $\boldsymbol{U}_p(0)\delta(\tau)$, in the case $\boldsymbol{U}_p(0) \neq 0$. eq. (6.8) can be compactly written as

$$m_e \frac{d\boldsymbol{U}_p(t)}{dt} = -\eta \boldsymbol{U}_p(t) - k(t) * \left(\frac{dU_p(t)}{dt} + U_p(0)\,\delta(t) \right) + \boldsymbol{S}(t) \tag{6.10}$$

where $m_e = m + m_a$ is the extended mass and "$*$" indicates convolution. The physical importance of the Basset contribution can be appreciated by considering the velocity autocorrelation tensor of a Brownian particle, $\boldsymbol{C}_v(t) = \langle \boldsymbol{U}_p(t) \otimes \boldsymbol{U}_p(0) \rangle$, where "$\otimes$" indicates the dyadic tensor product and "$\langle\cdot\rangle$" the ensemble average over the probability measure of the thermal fluctuations. Since $\langle \boldsymbol{S}(t) \otimes \boldsymbol{U}_p(0) \rangle = 0$, as it is physically reasonable to assume that the thermal fluctuations $\boldsymbol{S}(t)$ at time $t \geq 0$, are independent of (uncorrelated to) the velocity fluctuations at any previous time instant $t = 0$ [134, 133] (this principle is by some authors referred to as the principle of causality [169], and it essentially states the non-anticipativity of the action of thermal fluctuations as regards its effects on the particle velocity), by taking the tensorial product of both members of eq. (6.10) and averaging over the statistics of thermal fluctuations (the operations of time derivative and convolution commute with $\langle\cdot\rangle$), one obtains the evolution equation for $\boldsymbol{C}_v(t)$,

$$m^* \frac{d\boldsymbol{C}_v(t)}{dt} = -\eta \boldsymbol{C}_v(t) - k(t) * \left(\frac{d\boldsymbol{C}_v(t)}{dt} + \boldsymbol{C}_v(0) \right) \tag{6.11}$$

equipped with the isotropic initial condition

$$\boldsymbol{C}_v(0) = \langle U^2 \rangle \boldsymbol{I} \tag{6.12}$$

where $\langle U^2 \rangle$ is the squared variance of any entry $U_{p,h}(t)$, $h = 1, 2, 3$ of the particle velocity vector (proportional at thermal equilibrium to the temperature of the fluid). Therefore, due to this symmetry, the velocity autocorrelation function can be expressed as $\boldsymbol{C}_v(t) = \langle U^2 \rangle\, c_v(t)\, \boldsymbol{I}$, where the scalar function $c_v(t)$ satisfies eq. (6.11) with $c_v(0) = 1$. The occurrence of the Basset contribution determines a qualitative change in the long-term scaling of $c_v(t)$ with respect to the purely dissipative case (corresponding to considering the fluid motion in an instantaneous Stokes flow). In the latter case, the long-term decay is exponential, i.e., $c_v(t) = e^{-\eta\, t/m}$ while inertial effects induce an asymptotic power-law scaling $c_v(t) \sim t^{-\gamma}$, with $\gamma = 3/2$ in the free space [133, 92].

The application of eq. (6.10) in the Lagrangian analysis of particle motion, in the case the kernel $k(t)$ attains the Basset form expressed by eq. (6.9), raises three main issues:

- A computational issue, as the presence of a convolution in the equations of motion implies that the entire history of $\boldsymbol{U}_p(t)$ over the time interval $[0, t)$ should be stored in order to evaluate it;
- An analytical issue, associated with the singularity of the Basset kernel $k(t)$ at $t = 0$;

- A physical issue, related to the determination of the stochastic force $\boldsymbol{S}(t)$, in the case that inertial effects are accounted for.

The first problem is analyzed in the next section, in terms of modal representations. The second one is treated on physical grounds in Section 6.4. The last point, related to the determination of $\boldsymbol{S}(t)$, is one of the main issues of fluctuation–dissipation theories [134, 133]. To the best of our knowledge, a computationally valid approach to the determination of $\boldsymbol{S}(t)$ in the presence of the Basset term is lacking, although formal results have been proposed [11].

6.3 Modal Representation

The idea behind modal representations lies in the expression of the fluid inertial memory term entering the particle equation of motion as a linear superposition of elementary stochastic modes, susceptible of a simple evolution. The diction "stochastic" is used in this context, to pinpoint the fact that since $\boldsymbol{S}(t) \neq 0$, the velocity $\boldsymbol{U}_p(t)$ is itself a stochastic process, as well as any other process functionally dependent on $\boldsymbol{U}_p(t)$.

Let us consider eq. (6.10), and without loss of generality let us set $\boldsymbol{U}_p(0) = 0$. Since the problem of Brownian motion in the free space is isotropic, it is possible exclusively consider a scalar formulation of it, setting $U_p(t)$ instead of $\boldsymbol{U}_p(t)$. Let us assume in the remainder that the stochastic representation of $S(t)$ (replacing $\boldsymbol{S}(t)$ as a scalar formulation is considered) is known.

Consider a family of stochastic processes $y(t;\lambda)$ parameterized with respect to $\lambda \in [0, \infty)$ and fulfilling the equations

$$\frac{dy(t;\lambda)}{dt} = -\lambda\, y(t,\lambda) + q\, \frac{dU_p(t)}{dt} \tag{6.13}$$

where q is a constant to be determined. Let us suppose $y(t=0;\lambda) = 0$ so that

$$y(t;\lambda) = q \int_0^t e^{-\lambda\,(t-\tau)}\, \frac{dU_p(\tau)}{d\tau}\, d\tau \tag{6.14}$$

The inertial memory kernel can be expressed as a linear superposition of these processes. To this end, let $p(\lambda)$ the probability density of occurrence of $y(t;\lambda)$, so that $p(\lambda)\, d\lambda$ represents the infinitesimal weight factor in the representation of the memory inertial contribution. Thus, the particle equation of motion can be expressed as

$$m^* \frac{dU_p(t)}{dt} = -\eta\, U_p(t) - \underbrace{q \int_0^\infty p(\lambda)\, y(t;\lambda)\, d\lambda}_{I} + S(t) \tag{6.15}$$

The integral I entering eq. (6.15) can be rewritten in convolutional form as

$$I = \int_0^t \left[q \int_0^\infty p(\lambda)\, e^{-\lambda(t-\tau)}\, d\lambda \right] \frac{dU_p(\tau)}{d\tau}\, d\tau = k_p(t) * \frac{dU_p(t)}{dt} \tag{6.16}$$

thus defining the kernel $k_p(t)$.

Let us assume for $p(\lambda)$ the following expression

$$p(\lambda) = \begin{cases} A\,\lambda^{-1/2} & \lambda < \lambda_c \\ 0 & \text{otherwise} \end{cases} \tag{6.17}$$

where $\lambda_c > 0$, and A is the normalization constant such that $\int_0^\infty p(\lambda)\,d\lambda = 1$. In this case, setting $z = \lambda_c\,t$,

$$k_p(t) = \frac{q\,A}{\sqrt{t}} \int_0^{\lambda_c\,t} \frac{e^{-z}}{\sqrt{z}}\,dz \tag{6.18}$$

Let us observe that $k_p(0) = q$, while for $t > 0$, and for large λ_c, $\lambda_c t$ can be approximated by an infinite value, and thus

$$k_p(t) = \frac{q\,A}{\sqrt{t}} \int_0^{\infty} \frac{e^{-z}}{\sqrt{z}}\,dz = \frac{q\,A\,\pi}{\sqrt{t}} \tag{6.19}$$

The constant q can be always defined in order to match the asymptotics of the Basset kernel eq. (6.9). Therefore, the modal expansion eq. (6.15) provides an inertial kernel that does not match the singular behavior of the Basset kernel near $t = 0$, but still represents an excellent approximation of it for t large enough. The regularity of the inertial kernel will be questioned in the next section starting from physical arguments.

If one is interested in obtaining exactly the modal expansion for the Basset kernel, a slightly different parameterization can be chosen by considering the modes $y(t;k)$, $k \in [0,\infty)$, still satisfying the linear relaxation dynamics eq. (6.13), with the relaxation rates $\lambda = \lambda(k)$ depending quadratically on the parameter k, i.e.,

$$\lambda(k) = \lambda_0\,k^2 \tag{6.20}$$

with $\lambda_0 > 0$, consequently,

$$y(t;k) = q \int_0^t e^{-k^2(t-\tau)} \frac{dU_p(\tau)}{d\tau}\,d\tau \tag{6.21}$$

Assuming that all the modes at different ks concur uniformly in the expansion of the inertial force, i.e., that the weight function does not have a probabilistic meaning, the integral I in the k-representation becomes

$$I = \int_0^\infty y(t;k)\,dk = k_k(t) * \frac{dU_p(t)}{dt}\,, \qquad k_k(t) = q \int_0^\infty e^{-\lambda_0\,k^2 t}\,dk \tag{6.22}$$

providing

$$k_k(t) = \frac{q}{2}\sqrt{\frac{\pi}{\lambda_0\,t}} \tag{6.23}$$

and thus the parameters q and λ_0 can be always determined in order to exactly match the Basset kernel eq. (6.9).

6.3.1 Diffusional Field Representation

The quadratic spectral representation based on the dispersion relation eq. (6.20) suggests the Basset inertial term could be viewed as the consequence of the interaction of diffusional models associated with a scalar field with the particle. It is therefore interesting to further develop this field approach.

Let $u(x,t)$ be a scalar field of fluctuations, evolving according to a pure diffusion equation over the real line, perturbed by an impulsive forcing term $F(x,t)$

$$\frac{\partial u(x,t)}{\partial t} = \alpha \, \frac{\partial^2 u(x,t)}{\partial x^2} + F(x,t) \tag{6.24}$$

with $\alpha > 0$ and

$$F(x,t) = \delta(x - x_c)\, f(t) \tag{6.25}$$

where $f(t)$ is a generic function of time. The forcing $F(x,t)$ represents the action of the particle onto the field (corresponding to the fluid continuum) while the scalar field $u(x,t)$ represents the fluid flow. Set $u(x,t=0)=0$, the solution of eqs. (6.24) and (6.25) can be expressed in terms of the diffusional Green function as

$$\begin{aligned} u(x,t) &= \int_0^t d\tau \int_{-\infty}^{\infty} \frac{1}{\sqrt{4\,\pi\,\alpha\,(t-\tau)}} e^{-(x-x')^2/4\,\alpha\,(t-\tau)} F(x',\tau)\, d\tau \\ &= \int_0^t \frac{1}{\sqrt{4\,\pi\,\alpha\,(t-\tau)}} e^{-(x-x_c)^2/4\,\alpha\,(t-\tau)}\, f(\tau)\, d\tau \end{aligned} \tag{6.26}$$

Let $u_c(t) = u(x=x_c,t)$. From eq. (6.26) it follows that

$$u_c(t) = \frac{1}{\sqrt{4\,\pi\,\alpha}} \int_0^t \frac{f(\tau)}{\sqrt{t-\tau}}\, d\tau \tag{6.27}$$

which admits the same functional form of the Basset memory integral. This formal result has also been obtained in [195] (see also [95]), with a different approach, and with a purely computational motivation. Below, going beyond the pure mathematical formalism, the main interest is provide a physical interpretation of the field representation of the Basset force.

Let us consider a one-dimensional approximation of the momentum exchange between the fluid, with velocity $v(x,t)$, and the particle, with velocity $U_p(t)$. This can be modeled by considering a one-dimensional moment balance equations in the fluid of purely diffusional nature

$$\rho \, \frac{\partial v(x,t)}{\partial t} = \mu \, \frac{\partial^2 v(x,t)}{\partial x^2} + f(x,t) \tag{6.28}$$

where $f(x,t)$ is the force density exerted by the particle onto the fluid which can be written as an impulsive contribution centered at the particle center of mass x_c,

$$f(x,t) = \rho \, L_c \, \delta(x - x_c) \, \frac{dU_p(t)}{dt} \tag{6.29}$$

where, from dimensional analysis, the parameter L_c has the dimension of a length, and corresponds to length scale of inertial influence, in the fluid, due to the perturbation induced by the motion of the particle. From physical reasons, L_c is of the order of magnitude of the particle radius, and the choice

$$L_c = D = 2R_p \tag{6.30}$$

where D is the particle diameter, provides, as shown below, the correct value of L_c matching the Basset force. The inertial force exerted by the fluid onto the particle $F^{(i)}_{f\to p}$ can be viewed as a dissipative Stokesian contribution evaluated at the fluid velocity $v_c(t)$,

$$F^{(i)}_{f\to p} = -6\,\pi\,\mu\,R_p\,v_c(t) \tag{6.31}$$

Comparing Equations (6.24) and (6.25) with eqs. (6.28)–(6.30), and making use of eq. (6.27), it follows that

$$v_c(t) = \sqrt{\frac{\rho}{4\,\pi\,\mu}}\,D\int_0^t \frac{1}{\sqrt{t-\tau}}\,\frac{dU_p(\tau)}{d\tau}\,d\tau \tag{6.32}$$

and from eq. (6.31) one finally obtains

$$F^{(i)}_{f\to p} = -6\,\pi\,\mu\sqrt{\frac{\rho}{4\,\pi}}\,D\,R_p\,\frac{1}{\sqrt{t}} * \frac{dU_p(t)}{dt} = -6\,\sqrt{\pi\,\rho\,\mu}\,R_p^2\,\frac{1}{\sqrt{t}} * \frac{dU_p(t)}{dt} \tag{6.33}$$

that is exactly the Basset force. This result is physically interesting and requires some interpretation. It indicates that the inertial Basset contribution can be viewed as the inertial dissipation of the fluid elements nearby the solid particle, due to the perturbation exerted by the particle onto the fluid itself. This physical interpretation bears some analogies with Darwin's description of fluid inertial effects [51]. The fact that a scalar model correctly describes the fluid inertial effects onto particle dynamics is a remarkable property, as the fluid hydrodynamics involves vectorial entities, the velocity field $\boldsymbol{v}(\boldsymbol{x}, t)$, subjected to constraints, in the present case the solenoidal nature of $\boldsymbol{v}(\boldsymbol{x}, t)$, stemming from the incompressibility of a liquid phase, corresponding to the case of principal theoretical and engineering interest. Whether this would be a purely mathematical result, or a deeper physical property is a matter leaven open to future investigation. Interpreted on physical grounds, this result indicates that the fluid inertial contributions to the dynamics of immersed bodies are completely independent of the compressibility of the fluid. If this observation would be correct, it follows that in any isotropic problems, as the particle motion is in a unbounded fluid phase, a scalar field model would correctly describe the physics of a fluid–particle inertial interaction. This situation is altogether similar to the properties of the other inertial contribution, namely the added-mass term, which is independent of the constitutive equations in the fluid, and for this reason it can be estimated from the inviscid (Eulerian) approximation of the flow [138].

6.3.2 A Numerical Case Study

Let us consider the modal expansion in Equations (6.20)–(6.22) and its discretization with respect to k. Let $k_{\max}$ be the maximum value of k considered, and Δk the step size in the discretization. Assuming $q = 2/\sqrt{\pi}$, for the sake of normalization, the

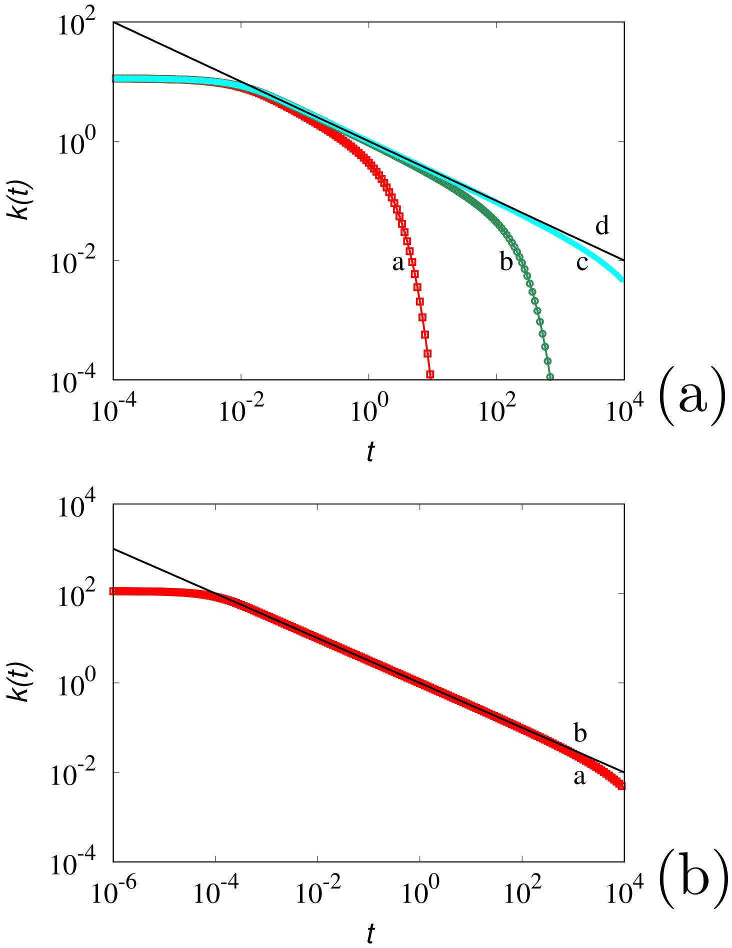

Figure 6.1. Behavior of the discretized $k_k(t)$ defined by eq. (6.34) for different discretizations. Panel (**a**) refers to $k_{\max} = 10$, lines and symbols (a) to (c) correspond to $\Delta k = 1,\ 0.1,\ 0.01$, respectively. Line (d) represents $k_\infty(t) = 1/\sqrt{t}$. Panel (**b**) $k_{\max} = 100$, $\Delta k = 0.01$ (line a), while line (b) depicts $k_\infty(t)$.

expression for $k_k(t)$ becomes

$$k_k(t) = \frac{2\,\Delta k}{\sqrt{\pi}} \sum_{i=1}^{N} e^{-(i\,\Delta k)^2\,t} \tag{6.34}$$

where $N = [k_{\max}/\Delta k]$ and $[x]$ represents the closest integer to the real-valued x. In the limit for $\Delta k \to 0$, and $k_{\max} \to \infty$, $k_k(t)$ defined by eq. (6.34) converges to $k_\infty(t) = 1/\sqrt{t}$. Figure 6.1a depicts the behavior of the discretized $k_k(t)$ at $k_{\max} = 10$ for decreasing values of Δk. As expected, as Δk decreases to zero, the deviations of $k_k(t)$ from $k_\infty(t)$ become negligible for $t > 1/k_{\max}^2$.

Similarly, the value of $k_{\max}$ controls the convergence to $k_\infty(t)$ at short time scales. Figure 6.1b depicts the behavior of $k_k(t)$ at $k_{\max} = 100$, $\Delta k = 0.01$. An accurate representation for $k_\infty(t)$ is achieved for $t > 10^{-4}$. The analysis of these data indicates that $k_{\max}$ controls the behavior of $k_k(t)$ near $t = 0$, which reaches a finite limiting value $k(0) \simeq k_{\mathrm{kmax}}$. This property seems to be a basic limitation of any discretization of the Basset force. In point of fact, as shown in the next section, the occurrence of a bounded value of $k_k(0)$ is a physical constraint derived from the viscoelastic nature of a liquid phase. And all the fluid, including water at room temperature, possesses a characteristic non vanishing relaxation time.

Consider eq. (6.10) for a macroscopic particle (radius greater than a millimeter or higher), for which the stochastic fluctuations could be neglected. Substituting on it the modal expansion eq. (6.34), it is obtained

$$\begin{aligned} m_e \frac{d\boldsymbol{U}_p(t)}{dt} &= -\eta \boldsymbol{U}_p(t) - \frac{2\,\beta\,\Delta k}{\sqrt{\pi}} \sum_{i=1}^{N} e^{-(i\,\Delta k)^2\,t} * \left(\frac{d\boldsymbol{U}_p(t)}{dt} + U_p(0)\,\delta(t) \right) \\ &= -\eta \boldsymbol{U}_p(t) - \frac{2\,\beta\,\Delta k}{\sqrt{\pi}} \sum_{i=1}^{N} \boldsymbol{z}_i(t) \end{aligned} \tag{6.35}$$

where $\beta = 6\,\sqrt{\pi\,\rho\,\mu}\,R_p^2$, as it stems from eq. (6.9), and $\boldsymbol{z}_i(t)$, $i = 1, \ldots, N$ is a system of N auxiliary degrees of freedom accounting for fluid inertial effects, the equations for which read

$$\begin{aligned} \frac{d\boldsymbol{z}_i(t)}{dt} &= -\mu_i\,\boldsymbol{z}_i(t) + \frac{d\boldsymbol{U}_p(t)}{dt} \\ &= -\left(\mu_i + \eta\right)\,\boldsymbol{z}_i(t) - \frac{2\,\beta\,\Delta k}{\sqrt{\pi}} \sum_{i=1}^{N} \boldsymbol{z}_i(t) \end{aligned} \tag{6.36}$$

where $\mu_i = (i\,\Delta k)^2$, and the impulsive initial contribution has been included into the initial condition for $\boldsymbol{z}_i(0) = \boldsymbol{U}_p(0)$.

Eq. (6.35) represents a major advantage of the model expansion compared to the more recent computational approaches for addressing inertial particle motion [95], as it reduces the integro-differential particle equations of motion to a system of ordinary differential equations that can be solved using standard numerical routines. The analysis here presented for a quiescent fluid can be straightforwardly extended to the presence of a macroscopic (e.g., pressure-driven) velocity field in the fluid phase.

6.4 Regularity of Inertial Kernels

The second main issue addressed in this contribution concerns the regularity of the inertial memory kernels $k(t)$, once basic physical requirements (such as the bounded propagation of any physical phenomenon, limited by the speed of light vacuo, as a consequence of relativity theory) are taken into account. In Section 6.2, it is shown that the Basset kernel diverges at $t = 0$, as seen in eq. (6.9). As explained below, this is a consequence of the infinite propagation velocity of the internal stresses that characterize the Newtonian constitutive eq. (6.5). This phenomenon is altogether analogous to the divergence of interfacial fluxes in heat/mass transfer parabolic problems in the presence of a discontinuity between the initial and the boundary conditions at a boundary. This problem can be resolved by removing the paradox of infinite propagation velocity intrinsic to any

Fickian/Fourier constitutive equation, simply considering the hyperbolic extension of the transport problem [81].

In the hydrodynamic case, the corresponding hyperbolic generalization merely consists in accounting for fluid viscoelasticity, which is a generic property of any liquid phases. In point of fact, even water at ambient conditions (temperature $T = 300$ K, pressure $p = 10^5$ Pa) behaves as a viscoelastic fluid, but its characteristic relaxation time, $\theta^c \simeq 1$ ps [49, 186], is so small that it can be neglected in the overwhelming majority of hydrodynamic problems, since the observation time scales in most of the practical cases of interest are widely larger than θ^c.

To begin with, let us consider the case of a viscoelastic fluid characterized by a single relaxation time θ^c (Maxwell fluid). Neglecting the nonlinear terms in the objective definition of the viscoelastic constitutive equation involving the Oldroyd upper convective derivative [159] (which are small for the typical conditions of Brownian and micrometric particles in microchannels), eq. (6.5) is replaced by the following viscoelastic constitutive equation:

$$\theta^c \frac{\partial \boldsymbol{\tau}}{\partial t} + \boldsymbol{\tau} = -\mu \left(\nabla \boldsymbol{v} + \nabla \boldsymbol{v}^T \right) \tag{6.37}$$

that in the Laplace domain takes the following simple expression:

$$\widehat{\boldsymbol{\tau}}(\boldsymbol{x}, s) = -\widehat{\mu}_e(s) \left[\nabla \widehat{\boldsymbol{v}}(\boldsymbol{x}, s) + \nabla \widehat{\boldsymbol{v}}(\boldsymbol{x}, s)^T \right] \tag{6.38}$$

where

$$\widehat{\mu}_e(s) = \frac{\mu}{\theta^c \, (s + 1/\theta^c)} \tag{6.39}$$

Consequently, the Laplace transform of $\widehat{\boldsymbol{F}}_{f \to p}(s)$ of the force subjected by the particle is still given by eq. (6.7), with the constant viscosity μ replaced by the function $\widehat{\mu}_e(s)$. As well known, this modifies the instantaneous dissipative Stokesian friction $\boldsymbol{F}^{(d)}_{f \to p}[\boldsymbol{U}_p(t)] = -\eta \, \boldsymbol{U}_p(t)$ into a memory term

$$\boldsymbol{F}^{(d)}_{f \to p}[\boldsymbol{U}_p(t)] = -\eta \, \frac{1}{\theta^c} \int_0^t e^{-(t-\tau)/\theta^c} \, \boldsymbol{U}_p(\tau) \, d\tau \tag{6.40}$$

while the inertial Basset term attains in the Laplace domain the form $-\widehat{k}(s) \, s \widehat{\boldsymbol{U}}_p(s)$ with

$$\widehat{k}(s) = \frac{\beta}{\sqrt{\theta^c}} \, \frac{1}{\sqrt{s \, (s + 1/\theta^c)}} \tag{6.41}$$

where $\beta = 6 \, \pi \sqrt{\rho \, \mu} \, R_p^2$. It is easy to see that the presence of a non-vanishing relaxation time $\theta^c > 0$ determines a finite value of $k(t)$ for $t = 0$. Enforcing the initial value theorem of Laplace transforms, it is obtained from eq. (6.41)

$$\lim_{t \to 0} k(t) = \lim_{s \to \infty} s \, \widehat{k}(s) = \frac{\beta}{\sqrt{\theta^c}} \tag{6.42}$$

In point of fact, the inverse Laplace transform of $\widehat{k}(s)$ is given by

$$k(t) = \frac{\beta}{\sqrt{\theta^c}} \, e^{-t/2\theta^c} \, I_0 \left(\frac{t}{2 \, \theta^c} \right) \tag{6.43}$$

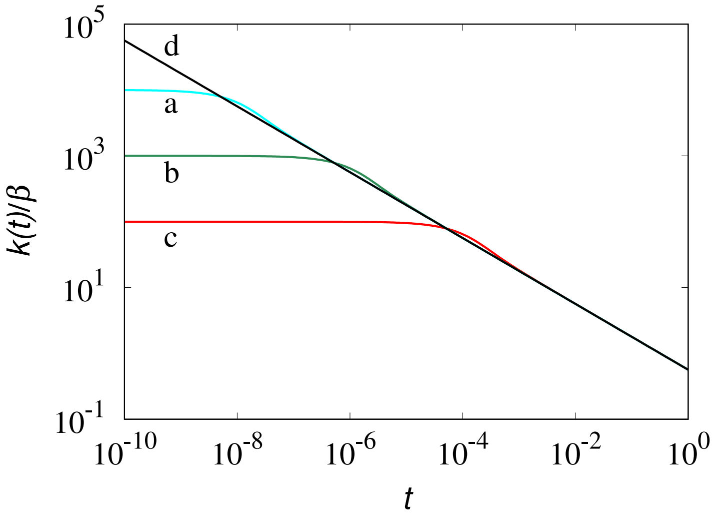

Figure 6.2. Rescaled inertial kernel $k(t)/\beta$, eq. (6.41) vs t for a simple Maxwell fluid, characterized by the relaxation time θ^c. Lines (a) to (c) refer to $\theta^c = 10^{-4}$, 10^{-6}, 10^{-8}, respectively. Line (d) depicts the asymptotic nondimensional Basset curve, $k(t)/\beta = 1/\sqrt{\pi\, t}$.

where $I_0(\xi)$ is the modified Bessel function of the first kind, which possesses the following asymptotic behaviors:

$$I_0(0) = 1\,, \qquad I_0(\xi) = \frac{e^{\xi}}{\sqrt{2\,\pi\,\xi}}\left[1 + O\left(\frac{1}{\xi}\right)\right] \tag{6.44}$$

From eq. (6.44), the asymptotics of the Newtonian Basset kernel is recovered for $t \gg \theta^c$. This phenomenon is depicted in Figure 6.2 for several values of θ^c. The viscoelastic kernel practically coincides with the Basset counterpart of a Newtonian fluid for $t > 5\,\theta_c$.

The occurrence of a finite value for $k(0)$ has been observed in Newtonian fluids once slip boundary conditions are enforced at the surface of the solid particle [78, 198, 199]. The physical reason for this occurrence, and the eventual analogy with the viscoelastic case, is still an open question.

6.4.1 Field-Theoretical Analysis

The result expressed by eq. (6.43) can be recovered from the field approach addressed in the previous section. The presence of viscoelastic effects characterized by a single relaxation time θ^c implies to substitute the parabolic diffusion model eq. (6.28) with the hyperbolic Cattaneo equation

$$\rho\,\theta^c \frac{\partial^2 v(x,t)}{\partial t^2} + \rho\,\frac{\partial v(x,t)}{\partial t} = \mu\,\frac{\partial^2 v(x,t)}{\partial x^2} + f(x,t) \tag{6.45}$$

while $f(x,t)$ is identical to eq. (6.29). The solution of this impulsive model, with $v(x,0) = \partial v(x,t)/\partial t|_{t=0} = 0$, takes the following form (see [191], p. 320):

$$v(x,t) = \frac{1}{2}\sqrt{\frac{\rho\,\theta^c}{\mu}}\,\frac{D}{\theta_c}\int_0^t e^{-(t-\tau)/2\,\theta^c}\, I_0\left(\frac{1}{2\,\theta^c}\sqrt{(t-\tau)^2-(x-x_c)^2\,\rho\,\theta^c/\mu}\right)\frac{dU_p(\tau)}{d\tau}\,d\tau \tag{6.46}$$

that for $x = x_c$, and $t \geq \tau$ reduces to

$$v_c(t) = \frac{1}{2}\sqrt{\frac{\rho}{\mu\,\theta^c}}\,D\int_0^t e^{-(t-\tau)/2\,\theta^c}\, I_0\left(\frac{t-\tau}{2\,\theta^c}\right)\frac{dU_p(\tau)}{d\tau}\,d\tau \tag{6.47}$$

providing the same expression for $k(t)$ derived above, as seen in eq. (6.43).

6.4.2 Extension to Complex Fluids

The analysis developed above for a viscoelastic fluid possessing a single relaxation time can be generalized to more complex and real fluids. The problem can be stated as follows. Consider a real fluid and suppose to have obtained from rheological experiments the functional form of the dissipation memory kernel $G(t)$ entering the expression of the dissipative contribution to the force exerted by the fluid on a spherical particle

$$\boldsymbol{F}^{(d)}_{f\to p}[\boldsymbol{U}_p(t)] = -6\,\pi\,R_p\int_0^t G(t-\tau)\,\boldsymbol{U}_p(\tau)\,d\tau \tag{6.48}$$

Does this information provide a way to quantify the inertial contribution, and specifically the expression for the generalized Basset force in this fluid?

This problem can be tackled as follows. The convolutional nature of eq. (6.48) suggests that the constitutive equation for the shear stresses is of the form

$$L_t[\boldsymbol{\tau}] = -\mu\,\left(\nabla\boldsymbol{v} + \nabla\boldsymbol{v}^T\right) \tag{6.49}$$

where L_t is a linear operator acting on the stress tensor $\boldsymbol{\tau}$, and containing its derivatives of any order n, $n = 0, 1, \ldots$, with respect to time, and eventually also its fractional time derivatives (Riemann–Liouville operators) [182]. In the Laplace domain, eq. (6.49) becomes

$$\widehat{\ell}(s)\,\widehat{\boldsymbol{\tau}}(\boldsymbol{x},s) = -\mu\,\left[\nabla\widehat{\boldsymbol{v}}(\boldsymbol{x},s) + \nabla\widehat{\boldsymbol{v}}(\boldsymbol{x},s)^T\right] \tag{6.50}$$

where $\widehat{\ell}(s)$ is a function of the Laplace variable s. eq. (6.50) coincides with eq. (6.38), and $\widehat{\mu}_e(s)$, coinciding with $\widehat{G}(s)$, is now expressed by

$$\widehat{\mu}_e(s) = \frac{\mu}{\widehat{\ell}(s)} = \widehat{G}(s) \tag{6.51}$$

The analysis developed above for a Maxwell fluid can be applied to this more general problem, providing for the Laplace transform of the inertial memory kernel the following expression:

$$\widehat{k}(s) = 6\,\sqrt{\rho}\,R_p^2\sqrt{\frac{\widehat{G}(s)}{s}} \tag{6.52}$$

The inverse Laplace transform $k(t)$ of $\widehat{k}(s)$ defined by eq. (6.52) cannot be obtained analytically for generic $\widehat{G}(s)$. Nevertheless, it is always possible to derive accurate representations for $k(t)$ enforcing eq. (6.52).

In order to make a practical example, consider the rheological data for polydimethilsiloxane at $T = 25$ °C reported in [159], for which an accurate representation involves the occurrence of $N = 5$ relaxation rates λ_h, $h = 1, \dots, N$,

$$G(t) = \sum_{h=1}^{N} a_h \, e^{-\lambda_h \, t} \tag{6.53}$$

where $\lambda_h = 1/\theta_h^c$, $h = 1, \dots, N$ are the relaxation rates i.e., the reciprocal of the relaxation times θ_h^c. The values for λ_h and for the expansion coefficients a_h can be found in [159] (p. 114), and the graph of the resulting $G(t)$ is depicted in Figure 6.3a. Applying eq. (6.52) to this case

$$\widehat{k}(s) = \alpha \sqrt{\frac{1}{s} \sum_{h=1}^{N} \frac{a_h}{s + \lambda_h}} \, , \qquad \alpha = 6 \, \pi \, \sqrt{\rho} \, R_p^2 \tag{6.54}$$

The graph of $k^*(s) = \widehat{k}(s)/\alpha$ is depicted in Figure 6.3b (symbols). The data can be accurately approximated over the time scales of interest by a linear combination of the inertial contributions obtained for the simple Maxwell fluid eq. (6.41), each of which is characterized by a different relaxation time

$$k^*(s) = \sum_{h=1}^{N_i} \frac{c_h}{\sqrt{s \, (s + b_h)}} \tag{6.55}$$

Making use of eq. (6.43), the memory inertial kernel $k(t)$ is given in this case by the expression

$$k(t) = \alpha \sum_{h=1}^{N_i} c_h \, e^{-b_h \, t/2} \, I_0 \left(\frac{b_h \, t}{2} \right) \tag{6.56}$$

For the use made above of the solutions obtained for the simple Maxwell fluid, each term of the form (6.41) in the Laplace domain, and (6.43) in the time domain, can be referred to as a "prototypical visco-inertial mode". In the present case, it is sufficient to consider the combination of $N_i = 2$ prototypical visco-inertial modes, and the resulting approximation is depicted in Figure 6.3b. The values of the parameters are $c_1 = 125$ a.u., $b_1 = 1.52$ s^{-1}, $c_2 = 420$ a.u., $b_2 = 65$ s^{-1}. The corresponding inertial memory kernel $k(t)$, i.e., the graph of eq. (6.56), is depicted in Figure 6.4.

From this practical example, it is possible draw the following conclusions:

1. Enforcing the constitutive model eq. (6.49), corresponding to the rheological description of a complex viscoelastic fluid, it is possible to derive the functional form of the fluid inertial kernel $k(t)$ from rheological data, i.e., from the functional form of $G(t)$;

2. The fluid inertial kernel $k(t)$ can be expressed as linear combination of a few prototypical visco-inertial modes;

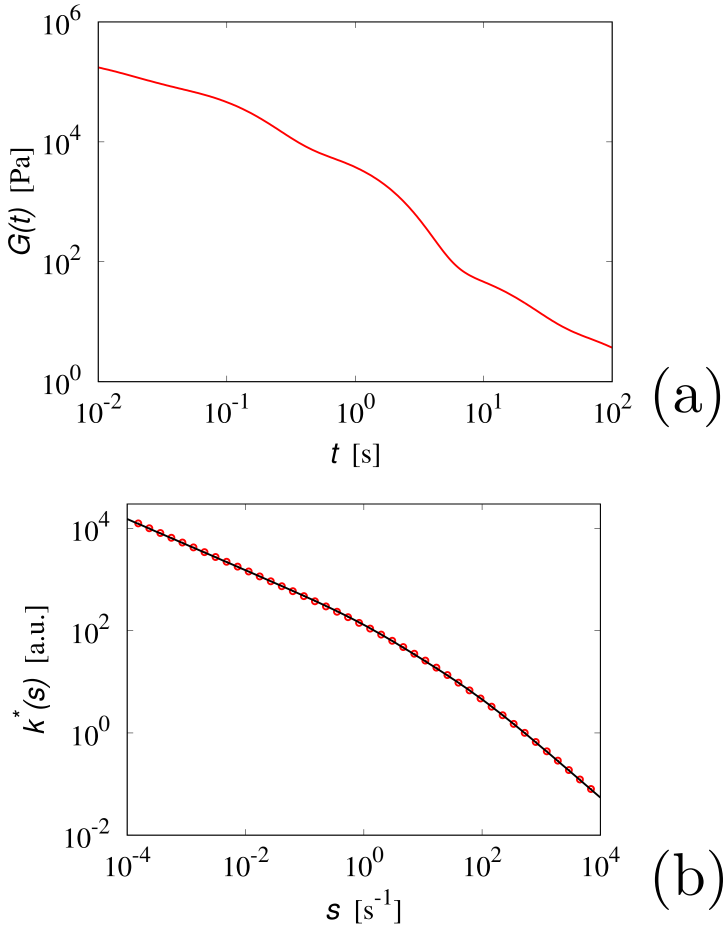

Figure 6.3. Panel (**a**) $G(t)$ vs t for polydimethilsiloxane at $T = 25$ °C. Panel (**b**) (symbols) $k^*(s) = \widehat{k}(s)/\alpha$ vs s for the same fluid, obtained from eq. (6.54). The solid line is the approximation of these data using $N_i = 2$, prototypical visco-inertial modes, as discussed in the main text.

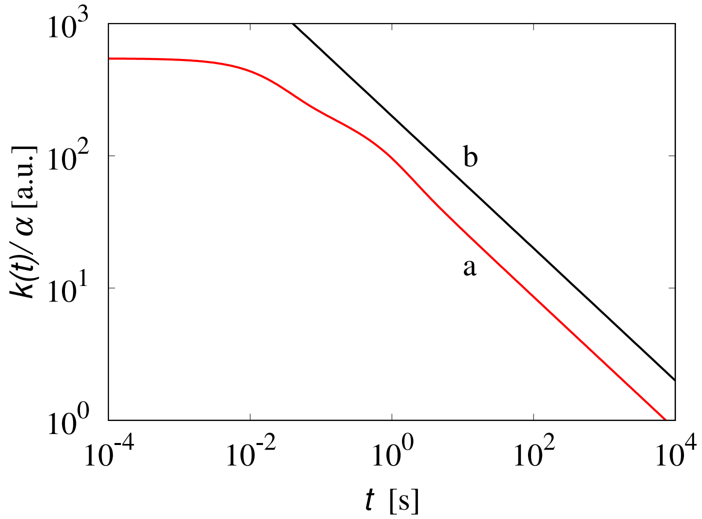

Figure 6.4. $k(t)/\alpha$ (line a) obtained from eq. (6.56) with $N_i = 2$ modes. Line (b) corresponds to the long-term scaling $k(t)/\alpha \sim 1/\sqrt{t}$.

3. The number N_i of modes required to provide an accurate representation of $k(t)$ does not necessarily coincide with the number N of dissipative (exponential) modes adopted for reconstructing $G(t)$.

Of course, it is possible to provide alternative representations of $k(t)$, e.g., adopting the modal decomposition discussed in Section 6.3. While for an accurate representation of the classical Basset kernel, a uncountable system of exponentially decaying modes is required, the physical constraint of bounded $k(t)$ permits to achieve accurate approximation for $k(t)$ using a finite (and relatively small) number of exponentially decaying modes.

6.4.3 Toward a Comprehensive Theory of Brownian Motion

To conclude, it is possible frame another central issue that takes advantage of the present theory. For a microparticle in a quiescent fluid (Brownian particle), the equations of motions in a real complex fluid, accounting for viscoelastic dissipation, fluid inertial effects and thermal fluctuations can be expressed in the form

$$m_e \frac{d\boldsymbol{U}_p(t)}{dt} = -h(t) * \boldsymbol{U}_p(t) - k(t) * \left(\frac{d\boldsymbol{U}_p(t)}{dt} + \boldsymbol{U}_p(0)\, \delta(t) \right) + \boldsymbol{S}(t) \tag{6.57}$$

where $h(t)$ is the viscoelastic kernel proportional to $G(t)$ defined by the linear functional form eq. (6.53), and $k(t)$ is the corresponding fluid inertial kernel, the properties of which have been addressed in the previous section. From rheological data, the viscoelastic kernel can be expressed as a linear combination of N modes, where usually $N < 10$ for most of the fluids [159], i.e., $h(t) = \sum_{j=1}^{N} h_j\, e^{-\lambda_j\, t}$. In a similar way, the fluid inertial kernel $k(t)$ analyzed in the previous section can also be accurately approximated by means of a system of exponentially decaying modes,

$$k(t) \simeq \sum_{i=1}^{N_i} k_i\, e^{-\mu_i\, t} \tag{6.58}$$

where the rates $\mu_i > 0$, $i = 1, \ldots, N_i$, are in general not related to the relaxation rates λ_j, $j = 1, \ldots, N$ and $N_i \gg N$. The property that $k(0)$ is bounded ensures, as discussed in the previous section, that the approximation eq. (6.58) can be arbitrarily accurate in the metrics of continuous functions. This means that for any $\varepsilon > 0$, there exist a finite N_i, and finite rates $\mu_i > 0$, $i = 1, \ldots, N_i$, such that $\left| k(t) - \sum_{i=1}^{N_i} k_i \, e^{-\mu_i \, t} \right| < \varepsilon$ for any $t \geq 0$. Consequently, eqs. (6.57) reduce to the form

$$m_e \, \frac{d\boldsymbol{U}_p(t)}{dt} \quad = \quad -\sum_{j=1}^{N} h_j \, e^{-\lambda_j \, t} * \boldsymbol{U}_p(t) - \sum_{i=1}^{N_i} k_i \, e^{-\mu_i \, t} * \left(\frac{d\boldsymbol{U}_p(t)}{dt} + \boldsymbol{U}_p(0) \, \delta(t) \right) + \boldsymbol{S}(t) \tag{6.59}$$

In order to solve these stochastic differential equations, the expression for $\boldsymbol{S}(t)$ should be determined, and it would constitute the generalization of the celebrated Kubo fluctuation–dissipation theorem of the second kind [133, 134], of which the original formulation is restricted to the pure dissipative case (i.e., to $k(t) = 0$). The analysis of this problem is beyond the scope of this contribution. However, the occurrence of a finite value of $k(0)$, coupled with the modal expansion of the memory kernels ($h(t)$ and $k(t)$) could provide a key physical and formal ingredients toward an elegant solution of this problem.

Conclusions

Starting from the elaboration and re-adaptation of results and methods in the analysis of particle motion in Stokes flows pioneered at the beginning of the 19th century by Hilding Faxén, and subsequently formalized and improved by Howard Brenner, Seagate Kim and many others, a new theoretical framework has been proposed in this dissertation to investigate transport properties of colloids in microfluidics.

The main goal of this dissertation has been to provide a theoretical framework for describing the complex hydromechanics of a particle in microfluidic systems, in a formally consistent way, suitable to be approached/approximated by numerical methods, accounting for the hydrodynamic effects that are involved when the dimensions of the flow device are reduced to length scale comparable to that of the transported particles, which is the common situation occurring in microfluidics.

Essentially the main points of the present theory are:

- a consistent bitensorial-distributional formalism of Stokesian singularities both in unbounded and bounded flow domains;
- the identification of the role of the dualism referred to as the Hinch-Kim dualism in the hydromechanical theory of particle motion in a Stokes flow, and the role played by the nature of the boundary conditions at the particle boundary;
- the use of this approach to develop a consistent theory of particle motion in confined Stokesian flows based on two main fundamental ingredients: the Green functions for the confinement, and the hierarchy of moments on the particle in algebraic ambient flows.

With the aim of providing a clear and unambiguous formalism for the singular solutions in Stokes flows, suitable to be extended to confined problems, the bitensorial formalism has been introduced in Chapter 2. The main motivation of this formalism is to make a clear distinction between source and field points of singular fields, and this proves to be useful even when the fluid domain is regarded as flat space, and it is parametrized with respect to Cartesian coordinates. A byproduct of this formalization has been a clear definition of the singularities characterizing Stokes flows, specifying the associated non-homogeneous equations and boundary conditions, and obtaining the most common unbounded singularities as a particular case of the more general bounded counterparts. Although this topic can be found in any monograph on Stokesian hydrodynamics [130, 194], the detailed description of some of the most common Stokesian singularities has never been, to the best of the author's knowledge, addressed in the hydrodynamic literature. In addition, enforcing the reciprocal symmetry of the Green function, it has been shown that it is possible to apply the operators both to the source and to the field point of the Stokeslet, in order to obtain the disturbance contribution to the flow field.

The main consequence of the latter result is that, whenever it is possible to define a reflection operator, this operator should coincide with the operator derived from moment theory furnishing the image system of singularity. This result, applied to the Green function in the flow bounded by a plane provides an alternative way for expressing the hydrodynamic singularities in a much simpler way than in the approach used by Blake [18] involving Fourier-Hankel transforms. The same approach has been also used to derive other non-trivial singularities, such as the Source Dipole and the Strainlet.

In Chapter 3, the formal structure of the operators describing the hydromechanics of an arbitrary body immersed in Stokes flow has been investigated: the singularity operator giving the disturbance flow due to the body being immersed in the fluid and the Faxén operator giving the moments on the body due to the fluid flowing around it. By considering moments of the volume forces on the body, a general expression for the singularity operator has been obtained. Specifically, a generic n-th order singularity operator can be obtained by defining (m, n)-th order geometrical moments as the m-th order moment of volume forces on the body immersed in a n-th order ambient flow singular at infinity. The analysis of this problem, by considering a vast class of boundary conditions of hydrodynamic interest, has shown that the Hinch-Kim dualism is not an intrinsic property of the Stokes flows due to Lorentz reciprocity of its governing equations, but it depends essentially on the nature of the interaction with the body. This is not a trivial conclusion, since other properties following from the reciprocity between thermodynamic forces and fluxes of the governing equations, such as the symmetry of the resistance matrix (following from the reciprocity of the Stokes equations and, primarily, from that of the Onsager relations [138]), are independent on the nature of the surface interaction (boundary conditions) between the body and the fluid.

The strength of this method is that the operators do have an explicit expression that allows us to investigate, case by case, the dualism, and to determine the physical conditions upon which this dualism applies. It is found that the Hinch-Kim dualism holds only for particular boundary conditions (although of great practical interest) such as for rigid particles, drop at the mechanical equilibrium or porous bodies modeled by the Brinkman equations), but it does not hold for other classes, such as elastic deforming bodies, deforming drops, non-Newtonian drops, and porous bodies modeled by the Darcy law.

It is interesting to observe that in the case Navier-slip boundary conditions are considered (for which it has been proved the validity of the Hinch-Kim dualism) the n-th order Faxén operator is determined by the n-th order surface traction on the body (i.e. the surface traction on the body immersed in a n-th order ambient flow). Therefore, by using Lorentz's reciprocal theorem in a suitable way, the 0-th, 1-st and 2-nd order surface tractions on a sphere with Navier-slip boundary condition have been calculated and, using these results, the 0-th, 1-st, 2-nd Faxén operators giving the moments up to the second order analytically derived for a rigid sphere. This result is of practical interest as it provides the disturbance field due to a sphere in an ambient flow up to the 2-nd order, corresponding to the case of a Poiseuille flow. In Chapter 4, enforcing the results obtained in the preceding chapters applied to the classical reflection method in the study of confined flows, the exact representation for the velocity field around a particle in confined fluids and for the hydrodynamic force, torque and higher-order moments acting on the particle have been derived. By means of a convergence analysis, it has been proved that these solutions are valid also for distances between particle and interfaces of the same order of the size of the particle. In the description of particle-fluid interactions in confined flow, the representation in terms of infinite matrices ($[N]$-matrix representing) proves to be, not only concise and elegant, but practically useful. Since the entries of the $[N]$-matrix are expressed in terms of well defined problems involving the geometry of the particle and of the confinement separately, it is possible to determine its entries by solving, either analytically or numerically, a family of Stokes problems in simpler domains, possessing, in many cases, symmetries that are missed in the confined case.

Transferring the theory to practical computational problems, the use of the truncation error estimates, associated with the truncation of the infinite matrices entering the theory with computationally feasible finite (truncated) counterparts represents a useful tool to check the accuracy of the numerical estimates. This analysis has been applied to the approximate expressions available in the literature. The practical examples treated in this dissertation represent only the very first application of this theory, the full strength of which, in dealing with confined geometries and practical problems, will be developed in forthcoming works.

Many of the results obtained in this thesis are applicable in a wider multi-scale sense and it can be viewed as part of the theory referred by Batchelor as "Microhydrodynamics" [106], which includes also more complex systems such as particle suspensions or particles transported in porous materials. In these systems the global macroscopic properties (effective viscosity, permeability, sedimentation rate, etc.) are emergent phenomena strictly related to the particle-particle and particle-confinement interactions existing at the microscopic level, that can be approached by means of homogenization techniques (moment analysis or multiscale expansions).

Two other important topics have been also addressed: the description of stochastic fluctuations in confined systems, and the extension to fluids more complex than the purely Newtonian case.

A generalized formulation of fluctuation-dissipation relations in confined geometries has been developed, and the corresponding overdamped approximation obtained. The influence of boundary conditions either at the particle or at the confinement walls has been discussed in connection with the Stokesian paradox of infinite touching time occurring for non-slip boundary conditions, showing that the presence of a finite slip length cures this pathology.

The extension to time-dependent Stokes regimes and to more complex fluids has been introduced in the last chapter, with the focus on showing that the occurrence of a finite propagation velocity of the shear stresses, characteristic of viscoelastic fluids, determines a regularization of the fluid inertial kernels with respect to the purely Newtonian case, for which the Basset kernel displays a power-law integrable singularity. Modal expansion of fluid inertial kernel in analogy with the classical exponentially decaying mode representation of linear viscoelasticity is also presented.

Bibliography

[1] B. J. Alder and T. E. Wainwright. Decay of the velocity autocorrelation function. *Phys. Rev. A*, 1(1):18, 1970.

[2] E. Barta and N. Liron. Slender body interactions for low reynolds numbers—part i: body-wall interactions. *SIAM J. on Appl. Math.*, 48(5):992–1008, 1988.

[3] E. Barta and N. Liron. Slender body interactions for low reynolds numbers—part ii: Body-body interactions. *SIAM J. Appl. Math.*, 48(6):1262–1280, 1988.

[4] A. B. Basset. *A treatise on hydrodynamics: with numerous examples*, volume 2. Bell and Company, 1888.

[5] G. K. Batchelor. *An introduction to fluid dynamics*. Cambridge university press, 1967.

[6] G. K. Batchelor. Slender-body theory for particles of arbitrary cross-section in stokes flow. *J. Fluid Mech.*, 44(3):419–440, 1970.

[7] G. K. Batchelor. The stress system in a suspension of force-free particles. *J. Fluid Mech.*, 41(3):545–570, 1970.

[8] G. K. Batchelor and J. T. Green. The determination of the bulk stress in a suspension of spherical particles to order c2. *J. Fluid Mech.*, 56(3):401–427, 1972.

[9] G. K. Batchelor and J. T. Green. The hydrodynamic interaction of two small freely-moving spheres in a linear flow field. *J. Fluid Mech.*, 56(2):375–400, 1972.

[10] M. Z. Bazant and O. I. Vinogradova. Tensorial hydrodynamic slip. *J. Fluid Mech.*, 613:125–134, 2008.

[11] D. Bedeaux and P. Mazur. Brownian motion and fluctuating hydrodynamics. *Physica*, 76(2):247–258, 1974.

[12] D. Bedeaux and P. Mazur. A generalization of faxén's theorem to nonsteady motion of a sphere through a compressible fluid in arbitrary flow. *Physica*, 78(3):505–515, 1974.

[13] C. W. J. Beenakker and P. Mazur. Is sedimentation container-shape dependent? *Phys. Fluids*, 28(11):3203–3206, 1985.

[14] E. Betti. Teoria della elasticità. *Il Nuovo Cimento (1869-1876)*, 7(1):69–97, 1872.

[15] S.M. Bezrukov, L. Schimansky-Geier, and G. Schmid. Brownian motion in confined geometries. *Eur. Phys. J. Spec. Top.*, 223(14):3021–3025, 2014.

[16] V. Biagioni, G. Balestrieri, A. Adrover, and S. Cerbelli. Combining electrostatic, hindrance and diffusive effects for predicting particle transport and separation efficiency in deterministic lateral displacement microfluidic devices. *Biosensors*, 10(9):126, 2020.

[17] X. Bian, C. Kim, and G. E. Karniadakis. 111 years of brownian motion. *Soft Matter*, 12(30):6331–6346, 2016.

[18] J. R. Blake. A note on the image system for a stokeslet in a no-slip boundary. *Math. Proc. Camb. Philos*, 70(2):303–310, 1971.

[19] J. R. Blake and A. T. Chwang. Fundamental singularities of viscous flow: Part i: The image systems in the vicinity of a stationary no-slip boundary. *J. Eng. Math.*, 8(1):23–29, 1974.

[20] M. Bordag, G. L. Klimchitskaya, U. Mohideen, and V. M. Mostepanenko. *Advances in the Casimir effect*. OUP Oxford, 2009.

[21] G. Bossis and J. F. Brady. The rheology of brownian suspensions. *J. Chem. Phys.*, 91(3):1866–1874, 1989.

[22] J. F. Brady and G. Bossis. Stokesian dynamics. *Annu. Rev. Fluid Mech.*, 20:111–157, 1988.

[23] H. Brenner. The slow motion of a sphere through a viscous fluid towards a plane surface. *Chem. Eng. Sci.*, 16(3-4):242–251, 1961.

[24] H. Brenner. Effect of finite boundaries on the stokes resistance of an arbitrary particle. *J. Fluid Mech.*, 12(1):35–48, 1962.

[25] H. Brenner. The stokes resistance of an arbitrary particle—iv arbitrary fields of flow. *Chem. Eng. Sci.*, 19(10):703–727, 1964.

[26] H. Brenner. *Interfacial transport processes and rheology*. Elsevier, 2013.

[27] H. Brenner and V. Ganesan. Molecular wall effects: Are conditions at a boundary "boundary conditions"? *Phys. Rev. E .*, 61(6):6879, 2000.

[28] H. Brenner and L. J. Gaydos. The constrained brownian movement of spherical particles in cylindrical pores of comparable radius: models of the diffusive and convective transport of solute molecules in membranes and porous media. *J. Colloid Interface Sci.*, 58(2):312–356, 1977.

[29] P. C. Bressloff and J. M. Newby. Stochastic models of intracellular transport. *Rev. Mod. Phys.*, 85(1):135–196, 2013.

[30] T. Brettschneider, G. Volpe, L. Helden, J. Wehr, and C. Bechinger. Force measurement in the presence of brownian noise: Equilibrium- distribution method versus drift method. *Phys. Rev. E Stat. Nonlin. Soft Matter Phys.*, 83(4), 2011.

[31] H. C. Brinkman. A calculation of the viscous force exerted by a flowing fluid on a dense swarm of particles. *Flow Turbul. Combust.*, 1:27–34, 1949.

[32] P.S. Burada, P. Hänggi, F. Marchesoni, G. Schmid, and P. Talkner. Diffusion in confined geometries. *ChemPhysChem*, 10(1):45–54, 2009.

[33] J. M. Burgers. On the motion of small particles of elongated form suspended in a viscous liquid. *Kon. Ned. Akad. Wet. Verhand.(Eerste Sectie)*, 16:113–184, 1938.

[34] R. E. Burgess. Brownian motion and the equipartition theorem. *Phys. Lett. A*, 42(5):395–396, 1973.

[35] S. Cerbelli, F. Garofalo, and M. Giona. Effective dispersion and separation resolution in continuous particle fractionation. *Microfluid. Nanofluidics*, 19(5):1035–1046, 2015.

[36] S. Cerbelli, M. Giona, and F. Garofalo. Quantifying dispersion of finite-sized particles in deterministic lateral displacement microflow separators through brenner's macrotransport paradigm. *Microfluid. and Nanofluid.*, 15:431–449, 2013.

[37] S. Chandrasekhar. Stochastic problems in physics and astronomy. *Rev. Mod. Phys.*, 15(1):1–89, 1943.

[38] T.-P. Cheng. *Einstein's Physics: Atoms, Quanta, and Relativity-Derived, Explained, and Appraised.* OUP Oxford, 2013.

[39] T. S. Chow and J. J. Hermans. Brownian motion of a spherical particle in a compressible fluid. *Physica*, 65(1):156–162, 1973.

[40] A. T. Chwang and T. Y.-T. Wu. Hydromechanics of low-reynolds-number flow. part 1. rotation of axisymmetric prolate bodies. *J. Fluid Mech.*, 63(3):607–622, 1974.

[41] A. T. Chwang and T. Y.-T. Wu. Hydromechanics of low-reynolds-number flow. part 2. singularity method for stokes flows. *J. Fluid Mech.*, 67(4):787–815, 1975.

[42] William Coffey and Yu P Kalmykov. *The Langevin equation: with applications to stochastic problems in physics, chemistry and electrical engineering.* World Scientific, 2012.

[43] R. G. Cooke. *Infinite matrices and sequence spaces.* Courier Corporation, 2014.

[44] R. G. Cox. The motion of suspended particles almost in contact. *Int. J. Multiph. Flow*, 1(2):343–371, 1974.

[45] R. G. Cox. The motion of suspended particles almost in contact. *Int. J. Multiph. Flow*, 1(2):343–371, 1974.

[46] R. G. Cox and H. Brenner. Effect of finite boundaries on the stokes resistance of an arbitrary particle part 3. translation and rotation. *J. Fluid Mech.*, 28(2):391–411, 1967.

[47] R. G. Cox and H. Brenner. The slow motion of a sphere through a viscous fluid towards a plane surface—ii small gap widths, including inertial effects. *Chem. Eng. Sci.*, 22(12):1753–1777, 1967.

[48] R. G. Cox and H. Brenner. The lateral migration of solid particles in poiseuille flow—i theory. *Chem. Eng. Sci.*, 23(2):147–173, 1968.

[49] A. Cunsolo, G. Ruocco, F. Sette, C. Masciovecchio, A. Mermet, G. Monaco, M. Sampoli, and R. Verbeni. Experimental determination of the structural relaxation in liquid water. *Phys. Rev. Lett.*, 82(4):775, 1999.

[50] H. Darcy. *Les fontaines publiques de la ville de Dijon: exposition et application des principes à suivre et des formules à employer dans les questions de distribution d'eau. . . un appendice relatif aux fournitures d'eau de plusieurs villes au filtrage des eaux.* Victor Dalmont, éditeur, 1856.

[51] C. Darwin. Note on hydrodynamics. *Math. Proc. Camb. Philos*, 49(2):342–354, 1953.

[52] G. D'Avino, F. Greco, and P. L. Maffettone. Particle migration due to viscoelasticity of the suspending liquid and its relevance in microfluidic devices. *Ann. Rev. Fluid Mech.*, 49:341–360, 2017.

[53] M. De Corato, F. Greco, G. D'Avino, and P. L. Maffettone. Hydrodynamics and brownian motions of a spheroid near a rigid wall. *J. Chem. Phys.*, 142(19):194901, 2015.

[54] S. R. De Groot and P. Mazur. *Non-equilibrium thermodynamics.* Courier Corporation, 2013.

[55] W. R. Dean and M. E. O'Neill. A slow motion of viscous liquid caused by the rotation of a solid sphere. *Mathematika*, 10(1):13–24, 1963.

[56] B. S. DeWitt and R. W. Brehme. Radiation damping in a gravitational field. *Ann. Phys.*, 9(2):220–259, 1960.

[57] R. Dey, C. M. Buness, B. V. Hokmabad, C. Jin, and C. C. Maass. Oscillatory rheotaxis of artificial swimmers in microchannels. *Nat. Commun.*, 13(1):2952, 2022.

[58] D. Di Carlo. Inertial microfluidics. *Lab. Chip*, 9(21):3038–3046, 2009.

[59] B. E. Dolata and R. N. Zia. Faxén formulas for particles of arbitrary shape and material composition. *J. Fluid Mech.*, 910:A22, 2021.

[60] S. Duhr and D. Braun. Thermophoretic depletion follows boltzmann distribution. *Phys. Rev. Lett.*, 96(16), 2006.

[61] L. Durlofsky, J. F. Brady, and G. Bossis. Dynamic simulation of hydrodynamically interacting particles. *J. Fluid Mech.*, 180:21–49, 1987.

[62] E. B. Dussan. On the spreading of liquids on solid surfaces: static and dynamic contact lines. *Annu. Rev. Fluid Mech.*, 11(1):371–400, 1979.

[63] E.B. Dussan. The moving contact line: The slip boundary condition. *J. Fluid Mech.*, 77(4):665–684, 1976.

[64] E. B. Dussan V. and S. H. Davis. On the motion of a fluid-fluid interface along a solid surface. *J. Fluid Mech.*, 65(1):71–95, 1974.

[65] G. D'Avino and P. L. Maffettone. Particle dynamics in viscoelastic liquids. *J. Non-Newton. Fluid Mech.*, 215:80–104, 2015.

[66] P. Ebenfelt and D. Khavinson. On point to point reflection of harmonic functions across real-analytic hypersurfaces in Rn. *J. Anal. Math.*, 68:145–182, 1996.

[67] A. Einstein. *Investigations on the Theory of the Brownian Movement.* Courier Corporation, 1956.

[68] H. Eslami and F. Mller-Plathe. Viscosity of nanoconfined polyamide-6,6 oligomers: Atomistic reverse nonequilibrium molecular dynamics simulation. *J. Phys. Chemi. B*, 114(1):387–395, 2010.

[69] X. Fan and I. M. White. Optofluidic microsystems for chemical and biological analysis. *Nat. Photon.*, 5(10):591–597, 2011.

[70] B. U. Felderhof. Force density induced on a sphere in linear hydrodynamics: Ii. moving sphere, mixed boundary conditions. *Phys. A: Stat. Mech. Appl.*, 84(3):569–576, 1976.

[71] B. U. Felderhof and R. B. Jones. Faxén theorems for spherically symmetric polymers in solution. *Phys. A: Stat. Mech. Appl.*, 93(3-4):457–464, 1978.

[72] B. Finzi and M. Pastori. *Calcolo tensoriale e applicazioni.* Zanichelli, 1979.

[73] T. Franosch, M. Grimm, M. Belushkin, F. M. Mor, G. Foffi, L. Forró, and S. Jeney. Resonances arising from hydrodynamic memory in brownian motion. *Nature*, 478(7367):85–88, 2011.

[74] E. Frey and K. Kroy. Brownian motion: a paradigm of soft matter and biological physics. *Ann. Phys.*, 517(1-3):20–50, 2005.

[75] G. P. Galdi and R. Rannacher. *Fundamental trends in fluid-structure interaction*. World Scientific, 2010.

[76] P. R. Garabedian. Partial differential equations with more than two independent variables in the complex domain. *J. Math. Mech.*, pages 241–271, 1960.

[77] C. Gardiner. *Stochastic methods*. Springer Berlin, 2009.

[78] R. Gatignol. On the history term of boussinesq–basset when the viscous fluid slips on the particle. *CR MECANIQUE*, 335(9-10):606–616, 2007.

[79] I. M. Gel'fand and G. E. Šilov. *Generalized functions: properties and operations*, volume 1. Academic Press New York, 1964.

[80] H. Ghassemi and E. Yari. The added mass coefficient computation of sphere, ellipsoid and marine propellers using boundary element method. *Pol. Marit. Res.*, 18(1):17–26, 2011.

[81] M. Giona. Generalized poisson-kac processes and the regularity of laws of nature. *Acta Phys. Pol. B*, 49(5), 2018.

[82] M. Giona, A. Brasiello, and S. Crescitelli. Stochastic foundations of undulatory transport phenomena: Generalized poisson–kac processes—part iii extensions and applications to kinetic theory and transport. *J. Phys. A*, 50(33):335004, 2017.

[83] M. Giona, G. Procopio, A. Adrover, and R. Mauri. New formulation of the navier–stokes equations for liquid flows. *J. Non-Equil. Thermody.*, 2022.

[84] M. Giona, G. Procopio, and R. Mauri. Hydrodynamic green functions: paradoxes in unsteady stokes conditions and infinite propagation velocity in incompressible viscous models. *Meccanica*, 57(5):1055–1069, 2022.

[85] A. J. Goldman, R. G. Cox, and H. Brenner. Slow viscous motion of a sphere parallel to a plane wall—i motion through a quiescent fluid. *Chem. Eng. Sci.*, 22(4):637–651, 1967.

[86] H. L. Goldsmith and S.G. Mason. The flow of suspensions through tubes. i. single spheres, rods, and discs. *J. Colloid Sci.*, 17(5):448–476, 1962.

[87] H. L. Goldsmith and R. Skalak. Hemodynamics. *Ann. Rev. Fluid Mech.*, 7(1):213–247, 1975.

[88] S. Goldstein. *Modern developments in fluid dynamics: an account of theory and experiment relating to boundary layers, turbulent motion and wakes*, volume 2. Clarendon Press, 1938.

[89] G. H. Golub and C. F. Van Loan. *Matrix computations*. JHU press, 2013.

[90] S. L. Goren. The hydrodynamic force resisting the approach of a sphere to a plane permeable wall. *J. Colloid Interface Sci.*, 69(1):78–85, 1979.

[91] O. Gorodetskyi, I. Vivat, M.F.M. Speetjens, and P.D. Anderson. Analysis of advective-diffusive transport in complex mixing devices by the diffusive mapping method. *Macromol. Theory Simul.*, 24(4):322–334, 2015.

[92] M. Grimm, S. Jeney, and T. Franosch. Brownian motion in a maxwell fluid. *Soft Matter*, 7(5):2076–2084, 2011.

[93] E. Guazzelli and J. F. Morris. *A physical introduction to suspension dynamics*. Cambridge University Press, 2011.

[94] William L Haberman and Rose M Sayre. Motion of rigid and fluid spheres in stationary and moving liquids inside cylindrical tubes. Technical report, David Taylor Model Basin Washington DC, 1958.

[95] G. Haller. Solving the inertial particle equation with memory. *J. Fluid Mech.*, 874:1–4, 2019.

[96] H. Han, Z. Huang, and W. Lee. Metal-assisted chemical etching of silicon and nanotechnology applications. *Nano Today*, 9(3):271–304, 2014.

[97] G. J. Hancock. The self-propulsion of microscopic organisms through liquids. *Proc. Math. Phys. Eng.*, 217(1128):96–121, 1953.

[98] J. Happel and H. Brenner. *Low Reynolds number hydrodynamics: with special applications to particulate media*. Springer Science & Business Media, 1983.

[99] J. O. Hardin, T. J. Ober, A. D. Valentine, and J. A. Lewis. Microfluidic printheads for multimaterial 3d printing of viscoelastic inks. *Adv. Mater.*, 27(21):3279–3284, 2015.

[100] H. Hasimoto. Slow motion of a small sphere in a cylindrical domain. *J. Phys. Soc. Japan.*, 41(6):2143–2144, 1976.

[101] H. Hasimoto. An extension of faxen's law te the ellipsoid of revolution. *J. Phys. Soc. Jpn.*, 52(10):3294–3296, 1983.

[102] H. Hasimoto. Lorentz's theorem on the stokes equation. *J. Eng. Math.*, 30(1-2):215–224, 1996.

[103] G. Hetsroni and S. Haber. The flow in and around a droplet or bubble submerged in an unbound arbitrary velocity field. *Rheol. Acta*, 9:488–496, 1970.

[104] R. Hill and G. Power. Extremum principles for slow viscous flow and the approximate calculation of drag. *Q. J. Mech. Appl*, 9(3):313–319, 1956.

[105] E. J. Hinch. An averaged-equation approach to particle interactions in a fluid suspension. *J. Fluid Mech.*, 83(4):695–720, 1977.

[106] E. J. Hinch. A perspective of batchelor's research in micro-hydrodynamics. *J. Fluid Mech.*, 663:8–17, 2010.

[107] B. P. Ho and L. G. Leal. Inertial migration of rigid spheres in two-dimensional unidirectional flows. *J. Fuid Mech.*, 65(2):365–400, 1974.

[108] BP Ho and LG Leal. Migration of rigid spheres in a two-dimensional unidirectional shear flow of a second-order fluid. *Journal of Fluid Mechanics*, 76(4):783–799, 1976.

[109] T. M. Ho, A. Razzaghi, A. Ramachandran, and K. S. Mikkonen. Emulsion characterization via microfluidic devices: A review on interfacial tension and stability to coalescence. *Adv. Colloid Interface Sci.*, 299:102541, 2022.

[110] L. M. Hocking. The effect of slip on the motion of a sphere close to a wall and of two adjacent spheres. *J. Eng. Math.*, 7(3):207–221, 1973.

[111] L. M. Hocking. A moving fluid interface on a rough surface. *J. Fluid Mech.*, 76(4):801–817, 1976.

[112] R. M. Höfer and J. J. L. Velázquez. The method of reflections, homogenization and screening for poisson and stokes equations in perforated domains. *Arch. Ration. Mech. Anal.*, 227(3):1165–1221, 2018.

[113] S. Hottovy, G. Volpe, and J. Wehr. Thermophoresis of brownian particles driven by coloured noise. *EPL*, 99(6), 2012.

[114] L. R. Huang, E. C. Cox, R. H. Austin, and J. C. Sturm. Continuous particle separation through deterministic lateral displacement. *Science*, 304(5673):987–990, 2004.

[115] K. Ichiki. Improvement of the stokesian dynamics method for systems with a finite number of particles. *J. Fluid Mech.*, 452:231–262, 2002.

[116] K. Ichiki and J. F. Brady. Many-body effects and matrix inversion in low-reynolds-number hydrodynamics. *Phys. Fluids*, 13(1):350–353, 2001.

[117] G. B. Jeffery. On the steady rotation of a solid of revolution in a viscous fluid. *Proc. London Math. Soc.*, 2(1):327–338, 1915.

[118] D. J. Jeffrey and Y. Onishi. Calculation of the resistance and mobility functions for two unequal rigid spheres in low-reynolds-number flow. *J . Fluid Mech.*, 139:261–290, 1984.

[119] R. E. Johnson and T. Y. Wu. Hydromechanics of low-reynolds-number flow. part 5. motion of a slender torus. *J. Fluid Mech.*, 95(2):263–277, 1979.

[120] I. P. Jones. Low reynolds number flow past a porous spherical shell. *Math. Proc. Camb. Philos.*, 73(1):231–238, 1973.

[121] R. B. Jones. Faxén theorems for a spherically symmetric polymer in time dependent compressible flow. *Phys. A: Stat. Mech. Appl.*, 95(1):104–116, 1979.

[122] Y. Kaneda. A generalization of faxén's theorem to nonsteady motion of an almost spherical drop in an arbitrary flow of a compressible fluid. *Phys. A: Stat. Mech. Appl.*, 101(2-3):407–422, 1980.

[123] A. Kang, J. Park, J. Ju, G. S. Jeong, and S. H. Lee. Cell encapsulation via microtechnologies. *Biomaterials*, 35(9):2651–2663, 2014.

[124] R. P. Kanwal. *Generalized functions: theory and applications*. Springer Science & Business Media, 2004.

[125] M. T. Kezirian. *Hydrodynamics with a wall-slip boundary condition for a particle moving near a plane wall bounding a semi-infinite viscous fluid*. PhD thesis, Massachusetts Institute of Technology, 1992.

[126] D. Khavinson and E. Lundberg. *Linear holomorphic partial differential equations and classical potential theory*. American Mathematical Soc., 2018.

[127] S. Kheifets, A. Simha, K. Melin, T. Li, and M.G. Raizen. Observation of brownian motion in liquids at short times: Instantaneous velocity and memory loss. *Science*, 343(6178):1493–1496, 2014.

[128] S. Kim. A note on faxen laws for nonspherical particles. *Int. J. Multiph. Flow*, 11(5):713–719, 1985.

[129] S. Kim. Singularity solutions for ellipsoids in low-reynolds-number flows: with applications to the calculation of hydrodynamic interactions in suspensions of ellipsoids. *Int. J. Multiph. Flow*, 12(3):469–491, 1986.

[130] S. Kim and S. J. Karrila. *Microhydrodynamics: principles and selected applications*. Courier Corporation, 2013.

[131] R. Klages, W. Just, and C. Jarzynski. *Nonequilibrium Statistical Physics of Small Systems: Fluctuation Relations and Beyond*. Wiley-VCH, 2013.

[132] P. E. Kloeden and E. Platen. *Numerical Solution of Stochastic Differential Equations*. Springer, 1992.

[133] R. Kubo. The fluctuation-dissipation theorem. *Rep. Prog. Phys.*, 29(1):255, 1966.

[134] R. Kubo, M. Toda, and N. Hashitsume. *Statistical physics II: nonequilibrium statistical mechanics*. Springer Science & Business Media, 2012.

[135] V. D. Kupradze and M. A. Aleksidze. The method of functional equations for the approximate solution of certain boundary value problems. *USSR Comput. Math. & Math. Phys.*, 4(4):82–126, 1964.

[136] M. Kuron, P. Stark, C. Holm, and J. De Graaf. Hydrodynamic mobility reversal of squirmers near flat and curved surfaces. *Soft Matter*, 15(29):5908–5920, 2019.

[137] O. A. Ladyzhenskaya. *The mathematical theory of viscous incompressible flow*. Gordon and Breach New York, 1969.

[138] L. D. Landau and E. M. Lifshitz. *Fluid Mechanics: Landau and Lifshitz: Course of Theoretical Physics, Volume 6*. Elsevier, 2013.

[139] L. D. Landau and E. M. Lifshitz. *Statistical Physics: Volume 5*. Elsevier, 2013.

[140] L. D. Landau, E. M. Lifshitz, A. M. Kosevich, and L. P. Pitaevskii. *Theory of elasticity: volume 7*. Elsevier, 1986.

[141] P. Langevin. Sur la théorie du mouvement brownien. *C. R. Acad. Sci. Paris*, 146:530–533, 1908.

[142] G. P. Langlois, M. Farazmand, and G. Haller. Asymptotic dynamics of inertial particles with memory. *J. Nonlinear Sci.*, 25:1225–1255, 2015.

[143] P. Lançon, G. Batrouni, L. Lobry, and N. Ostrowsky. Drift without flux: Brownian walker with a space-dependent diffusion coefficient. *EPL*, 54(1):28–34, 2001.

[144] P. Lançon, G. Batrouni, L. Lobry, and N. Ostrowsky. Brownian walker in a confined geometry leading to a space-dependent diffusion coefficient. *Phys. A: Stat. Mech. Appl.*, 304(1-2):65–76, 2002.

[145] E. Lauga. *The fluid dynamics of cell motility*. Cambridge University Press, 2020.

[146] E. Lauga, M. Brenner, and H. Stone. Microfluidics: The no-slip boundary condition. In *Springer Handbooks of Experimental Fluid Mechanics*, pages 1219–1240. Springer, 2007.

[147] E. Lauga and T. M. Squires. Brownian motion near a partial-slip boundary: A local probe of the no-slip condition. *Phys. Fluids*, 17(10):103102, 2005.

[148] L. G. Leal. *Advanced transport phenomena: fluid mechanics and convective transport processes*, volume 7. Cambridge University Press, 2007.

[149] S. H. Lee, R. S. Chadwick, and L. G. Leal. Motion of a sphere in the presence of a plane interface. part 1. an approximate solution by generalization of the method of lorentz. *J. Fluid Mech.*, 93(4):705–726, 1979.

[150] S. H. Lee, R. S. Chadwick, and L. G. Leal. Motion of a sphere in the presence of a plane interface. part 1. an approximate solution by generalization of the method of lorentz. *J. Fluid Mech.*, 93(4):705–726, 1979.

[151] L. Li, Y. Zhang, Y. Zhou, W. Zheng, Y. Sun, G. Ma, and Y. Zhao. Optical fiber optofluidic bio-chemical sensors: a review. *Laser Photonics Rev.*, 15(7):2000526, 2021.

[152] N. Liron and S. Mochon. Stokes flow for a stokeslet between two parallel flat plates. *J. Eng. Math.*, 10(4):287–303, 1976.

[153] N. Liron and R. Shahar. Stokes flow due to a stokeslet in a pipe. *J. Fluid Mech.*, 86(4):727–744, 1978.

[154] M. Lisicki. Four approaches to hydrodynamic green's functions–the oseen tensors. *arXiv preprint arXiv:1312.6231*, 2013.

[155] D. Lohse. Fundamental fluid dynamics challenges in inkjet printing. *Ann. Rev. Fluid Mech.*, 54:349–382, 2022.

[156] H. A. Lorentz. *Abhandlungen über theoretische Physik*. BG Teubner, 1907.

[157] J. H. C. Luke. Convergence of a multiple reflection method for calculating stokes flow in a suspension. *SIAM J. Appl. Math.*, 49(6):1635–1651, 1989.

[158] C. Luni, F. Michielin, L. Barzon, V. Calabrò, and N. Elvassore. Stochastic model-assisted development of efficient low-dose viral transduction in microfluidics. *Biophys. J.*, 104(4):934–942, 2013.

[159] C. W. Macosko. *Rheology principles, measurements and applications*. VCH Publishes, 1994.

[160] E. Z. Macosko, A. Basu, R. Satija, J. Nemesh, K. Shekhar, M. Goldman, I. Tirosh, A. R. Bialas, N. Kamitaki, E. M. Martersteck, et al. Highly parallel genome-wide expression profiling of individual cells using nanoliter droplets. *Cell*, 161(5):1202–1214, 2015.

[161] R. Mannella and P.V.E. McClintock. Ito versus stratonovich: 30 years later. *Fluct. Noise Lett.*, 11(1), 2012.

[162] J. H. Masliyah, G. Neale, K. Malysa, and T. G. M. Van De Ven. Creeping flow over a composite sphere: solid core with porous shell. *Chem. Eng. Sci.*, 42(2):245–253, 1987.

[163] H. Masoud and H. A. Stone. The reciprocal theorem in fluid dynamics and transport phenomena. *J. Fluid Mech.*, 879, 2019.

[164] C. Maul and S. Kim. Image systems for a stokeslet inside a rigid spherical container. *Phys. Fluids*, 6(6):2221–2223, 1994.

[165] C. Maul and S. Kim. Image of a point force in a spherical container and its connection to the lorentz reflection formula. In *The Centenary of a Paper on Slow Viscous Flow by the Physicist HA Lorentz*, pages 119–130. Springer, 1996.

[166] R. Mauri. A new application of the reciprocity relations to the study of fluid flows through fixed beds. *J. Eng. Math.*, 33:103–112, 1998.

[167] M. R. Maxey and J. J. Riley. Equation of motion for a small rigid sphere in a nonuniform flow. *Phys. Fluids*, 26(4):883–889, 1983.

[168] J. C. Maxwell. On the calculation of the equilibrium and stiffness of frames. *Lond. Edinb. Dublin Philos. Mag. J. Sci.*, 27(182):294–299, 1864.

[169] P. Mazur and D. Bedeaux. A generalization of faxén's theorem to nonsteady motion of a sphere through an incompressible fluid in arbitrary flow. *Physica*, 76(2):235–246, 1974.

[170] S. Michelin. Self-propulsion of chemically active droplets. *Ann. Rev. Fluid Mech.*, 55, 2022.

[171] W. H. Mitchell and S. E. Spagnolie. Sedimentation of spheroidal bodies near walls in viscous fluids: glancing, reversing, tumbling and sliding. *J. Fluid Mech.*, 772:600–629, 2015.

[172] J. Mo and M. G. Raizen. Highly resolved brownian motion in space and in time. *Ann. Rev. of Fluid Mech.*, 51:403–428, 2019.

[173] J. Mo, A. Simha, S. Kheifets, and M. G. Raizen. Testing the maxwell-boltzmann distribution using brownian particles. *Opt. Express*, 23(2):1888–1893, 2015.

[174] J. Mo, A. Simha, and M. G. Raizen. Brownian motion as a new probe of wettability. *J. Chem. Phys.*, 146(13):134707, 2017.

[175] H.K. Moffatt. Viscous and resistive eddies near a sharp corner. *J. Fluid Mech.*, 18(1):1–18, 1964.

[176] U. Mohideen and A. Roy. Precision measurement of the casimir force from 0.1 to 0.9 μ m. *Phys. Rev. Lett.*, 81(21):4549, 1998.

[177] H. Mori. Transport, collective motion, and brownian motion. *Prog. Theor. Phys.*, 33(3):423–455, 1965.

[178] B. Nasouri and G. J. Elfring. Higher-order force moments of active particles. *Phys. Rev. Fluids*, 3(4):044101, 2018.

[179] C.L. M. H. Navier. Mémoire sur les lois du mouvement des fluides. *Mémoires de l'Académie Royale des Sciences de l'Institut de France*, 6(1823):389–440, 1823.

[180] S. Neethirajan, I. Kobayashi, M. Nakajima, D. Wu, S. Nandagopal, and F. Lin. Microfluidics for food, agriculture and biosystems industries. *Lab Chip*, 11(9):1574–1586, 2011.

[181] F. T. Nieuwstadt and J. A. Steketee. *Selected papers of J. M. Burgers*. Springer Science & Business Media, 2012.

[182] K. Oldham and J. Spanier. *The fractional calculus theory and applications of differentiation and integration to arbitrary order*. Elsevier, 1974.

[183] M. E. O'Neill. A slow motion of viscous liquid caused by a slowly moving solid sphere. *Mathematika*, 11(1):67–74, 1964.

[184] M. E. O'Neill. A slow motion of viscous liquid caused by a slowly moving solid sphere: an addendum. *Mathematika*, 14(2):170–172, 1967.

[185] C. W. Oseen. *Hydrodynamik*, volume 1. Akad. Verl.-Ges., 1927.

[186] T. J. O'Sullivan, S. K. Kannam, D. Chakraborty, B. D. Todd, and J. E. Sader. Viscoelasticity of liquid water investigated using molecular dynamics simulations. *Phys. Rev. Fluids*, 4(12):123302, 2019.

[187] B. S. Padmavathi and T. Amaranath. Stokes flow past a composite porous spherical shell with a solid core. *Arch. Mech.*, 48(2):311–323, 1996.

[188] D. Palaniappan. Arbitrary stokes flow past a porous sphere. *Mech. Res. Commun.*, 20(4):309–317, 1993.

[189] M. Parmar, S. Annamalai, S. Balachandar, and A. Prosperetti. Differential formulation of the viscous history force on a particle for efficient and accurate computation. *J. Fluid Mech.*, 844:970–993, 2018.

[190] E. Poisson, A. Pound, and I. Vega. The motion of point particles in curved spacetime. *Living Rev. Relativ.*, 14:1–190, 2011.

[191] A. D. Polyanin. Handbook of linear partial differential equations for engineers and scientists. 2001.

[192] A. S. Popel and P. C. Johnson. Microcirculation and hemorheology. *Annu. Rev. Fluid Mech.*, 37:43–69, 2005.

[193] H. Power. On the rallison and acrivos solution for the deformation and burst of a viscous drop in an extensional flow. *J. Fluid Mech.*, 185:547–550, 1987.

[194] C. Pozrikidis. *Boundary integral and singularity methods for linearized viscous flow.* Cambridge University Press, 1992.

[195] S. G. Prasath, V. Vasan, and R. Govindarajan. Accurate solution method for the maxey–riley equation, and the effects of basset history. *J. Fluid Mech.*, 868:428–460, 2019.

[196] A. R. Premlata and H. H. Wei. Atypical non-basset particle dynamics due to hydrodynamic slip. *Phys. Fluids*, 32(9):097109, 2020.

[197] A. R. Premlata and H. H. Wei. Coupled faxen relations for non-uniform slip janus spheres. *Phys. Fluids*, 33(11):112003, 2021.

[198] A.R. Premlata and H.-H. Wei. The basset problem with dynamic slip: slip-induced memory effect and slip–stick transition. *J. Fluid Mech.*, 866:431–449, 2019.

[199] A.R. Premlata and H.-H. Wei. Atypical non-basset particle dynamics due to hydrodynamic slip. *Phys. Fluids*, 32(9):097109, 2020.

[200] G. Procopio and M. Giona. Stochastic modeling of particle transport in confined geometries: Problems and peculiarities. *Fluids*, 7(3):105, 2022.

[201] G. Procopio and M. Giona. Bitensorial formulation of the singularity method for stokes flows. *Math. Eng.*, 5(2):1–34, 2023.

[202] G. Procopio and M. Giona. On the singularity operator, the faxén operator and the hinch-kim's dualism for the hydromechanics of an arbitrary body in stokes flow. *Phys. Rev. Fluids*, in preparation, 2023.

[203] D. Psaltis, S. R. Quake, and C. Yang. Developing optofluidic technology through the fusion of microfluidics and optics. *Nature*, 442(7101):381–386, 2006.

[204] E. M. Purcell. Life at low reynolds number. *Am. J. Phys.*, 45(1):3–11, 1977.

[205] P. N. Pusey. Brownian motion goes ballistic. *Science*, 332(6031):802–803, 2011.

[206] M. G. Raizen and T. L. The measurement einstein deemed impossible. *Phys. Today*, 68(1):56, 2015.

[207] J. M. Rallison. Note on the faxén relations for a particle in stokes flow. *J. Fluid Mech.*, 88(3):529–533, 1978.

[208] J. M. Rallison. The deformation of small viscous drops and bubbles in shear flows. *Annu. Rev. Fluid Mech.*, 16(1):45–66, 1984.

[209] J. M. Rallison and A. Acrivos. A numerical study of the deformation and burst of a viscous drop in an extensional flow. *J. Fluid Mech.*, 89(1):191–200, 1978.

[210] M. M. G. Ricci and T. Levi-Civita. Méthodes de calcul différentiel absolu et leurs applications. *Math. Ann.*, 54(1):125–201, 1900.

[211] H. S. Ruse. An absolute partial differential calculus. *Q. J. Math.*, 1:190–202, 1931.

[212] H. S. Ruse. Taylor's theorem in the tensor calculus. *Proc. Lond. Math. Soc.*, 2(1):87–92, 1931.

[213] E. K. Sackmann, A. L. Fulton, and D. J. Beebe. The present and future role of microfluidics in biomedical research. *Nature*, 507(7491):181–189, 2014.

[214] P. G. Saffman. On the boundary condition at the surface of a porous medium. *Stud. Appl. Math.*, 50(2):93–101, 1971.

[215] J.M. Sancho, M.S. Miguel, and D. Dürr. Adiabatic elimination for systems of brownian particles with nonconstant damping coefficients. *J. Stat. Phys.*, 28(2):291–305, 1982.

[216] A. S. Sangani and G. Mo. An o (n) algorithm for stokes and laplace interactions of particles. *Phys. Fluids*, 8(8):1990–2010, 1996.

[217] D. H. Sattinger and O. L. Weaver. *Lie groups and algebras with applications to physics, geometry, and mechanics.* Springer Science & Business Media, 2013.

[218] G. Segre and A. Silberberg. Radial particle displacements in poiseuille flow of suspensions. *Nature*, 189(4760):209–210, 1961.

[219] H. M. Shapiro. *Practical flow cytometry.* John Wiley & Sons, 2005.

[220] H. S. Shapiro. *The Schwarz function and its generalization to higher dimensions.* John Wiley & Sons, 1992.

[221] A. Simha, J. Mo, and P.J. Morrison. Unsteady stokes flow near boundaries: The point-particle approximation and the method of reflections. *J. Fluid Mech.*, 841:883–924, 2018.

[222] O. Skurtys and J. M. Aguilera. Applications of microfluidic devices in food engineering. *Food Biophys.*, 3:1–15, 2008.

[223] M. Smoluchowski. Zur kinetischen theorie der brownschen molekularbewegung und der suspensionen. *Ann. Phys.*, 326(14):756–780, 1906.

[224] R. Smoluchowski, M. Kac, S. Chandrasekhar, and S. M. Ulam. *Marian Smoluchowski: Selected Scientific Works.* Wydawnictwa Uniwersytetu Warszawskiego, 2017.

[225] R. M. Sonshine, R. G. Cox, and H. Brenner. The stokes translation of a particle of arbitrary shape along the axis of a circular cylinder: Filled to a finite depth with viscous liquid i. *Appl. Sci. Res.*, 16:273–300, 1966.

[226] S. E. Spagnolie and E. Lauga. Hydrodynamics of self-propulsion near a boundary: predictions and accuracy of far-field approximations. *J. Fluid Mech.*, 700:105–147, 2012.

[227] A. M. Striegel and A. K. Brewer. Hydrodynamic chromatography. *Annu. Rev. Anal. Chem.*, 5:15–34, 2012.

[228] J. W. Swan and J. F. Brady. Simulation of hydrodynamically interacting particles near a no-slip boundary. *Phys. Fluids*, 19(11):113306, 2007.

[229] J. W. Swan and J. F. Brady. Particle motion between parallel walls: Hydrodynamics and simulation. *Phys. Fluids*, 22(10):103301, 2010.

[230] J. L. Synge. *Relativity: the general theory.* North-holland publishing company, 1960.

[231] J. L. Synge and A. Schild. *Tensor calculus*, volume 5. Courier Corporation, 1978.

[232] E. Undvall, F. Garofalo, G. Procopio, W. Qiu, A. Lenshof, T. Laurell, and T. Baasch. Inertia-induced breakdown of acoustic sorting efficiency at high flow rates. *Phys. Rev. Appl.*, 17(3):034014, 2022.

[233] P. Van Beek. A counterpart of faxen's formula in potential flow. *Int. J. Multiph. Flow*, 11(6):873–879, 1985.

[234] N. G. van Kampen. Itô versus stratonovich. *J. Stat. Phys.*, 24(1):175–187, 1981.

[235] C. Venditti, S. Cerbelli, G. Procopio, and A. Adrover. Comparison between one- and two-way coupling approaches for estimating effective transport properties of suspended particles undergoing brownian sieving hydrodynamic chromatography. *Phys. Fluids*, 34(4):042010, 2022.

[236] D.C. Venerus and H.C. Öttinger. *A modern course in transport phenomena.* Cambridge University Press, 2018.

[237] G. Volpe, L. Helden, T. Brettschneider, J. Wehr, and C. Bechinger. Influence of noise on force measurements. *Phys. Rev. Lett.*, 104(17), 2010.

[238] C. Y. Wang. Lid-driven stokes slip flow in a rectangular cavity. *Eur. J. Mech. B/Fluids*, 89:93–99, 2021.

[239] T. Wang, C. Yu, and X. Xie. Microfluidics for environmental applications. *Microfluidics in Biotechnology*, pages 267–290, 2020.

[240] S. Whitaker. Flow in porous media i: A theoretical derivation of darcy's law. *Transp Porous Media*, 1:3–25, 1986.

[241] G. M. Whitesides. The origins and the future of microfluidics. *Nature*, 442(7101):368–373, 2006.

[242] A. Widom. Velocity fluctuations of a hard-core brownian particle. *Phys. Rev. A*, 3(4):1394, 1971.

[243] E. Wong and M. Zakai. On the convergence of ordinary integrals to stochastic integrals. *Ann. Math. Stat.*, 36(5):1560–1564, 1965.

[244] E. Wong and M. Zakai. Riemann-stieltjes approximations of stochastic integrals. *Z. Wahrscheinlichkeit.*, 12(2):87–97, 1969.

[245] S. M. Yang. Motions of a sphere in a time-dependent stokes flow: A generalization of faxen's law. *Korean J. Chem. Eng.*, 4:15–22, 1987.

[246] A. K. Yetisen, M. S. Akram, and C. R. Lowe. Based microfluidic point-of-care diagnostic devices. *Lab Chip*, 13(12):2210–2251, 2013.

[247] M. Yew, Y. Ren, K. S. Koh, C. Sun, and C. Snape. A review of state-of-the-art microfluidic technologies for environmental applications: Detection and remediation. *Global Challenges*, 3(1):1800060, 2019.

[248] Q. Yu and P. N. Kaloni. A cartesian-tensor solution of the brinkman equation. *J. Eng. Math.*, 22(2):177–188, 1988.

[249] A. P. Yuda, P. Y. E. Koraag, F. Iskandar, H. S. Wasisto, and A. Sumboja. Advances of the top-down synthesis approach for high-performance silicon anodes in li-ion batteries. *J. Mater. Chem. A*, 9(35):18906–18926, 2021.

[250] J. Zhang, S. Yan, D. Yuan, G. Alici, N.-T. Nguyen, M. E. Warkiani, and W. Li. Fundamentals and applications of inertial microfluidics: A review. *Lab. Chip*, 16(1):10–34, 2016.

[251] J. Zinn-Justin. *From random walks to random matrices.* Oxford University Press, 2019.

[252] R. Zwanzig. Memory effects in irreversible thermodynamics. *Phys. Rev.*, 124(4):983, 1961.

[253] R. Zwanzig. Nonlinear generalized langevin equations. *J. Stat. Phys.*, 9(3):215–220, 1973.

[254] R. Zwanzig and M. Bixon. Hydrodynamic theory of the velocity correlation function. *Phys. Rev. A*, 2(5):2005, 1970.

[255] R. Zwanzig and M. Bixon. Compressibility effects in the hydrodynamic theory of brownian motion. *J. Fluid Mech.*, 69(1):21–25, 1975.

List of publications

- Procopio, G., Adrover, A. and Giona, M., 2021. Generalized Reflection Method for the Stokes Equation in Confined Geometries: Applications To Microfluidics and Particle Transport. *Chemical Engineering Transactions*, 86, pp. 1153-1158.
- Giona, M., Procopio, G. and Mauri, R., 2022. Hydrodynamic Green functions: paradoxes in unsteady Stokes conditions and infinite propagation velocity in incompressible viscous models. *Meccanica*, 57(5), pp. 1055-1069.
- Undvall, E., Garofalo, F., Procopio, G., Qiu, W., Lenshof, A., Laurell, T. and Baasch, T., 2022. Inertia-Induced Breakdown of Acoustic Sorting Efficiency at High Flow Rates. *Physical Review Applied*, 17(3), p. 034014.
- Procopio, G. and Giona, M., 2022. Stochastic Modeling of Particle Transport in Confined Geometries: Problems and Peculiarities. *Fluids*, 7(3), p. 105.
- Procopio, G. and Giona, M., 2023. Bitensorial formulation of the singularity method for Stokes flows. *Mathematics in Engineering*, 5(2), pp. 1-34.
- Venditti, C., Cerbelli, S., Procopio, G. and Adrover, A., 2022. Comparison between one-and two-way coupling approaches for estimating effective transport properties of suspended particles undergoing Brownian sieving hydrodynamic chromatography. *Physics of Fluids*, 34(4), p. 042010.
- Giona, M., Procopio, G., Adrover, A. and Mauri, R., 2022. New formulation of the Navier–Stokes equations for liquid flows. *Journal of Non-Equilibrium Thermodynamics* DOI: https://doi.org/10.1515/jnet-2022-0095.
- Procopio, G. and Giona, M., 2023. Modal representation of inertial effects in fluid-particle interactions and the regularity of the memory kernels. *Fluids*, 8(3), p. 84.
- Giona, M., Pezzotti, C. and Procopio, G., 2023. The fourfold way to Gaussianity: physical interactions, distributional models and monadic transformations. *Axioms*,12(3), p. 278.
- Giona, M., Pezzotti, C. and Procopio, G., 2023. Another normality is possible. Distributive transformations and emergent Gaussianity. arXiv preprint arXiv:2301.03925.
- Giona, M., Cocco, D., Procopio, G., Cairoli, A. and Klages, R., 2023. Stochastic hydrodynamic velocity field and the representation of Langevin equations. *submitted for publication.*
- Procopio, G. and Giona, M., 2023. On the Hinch-Kim dualism between singularity and Faxén operators in the hydromechanics of arbitrary bodies in Stokes flows. *submitted for publication.*
- Procopio, G. and Giona, M., 2023. On the theory of body motion in confined Stokesian fluids. *in preparation.*